MOLECULAR CHARACTERIZATION OF THE ZEBRAFISH *ff1b* GENE

QUEK SUE ING
(B. Applied Sc. (Hons), NUS)

A THESIS SUBMITTED

FOR THE DEGREE OF DOCTOR OF PHILOSOPHY

DEPARTMENT OF BIOLOGICAL SCIENCES

THE NATIONAL UNIVERSITY OF SINGAPORE

2009

ACKNOWLEDGEMENTS

I would like to express my deepest appreciation and gratitude to my thesis supervisor, Associate Professor Chan Woon Khiong, for his persistent patience, support, and dedication in guiding me to accomplish this research project. He has provided me enough guidance to become a good researcher, while given me opportunities to explore my own ideas and to carry out my own reseearch independently. He has really been an excellent advisor in both research and life.

I would also like to thank past and present lab members of Molecular Genetics Laboratory, especially Tan Siew Peng, Ng Sze Wai, Dr. Joelle Lai Chiu Yen, Dr. Mark Richards, Dr. Nicole Teoh Pick Har, Joanne Yeoh Yen Ni, and Chak Li Ling for their friendship and assistance in countless ways. Special thanks are given to Allan Tan Jee Hian for his skillful and promptly technical assistance, as well as valuable discussion about experiments and life. I would also like to thank Dr. Tian Hui for her assistance in generating the pBACff1bEx2EGFP construct, and Dr. Anusha Amali for her help in microinjecting the various deleted BAC constructs. Also, it would not have been possible for me to carry out this meaningful research without the high-quality pioneering work from Dr. Chai Chou.

My honest thanks are also addressed specifically to Prof. Chung Bon-Chu for her generosity in sharing the human *CYP11A1* promoter constructs and useful scientific discussion. In addition, my appreciation is also extended to Dr. Martin Lee Beng Huat, Dr. Pamela Mellon, and Dr. Zhou Yiting for their kindness in sharing the MA-10, LβT2, and 293T cell lines, respectively.

My sincere appreciation also goes to Associate Professor Low Boon Chuan and Dr. Liou Yih-Cheng for their encouragement and inspiring passion about scientific research throughout the course of this study. The appreciation also goes to colleagues along the Developmental and Cell Biology corridor especially Zhan Huiqing, Qingwei, Shirley Tan, Dr. Yihui, and Dr. Farooq for their helpfulness and friendliness in providing technical guidance on the experimental techniques with zebrafish.

It would not have been possible to complete this research project without the professional support from the technical staffs in the aquarium facility of DBS. My appreciation goes to past and present staffs of the zebrafish aquatirum, Mr. Subhas Balan, Wu Yi Lian, Loh Mun Seng, and Yan Tie for providing a good aquarium facility to work in and for their guidance in maintaining zebrafish. Particularly, the collection of good-quality zebrafish embryos as well as the general care for zebrafish would not have been so smooth and well done without the dedication from Mr. Subhas Balan.

On a more personal level, I would also like to thank those outside the laboratory and campus for their encouragement and support. I would like to thank my family for their support, understanding and unwavering belief that I will be able to achieved whatever I have aimed for. Special thanks to my dearest friends for providing accompany and entertainment no matter how tough is life. Most of all, I would like to thank my husband for his love, support, and comfort. Day in and day out, he has always been there for me, for better and for worse, in conflict and in tranquility. Finally, a sincere thank you to everyone who has made this thesis accomplished.

TABLE OF CONTENTS

SUMMARY

The nuclear receptor Ff1b has been established as the master regulator of the organogenesis and the function maintenance of interrenal gland in zebrafish, in reminiscent to its mammalian ortholog, SF-1. Despite the well defined expression profile, gene structure, and loss-of-function data for both Ff1b and SF-1, the molecular mechanisms underlying their regulatory functions and the upstream factors mediating their tissue-selective expression remain largely undefined. To better elucidate the transcriptional activity of Ff1b, the 5' proximal promoter of *cyp11a1*, a putative target gene of Ff1b, was isolated and analyzed. The characterization of this promoter with regards to Ff1b transactivation ability has ascertained the conserved role of Ff1b as the major transcriptional regulator in the steroidogenesis pathway.

To create an *in vivo* system for the functional studies of Ff1b, a transgenic zebrafish model was generated using a recombined BAC clone spanning 100 kb of *ff1b* locus with EGFP reporter inserted into Exon 2. The EGFP expression that faithfully recapitulates the endogenous *ff1b* expression in zebrafish embryos has proven useful for the lineage tracing of *ff1b*-expressing cells during embryonic development. The transgenic model has been used successfully for the fate tracing of interrenal cells from early stages of development following the morpholino knockdown of *ff1b* gene function and steroid inhibitor treatment using aminoglutethimide.

In an effort to characterize the genomic organization of *ff1b*, ~46 kb of genomic sequences encompassing zebrafish *ff1b* locus was determined. With the exception of the presence of an additional Intron IV, sequence analysis of *ff1b* locus revealed conserved genomic organization compared with human and mouse *SF-1* genes. Comparative genomics revealed that the presence of the extra intron in *ff1b* is likely to represent an ancestral feature of vertebrate *FF1* genes. Using a Red/ET recombination, a novel genomic deletion strategy has been adopted to delete two genomic fragments at the 5' flanking region and seven intronic sequences of *ff1b* from a recombined BAC plasmid that contains an EGFP reporter. When combined with transient microinjection assay into zebrafish embryos, an interrenal-specific enhancer is localized to Intron IV of *ff1b*. Computational analysis of Intron IV unravels *cis*-elements that potentially regulate the interrenal-specific expression of *ff1b*.

LIST OF TABLES

LIST OF FIGURES

ABBREVIATIONS

3β-Hsd	3β-hydroxysteroid dehydrogenase
ACTH	adrenocorticotrophic hormone
AF1	Activating function 1 domain
AF2	Activating function 2 motif
AG	aminoglutethimide
Amp	ampicilin resistance
BAC	bacterial artificial chromosome
cAMP	cyclic adenosine monophosphate
ChIP	chromatin immunoprecipitation
CNS	central nervous system
CRE	cAMP response element
CRH	arcuate nuclei
DBD	DNA binding domain
dpf	days post fertilization
EGFP	Enhanced green fluorescent protein
EMSA	electrophoretic mobility shift assay
FAdE	fetal adrenal enhancer
FBS	fetal bovine serum
FF1,Ftz-F1	fushi tarazu-factor 1
FRE	Ftz-F1 response element
FREd	distal FRE
FREp	proximal FRE
FSH	follicle stimulating hormone
HPA	hypothalamic-pituitary-adrenal
hpf	hours post fertilization
HPG	hypothalamic-pituitary-gonadal
HPS	hypothalamo-pituitary-steroidogenic
HRP	horse radish peroxidase
ISH	*in situ* hybridization
Kan^r	kanamycin resistance
KO	knockout
lacZ	β-galactosidase
LB	Luria-Bertani
LBD	ligand binding domain
LG	linkage group
LH	luteinizing hormone
LRH-1	Liver receptor homolog 1
MO	morpholino
NR	nuclear receptor
ORF	open reading frame

PBS	phosphate-buffered saline
PIS	pre-immune serum
POA	post-optic area
PVN	paraventricular nucleus
RLU	relative light unit
RT	room temperature
SEM	standard error mean
SF-1	Steroidogenic factor 1
StAR, star	steroidogenic acute regulatory protein
TFBSs	transcription factor binding sites
TSS	transcription start site
UTR	untranslated region
VMH	ventromedial hypothalamus
VMHE	ventromedial hypothalamus enhancer
YAC	yeast artificial chromosome

PUBLICATIONS

Tan J.H., **Quek S.I.**, and Chan W.K. (2005) Cloning, Genomic Organization, and Expression Analysis of Zebrafish Nuclear Receptor Coactivator, TIF2. Zebrafish *2(1) 33-46.*

Quek S. I. and Chan W.K. (2009) The transcriptional activation of zebrafish *cyp11a1* is dependent mainly on the nuclear receptor Ff1b. In review.

CHAPTER 1

Introduction

1.1 The hypothalamic-pituitary-steroidogenic organ (HPS) axis

In vertebrates, the endocrine system is composed of organs or glands that interact with one another via the release of chemical messenger called hormone into the blood stream. The major organs that constitute this system include the hypothalamus, pineal gland, pituitary gland, thyroid gland, thymus, adrenal gland, ovary, and testis. The endocrine system controls almost every biological process in a vertebrate including growth and development, metabolism, sexual and reproductive functions, normal tissue functions, as well as, determination of mood and behavior. Similar to the central nervous system (CNS), it helps us to respond properly to various stimulants, albeit in a much slower and adaptive manner. This is largely due to the difference in the nature of signaling molecules utilized in the two different but related systems. While the components of CNS interact with one another through rapid neurocrine signaling among neurons, the various organs in endocrine system integrate through hormones secreted into the blood stream. Although the effects of endocrine signaling are usually not as acute as the CNS, they often last longer.

Within the endocrine system, the hypothalamus functions like a control centre as it links the nervous system to the endocrine system through the pituitary gland (hypophysis) and subsequently sends signals to the relevant target organs to initiate the appropriate responses. The hypothalamus exerts its functions mainly by secreting and distributing hormones to the pituitary gland through the hypophyseal portal system (a highly specialized capillary network). Together, the two organs form the hypothalamic-pituitary axis that maintains the normal physiology of a vertebrate by

regulating homeostasis, immune response, and several behavioral changes. Among the major target organs under the control of hypothalamic-pituitary axis are the adrenal cortex and gonads (testis and ovary), which represent two of the major steroid-producing tissues in the endocrine system. In vertebrates, these organs collectively form the hypothalamic-pituitary-steroidogenic (HPS) axis which constitutes a central part of the endocrine system. The HPS axis can be further divided into hypothalamic-pituitary-adrenal (HPA) and hypothalamic-pituitary-gonadal (HPG) axes, as each of them is regulated by different sets of chemical messengers.

1.1.1 The HPS axis of higher vertebrates

The regions of hypothalamus that are involved in the regulation of the HPS axis include the paraventricular nucleus (PVN), post-optic area (POA), and arcuate nuclei, which send neuronal projections to the external zone of the median eminence (ME). The pituitary consists of two portions, which are known as the anterior (adenohypophysis) lobe and the posterior (neurohypophysis) lobe. In mammals, the adenohypophysis can be further subdivided into three regions: the pars distalis, pars intermedia, and pars tuberalis. As for the adenohypophysis, six main specialized cell types are distinguishable by the types of peptide hormones they synthesize. The activities of these cells are regulated by hypophysiotropic factors produced by specific neurons in the hypothalamus. Furthermore, the adenohypophysis receives hormonal signals from the hypothalamus via the hypophysial portal system.

Although the organs along the HPS axis function as an integrative system, the hormones that modulate the HPA and HPG axes are highly specialized. Along the HPA axis, corticotrophin-releasing hormone (CRH) is secreted by the PVN of hypothalamus in response to stress. The CRH is then delivered to the corticotrophs in the anterior lobe of pituitary gland to stimulate the production of POMC peptide.

POMC is eventually processed into adrenocorticotrophic hormone (ACTH) and secreted into the blood circulation, where it will reach ACTH receptors (melanocortin 2 receptors, MC2R) on the surface of adrenocortical cells. The hormone stimulation then triggers a series of signal transductions events that involve the cyclic adenosine monophosphate (cAMP) second messenger system to increase the production of steroids in the adrenal cortex. The synthesis and release of CRH is regulated by cortisol in a classic negative feedback loop mechanism to inhibit further secretion of ACTH in the anterior pituitary and CRH in the hypothalamus (Dallman *et al*., 1987; Kretz *et al*., 1999).

As for the HPG axis, secretion of gonadotropin-releasing hormone (GnRH) from the POA and arcuate nuclei of hypothalamus stimulates the secretion of gonadotropins from the gonadotropes in the pituitary gland. The two principal gonadotropins are luteinizing hormone (LH) and follicle stimulating hormone (FSH). By binding to the G-protein coupled, cAMP-dependent gonadotropin receptors on the target organ cells (primarily ovaries and testes), the gonadotropins elicit multiple responses that regulate reproductive development and function. Generally, LH stimulates the synthesis of androgens (mainly testosterone) in the ovary theca cells and testicular Leydig cells. LH also controls gamete release i.e. ovulation in females and spermiation in males as well as the formation of corpus luteum in females. In males, the effects of testosterone on genital and extragenital tissues are dominant. Not only is it required for the initiation and maintenance of spermatogenesis, it is also essential for the development and proper differentiation of the Wolffian duct. FSH, on the other hand, primarily modulates gamete maturation by controlling follicle development and spermatogenesis (Hillier, 2001; Sairam and Krishnamurthy, 2001).

Although the HPA and HPG axes are stimulated by distinctive signaling pathways and they eventually produce different classes of steroid hormones, there are evidences of interdependence between the two axes. For instance, while the adrenal cortex produce primarily glucocorticoids and mineralocorticoids, they also synthesize small amounts of androgens and they express low level of luteinizing hormone/chorionic gonadotropin receptors (LHCGR), a characteristic of gonad-specific G-protein coupled receptor (Pabon *et al*., 1996; Couzinet *et al*., 2001). Further investigations indicate that the adrenocortical responsiveness to gonadotropins might represent a pathological condition in the presence of elevated gonadotropin levels (Bernichtein *et al*., 2008).

1.1.2 The HPS axis of teleost

Teleosts possess a functional equivalent of the HPS axis though they are generally not as well studied as the mammalian system. Due to the vast adaptive radiation that they have gone through, teleosts display certain degree of variation in the architecture of their HPS axis. A few obvious differences can be found in the tissue organization of the organs that constitute the HPS axis, the hormone-secreting cell types, as well as, the major classes of active steroids. For example, the adrenal equivalent in teleost is known as interrenal and the basic anatomy is very different from that of mammals. This aspect will be discussed further in Section 1.2.

Generally, the teleostean and mammalian hypothalamus and pituitary are composed of essentially the same major components including the hypothalamus, adenohypophysis, and neurohypophysis. However, teleosts lack the pars tuberalis and their pars distalis are subdivided into a rostral and proximal portion (Bentley, 1998). In addition, the median eminence is absent and this is accompanied by the lack of a true hypothalamo-hypophysial portal system. Instead, the adenohypophysis is

extensively innervated by finger-like projections of the preoptic and hypothalamic neurons (Peter *et al*., 1990). As a result, the release of tropic hormones from the hypothalamus is mainly neuroglandular via direct peptidergic or aminergic innervation rather than neurovascular as found in tetrapods and many primitive fishes.

In sharp contrast to the mammalian system, most of the neurosecretory cells of the teleostan hypothalamus are located in the POA and the nucleus lateralis tuberis (NLT). The NLT represents the teleostean homolog of the mammalian arcuate nucleus and is responsible for the secretion of CRH and GnRH as well as a few other hypothalamic hormones including the arginine vasotocin (AVT). A few studies show that there might be two types of CRH-secreting cells: one located in the POA and the other in the NLT (Norris, 2006). There are experimental evidences suggesting that the CRH in the POA is responsible for its secretion while the CRH in the NLT is responsible for its synthesis. Other than these differences, the HPS axis of teleost is regulated largely by the same hormonal pathways as the mammals. The various peptide hormones including the CRH, GnRH, ACTH, LH, and FSH as well as their cognate receptors have been identified in many teleostan species. Nevertheless, the major classes of steroid hormones that are produced eventually in the interrenal and gonads differ slightly from that of mammals and other higher vertebrates.

1.2 The functional anatomy and embryonic morphogenesis of adrenals

1.2.1 The adrenal glands in mammals

Along the HPS axis, the adrenal glands represent one of the most important steroidogenic organs as the adrenal cortex produce two major classes of steroids (glucocorticoids and mineralocorticoids) that are indispensable to sustain life. Indeed, the removal of adrenals leads to fatality within just a few days, primarily due to the derangement in electrolyte balance, cardiac function, and inability to cope with

stressors. In mammals, the adrenal glands are located on top of the kidneys. Each adrenal gland is compartmentalized into two regions that are distinct in histological structure, embryonic origin, and physiological function. The adrenal cortex forms the outer part of adrenal and it is a factory for steroid hormones production. The medulla constitutes the inner part of adrenal and it releases catecholamines (adrenaline and noradrenaline).

The adrenal cortex is derived from the mesoderm germ layer (Hatano *et al*., 1996). An adrenocortical cell can be easily distinguished by the large number of lipid droplets and smooth endoplasmic reticulum as well as the presence of tubulovesicular mitochondria in their cytoplasm. The adrenal cortex is further compartmentalized into three concentric zones, namely *zona glomerulosa*, *zona fasciculata*, and *zona reticularis* from outside to inside. Each layer differs from one another in their characteristic arrangement of cells and major classes of steroid hormones produced. The outermost *zona glomerulosa* secretes primarily mineralocorticoids (mainly aldosterone) in response to increased levels of potassium or decreased blood flow to the kidneys, as part of the renin-angiotensin system. By increasing re-absorption of sodium and water, as well as, excretion of potassium, aldosterone plays a pivotal role in maintaining electrolyte balance. The *zona fasciculata* and *reticularis* produce glucocorticoids (cortisol in humans and corticosterone in mice) and weak androgens (dehydroepiandrosterone, DHEA), respectively, under the stimulation of ACTH. Glucocorticoids exert a broad range of important physiologic effects including the regulation of stress response and carbohydrate metabolism as well as the modulation of the immune functions. Its actions are mediated by intracellular glucocorticoid receptors via alterations of target gene expression (Payne and Adcock, 2001; Yudt and Cidlowski, 2002; Schoneveld *et al*., 2004).

The different classes of steroid hormones are synthesized from cholesterol via a series of biochemical reactions that are catalyzed by a battery of oxidative enzymes located in the mitochondria and endoplasmic reticulum. There are two major classes of steroidogenic enzymes, namely the steroid hydroxylases and hydroxysteroid dehydrogenases. Prior to the enzymatic synthesis, the free cholesterol from the cytoplasm need to be transported into the mitochondria by the steroidogenic acute regulatory protein (StAR). Within the steroidogenesis pathway (Fig. 1.1), the side-chain cleavage enzyme CYP11A1 (also known as P450SCC) catalyzes the first rate-limiting step by converting cholesterol into pregnenolone. Pregnenolone then serves as the immediate precursor for the synthesis of all other steroids. Typically, steroid hormones can be classified into five major classes, namely the glucocorticoids (mainly cortisol but species-dependent), mineralocorticoids (mainly aldosterone), androgens (mainly testosterone), estrogens (estrodiol and estrone), and progestagens (progesterone). The last three classes are collectively termed sexual or gonadal steroids. In humans, monkeys, hamsters, guinea pigs and fish, cortisol is the major glucocorticoid whereas in rodents, rabbits, birds, and snakes, corticosterone is the predominant glucocorticoid.

In contrast to the adrenal cortex, the adrenal medulla is derived from the embryonic neural crest cells, which are of ectoderm origin (Unsicker *et al*., 2005). It is composed mainly of chromaffin cells that produce catecholamine by converting tyrosine into adrenaline and noradrenaline (also called epinephrine and norepinephrine). Although the adrenal medulla and adrenal cortex was thought to be functionally independent, subsequent investigations have established anatomical and functional links between them. For example, medullary catecholamine secretion is under sympathetic control and paracrine control of cortisol. Conversely, the

neuropeptides and catecholamines synthesized by the adrenal medulla influence the steroidogenesis in adrenal cortex (Bornstein and Vaudry, 1998; Ehrhart-Bornstein *et al*., 1998; Ehrhart-Bornstein and Hilbers, 1998; Hinson *et al*., 1994).

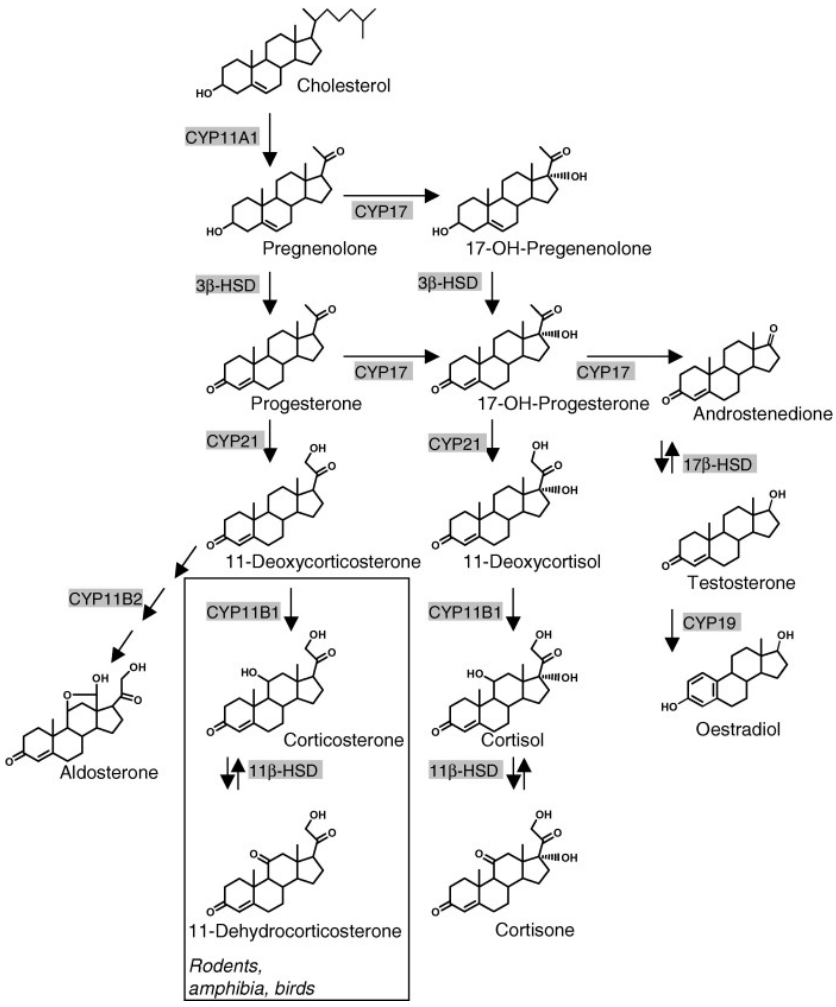

Figure 1.1 Biosynthesis pathways of adrenocortical and sexual steroids from cholesterol in tetrapods. The steroidogenic enzymes catalyzing the corresponding biochemical reaction are indicated with the arrow labels. The dominant glucocorticoid, corticosterone, in rodents, amphibian, and birds is indicated in box (taken from Bury and Sturm, 2007).

The morphogenetic events during the embryonic development of adrenals are well defined in mouse and human (Bland *et al*., 2003; Coulter, 2005; Else and Hammer, 2005; Hammer *et al*., 2005). In mouse, the adrenal cortex and gonads arise from common precursor cells that originate from the coelomic epithelium of the intermediate mesoderm at approximately embryonic day (E) 9.0. At E10.5, the

adrenal cortical precursor cells separate from the gonadal precursors. The neural crest cells then migrate to the growing and encapsulated adrenal cortex from E12.5 to E13.5, and differentiate to form islands of the catecholamine-producing chromaffin cells. In the fetal adrenal cortex of human and mice, there are two distinct layers namely the outer definitive (adult) zone and the inner fetal zone. The adrenal development is complete only after birth where the medullary islands coalesce to form a rudimentary medulla, and the fetal zone degenerates with the proliferation of definitive zone.

1.2.2 The interrenal gland in teleost

The teleostan equivalent of the adrenal cortex is the interrenal. The interrenal is embedded in the head kidney, which is located anterior to the pronephros (kidney). Similar to its mammalian counterpart, it is composed of two major types of cells namely the steroidogenic interrenal cells and the non-steroidogenic chromaffin cells which represent the homologs of mammalian adrenocortical and adrenomedullary cells respectively (Nandi, 1962; Grassi et al., 1997a; Rocha et al., 2001b). The structural organization of adrenocortical tissues and chromaffin tissues has been shown to vary greatly among evolutionarily divergent species (Fig. 1.2). In teleosts, the interrenal gland appears as a highly intermingled structure of steroidogenic and chromaffin cells.

In the early sixties, Nandi (1962) performed detailed examination of the structural organisation and the distribution of interrenal and chromaffin cells of the interrenal gland in 129 teleost species. According to his observations, the interrenal gland consists of structures such as streaks, lumps or cell strands, which are located in proximity to the posterior cardinal veins or their branches. The interrenal gland of

many teleosts has been found to be asymmetrically located at one side of the trunk (Nandi, 1962; Grassi et al., 1997b; Rocha et al., 2001a).

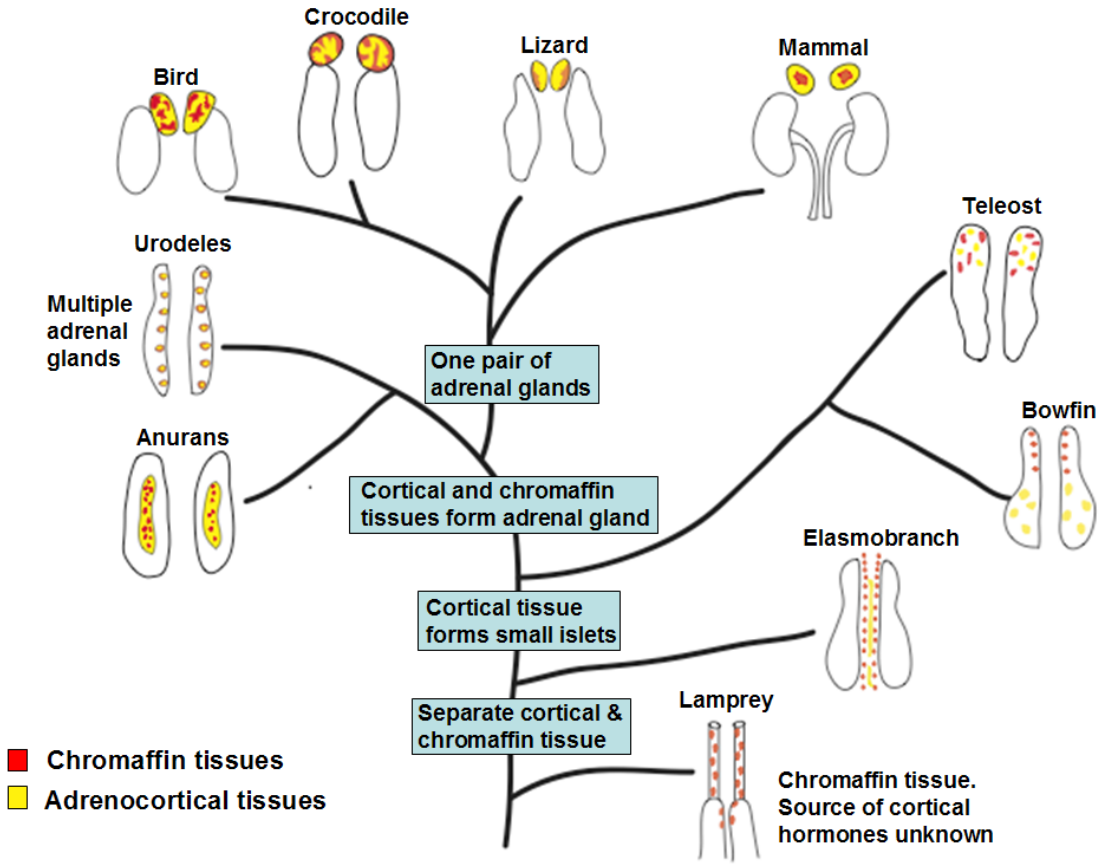

Figure 1.2 Structural organization of chromaffin and adrenocortical tissues in evolutionarily divergent lineages.

In terms of the steroidogenic capability, the interrenal glands of teleosts generally express similar sets of steroidogenic enzymes that catalyze cascade of steroid biosynthesis. One exception is the Cyp11b2 (aldosterone synthase) enzyme that catalyzes the final step for synthesis of aldosterone. Till date, the presence of mineralocorticoids in fishes remains debatable (Jiang *et al*., 1998; Nelson, 2003; Bury and Sturm, 2007; McCormick *et al*., 2008). In comparison to the steroidogenesis pathway in tetrapods, the steroidogenesis pathway in teleosts displays a few distinct features (Fig. 1.3). Firstly, the CYP17 enzyme catalyzes reactions that divert

corticosterone to the synthesis pathway of cortisol. In addition, teleosts lack CYP11B2 and have cortisol as their dominant corticosteroid.

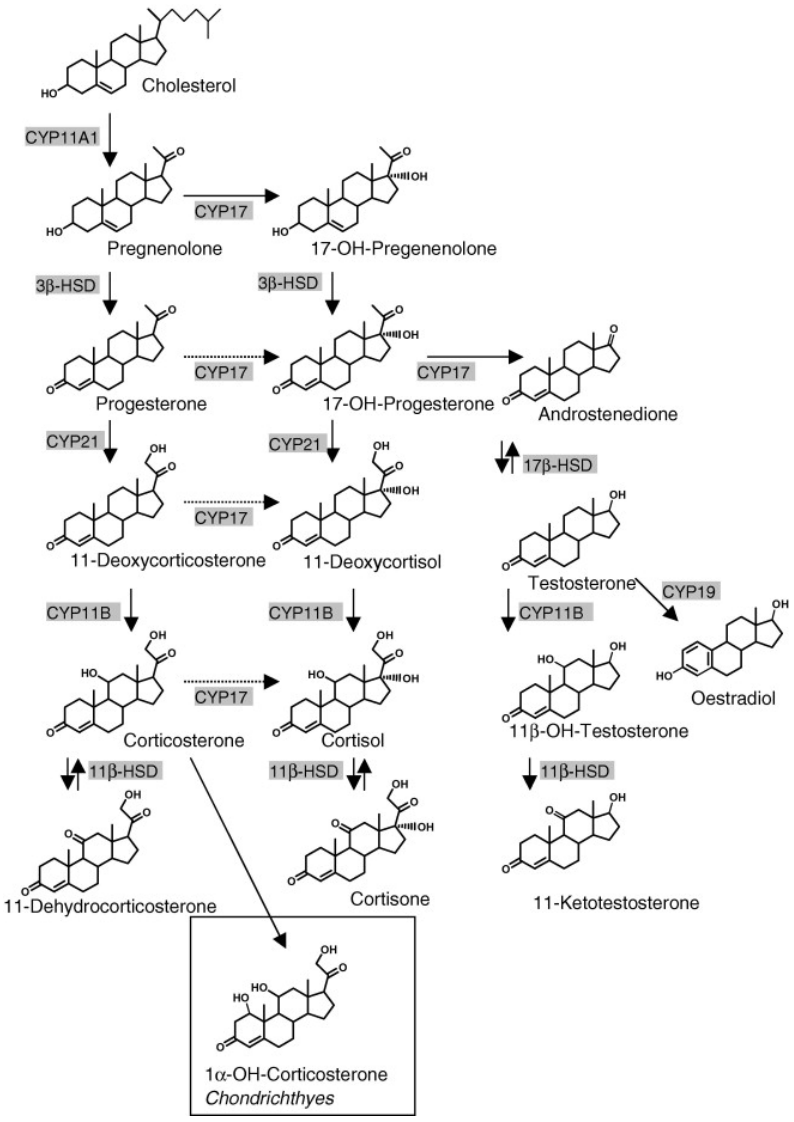

Figure 1.3 Biosynthesis pathways of adrenocortical and sexual steroids from cholesterol in fish. The steroidogenic enzymes catalyzing the corresponding biochemical reaction are indicated with the arrow labels. The dominant glucocorticoid is cortisol in teleost and the bioactive 1α-hydroxycorticosterone in Chondrichtyes (sharks and rays), as indicated in box (taken from Bury and Sturm, 2007).

1.2.3 The interrenal gland in zebrafish

For zebrafish, which is the model organism used in this study, the anatomy and early morphogenesis of interrenal has been recently reported (Hsu et al., 2003f).

Histological examination revealed the head kidney of adult zebrafish as fused bilateral lobes found in the anterior region of the kidney. *In situ* hybridization (ISH) assays using *cyp11a1* demonstrated that the steroidogenic interrenal cells are found in both lobes with the right gland bigger than the left one. Further examination of the interrenal cells with electron microscopy revealed a multiple layered epithelial organization that interposed with two distinct types of chromaffin cells (adrenaline and noradrenaline). Similar to mammalian adrenocortical cells, a large number of mitochondria can be seen in the cytoplasm of interrenal cells in zebrafish. However, the lipid droplets, a characteristic of steroidogenic cells in mammals, are not present in the zebrafish interrenal cells.

The morphogenetic movement of interrenal primordium in zebrafish has also been examined in detail by ISH analyses of *ff1b*, the earliest molecular marker for interrenal primordium (Chai and Chan, 2000b; Hsu et al., 2003b), as well as, that of steroidogenic enzymes such as *cyp11a1* and *3β-hsd*. The interrenal primordia first appeared as small and dispersed bilateral clusters ventral to the third somite at 20-22 hours post fertilization (hpf) (Chai and Chan, 2000a; Hsu et al., 2003g; Liu, 2007). By ~28 hpf, the primordia converged at the midline but further expansion of the interrenal cells placed them unevenly on both sides of the notochord again by 3 days post fertilization (dpf). At 3 dpf, a capsule-like structure of the interrenal gland formed but the epithelial structure and vascularization did not take place even at 5 dpf.

The morphogenetic movement of interrenal primordia has been demonstrated to be closely associated with the pronephric primordia (Hsu et al., 2003d) and also the endothelium cells (Liu and Guo, 2006). In addition, midline signaling has also been implicated in the morphogenetic movement of interrenal primordia, as the convergence of bilateral interrenal cells was shown to be defective in midline

patterning mutant such as *one-eyed pinhead* (*oep*), *squint* (*sqt*), and *floating head* (*flh*) (Chai and Chan, 2000c; Chai et al., 2003f; Hsu et al., 2003a). Besides, the Hedgehog (Hh)/Gli-mediated signaling pathway, which also represents a major signaling from the midline, has just recently been shown to modulate the interrenal morphogenesis in zebrafish by mediating the gene expression of *ff1b* and *wt1* (Bergeron *et al*., 2008).

1.3 Nuclear receptors NR5A: one of the key molecular players in the HPS axis

Nuclear receptors (NRs) are ligand-inducible transcription factors that regulate gene expression by interacting with specific DNA sequences upstream of their target genes and recruiting co-regulator protein complexes that modify chromatin templates and contact the basal transcription machinery. They represent one of the largest families of transcription factors, with 48 members identified in human (Robinson-Rechavi *et al*., 2001). Working in concert with other proteins, they regulate a variety of biological processes, including growth, development, metamorphosis, organogenesis, reproduction, and metabolic pathways (Carson-Jurica et al., 1990; Mangelsdorf et al., 1995; Giguere, 1999c; Smirnov, 2002; Gronemeyer et al., 2004). Many of the NRs play key roles in regulating the proper development and function of the HPS axis, and a good proportion of NRs bind steroids as their cognate ligands.

To date, more than 500 members of the nuclear receptor superfamily have been identified in animals ranging from hydra to human and a systematic classification dividing NRs into seven major groups have been established (Nuclear Receptors Nomenclature Committee, 1999; Germain *et al*., 2006). Considering the physiological importance of NRs, several publicly available online databases, including the Nuclear Receptor Signaling Atlas (NURSA; www.nursa.org) and the Nuclear Receptor database (NURBASE; http://www.ens-lyon.fr/LBMC/laudet/nurebase/nurebase.html)

have been established (Duarte *et al*., 2002; Ruau *et al*., 2004; Margolis *et al*., 2005; Lanz *et al*., 2006).

The NR5 sub-family of NRs, which is commonly known as Fushi-tarazu factor 1 (Ftz-F1), represents one of the most ancestral NR groups with essential functions in both invertebrates and vertebrates (Laudet and Adelmant, 1995; Laudet, 1997; Escriva *et al*., 2004). The *Ftz-F1* gene was initially identified in *Drosophila* as an activator that binds specifically to regulatory sequences of the segmentation gene, *fushi tarazu* (Ueda *et al*., 1990; Lavorgna *et al*., 1991). Members of the NR5 receptors have been reported from more than 40 species of invertebrate and vertebrate. The extensive distribution of FF1s and the highly conserved structure among the family members imply that members of this subfamily have critical function that might be conserved across the various phyla. As a key subject in this study, the *FF1* genes may be classified into two major subgroups namely the NR5A1 (SF-1/Ad4BP) and NR5A2 (LRH/FTF) based on sequence similarity and expression domains.

Members of FF1 sub-family share a typical structural organization with other members of NR superfamily (www.nursa.org). An FF1 receptor is composed of four functionally interacting domains (Fig. 1.4) which include: an Activating function 1 (AF1) domain at the N-terminus, a highly conserved DNA binding domain (DBD) that harbors a DNA-binding motif composed of two zinc fingers, a structurally conserved ligand-binding domain (LBD) and a highly variable hinge domain separating the DBD and the LBD (Giguere, 1999b; Li et al., 2003). The AF1 domain of NR5A members is relatively short as compared to other subfamilies of NRs. The NR5A members are also characterized by the presense of a conserved and unique Ftz-F1 box near the C-terminal region of their DBD (Pick *et al*., 2006). The Ftz-F1 box is known to stabilize the binding of NR5 receptors to their target DNA sequences by

interacting with nucleotides flanking the core recognition element (Wilson et al., 1993a; Li et al., 1999). Furthermore, the N-terminal LBD region in LRH-1 and SF-1, encompasses helices H1 to H3 of LBD, and is highly conserved in FF1 members and shares no sequence similarity with other receptor subfamilies (Giguere, 1999a).

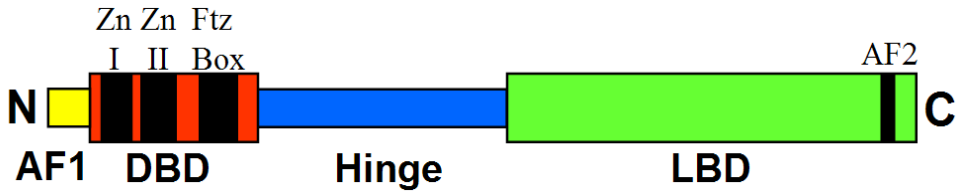

Figure 1.4 Structure/function domains in NR5A nuclear receptors. NR5A sub-family of nuclear receptors share structure/function domains with a typical nuclear receptor, which contains a variable N-terminal region (AF1), a conserved DNA binding domain (DBD), a variable hinge region, and a conserved ligand binding domain (LBD) with a conserved AF1 motif at its C-terminus.

1.3.1 NR5A1 (SF-1/Ad4BP) and NR5A2 (LRH-1/FTF)

NR5A1, which is commonly known as Steroidogenic factor-1 (SF-1), was first identified as a transcription factor with limited tissue distribution and recognized a conserved regulatory motif in the proximal promoter regions of genes encoding the cytochrome P450 steroid hydroxylases in mouse and bovine (Lala *et al*., 1992; Morohashi *et al*., 1992; Honda *et al*., 1993). In human, the *SF-1* gene is located on chromosome 9q33 and the gene product is a nuclear protein of approximately 54 kDa. SF-1 binds to target gene promoters as a monomer and recognizes variations of the DNA sequence PyCAAGGTCA (Rice et al., 1991; Wilson et al., 1993b), which will be referred to as FF1 response element (FRE) throughout the thesis. SF-1 displays high sequence homology to the drosophila Ftz-F1 receptor, which regulates the expression of *fushi tarazu* homeotic gene (Lavorgna *et al*., 1993). In mouse, the *Sf-1* locus also encodes three other transcripts that give rise to embryonic long terminal repeat-binding protein ELP1, ELP2, and ELP3 by alternative promoter usage and

differential splicing. However, subsequent studies demonstrated that SF-1 is the key factor that exerts a regulatory function in the HPS axis (Luo et al., 1995b; Ninomiya et al., 1995b; Kotomura et al., 1997).

Consistent with its role in the transcriptional activation of steroidogenic enzyme genes, *Sf-1* expression is restricted to a subset of endocrine tissues including the gonads, adrenal cortex, ventromedial hypothalamus, and the pituitary gonadotropes (Ikeda et al., 1994; Ingraham et al., 1994a; Morohashi et al., 1994; Ikeda et al., 1995b; Hammer and Ingraham, 1999). Interestingly, *Sf-1* is only weakly expressed in the placenta, although it is the major site of steroid production during pregnancy (Ikeda et al., 1993; Sadovsky et al., 1995c; Ramayya et al., 1997b), and placental development and steroid production was unaffected in *Sf-1* knockout mice (Sadovsky et al., 1995b). It was subsequently demonstrated that regulatory roles of SF-1 in inducing sterodogenic enzyme expression can be carried out by AP2 instead in the palcenta (Ben Zimra *et al*., 2002). In addition to the conventional steroidogenic tissues, *Sf-1* expression has also been detected in the skin (Patel *et al*., 2001) and spleen (Ramayya et al., 1997a; Morohashi et al., 1999a). Nevertheless, the physiological importance of its expression in these tissues has not been closely examined.

The liver receptor homologue 1 (LRH-1; NR5A2) or α-fetoprotein transcription factor (FTF) is the other member of the mammalian FF1 receptors. The expression of LRH-1 is abundant in the liver and intestine where it regulates genes encoding key enzymes in bile acids synthesis such as CYP7A and CYP8B1 (Castillo-Olivares and Gil, 2000b) as well as genes involved in cholesterol transport (Luo et al., 2001a; Schoonjans et al., 2002a). Intriguingly, LRH-1 regulates its target genes by binding to the same DNA response element, the FRE, as SF-1 (Lu *et al*., 2000).

It was conventionally assumed that *SF-1* expression is exclusive to endocrine tissues and *LRH-1* expression is exclusive to endoderm-derived tissues such as liver and intestine until the subsequent discovery of *LRH-1* expression in the ovaries of humans and rodents. The high level of *LRH-1* expression has been shown to be important in regulating the promoter activity of the steroid hydroxylase genes (Falender et al., 2003c; Sirianni et al., 2002b). However, *LRH-1* is expressed to a much lesser extent in the adrenal cortex of human (Wang *et al*., 2001). The high level of *LRH-1* expression in the ovaries implies a functional redundancy to *SF-1*. Nevertheless, in instances where *SF-1* and *LRH-1* are coexpressed, it can be extremely difficult to decipher the specificity of the target genes regulated by these two receptors because both of them bind FRE with equal affinities. For example, while SF-1 was assumed to regulate *CYP19* encoding the aromatase enzyme that converts androgen to estrogen (Fitzpatrick and Richards, 1993), expression patterns of these two receptors during follicular maturation in rat showed LRH-1, and not SF-1, as the major regulator of ovarian aromatase (Liu et al., 2003b).

1.3.2 NR5A subfamily members in zebrafish

In zebrafish, genes that belong to the FF1 family have been cloned and they have been established as orthologues of mammalian *SF-1* and *LRH-1*. To date, four Ff1s have been identified in zebrafish, namely Ff1a (Liu *et al*., 1997), Ff1b (Chai and Chan, 2000f), Ff1c (Xia, 2003), and Ff1d (Kuo et al., 2005g). During early embryonic development, only *ff1a* and *ff1b* are expressed. At 26 hpf, *ff1a* (*nr5a2*) shows a broader tissue expression pattern where its transcripts can be detected in the hypothalamus and trigeminal ganglion in the head region, and in the spinal neurons, somites and endodermal cells in the trunk (von Hofsten et al., 2001a; Kuo et al., 2005f; Sheela et al., 2005). In adult, *ff1a* is expressed in the brain, spinal cord, mandibular

arch and digestive organs. Ff1a is a close homologue of LRH-1 by sequence homology and functional analyses (Lin et al., 2000; Liu et al., 2000; von Hofsten et al., 2001b). On the other hand, *ff1b* (*nr5a1a*) has a more restricted expression profile in the ventromedial hypothalamus (VMH), interrenal gland, and gonads from embryonic development till adult stage (Chai and Chan, 2000d). Furthermore, Ff1b is found to play an essential role in the initiation of the interrenal primordium and its subsequent development and acquisition of steroidogenic capacity (Chai et al., 2003e; Hsu et al., 2004).

In contrast, *ff1c* is expressed only after the completion of embryonic development at 4 dpf and its expression in the adult fishes is ubiquitous, predominantly in the intestine, liver, ovary, muscle, and heart (Xia, 2003; Kuo et al., 2005e). The *ff1d* transcript is present throughout all stages of embryonic development, mainly in anterior and dorsal neural tissues in the head and trunk, including and VMH and pituitary (Kuo et al., 2005d; von Hofsten et al., 2005d). In addition, *ff1d* has been reported to be expressed transiently in the interrenal at ~30 hpf (von Hofsten et al., 2005c). In adult fishes, *ff1d* shows the highest level of expression in testis and with much lower expression in the brain, ovary, muscle, and heart (Kuo et al., 2005c; von Hofsten et al., 2005b). Although functional data of *ff1c* and *ff1d* genes are not available currently, the differential expression patterns of the four *ff1* genes indicate that they may have distinctive functions.

Both the DBD and LBD domains are highly conserved for all four zebrafish *ff1* genes, and they transactivate the basal promoter containing a consensus FRE (Liu et al., 2003d). The study of the four zebrafish *ff1* genes by phylogenetic analysis, genetic mapping, and comparative genomics have defined the evolutionary relationships among the four isoforms, as well as to tetrapod FF1s (Kuo et al., 2005b). Notably, the

orthology of *ff1a* to *NR5A2* is very apparent with data from phylogenetic analyses, chromosomal mapping and expression patterns. These findings suggest that the zebrafish *ff1a* and human *NR5A2* are derived from a single gene in their last common ancestor.

In contrast with *ff1a*, the evolutionary relationship of zebrafish *ff1b* and *ff1d* to tetrapod *NR5A1* and *NR5A2* are less clear in phylogenetic analysis. Nevertheless, the relationship of the two genes as gene duplicates are apparent, in that they are sisters in a phylogeny tree and they are localized on paralogous chromosomes compared with the genome of a related species that did not undergo whole-genome duplication (Amores et al., 1998b; Postlethwait et al., 1998; Taylor et al., 2003; Jaillon et al., 2004; Naruse et al., 2004). The tight association of *ff1b* and *ff1d* genes to an *NR6A1* co-orthologue as in humans indicates that the tandem duplication occurred before the divergence of human and zebrafish lineages.

The zebrafish *ff1c* is grouped into the third set of *ff1* genes, which include only teleostan representatives from pufferfish (Kuo et al., 2005a). The *ff1c* genes may thus come from genome-amplification events that occurred before the tetrapod/teleost divergence but was subsequently lost in the tetrapod lineage. This phenomenon where an ancient paralogue is retained in the fish lineage but was lost in the human lineage has been reported previously (Amores et al., 1998a). Genetic mapping has also revealed the conserved syntenies of the four *ff1* genes with *notch* paralogues in comparison to human NR5A paralogues. These chromosome segments conserved between the zebrafish and human genomes indicate a common ancestral origin. Most likely, the two NR5A groups arose before the divergence of mammalian and teleost lineages through a genome-amplification event.

1.4 NR5A1: the main player in development and function of HPS axis

Since its discovery in 1992, SF-1 (NR5A1) has emerged as a NR that is pivotal for the proper development and function of steroidogenic tissues. Consistent with this role, *SF-1* is expressed in all organs along the HPS axis and it modulates the development and maintenance of these organs at multiple levels along the HPS axis. In embryonic stem (ES) cells, stable expression of *SF-1* is sufficient to alter cell morphology, permit cAMP and retinoic acid-induced expression of the endogenous *CYP11A1* gene, and consequently promote steroidogenesis (Crawford *et al*., 1997b). This indicates that SF-1 is the master regulator in the specification and determination of steroidegenic lineage. Great insights into the endogenous function of SF-1 in embryonic development have been gained from SF-1 knockout (KO) mice studies. A few attempts of tissue-specific KO studies reported recently have provided important clues to SF-1 function in the VMH, pituitary, and gonads. On top of that, its functions in sex determination pathway and the maintenance of adrenal functions have long been established after nearly one and half decade of extensive research.

1.4.1 SF-1 in embryonic development: insights from knockout mice

Targeted disruption of *Sf-1* in mice was reported by three independent groups of researchers and they revealed the critical role of SF-1 in adrenal and gonadal development (Luo et al., 1994a; Sadovsky et al., 1995a; Shinoda et al., 1995d). The *SF-1* knockout (KO) mice exhibited adrenal and gonadal agenesis, male-to-female sex reversal of the internal and external genitalia regardless of genetic sex, impaired gonadotrope function, and ablation of VMH. In a separate study, the spleen of SF-1 KO mice was shown to be smaller with obvious defects in the splancnic vascularization and erythropoiesis (Morohashi et al., 1999b) although the precise function of SF-1 in the spleen has remained undefined till date.

The SF-1 KO pups completely lack adrenals and die shortly after birth presumably due to the lack of corticosteroids, as the mice can be maintained by administration of exogenous corticosteroids (Luo et al., 1995a). This observation implies the critical role of SF-1 not only in adrenal development but also in the biosynthesis of steroid hormones. It is important to note that the mesenchymal, adrenocortical, and gonadal precursor cells in these KO mice form at the correct time and place but undergo programmed cell death thereafter, indicating that SF-1 is not required for the initial specification of adrenogonadal primordia but is essential for their subsequent maintenance and differentiation. The complete lack of gonads and sex reversal phenomenon following the loss of SF-1 clearly indicate that it is involved not only in the organogenesis of gonads but also in the sex determination pathway. The molecular mechanisms underlying the complete regression of the adrenal and gonadal primordia remain largely unknown until now.

Contrary to the complete agenesis of adrenals and gonads, some of the dorsomedial region of VMH neurons persisted in SF-1 KO pups although they display severe defects. For instance, the VMH of SF-1 KO mice did not form discrete nucleus and further immuno-reactivity assays have revealed the markedly altered organization of the major cell types of VMH (Ikeda et al., 1995a; Shinoda et al., 1995c). Although the characteristic structures of VMH are present at E17, they progressively regress thereafter. A closer examination of these KO mice showed that the normal exclusion of GABA from the developing VMH did not take place (Dellovade et al., 2000a). Moreover, cells expressing neuropeptide Y, estrogen receptor α, and galanin displayed altered cell distribution, and so as the Islet-1- and Nkx2.1-expressing cells (Dellovade et al., 2000b; Davis et al., 2004b).

As the expression of SF-1 is restricted to only a sub-domain (gonadotrope) of pituitary, the pituitary gland develops normally. In the absence of SF-1, gonadotropes were formed but functionally impaired and they failed to express LHβ, FSHβ, and GnRH-R (Ingraham et al., 1994b; Shinoda et al., 1995b). Although SF-1 is not the sole determinant in the embryonic development of VMH and pituitary, it is important in shaping their normal architecture and function.

Although the global gene disruption of SF-1 has unraveled its crucial roles in embryonic development, the early postnatal death of KO pups has hindered further characterization of SF-1 functions. To partially solve this problem, *SF-1+/-* heterozygous KO has been generated. The mice display adrenal and gonadal hypoplasia but no major defect in the VMH and pituitary (Bland *et al*., 2000). As a result, the mice are unable to respond properly to stress stimulant, as measured by the levels of corticosteroid produced when they are subjected to inflammatory stress, food deprivation, and immobilization. The haploinsufficiency of SF-1 also revealed the dosage-sensitive effect of SF-1 action.

1.4.2 Tissue-specific knockouts of SF-1

With the advances in DNA engineering particularly the establishment of the Cre-loxP recombination system (Sauer and Henderson, 1988; Sauer and Henderson, 1989; Orban *et al*., 1992), tissue-specific knockouts of SF-1 are made possible. Using a transgene containing the Cre recombinase driven by the gonadotrope-specific promoter of αGSU gene, a loxP-modified SF-1 locus was selectively disrupted in the gonadotrope cells in pituitary (Zhao *et al*., 2001a; Zhao *et al*., 2001b). The resultant mice never mature sexually, and the testes and ovaries displayed severe hypoplasia although the VMH and adrenals appeared to be largely intact. The markedly decrease level of LH and FSH indicate that the absence of gonadotropins in global SF-1 KO

mice is of pituitary origin and not the secondary effect resulted from defect in GnRH production of VMH.

Using a similar strategy, SF-1 was selectively inactivated in the Leydig cells and granulosa cells with the allele of the anti-Müllerian hormone type 2 receptor knocked-in by a Cre-mediated strategy (Jeyasuria *et al*., 2004). In these mice, the adrenals develop and function normally, albeit at smaller size. In contrast, histological abnormalities were obvious in the testes from prenatal stages and spermatogenesis was impaired. Although female mice produced ovaries that were indistinguishable to the wild-type during embryogenesis and at birth, adult females were sterile, characterized by the absence of corpora lutea and the presence of hemorrhagic cysts in reminiscent of estrogen receptor alpha and aromatase KO mice.

The ablation of SF-1 specifically in the central nervous system (CNS) using a nestin-Cre/loxP recombination strategy has also been reported (Davis et al., 2004a; Kim et al., 2008; Zhao et al., 2008). In these mice, SF-1 expression was largely unaffected in the anterior pituitary, adrenals, and gonads; and the structural defects in VMH were largely similar to that of global SF-1 KO. Interestingly, these mice showed increased anxiety-like behavior, unravelling a regulatory role of SF-1 in a complex behavioral phenotype. In addition, novel target genes [Brain-derived neurotrophic factor (BDNF), corticotropin-releasing hormone receptor 2 (Crhr2), urocortin 3 (Ucn3), and cannabinoid-1 receptor (CB1R)] of SF-1 that potentially play a role in anxiety behaviour and energy homeostasis have been identified.

1.4.3 SF-1 in sex determination

In eutherian mammals, the basic principle underlying sex determination is the chromosomal genetic sex, which is determined at the time of fertilization by the presence or absence of the Y chromosome. This genetic determinant, however, needs

to be executed through the highly coordinated gene regulatory network along the HPG axis. SF-1 appears to be involved at all three levels of these events. *SF-1* is expressed in the VMH nucleus (Shinoda et al., 1995a) where it is regulated by GnRH (Haisenleder *et al*., 1996). In pituitary gonadotrope, SF-1 has been shown to regulate the gene expression of nitric oxide synthase, which mediates the gonadotropin release and sexual behaviour (Wei et al., 2002a). In the bipotential gonad, SF-1 expression was maintained together with the activation of a Y chromosome-located gene, *SRY*, along the testis determination and differentiation pathway but its expression was repressed by the dosage-sensitive sex reversal-adrenal hypoplasia congenita critical region on the X chromosome (DAX-1) just after the onset of ovarian differentiation (Tremblay and Viger, 2001b). The expression of SF-1 was restored in females at a later stage of embryogenesis. Besides DAX-1, SF-1 (in concert with SOX9, GATA-4 and WT1), was also able to stimulate MIS promoter activity in male gonadogenesis (De Santa et al., 1998c; Nachtigal et al., 1998a; Tremblay and Viger, 1999a; De Santa et al., 2000).

1.4.4 Ff1b as the earliest molecular marker and master regulator of interrenal development in zebrafish

Among the four *ff1* genes in zebrafish, *ff1b* shows the strongest homology to mammalian SF-1 in terms of protein sequence, expression pattern, and functional properties. Ff1b is the earliest known molecular marker for the zebrafish interrenal gland and it is also expressed in the VMH from early developmental stage (Chai and Chan, 2000e). Double *in situ* hybridization for *ff1b* and the steroidogenic markers, *cyp11a* and *3β-hsd*, showed that the expression of *ff1b* preceded the onset of steroidogenic identity by nearly 2 hr during the ontogeny of the interrenal (Chai et al., 2003d). Furthermore, *ff1b* and *wt1* seem to be co-expressed in the interrenal

primordium in a restricted time frame (Hsu et al., 2003h), and *wt1* may also participate in the interrenal development mediated by Ff1b (Hsu et al., 2003e).

Importantly, the disruption of *ff1b* gene function *in vivo* by antisense morpholino (MO) knockdown resulted in late larval morphological phenotype that suggests an impaired interrenal function (Chai et al., 2003c). The resultant morphants could be subdivided into four classes A to D according to the severity of phenotype (Fig. 1.5). When the *ff1b* gene function was knocked down by MO, the expression of *cyp11a1* and the enzymatic activity of 3β-Hsd were markedly reduced. A recent study that reported the isolation of DAX-1 in zebrafish has also demonstrated that *ff1b* knockdown abolished the expression of DAX-1 and that DAX-1 probably functions downstream of Ff1b in a regulatory cascade governing the proper development and function of interrenal gland (Zhao et al., 2006b). This observation implicates a direct involvement of *ff1b* in zebrafish interrenal development, which is highly reminiscent to the results obtained in mouse SF-1 knockout studies. This similarity observed between the two systems suggests a conserved regulatory program for adrenocortical development in evolutionarily divergent species.

1.4.5 Zebrafish Ff1s in sex determination

In contrast to mammals, the sex determination in zebrafish is a delicate process, which in many cases can be influenced by environmental factors. The mechanisms underlying zebrafish sex determination and differentiation are largely uncharacterized. By far, neither sex linked genes nor sex chromosomes have been identified in zebrafish. A number of genes have been linked to the process of sex determination or differentiation in zebrafish based on their orthology to mammalian counterparts and Ff1s are certainly one of them (von Hofsten and Olsson, 2005). Particularly, *ff1d* has been shown to be co-expressed with the anti-Mullerian hormone (amh) gene in the

ovary and testis, and it has been proposed as a promising candidate in regulating sex determination pathway in zebrafish (von Hofsten et al., 2005a).

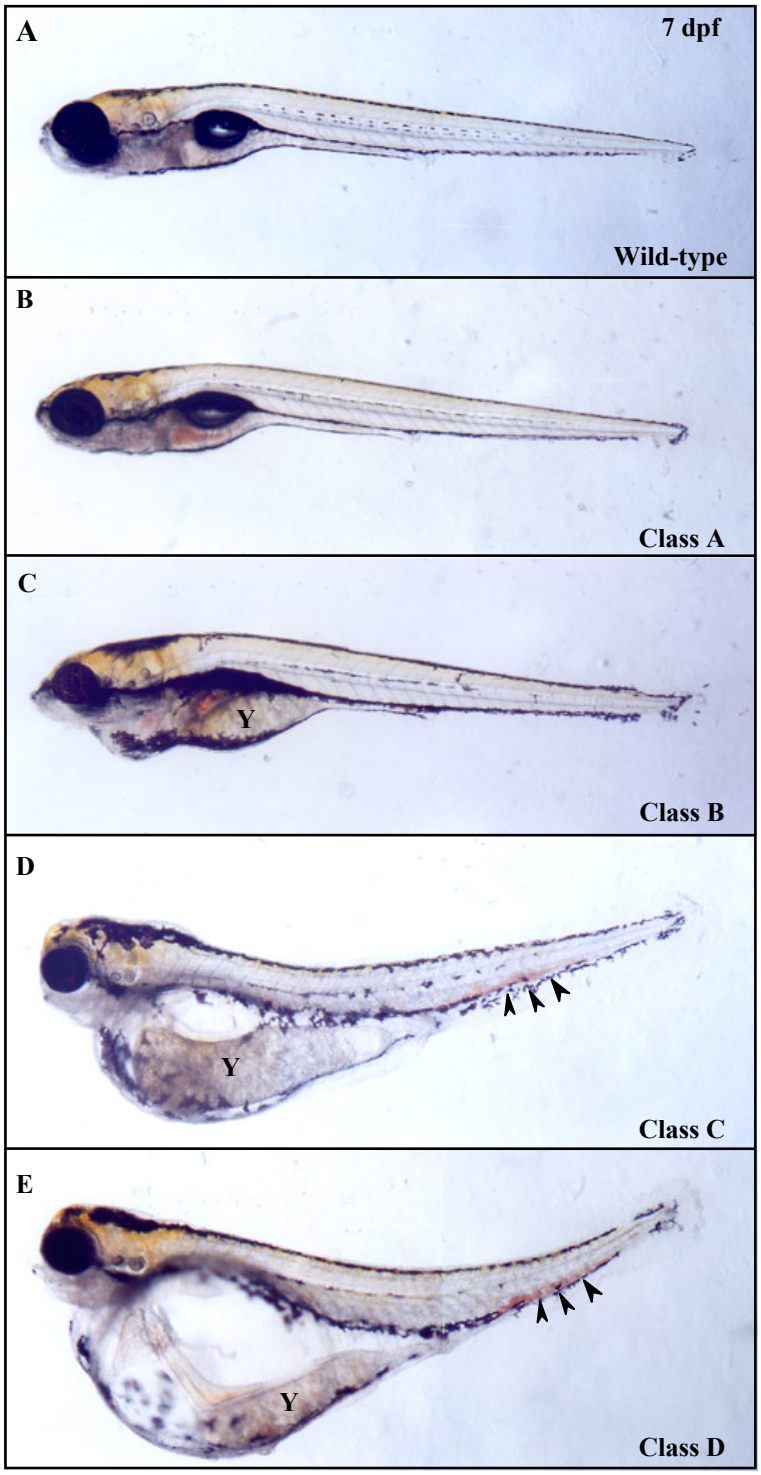

Figure 1.5 Morphological phenotypes of 7 dpf larvae microinjected with 11.25 µM ff1bMO per embryo (from Chai at el., 2003). (A) Wild-type, (B) Class A, (C) Class B, (D) Class C, and (E) Class D morphants. Classification was based on the severity of morphant phenotypes, mainly on the severity of subcutaneous edema. Arrowheads in (D) and (E) indicate blood island formation.

In line with the observations from mammals, gene dosage effects may be an influential factor involved in zebrafish sex determination. Based on their homology to mammalian orthologs and the expression profiles in the gonads, allelic variants and dosage effects of autosomal genes, the *ff1* genes, *sox9*, *wt1*, *amh*, *dmrt1* and *gata4* have been proposed to be involved in determining sex and directing gonad development in zebrafish (von Hofsten and Olsson, 2005). The recent isolation of DAX-1 homolog in zebrafish opens up the possibility of its involvement in the sex determination pathway (Zhao et al., 2006a). Nevertheless, the molecular interactions among the above factors remain to be characterized.

1.5 Transcriptional Regulation of SF-1

The highly selective expression of SF-1 along the HPS axis indicates its tight transcriptional regulation. However, the molecular mechanism underlying the tissue-specific expression of SF-1 is still not well understood. The first decade of research merely identified a number of *cis*-elements at the 5' flanking promoter region of SF-1 that modulate its basal transcription in transient transfection assays. Only in the last five years, the rapid advances in DNA engineering accelerated the study of regulatory elements that are responsible for the tissue-selective expression of SF-1. These studies made use of large DNA inserts, contained within yeast artificial chromosome (YAC) or bacterial artificial chromosome (BAC), spanning the entire genomic locus of SF-1 in combination with *in vivo* transgenic mice studies. The identification of several tissue-specific enhancers within the mouse *Sf-1* locus highlights the high level of complexity in SF-1 transcriptional regulation. Despite the successful identification of putative *cis*-elements and the accompanying *trans*-acting factors that could account for the tissue-specific expression of SF-1, the definition of the upstream regulators

that restrict adult expression, and signaling pathways that control SF-1 expression in the HPS axis during embryonic development are still lacking.

1.5.1 *Cis*-elements at the 5' proximal promoter

The mapping of regulatory elements governing SF-1 expression was possible once the genomic sequences were made available (Ninomiya et al., 1995a; Wong et al., 1996), and it began with the study of its 5' flanking promoter. Transient transfection studies using cell lines have identified a number of *cis*-elements that are required for *SF-1* expression. Notably, a 90 bp 5' promoter fragment spanning an E-box, a Sp1 (Splicing factor 1) site, and a CAT box is capable of activating reporter gene in testis and adrenocortical cells (Scherrer et al., 2002; Woodson et al., 1997b). The E-box that binds the ubiquitous USF factor has been shown to be essential for the transcriptional activation of SF-1 promoter in several heterologous cell lines (Nomura et al., 1995; Woodson et al., 1997a; Harris and Mellon, 1998b; Oba et al., 2000a). In addition, SOX9, a tissue-specific transcription factor, has also been implicated in inducing the expression of SF-1 in Sertoli and Y1 cells (Shen and Ingraham, 2002), while GATA-4 has been shown to moderately activate SF-1 expression in Sertoli cells (Tremblay and Viger, 2001a).

Despite the seemingly successful identification of putative *cis*-elements in the 5' promoter of SF-1 using *in vitro* transient transfection studies, subsequent *in vivo* transgenic mouse studies revealed that tissue-specific expression of SF-1 cannot be established with these genomic information (Stallings et al., 2002b; Wilhelm and Englert, 2002c; Zubair et al., 2002). For instance, while a 674-bp 5' promoter of mouse SF-1 could restrict lacZ expression to the gonads, the regulatory elements required to fully recapitulate the endogenous expression of SF-1 are missing (Wilhelm and Englert, 2002b). Furthermore, a 50 kb 5' flanking region of mouse SF-1 from a

BAC plasmid could direct the expression of EGFP reporter gene to most SF-1-expressing tissues but not the pituitary (Stallings et al., 2002a). By far, the most successful transgenic mouse study has come from an effort that utilized genomic locus of rat *Sf-1* gene spanning 153 kb, as the resultant transgene fully recapitulates the endogenous expression of *Sf-1* in mouse and the transgene was able to rescue SF-1 KO mice (Karpova et al., 2005c).

DNase I hypersensitivity mapping has also identified several potential regulatory regions within the *Sf-1* locus. One such domain surrounds the FRE in Intron I where the chromatin adopts an open structure in Y1 and adrenal cells, but is closed in liver, 3T3, and ECA2 cells (Ninomiya et al., 1996b; Nomura et al., 1996b). The second region is located 3' to Exon 7 of SF-1. Interestingly, a recent study identified three DNase I hypersensitive sites within the intergenic region between the mouse *Sf-1* gene and its upstream neighbor, germ cell nuclear factor (*Gcnf*) (Ishihara and Morohashi, 2005). Further dissection showed that one of the sites binds an insulator protein, CTCF, while the others are likely to be associated with nuclear matrix. These hypersensitive sites that are associated with CTCF and nuclear matrix were suggested to define an insulating boundary of histone acetylation between the two genes, and contribute to their distinct expression patterns in different tissues.

1.5.2 Auto-regulation of SF-1 gene expression

SF-1 has been proposed to autoregulate its own expression in rat and human through the FRE located in the first intron (Nomura et al., 1996d; Oba et al., 2000c). In transient transfection studies, mutation of this FRE decreased reporter gene activity in Y1 adrenocortical cells and the FRE was responsive to SF-1 overexpression in CV-1 cells (Nomura et al., 1996c). Furthermore, open chromatin structure surrounding the FRE has been revealed by DNase I hypersensitivity mapping (Ninomiya et al., 1996a;

Nomura et al., 1996a). Nonetheless, other investigations indicate that the FRE does not enhance transcription of SF-1 and the autoregulation of SF-1 might be species-dependent (Harris and Mellon, 1998a; Oba et al., 2000b). A more recent study has identified two highly conserved FREs within a fetal adrenal enhancer (FAdE) located in intron IV of mouse and human SF-1 gene (Zubair et al., 2006e). The two FREs were established to be essential to maintain an autoregulatory loop that is necessary for the maintenance of SF-1 expression in the fetal adrenal.

1.5.3 KO mice with downregulated SF-1 expression

Gene KO studies have been helpful in the identification of potential upstream regulator of SF-1 transcription on the basis that the loss of these genes is accompanied by downregulation or disappearance of *Sf-1* expression. One such example is the Wilm's tumor 1 (WT1) KO mice where SF-1 expression failed to initiate at all in the gonads (Wilhelm and Englert, 2002a). Similarly, the LIM homeobox protein Lhx-9 has been proposed to regulate *Sf-1* expression as Lhx-9 KO mice did not develop gonads and had markedly reduced *Sf-1* expression in their urogenital ridges (Birk *et al*., 2000). Besides WT1 and Lhx-9, the pre-B-cell transcription factor 1 (Pbx1) has also been implicated in the regulation of *Sf-1* expression due to the differentiation defects in adrenal and urogenital that are associated with minimal *Sf-1* expression in $Pbx^{-/-}$ mice (Schnabel *et al*., 2003). The Pbx1-dependent regulation of SF-1 expression in the mouse fetal adrenal has indeed been demonstrated recently (Zubair et al., 2006d).

1.5.4 Localization of tissue-specific regulatory DNA elements in intronic regions

A DNA fragment containing 153 kb of genomic sequences spanning the rat SF-1 locus has successfully recapitulated the endogenous expression of *Sf-1* in

transgenic mouse and the same region has been shown to rescue SF-1 KO mice (Karpova *et al*., 2005a; Karpova *et al*., 2005b). Using computational analysis based on evolutionarily conserved regions and observations from transgenic mouse studies, they have predicted potential regulatory elements for *Sf-1* expressing tissues.

Following this report, another laboratory has reported four additional transgenic mouse studies using long genomic regions spanning *Sf-1* locus to locate tissue-specific enhancers of SF-1 and all all them have delivered exciting findings (Shima et al., 2005c; Zubair et al., 2006c; Shima et al., 2008a; Zubair et al., 2008). By determining the lacZ reporter expression driven by overlapping genomic fragments spanning the mouse *Sf-1* locus in transgenic mice, Shima *et al*. (2005) successfully mapped a VMH-specific enhancer (VMHE) to Intron VI. A highly conserved equivalent of VMHE was also found in the human *SF-1* gene. By further deletion, a 503-bp core enhancer element has been identified (Shima et al., 2005b).

Using the same experimental approach as outlined in Shima *et al*. (2005), Zubair *et al*. (2006) successfully localized the fetal adrenal enhancer (FAdE) to Intron IV of mouse and human SF-1 gene. The 648-bp core FAdE was able to induce *lac*Z expression in the fetal adrenal gland with the *hsp68* basal promoter but the expression disappeared along with the regression of fetal adrenals. In the same study, a two-step regulation of SF-1 gene activation in the fetal adrenal has been proposed. The initial step involves the initiation of SF-1 transcription in the fetal adrenal by a Hox-Pbx-Prep1 complex and the continued expression of SF-1 is then maintained via an autoregulatory loop (Zubair et al., 2006b). Subsequently, the FAdE has been successfully used in lineage tracing of fetal adrenal cells during different stages of embryonic development (Ref, Zubair 2008). By monitoring transgene expression in

transgenic mouse, a direct link between the fetal zone and adult zone of adrenal cortex has been established.

An intronic enhancer for pituitary-specific expression of SF-1 has been recently localized to Intron VI of mouse *Sf-1* gene (Shima et al., 2008b). This enhancer functionally recapitulated the endogenous expression of SF-1 in the fetal Rathke's pouch right up to the adult pituitary gonadotrope. Similar to the FAdE and VMHE, the pituitary-specific enhancer consists of several elements conserved among animal species and mutational analyses confirmed the significance of these elements for the enhancer function. One of these elements was able to interact with pituitary homeobox 2 (Pitx2) *in vitro* and *in vivo*, indicating that Pitx2 regulates SF-1 gene transcription in the pituitary gonadotrope by interacting with the gonadotrope-specific enhancer.

1.6 Target genes of SF-1

SF-1 binds the extended consensus site of GTCAAGGTCA as a monomer. In all binding sites studied so far, the guanines are absolutely required and the two alanines preceding them are very highly conserved. For the remaining nucleotides, variations from the consensus are normally negligible (Busygina *et al*., 2005). As expected, SF-1 target genes can be found in all *SF-1*-expressing tissues. Generally, SF-1 target genes can be separated into those expressed in steroidogenic cells and non-steroidogenic cells [see Val *et al*. (2003) for an extensive review of SF-1 target genes]. Several studies have also highlighted the possible role of SF-1 in regulating a set of target genes that are actively involved in the signaling pathways modulating cell proliferation and/or apoptosis.

1.6.1 Steroidogenic targets of SF-1

The steroidogenic target genes of SF-1 encompass those that are transcriptionally modulated by SF-1 in the adrenals and gonads. Since its isolation in 1992, genes encoding steroidogenic enzymes represent the most dominant and well studied set of SF-1 target genes. Indeed, SF-1 has been shown to participate in the transcriptional regulation of all steroidogenic enzymes in the adrenal cortex and gonads with the exception of CYP11B2 (Bassett *et al*., 2002). In any case, SF-1 is required to activate the basal transcription of the target promoter and it seems to participate in the cAMP responsiveness of some of those target genes. The location of FREs in these promoter often overlap with that of the cAMP response elements (CREs) although SF-1 might not participate in cAMP responsiveness of all steroidogenic enzyme genes. Among the steroidogenic enzymes, CYP11A1 represents the most well characterized member in terms of SF-1 regulation as it catalyzes the first rate-limiting biochemical step in the steroidogenesis pathway. Two FREs mapped in the human CYP11A1 promoter have been implicated in both the basal transcription and hormone sensitivity of CYP11A1 gene (Hu et al., 2001; Guo et al., 2007c). In addition, SF-1 has been shown to regulate the cAMP-dependent transcription of CYP11A1 promoter in cooperation with AP-1 (Guo et al., 2007b; Lan et al., 2007).

Besides steroidogenic enzymes, SF-1 also controls the expression of genes encoding proteins that are involved in cholesterol transport and synthesis. These include the sterol carrier protein 2, SCP2 (Pfeifer *et al*., 1993); the sterol acute regulatory protein, StAR (Stocco, 2000); and the HMG-CoA synthase (Mascaro *et al*., 2000). Notably, a new class of genes encoding proteins that protect the steroidogenic cells against toxic by-products of steroidogenesis is emerging and SF-1 has also been implicated in their gene expression. These include the aldose reductase akr1-b7

(Aigueperse *et al*., 2001; Martinez *et al*., 2002; Val *et al*., 2002; Martinez *et al*., 2003) and the superoxide-dismutase 2 SOD2 (Chinn *et al*., 2002). The last subset of SF-1 target genes related to steroidogenesis are those encode for receptors of ACTH (Marchal et al., 1998; Naville et al., 1998; Naville et al., 1999; Winnay and Hammer, 2006; Lichtenauer et al., 2007a) and FSH (Heckert, 2001; Levallet *et al*., 2001), which regulate the hormone stimulated steroidogenesis of adrenals and gonads.

The other subset of SF-1 target genes covers those that are mostly expressed specifically in the gonads, and are involved in proper reproductive function and sexual determination and differentiation. They include DAX-1 (Burris *et al*., 1995; Kawabe *et al*., 1999), Mullerian inhibiting substance receptor (De Santa et al., 1998d), anti-Mullerian hormone gene (MIS) (De Santa et al., 1998b), small heterodimer partner (SHP) (Lee *et al*., 1999), scavenger receptor, class B, type 1 (SRB1) (Cao *et al*., 1997), insulin like 3 (Koskimies et al., 2002a), prolactin receptor (Hu *et al*., 1997), α-inhibin (Ito et al., 2000; Gummow et al., 2003b) and sex determining region Y (SRY) (De Santa et al., 2001b).

1.6.2 Non-steroidogenic targets of SF-1

The non-steroidogenic target genes of SF-1 mainly reside in the hypothalamus and pituitary. In SF-1 KO mice, the GnRH receptor and gonadotropins were not detected and SF-1 has been subsequently shown to regulate the gene promoter of GnRH receptor (Duval *et al*., 1997; Ngan *et al*., 1999; Pincas *et al*., 2001), αGSU (a common subunit of LH and FSH) (Fowkes *et al*., 2003), LHβ (Halvorson *et al*., 1996; Halvorson *et al*., 1998), as well as FSHβ (Jacobs et al., 2003b). In addition, SF-1 has also been demonstrated to regulate several hypothalamic genes that play important roles in the CNS. They include the N-methyl D-aspartate (NMDA) receptor, a non-specific cation channel that directly contributes to excitatory synaptic transmission

(Pieri *et al*., 1999); the neuronal nitric oxide (NO) synthase that modulates the secretion of GnRH (Wei et al., 2002b); and oxytocin that acts as a neurotransmitter and involved in female reproduction (Wehrenberg *et al*., 1994).

1.6.3 Beyond reproductive function and steroidogenesis: SF-1 in cell proliferation and apoptosis?

Several observations have highlighted that target genes activated by SF-1 should extend beyond the broad classes that have been discussed. For instance, the presence of adrenal and gonadal anlage and their subsequent regression by apoptosis in SF-1 KO mice clearly indicate a role of SF-1 in cell proliferation or apoptosis (Luo et al., 1994b). SF-1 has also been demonstrated to modulate the proliferation rate of rat ovarian surface epithelial cells (Nash *et al*., 1998). A recent study demonstrated that increased dosage of SF-1 triggered cell proliferation and cancer development of adrenocortical cells (Doghman *et al*., 2007). Importantly, the transcriptional regulating protein of 132 kDa (TreP-132), which is expressed in steroidogenic tissues and known to acts as a coregulator of SF-1 (Gizard et al., 2002b), has been demonstrated to control cell proliferation by regulating the expression of cyclin-dependent kinase inhibitors p21WAF1/Cip1 and p27Kip1 (Gizard *et al*., 2005).

1.7 LRH-1: diverse functions in development, metabolism, and steroidogenesis

The expression domain of LRH-1 (NR5A2) is slightly broader than that of SF-1. LRH-1 is expressed since early developmental stage and it is absolutely required for proper endoderm development. It is dominantly expressed in endoderm-derived tissues including liver, intestine, and exocrine pancreas. Its transcripts can also been detected in the ovary, adrenal, and testis but the expression seems to be species-dependent. The molecular mechanisms by which LRH-1 regulates the cholesterol and bile acid homeostatic pathways are well characterized while its function in ovarian

steroidogenesis is emerging just recently [for review, see (Fayard et al., 2004b; Lee and Moore, 2008)].

1.7.1 LRH-1 in endoderm development

Lrh-1 is abundantly expressed in mouse embryonic stem cells (Gu et al., 2005c; Gao et al., 2006) and its expression can be detected as early as preimplantation stage (Pare et al., 2001a; Pare et al., 2004a; Gu et al., 2005b). Homozygous disruption of *Lrh-1* gene in mice is embryonic lethal and the developing embryos do not survive beyond E7.0, the gastrulation stage (Pare et al., 2004b; Gu et al., 2005a; Labelle-Dumais et al., 2006b). In LRH-1 KO mice, the primitive streak morphogenesis and mesoderm formation are severely impaired although the anterior-posterior specification is unaffected (Labelle-Dumais et al., 2006a). LRH-1 is actively involved in the transcriptional cascade governing the proper endoderm differentiation and hepatic determination. Its expression is tightly regulated by early endodermal markers including GATA4, GATA6, and HNF4, as well as by other developmental transcription factors from the basic helix-loop-helix, homeodomain, and NR families (Pare et al., 2001b; Annicotte et al., 2003a). On the other hand, LRH-1 has been shown to regulate the expression of a number of liver-specific genes including Forkhead box a2 (*Foxa2)*, hepatocyte nuclear factor 1α *(HNF1α)*, *HNF3β*, and *HNF4* (Rausa et al., 1999; Pare et al., 2001c). Furthermore, it has been implicated as a downstream target of pancreatic and duodenal homeobox 1 (Pdx1), which is a homeobox factor that is essential for pancreatic development (Annicotte et al., 2003b). These findings collectively indicate that LRH-1 is acting downstream of transcription factors that are important for early endoderm specification but upstream of genes involved in the development of hepatopancreatic lineages.

1.7.2 LRH-1 in cholesterol reverse transport and bile acid homeostasis

Besides serving as the precursor for steroidogenesis, cholesterol also mediates other important cellular functions including membrane biogenesis as well as the biosynthesis of bile acids. LRH-1 participates in reverse cholesterol transport from peripheral tissues to the liver by mediating the transcription regulation of cholesteryl-ester-transfer protein (CETP) and scavenger receptor class B type I (SR-BI). LRH-1 potentiates the cholesterol-induced expression of CETP in concert with oxysteroid-activated NRs Liver X Receptor (LXR) α and LXRβ (Luo et al., 2001b). Besides, LRH-1 binds FREs present in the murine and human SR-BI promoters and the expression of SR-BI is found to be reduced in $LRH1^{+/-}$ mice (Schoonjans et al., 2002b).

LRH-1 also participates in the regulation of the bile acid (BA) synthesis pathway in concert with several other NRs. Briefly, LRH-1 regulate the expression of cholesterol 7α-hydroxylase (CYP7A1) and sterol 12α-hydroxylase (CYP8B1) in cooperation with LXRα, Farnesoid X receptor (FXR) and SHP (Castillo-Olivares and Gil, 2000a; Goodwin et al., 2000; Lu et al., 2000b; Yang et al., 2002; Castillo-Olivares et al., 2004). In addition, LRH-1 also regulates the expression of several genes involved in lipoprotein assembly and lipid re-absorption including the pancreatic enzyme carboxyl ester lipase (CEL) (Fayard *et al*., 2003), ileal apical sodium-dependent BA transporter (ASBT) (Chen *et al*., 2003), and enterocytic multidrug-resistance protein 3 (MRP3) (Inokuchi *et al*., 2001).

1.7.3 Emerging roles of LRH-1 in steroidogenesis

Following the discovery of its abundant expression in the ovary in several species studied, it is now clear that LRH-1 modulates steroidogenesis cooperatively with SF-1 in the ovary (Boerboom et al., 2000b; Sirianni et al., 2002a; Falender et al.,

2003a; Hinshelwood et al., 2003b; Liu et al., 2003a). LRH-1 expression is restricted to the corpus luteal cells and follicular granulosa cells in all stages of development, whereas SF-1 expression is primarily found in the theca and interstitial cells. Besides differential expression in distinct ovarian cell types, the two NRs are differentially regulated by estradiol, FSH, and LH during the estrous cycle (Boerboom et al., 2000a; Falender et al., 2003b). LRH-1 has been demonstrated to regulate the expression of SR-BI and CYP19 in the granulosa cells (Hinshelwood et al., 2003a; Liu et al., 2003c; Schoonjans et al., 2002c). Moreover, LRH-1, rather than SF-1, regulates the expression of 3β-hydroxysteroid dehydrogenase type II (HSD3B2) in the human corpus luteum, which primarily produces progesterone (Peng *et al*., 2003). These observations suggest that LRH-1 may play a more important role in female sexual function compared to SF-1, whose role is more dominant in male sexual determination (Fayard et al., 2004a). The ovarian expression of LRH-1 in a stage-specific manner also raises the possibility that LRH-1 may have specific roles in modulating luteal and follicular functions.

An overexpression study of SF-1 and LRH-1 demonstrated that they exert qualitatively similar actions to stimulate the production of estrogen and progesterone in rat granulosa cells (Saxena *et al*., 2007). Since the binding specificity for FRE by SF-1 and LRH-1 is similar, they could potentially activate the same target genes if their expression domains overlap. Indeed, it has been reported that molecular switching between SF-1 and LRH-1 exist if they are co-expressed in the same cell. Hormonal stimulation of GRMO2 granulosa cell lines with forskolin resulted in a dynamic switching of SF-1 and LRH-1 at the inhibin α-subunit gene promoter such that SF-1 is replaced by LRH-1 (Weck and Mayo, 2006).

1.8 Modulation of transcriptional activity of NR5A receptors

It is now recognized that the activity of NRs can be modulated by at least three distinct mechanisms. Firstly, conformational changes of NRs can be induced by binding of a small lipophilic ligand or interacting partner in heterodimer complexes. Secondly, NRs activity can be modified by covalent modification, usually in the form of phosphorylation, and they are regulated by signaling events or during the cell cycle. Lastly, the transcriptional activities of NRs are dependent on protein-protein interactions, generally through contacts with other transcription factors and coregulators, including NRs themselves. All three mechanisms can either work individually or in concert with each other to exert NR function.

1.8.1 Identification of physiological ligands

For ligand-dependent receptors, hormone binding induces conformational changes that include a critical repositioning of the C-terminal helix H12 within the AF2 region (Nolte *et al*., 1998). Like other NRs, LRH-1 and SF-1 possess an intact and functional AF2 region (Galarneau *et al*., 1996; Ito *et al*., 1997). Intriguingly, both NRs are thought to be constitutively active as they are able to activate reporter constructs in the apparent absence of exogenous ligand in most cell lines. The proposal of oxysterols as a physiological ligand of SF-1 was largely controversial because these steroids fail to alter the activity of SF-1 in most cellular contexts, or elicit conformational changes predicted upon ligand binding (Lala *et al*., 1997; Mellon and Bair, 1998; Desclozeaux *et al*., 2002). Thus, SF-1 and LRH-1 remained as orphan NR until the high-resolution structures of both receptors are solved.

The X-ray crystallography structure of the mouse LRH-1 LBD was first reported by Sablin *et al*. (2003). The structure revealed a fold that resembled that of the known agonist-bound LBD structure with a large but empty ligand-binding pocket

as result of the tight packing of bulky hydrophobic residues, which is indicative that LRH-1 could remain constitutively active in the absence of a ligand (Sablin *et al*., 2003). In opposition to this, a subsequent attempt to solve the X-ray structure of LRH-1 and SF-1 LBD from mouse and human revealed that phosphotidyl inositol second messengers were the cognate ligands and that ligand binding was necessary to achieve maximal NR activity (Krylova *et al*., 2005). According to their evolutionary analysis of structure-function relationships across the NR5A subfamily, ligand binding represents the ancestral state of NR5A receptors and was probably diminished or altered uniquely in the rodent LRH-1 lineage. Intriguingly, a third study published on the X-ray crystal structure of human SF-1 and LRH-1 LBD demonstrated that the ligand-binding pocket of both NRs could use a wide range of phospholipid molecules as ligands (Wang *et al*., 2005). Obviously, the dependency of the two NRs on their potential ligands *in vivo* remain to be tested with more transient transfections and biochemical assays.

1.8.2 Covalent modifications that modulate the activities of NR5A receptors

The study of post-translational modifications of SF-1 revealed several signaling pathways that potentially regulate its transcriptional activity. SF-1 was first found to be phosphorylated in ovary granulosa cells following FSH stimulation (Carlone and Richards, 1997). The protein kinase A (PKA), which has been implicated in the stimulation of many SF-1 target genes expression, was able to phosphorylate the LBD and N-terminal region of SF-1 (De Santa et al., 2001a; Zhang and Mellon, 1996). In another study, SF-1 was shown to be phosphorylated at Ser-203 in AF1 domain by the extracellular signal-regulated kinase 2 (ERK2) in the ras/MAPK signaling pathway (Hammer *et al*., 1999). More importantly, mutation of Ser-203 to an alanine residue markedly decreased the activation potential of SF-1 by

50%. Besides, phosphorylation of Ser-203 enhances the recruitment of cofactors TIF2 and SMRT, and stabilized the structure of LBD in SF-1. Phosphorylation of LRH-1 at serine 238 and 243 has also been reported and it led to the stimulation of its transactivation activity (Lee *et al*., 2006).

Besides phosphorylation, SF-1 has been shown to be acetylated *in vivo* by the acetylase GCN5 and this modification stimulates its transcriptional activity (Jacob *et al*., 2001). Lastly, SF-1 is known to be covalently modified by small ubiquitin-like modifier 1 (SUMO). The SUMOylation of SF-1 was first identified by its protein-protein association with components of SUMOylation pathway and SF-1 can be SUMOylated at Lys-119 and Lys-194 *in vitro* (Komatsu *et al*., 2004). Subsequent investigations reveal that SUMOylation modification of SF-1 protein primarily represseed its transcriptional activity on its target genes (Lee *et al*., 2005; Campbell *et al*., 2008; Yang *et al*., 2008).

1.8.3 Protein-protein interactions with coregulators

To achieve transcriptional activation of target genes, DNA-bound NRs were originally believed to directly recruit general transcription factors (GTFs) to the preinitiation complex. Subsequent research revealed, however, that most NR regulated transcription events require intermediary factors, the so-called coregulators, which often constitute subunits of larger multiprotein complexes that act at several functional levels including chromatin remodeling, enzymatic modification of histone tails, or modulation of the preinitiation complex via interactions with RNA polymerase II and GTFs.

Most NR coregulators can be further subdivided into coactivators and corepressors, respectively, depending on whether they mediate transcriptional activation or repression. Many of the NR-coregulator interactions occur through the

LXXLL motif of NRs (Jepsen and Rosenfeld, 2002; Savkur and Burris, 2004). Furthermore, it has become clear that coactivation or corepression is not necessarily an intrinsic feature of a given coregulator but can depend on the target gene and cell-type specific context, *i.e.* some coregulators can function either as a coactivator or a corepressor in a context-dependent manner (Nagy and Schwabe, 2004; Kishimoto *et al*., 2006; O'Malley *et al*., 2008; Wolf *et al*., 2008).

Similar to many other NRs, SF-1 interacts with a wide range of coregulators to modulate the transcription of its target genes. The known interactors characterized so far include steroid receptor coactivator 1, SRC1 (Crawford et al., 1997a; Ito et al., 1998), coactivator TIF2 and p/CIP (Borud *et al*., 2002), corepressor RIP140 (Sugawara *et al*., 2001), DAX1 (Hanley et al., 2001; Koskimies et al., 2002b), androgen receptor (Jorgensen and Nilson, 2001), hMBF1 (Kabe *et al*., 1999), β-catenin (Gummow et al., 2003a; Mizusaki et al., 2003), Sp1 (Sugawara *et al*., 2000), Ptx1 (Tremblay *et al*., 1999), Egr-1 (Tremblay and Drouin, 1999), CREB binding protein (Monte *et al*., 1998), TreP-132 (Gizard et al., 2002a), paired-like homeodomain transcription factor 1 (Tremblay et al., 1998b), pituitary specific transcription factor 1 (Tremblay et al., 1998a), nuclear factor Y (Jacobs et al., 2003a), estrogen receptor alpha (Drean *et al*., 1996), nuclear receptor co-repressor 2 (Crawford *et al*., 1998), CCAAT/enhancer binding protein (Reinhart *et al*., 1999), dead box polypeptide 20, 103KD (Ou *et al*., 2001), Zip67 (Borud *et al*., 2003), GATA4 (Tremblay and Viger, 1999b), small nuclear RING finger protein (Curtin *et al*., 2004), AP1 (Guo *et al*., 2007a), and Foxl2 (Wang *et al*., 2007). In the sex determination pathway, SF-1 has been shown to regulate the gene expression of the *MIS* gene in physical association with WT1 and SRY-related HMG box 9 (SOX9) (De Santa et al., 1998a; Nachtigal et al., 1998b; Gurates et al., 2002; Gurates et al., 2003).

Furthermore, Pbx1 together with SF-1 have been shown to act synergistically on Mcr-2 promoter (ACTH receptor) to modulate adrenocortical growth as well as steroidogenesis (Lichtenauer et al., 2007b).

The transcriptional activity of LRH-1 has also been shown to be mediated by interactions with a wide range of coregulator although the list of interactors is not as extensive as SF-1. The small heterodimer protein (SHP) (Lu et al., 2000a; Lee and Moore, 2002; Li et al., 2005), prospero-related homeobox factor (Prox1) (Qin *et al*., 2004), silencing mediator for retinoic acid receptor and thyroid hormone receptor (SMRT) (Xu *et al*., 2003) and sterol regulatory element-binding protein (SREBP) (Kanayama *et al*., 2007) have been implicated as transcriptional corepressor of LRH-1. In addition, steroid receptor coactivator 1 (SRC-1) (Xu *et al*., 2004) and β-catenin (Botrugno *et al*., 2004) have both been reported to interact with LRH-1 and potentiates its transcriptional activity. Following the discovery of LRH-1 expression in the ovary, several coregulators that mediate LRH-1 transcriptional activity at the gene promoter of steroidogenic enzymes have been identified. These include the peroxisome proliferator-activated receptor gamma coactivator-1alpha (PGC-1α) and retinoid X receptor (RXR) (Safi *et al*., 2005) as well as PIASy, the shortest member of the protein inhibitor of activated STAT family (Hsieh *et al*., 2008). A recent study showed that the LXXLL-related motifs in DAX-1, which is well documented as the coregulator of SF-1, have target specificity for both SF-1 and LRH-1 (Suzuki *et al*., 2003).

For zebrafish Ff1s, Prox1 has been implicated as a novel corepressor of Ff1b and both of them work in conjunction to regulate the development of the zebrafish interrenal primordium (Liu et al., 2003e). It is postulated that Prox1 can form a repressor complex with Ff1b, which subsequently regulates the target genes in the

interrenal development. Just recently, antisense morpholino knockdown of *wt1* in zebrafish showed that Wt1 plays an important role in the development of both pronephric and interrenal primordia in coordination with Ff1b (Hsu et al., 2003c). Therefore, Wt1 might be a potential coregulator that can physically interact with Ff1s in modulation of their activities. In addition, the transcriptional intermediary factor 2 (TIF2), which belongs to the p160 coactivators family, has been shown to interact strongly with Ff1b and Ff1c (Tan *et al*., 2005). As zebrafish Ff1s share a high homology to their mammalian homologues, the list of coregulators that mediate their transcriptional activity will continue to grow.

1.9 Aims of this study

The focus of the present study was on *ff1b*, which is the most well studied member among the four zebrafish *ff1* genes isolated. As a follow-up to previous studies carried out in our laboratory that explored the cloning, genomic organization, expression pattern, and loss-of-function studies in relation to *ff1b*, this research project was initiated with the long-term objective to understand the regulatory mechanisms governing the expression and transcriptional activity of *ff1b* in the organogenesis and maintenance of mature zebrafish interrenal gland.

While Ff1b functions as a master regulator gene in the specification of interrenal primodium (Chai et al., 2003b), nevertheless, the upstream *cis*-acting elements and their corresponding *trans*- factors that modulate the expression and transcriptional activity of Ff1b, have not been defined. Furthermore, unanswered questions remained concerning the downstream effectors of Ff1b, particularly as the target genes that are activated by Ff1b for steroidogenesis and maintenance of endocrine function maintenance are likely to be different from that for organogenesis. For the later, many of these downstream gene targets are likely to encompass classes

of genes that are involved in apoptosis, cell proliferation, vascularization, and restriction of expansion domain for organogenesis.

While the relevance of SF-1 KO mice studies cannot be questioned, they have nevertheless also highlighted the difficulty of using a mammalian system to study the *in vivo* gene functions. Even with the development of tissue-specific KO approach, the investigation of adrenal organogenesis in mammalian system remains a great challenge due to its *in utero* development. In this regard, the zebrafish model complements the mammalian system perfectly in that it allows discoveries that are otherwise not possible, especially if they required direct embryonic manipulation or when combined with both forward and reverse genetic approaches, which are well established in zebrafish model. In the last decade, zebrafish has emerged as a popular model organism for a wide spectrum of endocrinology studies (McGonnell and Fowkes, 2006). The zebrafish endocrine system is sufficiently similar in comparison to human and mouse, thereby allowing the experimental findings to be broadly applicable among these vertebrate models. Besides, the transparency and rapid development of zebrafish embryos enable live imaging and developmental study of endocrine organs, as well as embryonic and molecular micromanipulation. Furthermore, injections of DNA, RNA, and morpholino oligo, cell transplantation, and many other molecular and histochemical techniques are well established in zebrafish (Westerfield, 2000). The wide variety of both forward and reverse genetic approaches can be readily employed to decipher gene function. As a vertebrate, zebrafish displays many experimental advantages of invertebrate models including the ease of maintainance under laboratory conditions, large number of offsprings (a few hundred eggs weekly), external fertilization, short development and generation time, just to mention a few.

While the overall endocrine function of Ff1b is conserved with mammalian SF-1, subtle differences still exist and some of these differences have indeed highlighted the advantages of zebrafish model in comparison to mammalian models. For instance, the knockdown of *ff1b* gene function in zebrafish is not embryonic lethal (Chai et al., 2003a), probably due to the maternal store or alternate site of corticosteroids synthesis. Thus, *ff1b* morphants of zebrafish can be easily subjected to a wide range of experimental manipulations, including direct treatment with chemical or corticosteroids, co-injection of overexpression constructs, as well as, imaging analyses from early stages of embryonic development. With the established role of Ff1b as a master regulator of interrenal development, it is now plausible to generate a faithful transgenic marker using *ff1b* gene. Obviously, a fluorescent lineage tracer of *ff1b* in zebrafish is likely to provide a higher level of versatility and convenience than that of SF-1 in the mouse model, mainly due to the possibility of live imaging in zebrafish embryos.

In this research project, three major lines of research that have been undertaken will eventually lead us to achieving the long-term goal of deciphering *ff1b* gene functions in the morphogenesis of the interrenal gland. Despite the well defined central role of Ff1b in interrenal development, the supporting evidence of its *in vivo* function as a transcription factor is still lacking.The first objective is directed at the establishment of Ff1b as a *bona fide* transcription factor and we will use the 5' promoter of *cyp11a1*, a putative target gene of Ff1b, to study this aspect. The establishment of the association of Ff1b with the *cyp11a1* promoter would aid to generate an endogenous target gene promoter for the detailed study of Ff1b transcriptional activity.

For the second objective, we aim to establish a stable transgenic zebrafish line that will allow lineage tracing of *ff1b*-expressing cells, particularly those in the interrenal gland, using EGFP as the fluorescent marker. The resultant transgenic line would create an *in vivo* model for the visualization of *ff1b*-expressing cells throughout the developmental process, thereby enabling a much more detailed and close examination of the morphogenetic events that are taking place during the organogenesis of the interrenal gland. Furthermore, the stable transgenic zebrafish will allow the isolation of pure populations of *ff1b*-expressing cells for a variety of cellular and molecular analyses to identify the upstream regulators, interacting partners, and downstream target genes of Ff1b.

The third objective is the identification of *cis*-regulatory elements that control the tissue-specific expression of *ff1b* in zebrafish, particularly that in the interrenal gland. Although tissue-specific enhancers, such as VMHE and FAdE, are conserved between mouse and human (Shima et al., 2005a; Shima et al., 2008c; Zubair et al., 2006a), sequences that share sufficient homology to these enhancers could not be mapped in zebrafish *ff1b* through biocomputational analysis and comparison. The close examination of *ff1b* locus and the identification of tissue-specific enhancers for *ff1b* would aid to unravel the commonalities and disparities between the transcriptional regulation of *ff1b* and *SF-1*. This would be useful in defining the evolutionary mechanisms that have taken place to shape the current gene function of *ff1b* and *SF-1*, and probably also other *FF1* genes. This requires the sequencing of a major portion of the *ff1b* genomic locus to fully establish the sequence information. Subsequently, a recombination-based deletion study of the *ff1b* locus, in combination with transient transgenesis, in zebrafish embryos has been adopted to identify enhancer elements that are responsible for the tissue-specific expression of *ff1b*.

CHAPTER 2

Materials and Methods

2.1 Purification of plasmids from bacterial culture

Small-scale purification of plasmids < 20 kb in size intended for cloning, sequencing, and clone screening was carried out from 2 - 3 ml of DH10B or DH5α *E. coli* bacterial culture. The isolation of plasmid DNA was performed with the QIAprep® Spin Column (QIAGEN GmbH, Germany) or with the spin column from High-Speed Plasmid Mini Kit (Geneaid, Taiwan).

Large-scale purification of plasmids < 20 kb in size and bacterial artificial chromosome (BAC) plasmids from bacteria intended for microinjection or transfection experiments was carried out using QIAGEN Plasmid Endofree Midi/Maxi Kit with the following modifications for BAC DNA. For the purification of BAC DNA, at least 400 ml of bacteria culture was used and the resulting lysate was treated as two Maxiprep reactions and passed through either one QIAGEN-tip 500 or two QIAGEN-tip 100. Elution buffer was pre-heated to 65°C when purifying BAC DNA and the final DNA pellet was dissolved overnight at 4°C in TE buffer, after which the DNA was stored at 4°C.

2.2 Subcloning techniques

All general subcloning and DNA manipulation techniques including restriction endonucleases digestions, ligations, and PCR amplification of DNA fragments were performed according to protocols described in Sambook and Russel (2000) as well as the corresponding manufacturer's manual. The enzymes used were mostly purchased from New England Biolabs Inc (MA, USA), Promega Corp. (WI, USA), Roche

(Switzerland), and Invitrogen (CA, USA). The DNA fragments generated by PCR or restriction digestion were purified using QIAquick PCR Purification Kit (QIAGEN) or gel-purified using QIAquick Gel Extraction Kit (QIAGEN).

2.3 Site-directed mutagenesis

Mutagenesis on the desirable site in a plasmid DNA was generated using the Quickchange® XL Site-directed Mutagenesis Kit (Stratagene, CA, USA). Briefly, the pairs of mutagenic primers were designed following the guidelines described in the manufacturer's manual and complementary oligonucleotide primers were ordered from 1stBASE (Singapore) or Research Biolabs (Singapore). Mutant strands were synthesized from the parental plasmid by PCR amplification using the complementary mutagenic oligonucleotides. Reactions were set up in a final volume of 50 µl and contained 1X Pfu reaction buffer, 10 ng of template DNA, 125 ng of the each oligonucleotide primers, 0.2 mM of each dNTPs, 3 µl of Quickchange Solution (to facilitate replication of large plasmids), and 1 µl of *PfuTurbo* DNA polymerase (2.5 U/ µl).

Following PCR amplification, 1 µl of *Dpn* I restriction enzyme was added directly into the PCR reaction mixture and the resulting mixture was incubated at 37°C to digest the non-mutated, methylated parental DNA strands. Two microlitre of this final reaction mixture was transformed into 50 µl of home-made electrocompetent cells of DH10B (transformation efficiency ~10^9 cfu/µg). Half or all of the transformed cell mixture was then plated onto LB plates with appropriate antibiotics selection and the LB plates were incubated overnight at 37 °C to obtain single colonies. To screen for the successfully mutagenized construct, plasmids were subsequently isolated from 8 – 10 colonies and sent for sequencing to identify the correctly mutagenized clone. The efficiency of mutagenesis is normally 20 – 50 %.

2.4 Genome walking for the isolation of putative promoter regions of zebrafish steroidogenic genes

The putative promoter regions of the zebrafish steroidogenic genes including *cyp11a1*, *star*, *cyp17*, and *3β-hsd* were isolated by a modified genome walking method (Siebert *et al*., 1995). Briefly, 2 μg of zebrafish genomic DNA was separately digested with five different restriction enzymes that leave 3' overhangs, namely *Bst*XI, *Nsi*I, *Pst*I, *Sac*I and *Sph*I. Following purification by phenol: chloroform: isoamyl (25:24:1, PCI) extraction, each pool of digested DNA fragments was subjected to homopolymeric dC-tailing in 40 μl reactions containing 0.2 mM dCTP, 10 mM Tris-Cl (pH 8.4), 25 mM KCl and 1.25 mM $MgCl_2$ and 38.4 U of TdT for 1 h at 37°C. Only " 3' overhang cutters" were used as TdT tends to extend more readily from 3' overhangs than from 5' overhangs or flushed double-stranded DNA ends. The poly (dC) tail serves as a priming site for the anchored adapter primer, ANC1 (5'-GAGGTCGACGGGIIGGGIIGGGIIGH-3'), which contains doublets of deoxyinosine residues (I) to prevent the formation of strong G-C clamps when anealed to the poly (dC) stretch.

Hemi-nested PCR was performed with aliquots of each pool of DNA fragment using the Expand™ Long Template PCR System (Roche) with ANC1 and gene-specific primers (Table 2.1). One μl (~40 ng) of genomic DNA was used for primary PCR. An initial denaturation step at 94°C for 2 min was followed by an extension at 68°C for 15 min to generate the second strand of template DNA. Cycling conditions for primary PCR were: 25 cycles of 94°C for 20 sec, annealing for 30 sec, 68°C for 8 min followed by a final extension at 68°C for 10 min. From 25 μl of primary amplified product, 1 μl was used as template for secondary PCR. Cycling parameters for secondary PCR were essentially the same as for primary PCR except that initial

denaturation was reduced to 1 min. The annealing temperature during cycling was set according to the calculated T_m of the gene-specific primer used. Amplified fragments were checked and identified by gel electrophoresis of the PCR product. The distinct bands on gel were then cloned into pGEM-T vector and sequenced to identify clones that contain the 5' flanking region of the four genes aforementioned. The promoter fragments carrying the putative 5' promoter sequences were subsequently cloned into pEGFP-1 and pGL3Basic vector for transient expression studies in cell lines and zebrafish embryos.

Table 2.1 Primers designed for the isolation of 5' flanking promoter of the following steroidogenic genes by genome walking.

cyp11a1	zfP450SCCr2	5' CCATAATTCGGTGGACATTCCTG 3'
	zfP450SCCr3	5' TGAAGGCAAGGACACTGAGCAG 3'
star	zfStARr3	5'- CTGTCATATTTCTCATGTGTCTG -3'
	zfStARr4	5'- GTCTGTAAGAAATGCCAGCACAC -3'
cyp17	zfP450C17r2	5' ATCTCCTTCGCATGATGGTGG 3'
	zfP450C17r3	5' CACCAGGCTCAGCAGACTCC 3'
3β-hsd	zf3bHSDr1	5' TGATGGCGTCACGTGTTGTCG 3'
	zf3bHSDr2	5' GATTCGAGACAATGCGGTGTC 3'

2.5 Bioinformatic analysis of transcription factor binding sites

Genomic sequences were searched for putative transcription factor binding sites using the MatInspector program (Cartharius *et al*., 2005) at the online genomatix server http://www.genomatix.de/. Analyses of sequences were performed against the MatInspector library of transcription factor binding sites (TFBSs) weight matrices (version 6.0 or 7.1). Matrix group selected includes general core promoter elements and vertebrates. Matrix filter was set to include all tissue associations. Only binding sites that showed a matrix similarity score of > 0.90 were considered significant. A

perfect match to the matrix was assigned 1.00 (each sequence position corresponds to the highest conserved nucleotide at that position in the matrix). Putative transcriptional *cis*-elements that might play a regulatory role were then presented as a schematic diagram.

2.6 Preparation of electrocompetent bacterial cells

DH10B strain of *E. coli* bacterial cells were inoculated into 10 ml of LB media alone or supplemented with the necessary antibiotics for plasmid and/or BAC selection. Culture was grown at 37 °C with vigorous shaking at 250 rpm overnight until OD_{600} reaches 1.2 – 1.8 the next morning. For bacterial cells harboring the pRed/ET plasmid, culture was grown at 30°C. The overnight culture was then diluted with ~200 ml of fresh LB media (pre-warmed to room temperature, RT) so that the OD_{600} of the fresh culture reads ~0.1. The fresh culture was incubated at 37°C or 30°C with vigorous shaking for 2 – 3 h until OD_{600} reaches 0.35 – 0.45. The growth of culture was monitored for OD_{600} with spectrophotometer at every 30 min. In the case where the bacterial cells will be used for homologous recombination, 8 ml of 10% L-arabinose was added to the culture at the beginning of incubation and the temperature was adjusted from 30°C to 37°C when OD_{600} reaches ~0.2. The final culture at log phase (OD_{600} = 0.35-0.45) was then chilled in ice water bath for 20-30 min with occasional swirling.

The chilled culture was centrifuged at 5,000 rpm for 15 min at 4°C to harvest bacterial cells. The cell pellet was subsequently rinsed with 200 ml of ice-cold sterile MQ water followed by 100 ml and 20 ml of ice-cold 10% glycerol. The cell pellet was thoroughly resuspended in the rinsing solution by pipetting up and down prior to every centrifugation using serological pipette. Following the final wash with 10 % glycerol, the bacterial pellet was resuspended in 500 µl of 10 % glycerol by gentle

swirling. The OD_{600} of bacterial cell suspension was measured at 1:100 dilution using spectrophotometer. Each 1.0 OD_{600} corresponds to 2.5 X 10^8 cells/ml. The bacterial cell suspension was then adjusted to a final concentration of 2 to 3 X 10^{10} cells/ml and aliquoted (50 µl each) into sterile and pre-chilled microfuge tubes. Finally, the cells were snap-freezed in liquid nitrogen and stored at -80°C until use.

2.7 Transformation of *E. coli* bacteria

Supercoiled plasmid DNA was transformed into *E. coli* bacteria by chemical method. For each transformation, 100 µl of thawed DH10B or DH5α competent cells was added into a microfuge tube containing ~10 ng of plasmid DNA and mixed by tapping. The mixture was left on ice for 20 – 30 min after which heat shock treatment was performed for 5 min at 37°C. The tube was immediately placed back on ice, followed by the addition of 1 ml of LB media. The bacterial culture was then incubated at 37°C for 1 h with shaking at 200 rpm for recovery of the competent cells. The appropriate amount (~50 µl) of transformation mix was then plated onto selective LB agar plates with antibiotics and incubated for 16 – 20 hr at 37°C.

Electroporation was adopted for transformation of linear DNA fragments (for homologous recombination), BAC plasmids, mutagenized and freshly ligated plasmid DNA into *E. coli* bacteria. DH10B electrocompetent cells was thawed on ice and mixed with 1 – 3 µl of DNA construct to be transformed. The mixture was left on ice for 2 – 3 min while the Gene Pulser (Bio-Rad) was set to a capacitance of 25 µFarad, pulse controller to 200 ohms, and voltage to 1.8 kV. The mixture was then transferred from microfuge tube to a fresh pre-chilled 0.1 cm cuvette (Bio-Rad) and pulsed in the electroporation chamber so that the time constant reads 4 – 5 msec. Cells were allowed to recover in 1 ml of LB or SOC at 37°C with gentle shaking at 200 rpm for

45 – 70 min. The appropriate amount (usually 100 µl) of transformation mix was then plated onto selective LB agar plates with antibiotics and incubated for 16-20 h at 37°C.

2.8 Red/ET homologous recombination

Red/ET recombination, also referred to as λ-mediated recombination, relies on homologous recombination *in viv*o in *E. coli* bacteria. The recombineering process is catalyzed by a pair of phage-derived proteins RecE and RecT that have been placed under L-arabinose induction and require a temperature shift from 30°C to 37°C for homologous recombination to take place (Zhang *et al*., 1998). In the presence of the recombination proteins, homologous recombination between a linear DNA molecule (e.g. a PCR product) and a circular DNA (plasmid, BAC, or *E. coli* chromosome) can occur with as little as 42 bp homologous sequence. This exchange of genetic material between two DNA molecules in a precise, specific, and accurate manner has opened up a wide range of modifications (insertions, deletions, point mutations, fragment exchanges) of DNA molecules of any size and at any chosen position. In this study, various BAC constructs were modified by DNA engineering based on homologous recombination. The desired modifications were introduced using the Counter-Selection BAC Modification kit from Gene Bridges (Dresden, Germany).

2.8.1 Insertion of an EGFP-Kan^r cassette into ff1bBAC2

An EGFP-Kan^r was designed to be inserted into nucleotide 338 within codon 25 in Exon 2 of *ff1b* so that the resultant EGFP expression was regulated by the endogenous *ff1b* locus. The EGFP-Kan^r donor fragment was generated by PCR amplification with primers ff1bEx2EGFPKan/4170F (5'-ACGGTGATGGACTTCA GAGC-3') and ff1bEx2EGFPKan/6457R (5'-ACTGATGTGAGTATTCGCAGC-3') from pUC18Ff1bEx2EGFPKan (-NotI) containing genomic sequences of *ff1b*

flanking the EGFP-Kan^r selectable marker (Fig. 2.1). The original *Not* I restriction site located between EGFP and Kan^r coding sequences was removed by restriction digestion with *Not* I followed by Klenow fill-in and ligation. The removal of the internal *Not* I site was necessary to enable the release of the whole genomic insert emcompassing *ff1b* locus from the pBeloBAC-11 vector backbone for stable transgenesis studies following successful recombination. The size of this DNA donor fragment (2288 bp) was checked by gel electrophoresis. This linear DNA fragment was subsequently purified through Qiagen gel extraction column and DNA concentration was measured by Nanodrop spectrophotometer.

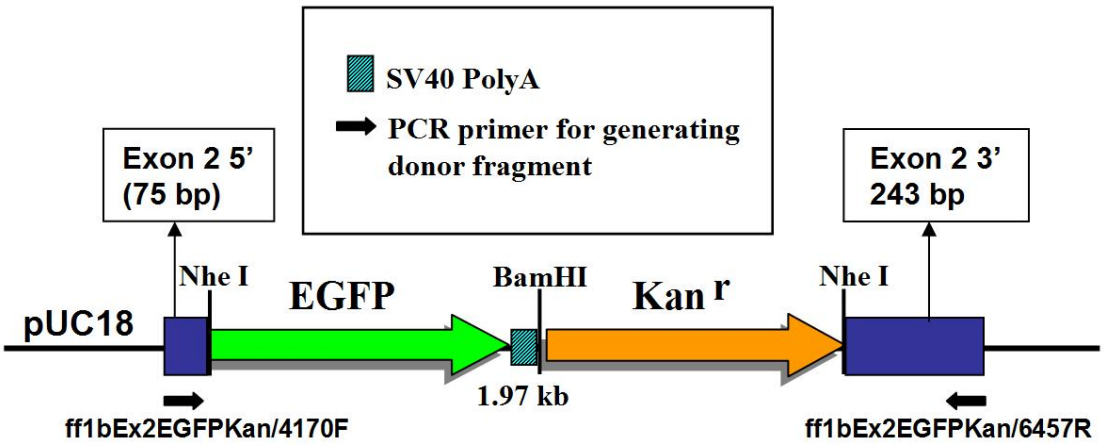

Figure 2.1 Schematic diagram representing pUC18Ff1bEx2EGFPKan (-NotI) as template for PCR amplification of donor fragment ff1bEx2EGFPKan. Positions of primers used to generate the donor fragment were indicated by black arrows. Sizes of *ff1b* genomic sequences flanking the insertion site in Exon 2 were indicated by Ex2 5' and 3'.

Concurrently, bacterial cells were prepared to undergo homologous recombination with the above donor fragment. The BACff1b2 plasmid carrying ~100 kb of zebrafish genomic sequence encompassing *ff1b* locus (Chai, 2002) was first transformed into DH10B electrocompetent cells by electroporation (Section 2.6). The pRed/ET plasmid, which encodes the phage-derived proteins RecE and RecT that catalyze homologous recombination, was then transformed into the bacterial cells

harboring the BAC plasmid by a modified electroporation protocol in the manual (Genebridges). Briefly, bacteria containing the BACff1b2 plasmid was grown in 1 ml of LB medium supplemented with chloramphenicol (15 μg/ml) in a 1.5 ml microcentrifuge tube at 37°C with 16 hr vigorous shaking (1000 rpm) using a table-top thermomixer (Eppendorf). The next day, a microcentrifuge tube containing fresh 1.4 ml LB medium supplemented with chloamphenicol were set up with 30 μl of overnight culture. This diluted culture was then grown for 2 – 3 h at 37°C with shaking at 1000 rpm in a table-top thermo-mixer (Eppendorf). Cells were then centrifuged for 30 sec at 11,000 rpm in a chilled microfuge benchtop centrifuge at 2°C. The cell pellet was washed twice with 1 ml of chilled sterile MQ water after which the final pellet was resuspended in ~30 μl of water remaining in the microcentrifuge tube. The cell suspension was mixed with 1 μl (20 ng) of pRed/ET plasmid on ice and electroporation was carried out as described in Section 2.6. Transformed bacteria were grown on LB agar plates supplemented with chloramphenicol (15 μg/ml) and tetracycline (3 μg/ml) selecting for BACff1b2 and pRed/ET plasmid, respectively at 30°C. Incubation was carried out in dark as tetracycline is light sensitive. Furthermore, as pRed/ET is a derivative of a termo-sensitive pSC101 replicon(Miller *et al*., 1995), the incubation temperature was maintained at 30°C.

Following the transformation of pRed/ET plasmid, the bacteria were now ready to undergo homologous recombination with the linear donor Ex2EGFPKan fragment. The bacteria were made electro-competent as described in section 2.11 prior to electroporation. Subsequently, 150 – 250 ng of Ex2EGFPKan donor fragment was electroporated into 50 μl of electrocompetent DH10B cells ($3x10^{10}$cells/ml) containing BACff1b2 and pRed/ET plasmids. The transformation mixture was plated onto LB agar plates supplemented with chloramphenicol (15 μg/ml) and kanamycin

(15 μg/ml) to select for bacterial cells that had the EGFP-Kan cassette successfully inserted into the BACff1b2 plasmid by homologous recombination. To screen for the successfully recombined clones, 10 – 20 colonies were subjected to colony PCR using primers spanning the insertion junction (one primer within the Kan CDS and the other located ~100 bp 3' to the donor fragment).

Subsequently, large-scale BAC plasmid isolation was carried out using QIAGEN Plasmid Endofree Maxi Kit (Section 2.1) from bacterial clone that showed positive results in colony PCR screening. The insertion was verified by DNA sequencing and the BACff1b2 that had the EGFP-Kan^r cassette successfully inserted into Exon 2 was named pBACff1bEx2EGFPKan.

2.8.2 Truncations of specific genomic regions from pBACff1bEx2EGFPAmp by counter-selection strategy

When it was not desirable to leave a selectable marker (e.g. kanamycin) at the recombination site, i.e. truncation of specific genomic sequences from the above recombined BAC plasmid, a two-step recombineering strategy termed counter-selection was employed. To begin, PCR product containing *rpsL-neo* counter selection cassette flanked by homology arms targeting the site to be truncated were electroporated into the L-arabinose-induced bacteria (Fig. 2.2). This selection cassette was inserted into the BAC at the first recombination step and the resulting recombined plasmid can be retrieved by kanamycin resistance selection. In the second step, the induced cells were electroporated with PCR product containing a non-selectable marker i.e. only the right and left homology arms from the first step. As the *E. coli* DH10B strain carries a mutation in the *rpsL* gene, it is streptomycin-resistant. The removal of *rpsL-neo* cassette together with the replacement of non-selectable DNA

can be identified by streptomycin resistance selection, as the *rpsL* gene renders the bacteria streptomycin sensitivity in the first step of recombination.

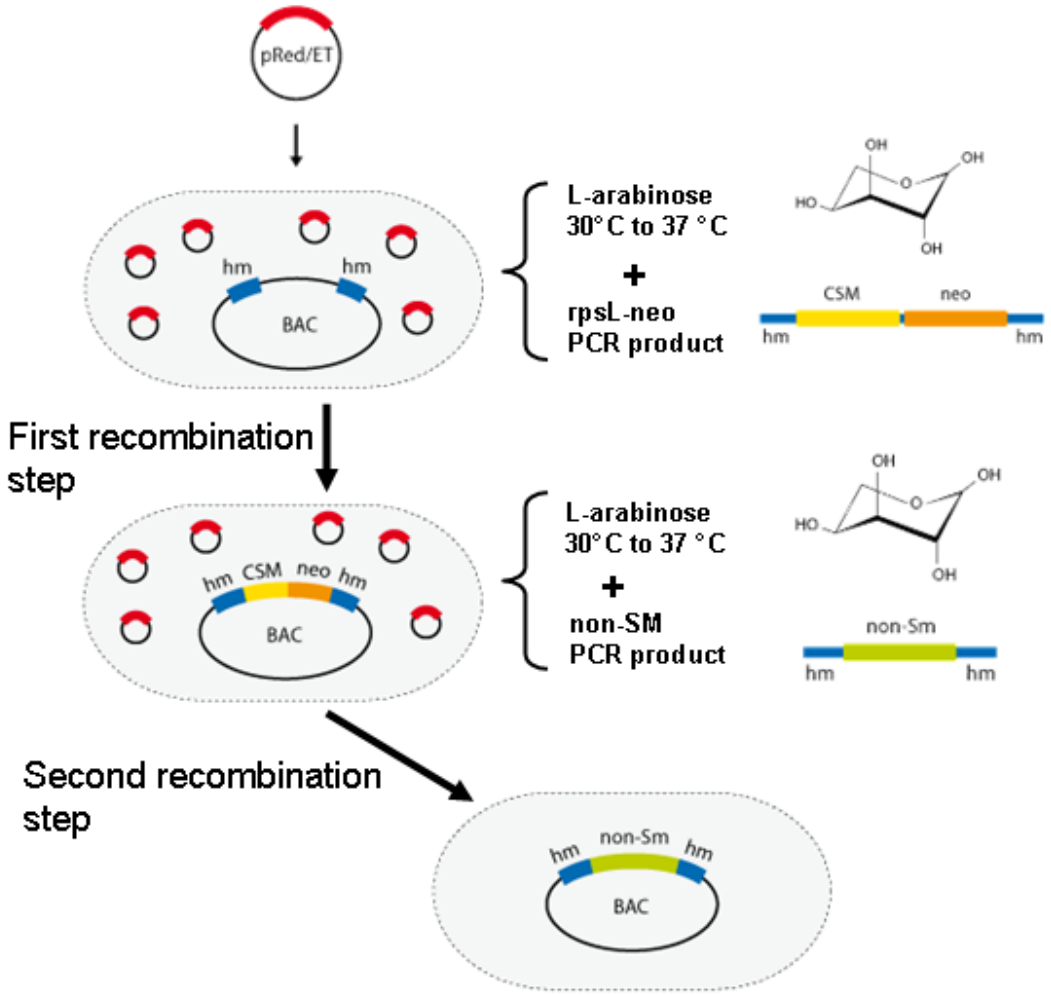

Figure 2.2 Schematic representation of modification of BAC-of-interest by homologous recombination based on counter-selection method. The pRed/ET plasmid is first transformed into the E. coli host that carries the BAC to be modified. The expression of genes mediating Red/ET recombination is induced by adding L-arabinose and a temperature shift from 30°C to 37 °C. Following induction, PCR product containing rpsL-neo counter selection cassette flanked by homology arms are electroporated into the bacteria. This selection cassette is inserted into the BAC at the first recombination step and can be retrieved by kanamycin resistance selection. In the second step, the induced cells are electroporated with PCR product containing the non-selectable marker (non-sm), which can either be just an oligonucleotide harboring the right and the left homology arms of the selection cassette and a point mutation (control reaction) or a gene flanked by homology arms. The removal of *rpsL-neo* cassette together with the replacement of non-selectable DNA can be identified by streptomycin resistance selection, as the *rpsL* gene renders the bacteria streptomycin sensitivity after the first step of recombination.

2.8.2.1 Replacement of Kan resistant gene with an Amp resistant gene

As the pBACff1bEx2EGFPKan BAC palsmid (Section 2.8.1) carries a kanamycin resistance gene, it is not suitable to be used in counter-selection scheme, which requires a kanamycin selection to identify successful recombination in the first step. Therefore, a replacement of the kanamycin resistance gene with ampicilin resistance gene was carried out by Red/ET recombination by a protocol that is essentially the same as that described in Section 2.8.1.

The β-lactase (Amp) gene flanked by right and left homology arms targeting the immediate 60 bp upstream and downstream of kanamycin CDS in pBBff1bEx2EGFPKan was generated by PCR amplification using the Advantage2 polymerase system (Clontech). The forward and reverse primers used were Ff1bEx2/AmpF:5'ATATCATCATGAACAATAAAACTGTCTGCTTACATAAAC AGTAATACAAGGGGTGTT*ATGAGTATTCAACATTTCCGTGTCG*3' and Ff1bEx2/AmpR: 'AGGTCAGAAAGCCGCTAGCGTAATGCTCTGCCAGTGTTAC AACCAATTAACCAATTCTGA*TTACCAATGCTTAATCAGTGAGGC*3' respectively, with sequences in *italic* denoting priming sites in β-lactase (Amp) gene. The resulting recombined BAC plasmid, with the ampicilin resistance gene replacing the original kanamycin resistance gene, was named pBACff1bEx2EGFPAmp. The BAC plasmid was now ready to go through any modification by the two-step counter selection method.

2.8.2.2 Truncations of specific genomic regions from pBACff1bEx2EGFPAmp

To carry out the first step of recombination, various *rpsL-neo* fragments carrying homology arms (60 bp for each side) targeting sites to be truncated in pBACff1bEx2EGFPAmp were generated by PCR amplification using the long PCR primers listed in Table 2.2. All long primers (80 bp) were synthesized by Sigma-Proligo (Singapore). These linear DNA fragments (~1.4 kb) generated by PCR were gel-purified and ~150 – 250 ng of DNA was electroporated into electrocompetent DH10B bacteria carrying the pBACff1bEx2EGFPAmp and pRed/ET plasmids. Bacterial cells that had the *rpsL-neo* selectable marker inserted into the target sites, in replacement of the genomic region that had been truncated, were identified by kanamycin selection. Bacterial clones that had successfully undergone homologous recombination were verified by colony PCR screening. Ten to 20 bacterial colonies were selected and individually lysed in PCR water by heating at 95°C for 10 min. The resultant lysate was used as DNA template in PCR reactions with primers spanning the insertion site. The forward primer (RpsLneo843F: 5'CCGAGAAAGTATCCATC ATGG 3' lied within the neo CDS and the reverse primer was designed to be located ~100 – 150 bp downstream of *rpsL-neo* donor fragment. Sequences of reverse primers that were used to check for successful integration of *rpsL-neo* cassette at targeted genomic regions are listed in Table 2.4.

To complete the second step of recombination, long primers (120 bp) spanning just the right and left homology arms (Table 2.3) of the first set of primers (for *rpsL-neo* amplification) were synthesized and annealed. Annealing was done by heating both forward and reverse oligonucleotides (1:1 mixture) to 100ºC for 5 min and cooling the mixture down in an insulated box left at RT overnight.

Table 2.2 Long primers used in the first recombination step of counter-selection to replace genomic sequences to be truncated with *rpsL-neo* selectable marker.

Region to be deleted	Primer name	Primer sequence (80 bp each, 5' to 3')
5'10kb	5'10kb RpsLneoF	ATACCATATTTGCAAGATTAATGACCTACAACAATGAAGGTGG AAATGAAGGCCAGTCGC*GGCCTGGTGATGATGGCGGGATCG*
	5'10kb RpsLneoR	TTAATCATTACTGACCCTGCTGAAAAATCCAGCTTAAACCAGC CTAGGATGGTTAGCTGG*TCAGAAGAACTCGTCAAGAAGGCG*
5'20kb	5'20kb RpsLneoF	ATACCATATTTGCAAGATTAATGACCTACAACAATGAAGGTGG AAATGAAGGCCAGTCGC*GGCCTGGTGATGATGGCGGGATCG*'
	5'20kb RpsLneoR	TTCATTCCGCTGTGGCGACCCCAGATTAATAAAGGGACTAAGC CGACAAGAAAATGAATG*TCAGAAGAACTCGTCAAGAAGGCG*
Intron I	Int1Del RpsLneoF	AACATCTCTAGCCTTATTATTTTAATACGCATCATTTTAGTGTG ACACTTTAATATTGAG*GGCCTGGTGATGATGGCGGGATCG*
	Int1Del RpsLneoR	ATCTCCACACACCGGGCAAAGCTCCTCCAAATCCTCATCTGCT CTGAAGTCCATCACCGT*TCAGAAGAACTCGTCAAGAAGGCG*
Intron II	Int2Del RpsLneoF	TTGGTTGTAACACTGGCAGAGCATTACGCTAGCGGCTTTCTGA CCTGCGAAAGTTGTAAG*GGCCTGGTGATGATGGCGGGATCG*'
	Int2Del RpsLneoR	GTCCTGGTTCTGTGTGCACGTGTATCTCTTGTTATTCTGAACTG TCCTCTTGAAAAAACC*TCAGAAGAACTCGTCAAGAAGGCG*
Intron III	Int3Del RpsLneoF	GGAAAAGATGTCCGTTCTGCCGCTTCCAGAAGTGTCTGAGTGT CGGCATGAGACTTGAGG*GGCCTGGTGATGATGGCGGGATCG*'
	Int3Del RpsLneoR	CTCGCTTGTACATTGGGCCAAACTTATTTCTTCCACCTCTCATC CGGTCTGCACGCACAG*TCAGAAGAACTCGTCAAGAAGGCG*
Intron IV	Int4Del RpsLneoF	CCGCCGCTGGTGCTGGAGCTGCAGAGCTGCGACCCAGATGAG GAGCAGGTATGAAGCAAA*GGCCTGGTGATGATGGCGGGATCG*
	Int4Del RpsLneoR	CTCCAGCTTTCCTCTGCCGCTCTGCTCCTGGTGGAGATACGCGC AGATCTTTCCTCTCAC*TCAGAAGAACTCGTCAAGAAGGCG*
Intron V	Int5Del RpsLneoF	GACGCTCTTCTCTATCGTGGAGTGGGCGAGAAGCTGTGTCTTC TTCAAGGAACTAAAGGT*GGCCTGGTGATGATGGCGGGATCG*
	Int5Del RpsLneoR	ATGTGATCCAGAAGCAGCAGCTCGCTCCAGCAGTTATGCAGCA GACGCATCTGATCGCCC*TCAGAAGAACTCGTCAAGAAGGCG*
Intron VI	Int6Del RpsLneoF	ATCTGCAGACAGGTGCATCATGGGAGAGACGGCAGCCTGCTG CTCATCACAGGACAGGAG*GGCCTGGTGATGATGGCGGGATCG*
	Int6Del RpsLneoR	CCCTCGCTCAACCATGCTGGACAGAGGAGGACCAGCGTCCAA CACCGCCGACAGCTCCAC*TCAGAAGAACTCGTCAAGAAGGCG*
Intron VII	Int7Del RpsLneoF	TGCTGCAGGTGGACAGCAGAGAGATGGCCTGTCTGAAGTTCCT CATCCTCTTCAACCCCA*GGCCTGGTGATGATGGCGGGATCG*
	Int7Del RpsneoR	CCCCGTTCACCTGCTCCTGCACGCTCTCCACAAACTGCGGGTT CTCCAGGAGCTTCACGT*TCAGAAGAACTCGTCAAGAAGGCG*

Oligonucleotide sequences in italic denote primer sequence that annealed to the *rpsL-neo* DNA template during PCR amplification.

Table 2.3 Long primers used in the second recombination step of counter-selection to replace *rpsL-neo* selectable marker with the left and right homology arms.

Region to be deleted	Primer name	Primer sequence (120 bp each, 5' to 3')
5'10kb	5'10kbDelF	ATACCATATTTGCAAGATTAATGACCTACAACAATGAAGGTGG AAATGAAGGCCAGTCGCCCAGCTAACCATCCTAGGCTGGTTTAA GCTGGATTTTTCAGCAGGGTCAGTAATGATTAA
	5'10kbDelR	TTAATCATTACTGACCCTGCTGAAAAATCCAGCTTAAACCAGCC TAGGATGGTTAGCTGGGCGACTGGCCTTCATTTCCACCTTCATT GTTGTAGGTCATTAATCTTGCAAATATGGTAT
5'20kb	5'20kbDelF	ATACCATATTTGCAAGATTAATGACCTACAACAATGAAGGTGG AAATGAAGGCCAGTCGCCATTCATTTTCTTGTCGGCTTAGTCCC TTTATTAATCTGGGGTCGCCACAGCGGAATGAA
	5'20kbDelR	TTCATTCCGCTGTGGCGACCCCAGATTAATAAAGGGACTAAGCC GACAAGAAAATGAATGGCGACTGGCCTTCATTTCCACCTTCATT GTTGTAGGTCATTAATCTTGCAAATATGGTAT
Intron I	Int1DelF	AACATCTCTAGCCTTATTATTTTAATACGCATCATTTTAGTGTGA CACTTTAATATTGAGACGGTGATGGACTTCAGAGCAGATGAGG ATTTGGAGGAGCTTTGCCCGGTGTGTGGAGAT
	Int1DelR	ATCTCCACACACCGGGCAAAGCTCCTCCAAATCCTCATCTGCTC TGAAGTCCATCACCGTCTCAATATTAAAGTGTCACACTAAAATG ATGCGTATTAAAATAATAAGGCTAGAGATGTT
Intron II	Int2DelF	TTGGTTGTAACACTGGCAGAGCATTACGCTAGCGGCTTTCTGAC CTGCGAAAGTTGTAAGGGTTTTTTCAAGAGGACAGTTCAGAATA ACAAGAGATACACGTGCACACAGAACCAGGAC
	Int2DelR	GTCCTGGTTCTGTGTGCACGTGTATCTCTTGTTATTCTGAACTGT CCTCTTGAAAAAACCCTTACAACTTTCGCAGGTCAGAAAGCCGC TAGCGTAATGCTCTGCCAGTGTTACAACCAA
Intron III	Int3DelF	GGAAAAGATGTCCGTTCTGCCGCTTCCAGAAGTGTCTGAGTGTC GGCATGAGACTTGAGGCTGTGCGTGCAGACCGGATGAGAGGTG GAAGAAATAAGTTTGGCCCAATGTACAAGCGAG
	Int3DelR	CTCGCTTGTACATTGGGCCAAACTTATTTCTTCCACCTCTCATCC GGTCTGCACGCACAGCCTCAAGTCTCATGCCGACACTCAGACAC TTCTGGAAGCGGCAGAACGGACATCTTTTCC
Intron IV	Int4DelF	CCGCCGCTGGTGCTGGAGCTGCAGAGCTGCGACCCAGATGAGG AGCAGGTATGAAGCAAAGTGAGAGGAAAGATCTGCGCGTATCT CCACCAGGAGCAGAGCGGCAGAGGAAAGCTGGAG
	Int4DelR	CTCCAGCTTTCCTCTGCCGCTCTGCTCCTGGTGGAGATACGCGC AGATCTTTCCTCTCACTTTGCTTCATACCTGCTCCTCATCTGGGT CGCAGCTCTGCAGCTCCAGCACCAGCGGCGG
Intron V	Int5DelF	GACGCTCTTCTCTATCGTGGAGTGGGCGAGAAGCTGTGTCTTCT TCAAGGAACTAAAGGTGGGCGATCAGATGCGTCTGCTGCATAA CTGCTGGAGCGAGCTGCTGCTTCTGGATCACAT
	Int5DelR	ATGTGATCCAGAAGCAGCAGCTCGCTCCAGCAGTTATGCAGCA GACGCATCTGATCGCCCACCTTTAGTTCCTTGAAGAAGACACAG CTTCTCGCCCACTCCACGATAGAGAAGAGCGTC
Intron VI	Int6DelF	ATCTGCAGACAGGTGCATCATGGGAGAGACGGCAGCCTGCTGC TCATCACAGGACAGGAGGTGGAGCTGTCGGCGGTGTTGGACGC TGGTCCTCCTCTGTCCAGCATGGTTGAGCGAGGG
	Int6DelR	CCCTCGCTCAACCATGCTGGACAGAGGAGGACCAGCGTCCAAC ACCGCCGACAGCTCCACCTCCTGTCCTGTGATGAGCAGCAGGCT GCCGTCTCTCCCATGATGCACCTGTCTGCAGAT
Intron VII	Int7DelF	TGCTGCAGGTGGACAGCAGAGAGATGGCCTGTCTGAAGTTCCTC ATCCTCTTCAACCCCAACGTGAAGCTCCTGGAGAACCCGCAGTT TGTGGAGAGCGTGCAGGAGCAGGTGAACGGGG
	Int7DelR	CCCCGTTCACCTGCTCCTGCACGCTCTCCACAAACTGCGGGTTC TCCAGGAGCTTCACGTTGGGGTTGAAGAGGATGAGGAACTTCA GACAGGCCATCTCTCTGCTGTCCACCTGCAGCA

Table 2.4 Primer sequences used to check for successful recombination in two-step counter selection to delete specific genomic regions.

Region to be deleted	Primer name	Length (bp)	Primer sequences (5' to 3')
5'10kb	5'10kbChkF	21	GACCTACAACAATGAAGGTGG
	5'10kbChkR	23	GCGCTTTTACAATGTAGATTGTG
5'20kb	5'20kb ChkF	21	GACCTACAACAATGAAGGTGG
	5'20kb ChkR	23	AGACGCTCAGATATTTCCCAGAG
Intron I	Int1DelChkF	21	CACGTCCATATAGGAGGCTTG
	Int1DelChkR	21	AGCGTAATGATAACCGGACAC
Intron II	Int2DelChkF	20	CACGACATTCAACCTACCCC
	Int2DelChkR	21	TCCTCTGAGTTTTGTCGATGC
Intron III	Int3DelChkF	21	GCATCGACAAAACTCAGAGGA
	Int3DelChkR	20	GAGCCGTAATTCTGCAGAGC
Intron IV	Int4DelChkF	20	CAGTGTCCCCATAAACCCTG
	Int4DelChkR	22	GAGCCGTACCTTTAGTTCCTTG
Intron V	Int5DelChkF	20	CTTCAGCCTGCTGTGTGTCA
	Int5DelChkR	20	CATGATGCACCTGTCTGCAG
Intron VI	Int6DelChkF	20	CTGCAGACAGGTGCATCATG
	Int6DelChkR	21	GGATGAGGAACTTCAGACAGG
Intron VII	Int7DelChkF	20	CAGGTGGACAGCAGAGAGAT
	Int7DelChkR	20	TCTCGATCAGCAGGTTGTTG

The annealed oligonucleotides were subsequently used as the donor DNA fragment in the second step of counter-selection where ~150 – 250 ng of annealed oligonucleotides were electroporated into electrocompetent bacteria harboring the respective recombined BAC plasmid constructs from the first recombination and pRed/ET plasmid. For instance, annealed Int1DelF and Int1DelR primers were electroporated into bacterial cells containing pBACff1bEx2EGFPAmp plasmid having *ff1b* Intron I replaced by the *rpsL-neo* selectable marker in the first recombination step of counter-selection. As an example, Intron I was eventually truncated without leaving a selectable marker when the *rpsL-neo* cassette was

replaced by the Int1Del oligonucleotides in the second recombination step. Bacterial cells that had successfully undergone this second step of recombination could be retrieved by streptomycin (50 μg/ml) selection. Positive clones were confirmed by colony PCR as described for the first recombination step. The reverse primers used to screen for positive clones were essentially the same as the first recombination step while the forward primers were as listed in Table 2.4.

2.9 Tissue culture

The mouse Y1 adrenocortical cells obtained from the American Type Culture Collection (ATCC) were maintained in Ham's F12K medium supplemented with 10% horse serum (HS) and 2.5% fetal bovine serum (FBS). Chinese hamster ovary cells (CHO-K1; ATCC) were maintained in Ham's F12K medium supplemented with 10% FBS. The mouse LβT2 gonadotrope cells (a kind gift from Dr. P. Mellon, UCSD) were maintained in Dulbecco's modified Eagle's medium (DMEM) supplemented with 10% FBS, 2 mM L-glutamine, and 1 mM sodium pyruvate. The mouse MA-10 Leydig tumor cells (a kind gift from Dr. Martin Lee, Department of Physiology, NUS) were maintained in Waymouth's medium supplemented with 15% HS and 25 mM Hepes (pH 7.4). The human 293T kidney cells were maintained RPMI medium supplemented with 10% FBS. The human HepG2 hepatoma cells were maintained in DMEM supplemented with 10 % FBS.

All cell lines were maintained at 37ºC in 5% CO_2 with penicillin (100 U/ml) and streptomycin (100 μg/ml) added into the culture media. All basal media were purchased from Gibco, Invitrogen. Cells were routinely grown to 80-90% confluency prior to seeding for transfections or passages. For passages, media was removed from monolayer cells and cells were washed once with 1X PBS. Monolayer cells were then treated with 2 – 3 ml of 0.25 % trypsin-EDTA at RT for 3 min after which 8 – 9 ml of

media (with serum) was added to inhibit trypsin. Cells were routinely passaged at a ratio of 1:4 to 1:6.

2.10 Transient transfection

On the day before transfection, cells were seeded in 24-well tissue culture plates at a density of 0.8 – 1.5 x 10^5 cells per well so that cells were 60-80 % confluent by the time of transfection. All transfections were carried out using Fugene 6 transfection reagent (Roche, Switzerland) except for MA-10 cells, which were transfected using Lipofectamine 2000 transfection reagent (Invitrogen) following the manufacturer's protocol with optimization of plsmid: transfection reagent ration. When Fugene 6 transfection reagent was used, 0.4 μg of each luciferase reporter plasmid, 2 ng of pRL-SV40 (as a transfection efficiency control), and 0.6 μl of Fugene 6 transfection reagent were added into each well. When Lipofectamine 2000 was used, 0.8 μg of each luciferase reporter plasmid, 2 ng of pRL-SV40, and 4 μl of Lipofectamine 2000 transfection reagent were added into each well. Cells were harvested at 24 h following transfection and lysed in 1× passive lysis buffer provided in the Dual Luciferase reporter assay system (Promega) for dual-luciferase assay.

2.11 Dual-Luciferase assay

The dual-luciferase assay was carried out using reagents and experimental protocol provided by the manufacturer of Dual-Luciferase Reporter Assay System (Promega). For transfected cells, media was removed and cells were washed with 1X PBS, after which 100 μl of 1X passive lysis buffer was added into each well of 24-well tissue culture plate. The cells were left to lyse at RT for 15 min with gentle shaking (~50 rpm) and the lysed cells were kept on ice thereafter until luciferase measurement was completed. For microinjected embryos, 50 embryos were

dechorionated manually and homogenized in 100 µl of 1X passive lysis buffer by pippeting up and down until no big clumps of tissues were visible. Lysis was left to proceed on ice for 10 – 15 min and the samples were kept on ice until luciferase measurement is completed.

The LAR II and Stop & Glo® reagents required for the dual-luciferase assay were warmed up to RT at least 30 min before measurement. To start measuring luciferase activity, 20 µl of homogenate from transfected cells or microinjected zebrafish embryos was transferred into a borosilicate glass tube (12 x 75 mm; Fisher-Scientific) that fits perfectly into the measurement chamber of the Lumat LB9507 luminometer (Berthold, Australia). One hundred µl of LARII mixture was added into the homogenate and firefly luciferase activity was assayed over a 10 sec measurement period. The glass tube was quickly taken out from the luminometer and 100 µl of Stop & Glo® after which the *Renilla* luciferase activity was measured. The firefly luciferase activity of a particular luciferase construct was normalized by the *Renilla* luciferase activity conferred by the pRL-SV40 construct. Data are presented as the mean ± SD (standard deviation) of the average of four independent transfections, which were repeated at least once to ascertain the reproducibility of the data.

2.12 Immunoblot detection of biotin-labeled Ff1b produced by coupled *in vitro* transcription and translation

Ff1b protein was produced *in vitro* using the TNT® T7 quick coupled transcription/translation system (Promega) for electrophoretic mobility shift assay. To verify the identity of the Ff1b protein (~50 kDa) produced by this method, the translated proteins were biotinylated, separated on PAGE gel, and subsequently detected by chemi-luminescence using the Transcend™ Non-Radioactive Translation Detection System (Promega).

To set up the *in vitro* transcription/translation reaction, 40 µl of TNT® quick master mix, 1 µl of methionine (1 mM), 1 µl of Transcend^{TM} biotin-lysyl-tRNA, and 1 µl of DNA template pCDNA3.1ff1b (1 µg/µl) were mixed thoroughly in a PCR tube. Reaction volume was adjusted to a final volume of 50 µl with sterile MQ water after which incubation was carried out in a PCR machine at 30ºC for 90 min. A negative control reaction was set up by replacing the pCDNA3.1ff1b template with empty pCDNA3.1 vector. After incubation, a 1 µl aliquot was removed and mixed with 11 µl 1X SDS sample buffer and the mixture was heated at 70ºC for 15 min to denature the proteins. The denatured samples were subjected to SDS-PAGE in a 10% PAGE gel after which the gel was equilibrated in Towbin transfer buffer (2.5 mM Tris, 19.2 M glycine, 0.1% SDS, 20% methanol) for 20 min at RT. Concurrently, PVDF membrane (Bio-Rad) was activated by submerging in methanol for 2 – 3 sec and equilibrated in Towbin transfer buffer for 20 min at RT.

Proteins were transferred to a PVDF membrane using the Trans-blot Semy-dry apparatus (Bio-Rad) at 15 V for 20 min. Blocking was carried out by incubating the membrane in 1X Tris-buffered Saline with Tween-20 (TBST; 150 mM NaCl, 0.1% Tween-20, 10 mM Tris-Cl, pH7.4) with gentle shaking (~50 rpm) for 1 hr at RT. After blocking, the PVDF membrane was incubated in 1:7500 dilution of Streptavidin-Horse Radish Peroxidase (Streptavidin-HRP; Pierce, IL, USA) with gentle shaking for 1 hr at RT. This was followed by 3 x 5 min washes with 1X TBST and another 3 x 5 min washes with sterile MQ water. The membrane was immersed in substrate solution, which is composed of stable peroxide buffer and luminol/enhancer solution (SuperSignal West Pico Chemiluminescent substrate, Pierce) for 1 – 2 min. Finally, chemiluminescence from the biotin-labeled Ff1b protein was detected by exposing the PVDF membrane to Fuji X-ray film for 1 min in dark.

2.13 Electro-mobility shift assays (EMSA)

Electrophoretic mobility shift assays (EMSA) were performed using the LightShift Chemiluminescent EMSA kit (Pierce). Oligonucleotides containing the putative *cyp11a1* distal (FREd) and proximal (FREp) FREs and the mutated versions of each FRE (Table 2.3) was synthesized and labeled with biotin using the biotin 3' end DNA labeling kit (Pierce). Core regconition sequences of FREs are underlined and mutated residues were highlighted in bold. For each labeling reaction, 50 nmol of single-stranded oligonucleotides was labeled at their 3' end with biotin-11-UTP. The labeled oligonucleotides were subjected to chloroform extraction and complementary oligonucleotides at equal amount were annealed. Annealing was done by heating each pair of oligonucleotides to 100ºC in water bath in a 2 L beaker for 5 min and cooling down to RT slowly in an insulated box overnight.

Table 2.5 Ftz-f1 response elements (FREs) mapped in the zebrafish *cyp11a1* promoter analyzed by electrophoretic mobility shift assay.

Distal FRE	zsccFREdF	5'-GTTGACCTTGGGAAAAGTAAATG-3'
	zsccFREdR	5'-CATTTACTTTTCCCAAGGTCAAC-3'
Mutated distal FRE	zsccFREdMutF	5'-GTTGACCT**C**GG**TG**AAAGTAAATG-3'
	zsccFREdMutR	5'-CATTTACTTT**CA**CC**G**AGGTCAAC-3'
Proximal FRE	zsccFREpF	5'-GTAGTTCATTGTCCTTGACCTGTG-3'
	zsccFREpR	5'-CACAGGTCAAGGACAATGAACTAC-3'
Mutated proximal FRE	zsccFREpMutF	5'-GTAGTTCATT**CA**CC**G**TGACCTGTG-3'
	zsccFREpMutR	5'-CACAGGTCA**C**GG**TG**AATGAACTAC-3'

Core recognition sequences of FREs are underlined and mutated residues were highlighted in bold.

Ff1b protein was produced by *in vitro* transcription and translation from pcDNA3.1ff1b (Liu *et al*., 2003) using the TNT® T7 quick coupled transcription/translation system (Promega). The identity of Ff1b protein produced by

this method was verified as described in Section 2.12. For each binding reaction, 8 µl of the *in vitro* translated mixture of Ff1b was mixed with 1 µg of Poly dI·dC and 20 fmol of the corresponding biotin-labeled DNA probes in 1x binding buffer (10 mM Tris, pH7.5; 100 mM KCl; 1 mM DTT) with a total reaction volume of 20 µl. Reactions were carried out at 25ºC for 20 min. Unbound labeled DNA was separated from protein-DNA complexes by electrophoresis at 100 V in a 5 % acrylamide-0.5% Tris-bovate-EDTA (TBE) gel for approximately 45 min, transferred onto a zeta-probe membrane (Bio-Rad) by electroblotting, and UV cross-linked. Chemi-luminescence from the biotin-labeled DNA bands was detected by exposing the zeta-probe membrane (Bio-Rad) to Fuji X-ray film for 3 – 5 sec in dark.

2.14 Development of Ff1b polyclonal antibodies

A polyclonal antibody for Ff1b was raised against amino acid residues 234-248 (CAYLHQEQSGRGKLE) of Ff1b protein, which corresponds to the N-terminus of ligand binding domain (Fig. 2.3) by Biogenes (Gmbh). This epitope was selected based on the likelihood of antigenicity based on computational analysis using the program Antheprot (Release 5). This peptide sequence was compared to the other Ff1 proteins of zebrafish and a BLAST search was performed against the NCBI protein database to ensure that cross-reactivity to other zebrafish proteins is minimal.

```
Ff1b    --------LVLELQSCDPDEEQVRGKICAYLHQEQSGRGKLEKSRPFSLLCVMADQTLFS 266
Ff1aE   --------LVVELLKCEPDEPQVQAKILAYLQQEQASRGKHEKLNTFGLMCKMADQTLFS 331
Ff1c    STTAPSSFFLNQLLQAEPDEKQLCMRVLASLQREQACRGKHDRLNTFSIMCKMADQTLFG 351
Ff1d    STTAPSSFFLNQLLQAEPDEKQLCMRVLASLQREQACRGKHDRLNTFSIMCKMADQTLFG 351
                :: :* ..:*** *:  :: * *::**: *** :: ..*.::* *******.
```

Figure 2.3 Location of epitope chosen for the generation of Ff1b polyclonal antibody. An epitope spanning 15 amino acid residues of Ff1b at the N-terminal region of ligand binding domain was chosen for the generation of custom-raised polyclonal antibody in rabbit. The residues are highlighted in purple and the alignment with the other three Ff1 isoforms at the corresponding region is shown.

The 15-residues peptide was synthesized by Biogenes and the resultant peptide was conjugated to the carrier protein LPH to ensure the immunogenicity of the peptide. According to the immunization protocol of Biogenes, pre-immune serum was collected from two rabbits (#1659 and #1660) on day 0. Immunization of the rabbits was carried out over a period of two months on day 7, 14, 28, and 56. Bleeding of the immunized rabbits was performed on day 35 and 63 and the polyclonal antibodies produced were delivered as crude antiserum. The reactivity of the antibody produced was tested by Western blot and a clear band corresponding to the size of Ff1b (~50 kDa) was detected in ovary protein extract from an adult zebrafish female. The antiserum produced from rabbit #1660 gave rise to a stronger band as compared to that from rabbit #1659, and thus, the #1660 antiserum of Ff1b was subsequently used for chromatin immunoprecipitation (ChIP) assays.

2.15 Chromatin Immunoprecipitation (ChIP)

ChIP assays were carried out using the ChIP assay kit (Upstate). For every ChIP assay, ~1 X 10^6 of cells was needed and this was estimated to be ~25 mg of ovary tissues by a cell count using hemocytometer. To begin, ovary tissues were freshly extracted from a zebrafish female adult and ~25 mg was placed into each 1.5 ml microcentrifuge tube for each ChIP assay. The ovary tissue was briefly homogenized in 1X PBS using a telfon pestle that was fitted to the 1.5ml microcentrifuge tube until no big clump of tissue was visible. The homogenate was subsequently treated with 1% formaldehyde for 15 min on a nutator at RT. Following the cross-linking of DNA/protein, cells were pelleted by centrifugation at 2000 rpm for 4 min at 4ºC. The cell pellet was then washed twice with chilled 1 x PBS supplemented with a cocktail of protease inhibitor (1 mM PMSF, 1 μg/ml aprotinin, and 1 μg/ml pepstatin A). The washed cell pellet was resuspended in 200 μl of SDS

Lysis Buffer (1% SDS, 10 mM EDTA, 50 M Tris, pH 8.1) followed by 10 min incubation on ice. Lysate was subjected to sonication to shear DNA to length between 200 and 800 bp. Using a Vibra Cell sonicator VC505 equipped with a 3 mm tip and set to 20% of the maximum amplitude (100 V), 14 x 10-sec pulses, separated by a 4 min interval, were shown to be the optimal condition for this amount of ovary lysate.

Sonicated samples were centrifuged for 10 min at 13,000 rpm in a 1.5 ml microcentrifuge tube at 4ºC, and the supernatant was transferred (~200 µl each) into a new 2 ml tube. One tenth of the sonicated supernatant was kept at -20°C and used as positive control for PCR analysis later on. The remaining cell supernatant was then diluted 10-fold with ChIP Dilution Buffer (0.01 % SDS, 1.1 % Triton X-100, 1.2 mM EDTA, 167 mM NaCl, 16.7 mM Tris-HCl, pH 8.1).

To reduce non-specific background, the diluted cell supernatant was pre-cleared with 75 µl of Protein A agarose/salmon sperm DNA (50% slurry) for 30 min at 4°C on a nutator. The 50% slurry of Protein A agarose/salmon sperm DNA was provided by the ChIP assay kit as 1.5 ml packed beads containing 600 µg of sonicated salmon sperm DNA, 1.5 mg of BSA and ~4.5 mg of recombinant protein A resuspended in TE buffer, pH 8.0, containing 0.05 % of sodium azide to a final volum of 3 ml. Agarose was pelleted by centrifugation at 1,000 rpm at 4°C for 1 min after which the supernatant was transferred to a fresh 2 ml tube. Twenty µl of immunoprecipitating antibody (Ff1b antiserum) was added into each tube and incubated overnight at 4°C on a nutator. As a negative control, immunoprecipitation was always performed with the same amount of pre-immune serum in parallel.

The next day, 60 µl of protein A agarose/salmon sperm DNA (50% slurry) was added into each tube and incubated for 1 hr at 4°C on a nutator. Agarose was pelleted by centrifugation at 1,000 rpm at 4°C for 1 min. The supernatant was carefully

removed and discarded. The agarose beads were then washed with 1 ml of each of the following buffers sequentially (provided as part of the ChIP assay kit). Each washing was carried out for 4 min at 4°C with shaking on a nutator.

i) Low Salt Immune Complex Wash Buffer (0.1% SDS, 1% Triton X-100, 2 mM EDTA, 150 mM NaCl, 20 mM Tris-HCl; pH 8.1)

ii) High Salt Immune Complex Wash buffer (0.1 % SDS, 1% Triton X-100, 2 mM EDTA, 500 mM NaCl, 20 mM Tris-HCl; pH 8.1)

iii) LiCl Immune Complex Wash Buffer (0.25 M LiCl, 1% IGEPAL-CA630, 1% deoxycholic acid sodium salt, 1 mM EDTA, 10 mM Tris; pH 8.1)

iv) TE Buffer (1 mM EDTA, 10 mM Tris-HCl; pH 8.0), twice

The histone complexes were eluted from antiserum by adding 250 µl of elution buffer into each tube. Elution buffer was prepared fresh by mixing an equal volume of 2% SDS with 0.2 M $NaHCO_3$. Samples were tapped briefly and incubated at RT for 15 min on a nutator with gentle shaking. The agarose beads were spun down as above and the eluates were transferred and pooled into a new 1.5 ml microcentrifuge tube for each sample. Elution was repeated one more time to produce ~500 µl of eluates in total for each ChIP sample. To reverse cross linking, 20 µl of 5M NaCl was added into each eluate and heated at 65°C in a heat block for 4 h. Cross linking reversal was also done on input samples where 1 µl of 5 M NaCl was added for each 20 µl of input sample. If necessary, samples were stored at -20°C.

Following the cross-linking reversal, 10 µl of 0.5 M EDTA, 20 µl of 1 M Trsi-HCl (pH 6.5), and 2 µl of 10 mg/ml Proteinase K were added to each eluate and incubated for 1 hr at 45°C in a heat block. DNA was then recovered by PCI extraction using heavy phase lock gel (1.5 ml, Eppendorf) and ethanol precipitation. Briefly, equal volume of eluate and PCI (25:24:1) solution (~500 µl each) was mixed in each of the 1.5 ml phase lock gel tube with vigorous shaking for ~1 min. The mixtures were then spun at 13,000 rpm, RT, for 5 min to separate the organic and aqueous

phases. The upper aqueous phase was transferred into a fresh 2 ml microcentrifuge tube. One µl of glycogen (Roche, 20 mg/ml) was added into each ChIPed sample or 0.3 µl for the input sample prior to ethanol precipitation to increase the visibility of the small DNA pellet. Subsequently, 2.5 volume (1250 µl) of chilled absolute ethano was added and DNA was allowed to precipitate at -20 °C for 2 hr to overnight. Precipitated DNA was then spun down at 14,000 rpm, 15 min at 4°C. The visible DNA pellet was then washed with 1 ml of chilled 70% ethanol and the final pellet was air-dried for about 10 min at RT, and resuspended in 20 µl of MQ water.

The immunoprecipitated DNA samples were analyzed for enrichment in the genomic region of interest by PCR analyses. Standard PCR reactions were set up using Promega GoTaq® polymerase system with primers targeting FREd and FREp regions within *cyp11a1* promoter. As negative control, a pair of primers targeting the *keratin8* promoter region, where FRE is absent, was included. About 3 – 5 µl of DNA was used for each 20 µl PCR reaction. Cycling parameters were 95 °C for 5 min and 30 cycles of 95°C for 30 sec, 56°C for 30 sec, 72°C for 1 min followed by a final elongation step at 72°C for 10 min. Ten µl of each PCR product was checked using 1.2% TAE gel with the 100 bp DNA ladder to determine the sizes of amplicon.

2.16 General maintenance of zebrafish

Fish stocks were maintained in the S2-L2 aquarium facility of the Department of Biological Sciences, National University of Singapore. Embryos were obtained by natural spawning and cultured in egg water medium at 28.5°C (Westerfield, 2000). Egg water is composed of instant ocean sea salt (60 µg/ml) and methylene blue (30 µg/ml). Staging of embryos was carried out according to Kimmel et al., (1995). Embryos meant for histological analysis were treated with 0.03% phenylthiourea (Sigma, MO, USA) from ~10 hpf, to inhibit melanin pigment formation (Karlsson *et*

al., 2001). Feeding was initiated for larva at 4 – 5 dpf with larval diet (Aquatic Eco-systems Inc, FL, USA). At about 8 – 10 dpf, artemia feeding was initiated. Up to 50 larvae were maintained in a 1 L tank until they were 3 – 4 weeks old. The juvenile fishes were eventually transferred and maintained in 2.5 L tanks in the AHAB aquarium system. No more than 25 adult fishes were kept in one 2.5 L tank at a time.

2.17 Generation of the ff1bEx2EGFP stable transgenic zebrafish line

The ff1bEx2EGFP transgenic line was generated using DNA insert released from BAC plasmid pBACff1bEx2EGFPKan by *Not* I digestion. This insert encompasses ~100 kb of zebrafish genomic sequences including the *ff1b* locus (~25 kb) with the EGFP-Kan^r cassette inserted into Exon 2 of *ff1b* by homologous recombination (Section 2.8.1). To generate a linear DNA fragment from pBACff1bEx2EGFPKan, 20 – 30 μg of BAC plasmid was digested by *Not* I restriction enzyme at 37°C overnight. The digested DNA was purified by PCI extraction using heavy phase lock gel (1.5 ml, Eppendorf) and ethanol precipitation. Briefly, equal volume of phenol: chloroform: isoamyl (25: 24: 1) was added into the overnight digestion mixture in a 1.5 ml microcentrifuge tube containing 300 μl of phase lock gel. The tube was sealed with parafilm and shaked on a rocking platform at RT for 30 min. The aqueous and organic phase was separated by centrifugation at 13,000 rpm for 5 min at RT. The upper phase was transferred to a fresh 1.5 ml tube and DNA was precipitated with an equal volume of isopropanol. The mixture was inverted for about 10 times to thoroughly mix and immediately centrifuged at 13,000 rpm for 15 min at 4°C. The DNA pellet was washed twice with 70 % ice-cold ethanol and the DNA pellet was finally resuspended in an appropriate volume of 1X TE buffer (~50 μl).

For microinjection, the purified pBACff1bEx2EGFPKan/NotI fragment was diluted to a final concentration of 50 ng/µl in 1x Danieau's buffer containing 0.05% phenol red. About 4.6 nl of this injection solution was microinjected into the animal pole of wild-type zebrafish embryos at one-cell stage. At 36 to 48 hpf, injected embryos were screened for GFP fluorescence. Only those embryos carrying strong GFP signal in *ff1b*-expressing tissues (interrenal and VMH) were selected and maintained to adulthood. When fishes reached adult stage (3-4 months), they were inter-bred to screen for positive founder that could give rise to progeny showing GFP expression at the above tissues. F_1 progeny was grown up to adulthood and out-crossed with wild-type zebrafish to produce F_2 progeny. The F_2 progeny and subsequent generations were in-crossed among siblings to produce the next generation.

2.18 Microinjection of DNA constructs and morpholinos

Micropipettes were prepared from 3.5-inches borosilicate glass capillaries with an internal diameter of 0.5 mm (WPI, Florida, USA) on a Model PC-10 Micropipette puller (Narishige, Tokyo, Japan). Pulled capillaries were cut manually with sterile blade under 40X magnification of a Bausch & Lomb dissection microscope at an angle of ~45° to produce slanted and sharp tips. Cut capillaries were back-filled with mineral oil (Sigma) using a 10 ml syringe fitted with an 18.5 gauge needle. Capillaries were placed horizontally upon two rows of blue tack plastic adhesive in 140 mm petri dishes for storage prior to use.

Freshly laid embryos were collected in egg water and transferred onto a 90 mm petri dish containing 1.5% agarose with trenches for fitting embryos using a pasteur pipette (Westerfield, 2000). Excess water surrounding the embryos was removed by aspiration although a small amount of water must be retained to keep the embryos

moist. Microinjection was performed using a Nanoliter 2000 injector (WPI, Florida, USA) equipped with a micromanipulator to enable rapid fine insertion and withdrawal of the micropipettes during the process of microinjection. The polished borosilicate glass capillary was fixed onto the pistol of Nanoliter 2000 injector. Excess mineral oil was removed by wiping with paper towel. Mineral oil in the capillary was emptied by pushing the 'Empty' button until the stainless steel needle in the pistol reached 1/3 of the capillary to ensure proper fixation of capillary. The injection solution containing DNA or morpholino was back-filled into the capillary by placing the tip of capillary into 2 – 3 µl injection solution and pushing the 'Fill' button at the same time. After microinjection, embryos were cultured in egg water at 28.5°C.

DNA constructs were microinjected at a concentration of 50 ng/µl in 1X Danieu's buffer (58 mM NaCl, 0.7 mM KCl, 0.4 mM $MgSO_4$, 0.6 mM $Ca[NO_3]_2$) and 0.25% phenol red. About 450 pg (4.6 nl) was delivered by direct injection into the animal pole of one-cell stage embryos. For all DNA constructs and morpholinos, the injection solution was stored at 4°C for up to a week, after which fresh injection solution must be prepared.

Morpholinos were designed and synthesized by Genetools LLC (OR, USA). A stock solution of 2 mM was prepared by dissolving the lyophilized powder in MQ water and stored at -80°C. The required injection concentration was diluted from the stock solution into 1X Danieau's buffer containing 0.05% phenol red. Morpholino solutions were delivered into the yolk directly underlying the blastodisc. Microinjected embryos were maintained in egg water in 100 mm petri dish and no more than 100 embryos were allowed in one dish. At about 5 to 6 hours after microinjection, dead embryos were removed and egg water was changed every 3 to 4 days or whenever they turned turbid. At ~30 hpf, morpholino-microinjected embryos

were checked under microscope for non-specific toxic effects including reduction of the head and eyes, an amorphous appearance of cells in the body, downward curving body axis and edema of the pericardial and yolk sac. Only embryos that showed normal phenotype at this stage were allowed to develop further for subsequent molecular or histological analyses.

2.19 Microscopic imaging of EGFP expression in zebrafish embryos and larvae

EGFP expression in live embryos and larvae (transgenic or plasmid-injected) was monitored for UV epifluorescence with a Zeiss Axiovert 25 inverted microscope. Embryos or larvae were anaesthetized in 0.001% 2-phenoxyethanol after which they were transferred to concave borosilicate glass slides or optical chambers covered with borosilicate cover slip of 0.15 mm thickness. To strictly prevent the embryos or larvae from moving around, they were embedded in 1.5% agarose at different orientations on a concave glass slide prior to microscopic analyses. The fixed embryos or larvae were manipulated to different orientations the same way for microscopic analyses.

Epifluorescence pictures were captured using the Zeiss Axiovert 200M microscope with imaging software AxioVision (version 4.3). The illumination of EGFP fluorescence was achieved through excitation from a high pressure mercury lamp (50-watt, Zeiss) using filter sets 38 of Zeiss (BP 470/40, FT 495, BP 525/50). Images were captured with exposure time set automatically. Exposure time normally falls into the range of 500 msec to 1 sec and manual adjustment was made whenever necessary to achieve the optimal fluorescence.

Confocal images were taken using Olympus IX70 microscope equipped with FluoView300 imaging software using 488 nm excitation and 510-550 nm band-pass filters. Images were captured in Kalman mode (2X) with PMT voltage set to 600 to 700 V. Gain and Offset were always set as 1.0 to achieve the lowest background noise.

Three dimensional images were always consolidated from serial optical sections, which were taken at ~2 or 3 μm intervals using a 10X or 20X Plan-Neofluar objective lenses. Raw image collection and processing were performed using the Olympus FluoView software (version 1.7a).

2.20 Cryostat sectioning of transgenic ff1bEx2EGFP zebrafish embryos

Samples were prepared for cryostat sectioning essentially as described in Chapter 8 of the Zebrafish Book (Westerfield, 2000). Sections of 20 μm thickness were collected on a Leica CM1900 Cryostat (Leica, Germany). Images of cryo-sections were captured using the Zeiss Axiovert 200M equipped with imaging software AxioVision (version 4.3) or using confocal microscope (Olympus IX70) equipped with Olympus FV300 imaging software.

2.21 Isolation of genomic DNA from zebrafish larvae

Zebrafish larvae were kept in egg water at 28°C until 7 dpf. Genomic DNA was prepared from a single larva (transgenic or wild-type). Each larva was transferred into a 1.5 ml microcentrifuge tube and rinsed with 1 ml of sterile MQ water and as much as liquid was removed before the addition of 100 μl of gDNA extraction buffer (10 mM Tris pH8.2, 10 mM EDTA, 200 mM NaCl, 0.5% SDS). Proteinase K and RNase A were freshly added into the extraction buffer to a final concentration of 200 μg/ml and 100 μg/ml respectively. Samples were incubated in a 55°C incubator with gentle shaking for 5 hr after which DNA was precipitated with 0.1 volume of 3 M sodium acetate (pH 5.2) and 2.5 volume of ice-cold absolute ethanol. Samples were mixed well and incubated at RT for 15 minutes before they were centrifuged at 13,000 rpm for 5 minutes. The supernatant was then removed and DNA pellet was rinsed with 70% ethanol once and centrifuged again. The final DNA pellet was allowed to air dry

after which it was dissolved in 50 µl of 10 mM Tris-HCl buffer. Integrity and quantity of the purified DNA was assessed on 0.7% agarose gel and by Nanodrop spectrophotometer measurement. About 2 – 3 µl of DNA was used as template in each PCR reaction for the detection of transgene or endogenous gene by PCR amplification using Promega GoTaq® polymerase.

2.22 Treatment of zebrafish embryos with aminoglutethimide (AG)

Crystalline aminoglutethimide (Sigma) was first dissoved in 0.2 N HCl to a concentration of 0.2M and then diluted to 1 mM in egg water. The volume of 1M HEPES (pH 7.9) required to adjust the 1 mM aminoglutethimide solution to pH 7.4 was determined as 50 µl for every 30 ml of egg water(Chan and Tan, 1988), and equal amount of HEPES was added to other embryos cultures in the same experiment to control for any effects that may be caused by HEPES. The final concentration of HEPES added was 2.5 nM and did not produce any observable defects in embryos. Embryos were treated from 8 hpf onwards till 10 dpf and aminoglutethimide was renewed at 5 dpf. For every treatment, about 100 embryos or larvae were maintained in 120 ml of egg water in a 250 ml beaker.

CHAPTER 3

Ff1b as a transcriptional regulator of *cyp11a1*

3.1 Introduction

Zebrafish *ff1b* displays remarkable homology to mammalian *SF-1* at many levels including gene and protein structure, expression profile and gene function (Chai and Chan, 2000; Chai, 2002; Chai *et al*., 2003). Morpholino knockdown of *ff1b* gene function led to the ablation of steroidogenic interrenal cells, as characterized by the downregulation of *cyp11a1* transcripts and 3β-Hsd enzymatic activity (Chai *et al*., 2003; Hsu *et al*., 2003). Furthermore, *ff1b* morphants displayed late morphological defects that were indicative of diminished osmoregulation, which was most likely attributed to corticosteroids deficiency (Chai *et al*., 2003). This is highly reminiscent to the findings from *Sf-1* knockout studies in mice where the pups lacked adrenal development and died shortly after birth due to glucocorticoid and mineralocorticoid deficiency (Luo *et al*., 1994; Sadovsky *et al*., 1995; Shinoda *et al*., 1995). These findings point to the conserved roles of Ff1b in the transcriptional regulation of genes encoding key steroidogenic enzymes involved in the steroid biosynthesis pathway.

In mammals, SF-1 has long been established as a key transcriptional regulator of genes encoding steroidogenic enzymes. Indeed, SF-1 was initially identified based on its ability to bind and activate the gene promoter of steroidogenic enzymes CYP11A1, CYP11B1, and CYP21 (Morohashi *et al*., 1992; Rice *et al*., 1991). As discussed in Section 1.7, SF-1 participates in regulating the expression of almost all adrenal and testicular steroidogenic genes including the steroid acute regulatory protein *StAR*, hydroxysteroid dehydrogenases (*HSD3B* and *HSD11B*), and those encoding P450 cytochrome enzymes in the P450 family (*CYP11A1*, *CYP11B1*,

CYP17 and *CYP21*). In most of these studies, the transcriptional regulatory effect of SF-1 on steroidogenic genes was demonstrated by transient transfection studies and a majority of them focus on *CYP11A1* gene promoter, which is by far the best characterized gene promoter regulated by SF-1, especially with regard to its responsiveness to cAMP induction (Ahlgren *et al*., 1999; Chen and Guo, 2000; Guo *et al*., 1994; Guo *et al*., 2007a; Lan *et al*., 2007; Pestell *et al*., 1993; Sher *et al*., 2007; Watanabe *et al*., 1994). This is not surprising because *CYP11A1* encodes the very first enzyme that catalyses the first, rate-limiting step in steroidogenesis and is known to be highly conserved throughout vertebrate evolution (Norris, 2006).

In view of the apparent conservation of the major steroidogenic pathway between mammals and teleosts (Hsu *et al*., 2006; Hu *et al*., 2001a), it is reasonable to postulate that Ff1b is responsible for regulating the steroid hydroxylases in zebrafish. The effect of Ff1b transcriptional activity on the putative target promoter of steroidogenic genes, however, had not been dissected before this study was conducted. The isolation of gene promoters that are responsive to Ff1b transcriptional activity would aid our understanding of how Ff1b regulate its target genes and also in ascertaining its functional analogy to its mammalian counterpart, SF-1, in the regulation of steroidogenesis.

On this basis, we isolated the 5' upstream flanking sequence of several zebrafish steroidogenic genes, namely *cyp11a1, star, cyp17, and 3β-hsd*, which could potentially be regulated by Ff1b. By computational analysis, *cis*-acting regulatory elements that could potentially regulate the expression of these genes were identified. Importantly, putative FREs have been mapped at the promoter of *cyp11a1*, *cyp17*, and *star*. Transgenesis studies in zebrafish embryos and transient transfection studies in Y1 cells established the 1.7 kb zebrafish *cyp11a1* promoter as a functional promoter

and it was subsequently used to dissect the regulatory functions of FREs and Ff1b. The functions of the two FRE mapped in the *cyp11a1* promoter were examined closely by a series of deletion and mutagenesis studies in Y1 cells. Subsequent characterization by EMSA and ChIP assay demonstrated that Ff1b bound both FREs, and the binding to the distal FRE seemed to be stronger than that of proximal FRE. These combined approaches have established Ff1b as the central regulator of the basal transcriptional activity of the 1.7 kb *cyp11a1* promoter. These data present the first experimental evidence showing the transcriptional regulatory effect of Ff1b on the expression of steroidogenic enzymes, and thus, steroidogenesis in zebrafish.

3.2 The isolation and analyses of gene promoters potentially regulated by Ff1b

As the zebrafish genome database was not yet available back when this study was initiated, the 5' promoter region of *cyp11a1* was isolated by a modified genome walking method. Gene-specific primers were also designed to isolate the 5' upstream promoter of three other steroidogenic enzyme genes, namely *cyp17*, *star*, and *3β-hsd*. The transcriptional regulation of these four genes was expected to be highly important, as they encode enzymes sitting on the top of steroidogenesis pathway. They are abundantly expressed in all steroidogenic tissues and their expression levels are likely to be higher than those enzymes catalyzing the peripheral reactions in the same pathway because they are required for the synthesis of all classes of steroid hormones (Payne and Hales, 2004; Sewer *et al*., 2007). The 5' upstream promoter fragments of these steroidogenic genes at various lengths were cloned into pGEM-T vector and sequenced, after which the sequences were computationally analyzed for transcription factor binding sites (TFBSs). Subsequently, the transcriptional activities of these promoter fragments were assessed experimentally in zebrafish embryos and Y1 adrenocortical cell line.

3.2.1 *In silico* identification of *Ftz-F1* response elements in the 5' putative promoter of steroidogenic enzyme genes

Sequencing data of the four putative 5' promoters for *cyp11a1*, *cyp17*, *star*, and *3β-hsd* showed that the isolated sequences span 1735, 2676, 1262, and 1233 bp, respectively. The sequences were subsequently compared to the zebrafish genome database at Ensembl Genome browser (http://www.ensembl.org/Danio_rerio/Info/Index), which became available online as this study was ongoing. The genomic sequences of the above four genes were mapped to the 5' promoter of gene entry ENSDARG00000002347, ENSDARG00000006137, ENSDARG00000033566, and ENSDARG00000019747, respectively, at the Ensembl database.

The 5' upstream putative promoter sequences (upstream of the predicted transcription start site, TSS +1) were then analyzed bioinformatically for TFBS using the Genomatix MatInspector server online at http://www.genomatix.de/ (Cartharius *et al*., 2005). The resulting matches for TFBSs were saved in Microsoft Excel format and analyzed manually for binding sites that are potentially relevant to the regulation of steroidogenic genes. Only TFBSs that showed a matrix similarity score of >0.90 were considered significant. A perfect match to the matrix would be assigned a score of 1.00 (each sequence position corresponds to the highest conserved nucleotide at that position in the matrix).

When screening the TFBSs predicted by MatInspector, attention was paid particularly to binding sites predicted for Vertebrate Steroidogenic Factor, which include LRH-1 and SF-1, with consensus sequence CAAGgtca, where nucleotide in capital letters denotes the core sequence used by MatInspector. It has been shown previously that Ff1b binds to the same consensus site as SF-1 and LRH-1 (Liu *et al*., 2003) and these binding sites are termed *Ftz-F1* response element (FRE) throughout

this study. Besides FRE, *cis*-elements that have previously been implicated in the transcriptional regulation of steroidogenic genes including cAMP responsive element (CRE) and binding sites for Sp1, AP-1, and Nuclear Factor-1 (NF-1) have also been highlighted (Chou *et al*., 1996; Guo *et al*., 2003; Watanabe *et al*., 1994). In addition, binding sites of transcription factors or coregulators that have been previously shown to interact physically with SF-1 in mediating its transcriptional activity such as SOX factors, GATA factors, WT1 were highlighted (De Santa *et al*., 1998; Nachtigal *et al*., 1998; Shi *et al*., 2008; Tremblay and Viger, 1999). These matches were manually translated into schematic diagram that shows the relative positions of each *cis*-element drawn to scale (Fig 3.1).

Notably, at least one FRE (except for *3β-hsd*) was predicted in each of the four promoters analyzed (Fig. 3.1). For *cyp11a1* and *cyp17*, two putative FREs were mapped at locations proximal (within 100 bp) and distal (-1500 to -1000 bp) to the predicted TSS. The *star* promoter contains only one FRE at -661 to -648 while the *3β-hsd* promoter contains no FRE. In all four promoters, binding sites for GATA factors, SOX factors, WT1, Sp1, and AP-1 that could potentially interact with Ff1b to modulate its transcriptional activity were identified at several locations. Among these factors, Sp1 and AP-1 have been implicated in the transcriptional activation of human CYP11A1 promoter (Guo *et al*., 2007b). In addition, three CREs were predicted in all four promoters indicating that they could potentially respond to cAMP, which serves as an important messenger in modulating the regulation of steroid synthesis. Lastly, motifs for NF-1, which has been implicated in the transcriptional regulation of human steroidogenic genes (Chou *et al*., 1996), were also identified in the putative promoter regions of *cyp17* and *3β-hsd*.

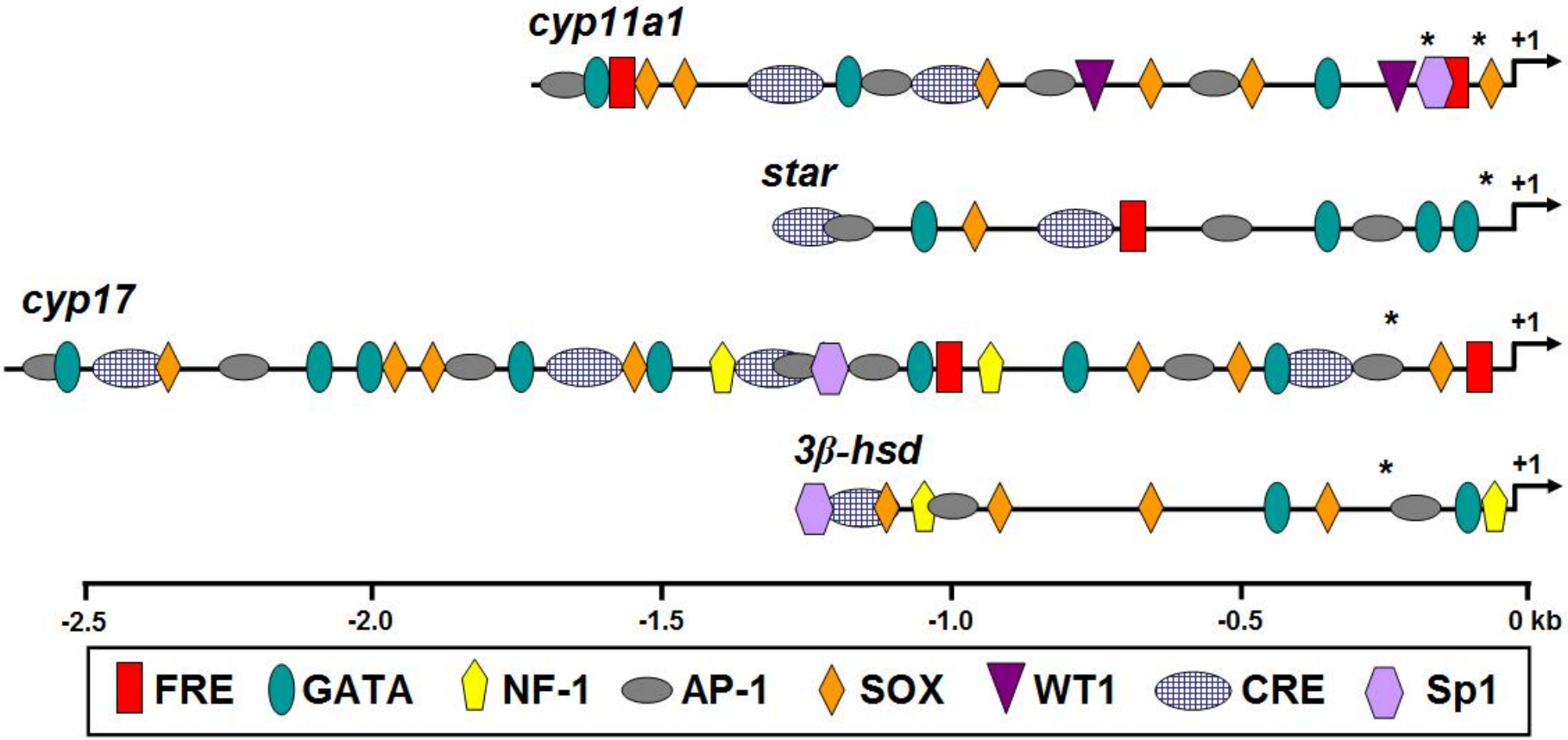

Figure 3.1 Identification of *cis*-elements that could potentially regulate the expression of zebrafish steroidogenic genes, including *cyp11a1*, *star*, *cyp17*, and *3β-hsd*. The 5' promoter sequences of the above four zebrafish genes spanning 1735, 2676, 1262, and 1233 bp respectively were extracted from Ensembl genome browser *in silico*. Binding sites of the transcription factors indicated were predicted using the web-based MatInspector program. Only binding sites for transcription factors that have previously been implicated in the transcriptional regulation of steroidogenic gene promoter or in SF-1 transcriptional activity were shown. The location of TATA boxes predicted in proximity to the predicted transcription start site +1 were shown in asterisk (*).

Taken together, *in silico* analysis of the putative gene promoters of *cyp11a1*, *star*, *cyp17*, and *3β-hsd* revealed important *cis* – acting elements that could potentially regulate their expression. The *cyp11a1* and *cyp17* promoter stand out among the four promoters, as both of them possess two FREs providing a promising site of regulation for Ff1b.

3.2.2 Assessment of promoter activity by transient transgenesis in zebrafish embryos

To determine whether these promoters could drive the expression of EGFP reporter gene specifically to steroidogenic tissues, the promoter regions of *cyp11a1*, *star*, *cyp17*, and *3β-hsd* were subcloned from pGEM-T vector into pEGFP-1 vector. The resulting EGFP expression constructs were then microinjected into zebrafish embryos at 1-2 cell stage and the embryos were monitored for EGFP expression at early developmental stages from 32 hpf to 3 dpf. Observation from the microinjection experiment is summarized in Table 3.1.

Table 3.1 The 1.7 kb *cyp11a1* promoter drives tissue-specific expression in zebrafish embryos.

Gene	Source of genomic library	Length of putative promoter isolated	Site of EGFP expression in zebrafish embryos
cyp11a1	*Sph* I	1735 bp	Interrenal and genital ridge
star	*Nsi* I	1262 bp	No expression
cyp17	*Sph* I	2676 bp	No expression
3β-hsd	*Sph* I	1233 bp	No expression

Out of the four promoters studied, only the 1.7 kb promoter of *cyp11a1* specifically expressed EGFP in the interrenal and genital ridge from ~32 hpf onwards (Fig. 3.2). The percentage of fluorescent embryos was, however, only ~10-15% (n = 358) indicating that the promoter activity is not at its full complement. Nevertheless,

the 5' putative promoter of *cyp11a1* stands out as the best target promoter candidate for characterization in relation to Ff1b transcriptional activity, as it drives the expression of EGFP reporter genes specifically to the tissues (interrenal and genital ridge) where Ff1b is endogenously expressed. This met our original intention to study the gene promoter of Cyp11a1 as the first rate-limiting step in steroidogenesis.

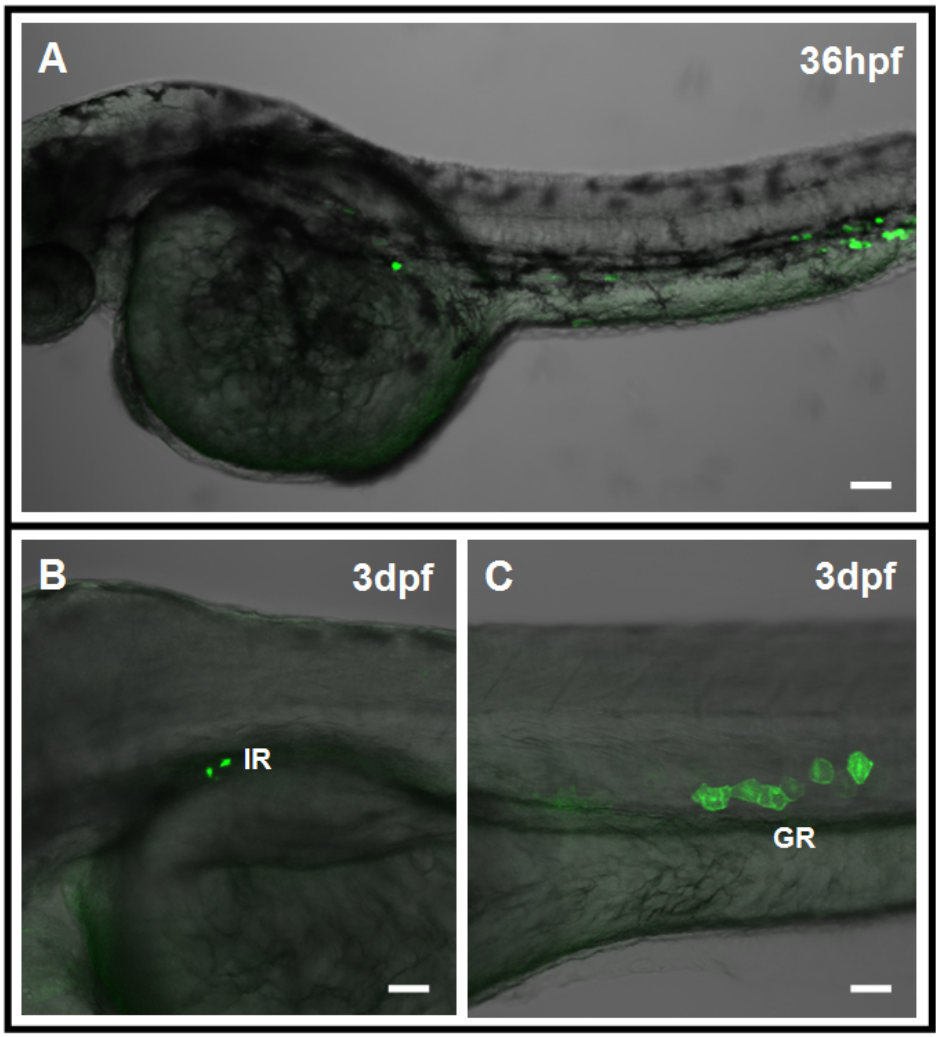

Figure 3.2 The 1.7 kb zebrafish *cyp11a1* promoter targets EGFP specifically to the steroidogenic tissues, the interrenal and genital ridge, at early stages of development. The 1.7 kb zebrafish *cyp11a1* promoter was cloned into pEGFP-1 vector and microinjected into zebrafish embryos at 1-2 cell stage. Injected embryos were monitored for EGFP expression from 32 hpf onwards until 3 dpf. Scale bar, 100 μm. Abbreviations: IR, interrenal; GR, genital ridge.

3.2.3 Assessment of promoter activity by transient transfections in Y1 adrenocortical cells

Following the initial assessment of promoter activity in zebrafish embryos, the promoter fragments were concomitantly cloned into pGL3Basic luciferase reporter vector for transient expression studies in Y1 adrenocortical cells, which endogenously express SF-1 (Rainey *et al*., 2004). These plasmids containing the corresponding promoter fragments upstream to the luciferase reporter gene were transiently transfected into Y1 cells after which cells were harvested for dual-luciferase assay. In agreement with the observations from microinjection experiment, only the 1.7 kb *cyp11a1* promoter was able to activate the luciferase reporter to a level that was ~12-fold of the promoterless pGL3Basic vector (Fig. 3.3). It is intriguing that the other three gene promoters were not functional in Y1 cells despite the fact that two out of three promoter possess at least one FRE. This might be due to the presence of repressor element or the absence of crucial *cis*-elements that are required to activate transcription from the three promoter. Collectively, the transient transgenesis in zebrafish embryos and transient transfection studies in Y1 demonstrated the functionality of the 1.7 kb *cyp11a1* promoter of zebrafish. Subsequent molecular characterization with regard to Ff1b transcriptional activity focused on this 5' promoter region of *cyp11a1*.

3.3 Comparison of *cis*-elements in the 1.7 kb promoter of zebrafish *cyp11a1* to its counterpart in other species

The 1.7 kb putative promoter sequence of *cyp11a1* matches database location 158,905-160637, Contig AL929050.6 of chromosome 25 at the Ensembl genome browser of zebrafish (Zv 7, 2007). When 2 kb of zebrafish *cyp11a1* 5' flanking sequence was compared to the green spotted pufferfish *Tetraodon nigroviridis*, mouse,

and human *cyp11a1*, with regard to the *cis*-elements predicted by MatInspector, conserved modules of binding sites for transcription factors SF-1, GATA factors, AP-1, Sox-related factors and WT1 were evident (Fig. 3.4).

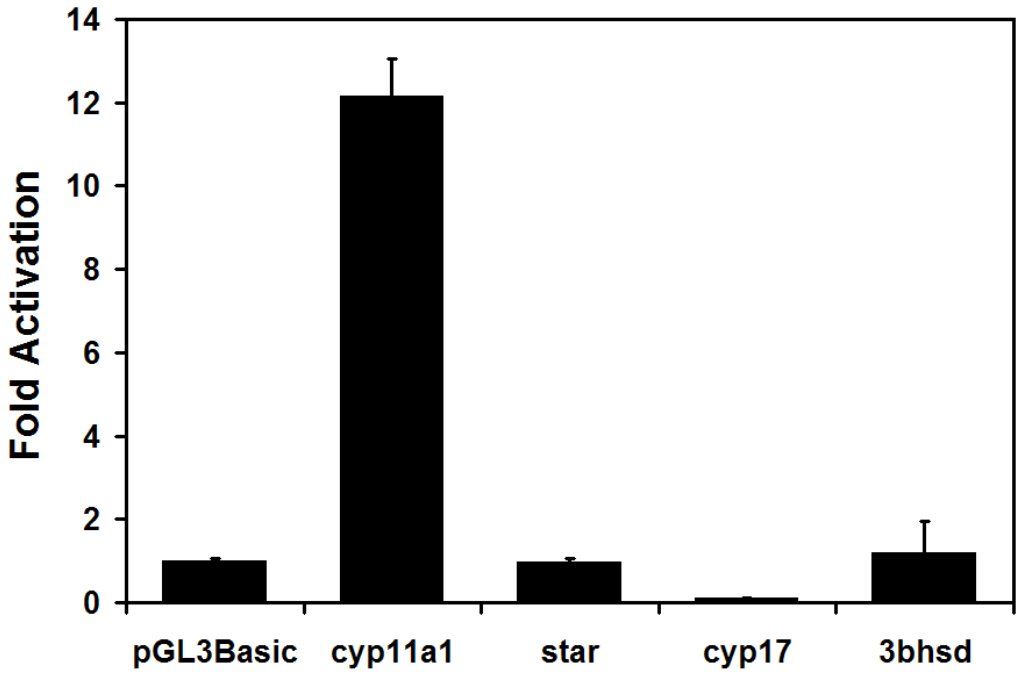

Figure 3.3 Evaluation of promoter activity of zebrafish *cyp11a1*, *star*, *cyp17*, and *3β-hsd* in Y1 adrenocortical cells. The four putative promoters were cloned upstream to luciferase in pGL3Basic vector and transfected into Y1 adrenocortical cells. Renilla luciferase expression vector, pRL-SV40, was co-transfected for normalization of transfection efficiency. Data are expressed as fold activation above the normalized luciferase activity measured from cells transfected with promoterless pGL3Basic vector (adjusted to 1-fold) in one representative experiment, and represent the mean of luciferase activity ± SEM ($n = 4$).

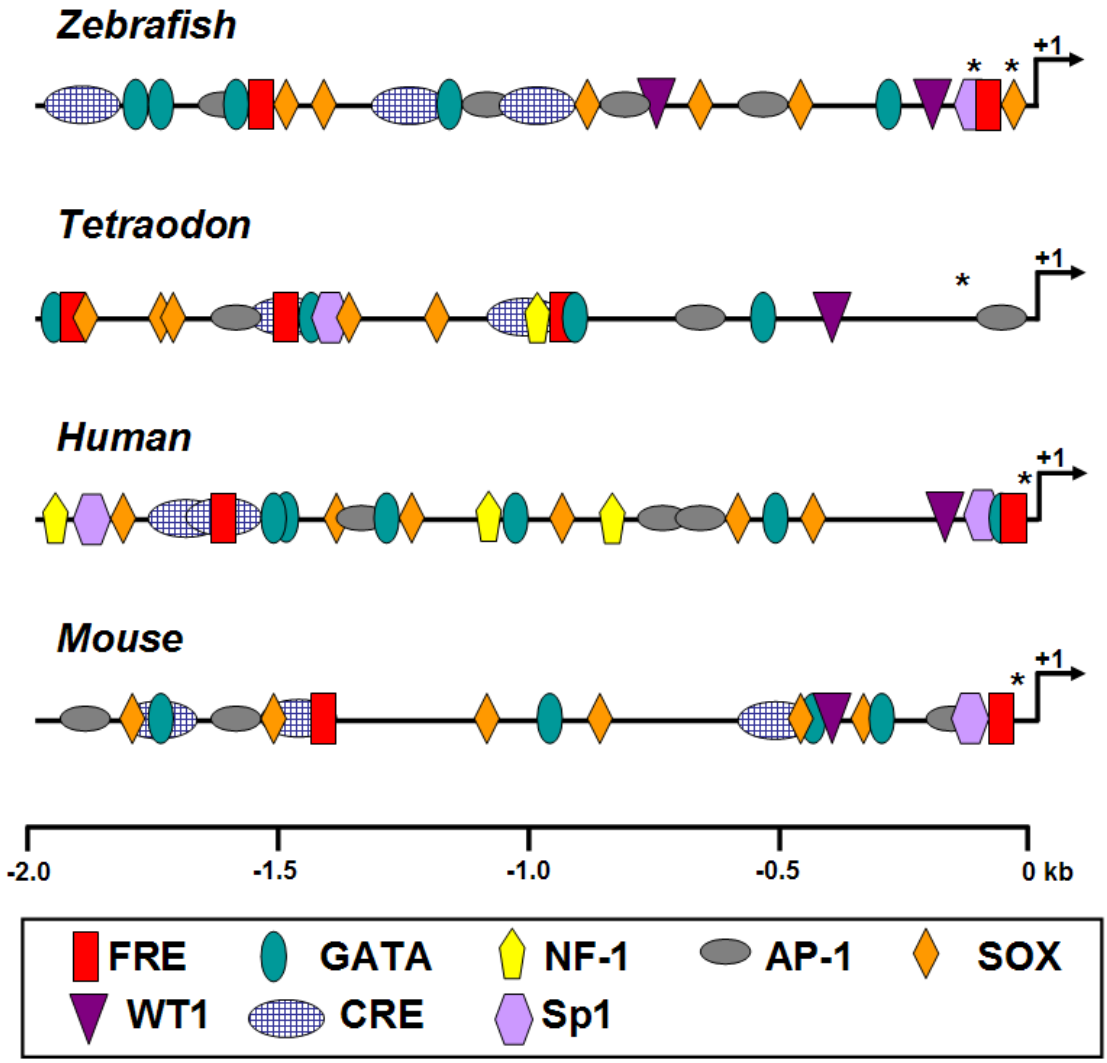

Figure 3.4 Conservation of *cis*-elements predicted in the 5' flanking promoter region of zebrafish *cyp11a1* in comparison to the equivalent 2 kb region in the gene promoter of Tetraodon, human, and mouse. Binding sites of the transcription factors indicated were predicted using the web-based MatInspector program. Only binding sites for transcription factors that have previously been implicated in the transcriptional regulation of *CYP11A1* promoter or in SF-1 transcriptional activity were shown. The conserved elements are indicated by different shapes in different colours. The location of TATA boxes identified in proximity to the transcription start site +1 are indicated by asterisk (*).

At least two cAMP response element (CRE) were identified in the 5' promoter of all species. There are at least two FREs within the 5' promoter region and the location of these binding sites is highly conserved across zebrafish, human, and mouse. In this study, two putative FREs that have been predicted within the 1.7 kb promoter are designated proximal FRE (FREp) at -68/-56 bp and distal FRE (FREd) at -1484/-1472 bp relative to the predicted TSS +1. Two TATA boxes have been identified upstream (-116/-100) and downstream (-43/-27) to the FREp but the actual TSS has yet to be determined experimentally. Collectively, the *in silico* comparison of the of zebrafish *cyp11a1* promoter to human, mouse, and tetraodon pufferfish revealed highly conserved *cis*-elements that are likely to play a role in modulating their expression. Most importantly, locations of FREs mapped are highly conserved across different species indicating their crucial roles in mediating the regulation of the *cyp11a1* gene.

3.4 Activity of the zebrafish 1.7 kb *cyp11a1* promoter in comparison to its human counterparts

Considering the high degree of conservation between the human and zebrafish *cyp11a1* promoter, we wanted to find out whether the two promoters exhibit similar niche of activity. The human promoter has been well characterized in terms of the functional importance of the two FREs and the minimal length required to recapitulate the endogenous *CYP11A1* expression (Guo *et al*., 1994; Hu *et al*., 2001b). In a transgenic mouse study, it has been reported that the 4.4-, 2.3-, and 1.7 kb promoter of human *CYP11A1* could drive *lacZ* reporter expression specifically to the adrenal and gonads (Hu *et al*., 1999; Hu *et al*., 2001b). It would be interesting to look at the activity of the 1.7 kb human promoter in comparison to the zebrafish promoter by trangenesis studies in zebrafish embryos and different mammalian cell lines of steroidogenic and non-steroidogenic origins.

3.4.1 Assessment of promoter activity and responsiveness to *ff1b* overexpression in zebrafish embryos

The human *CYP11A1* promoter spanning 4.4-, 2.3-, and 1.7 kb (kind gift from Prof. B.C. Chung, Academia Sinicia, Taiwan) that have been shown previously to drive tissue-specific expression of *lac*Z in transgenic mice were cloned into pEGFP-1 vector and microinjected into zebrafish embryos. Since the zebrafish and human promoters contain highly conserved *cis*-regulatory elements, it is reasonable to hypothesize that they would display similar level and niche of activity. To our surprise, none of the human promoter fragments were able to target EGFP expression specifically to steroidogenic tissues in zebrafish embryos. Observation for tissue-specific EGFP expression was initiated from 24 hpf onwards until 10 dpf and no trace of EGFP expression was seen at all.

To quantify the promoter activity and to evaluate their responsiveness to *ff1b* overexpression in zebrafish, the above promoter fragments were cloned into pGL3Basic vector and the resulting human or zebrafish *cyp11a1-luc* reporter plasmids were microinjected into zebrafish embryos for transactivation assay as described previously (Liu *et al*., 2003). While the microinjection of various *cyp11a1*-luc plasmids measured the intrinsic promoter activity, the co-injection of these promoter constructs with overexpression plasmid of *ff1b* measured their responsiveness to Ff1b transcriptional activity. Since *ff1b* is not expressed maternally and its zygotic expression initiates only after 20 hpf, zebrafish embryos provide a good *in vivo* context for evaluating the effects of Ff1b transcriptional activity on these promoter. In all microinjection experiments, plasmid pRL-SV40 was co-injected to allow for normalization of luciferase activity. The embryos were harvested and homogenized for luciferase assay at 14 hpf.

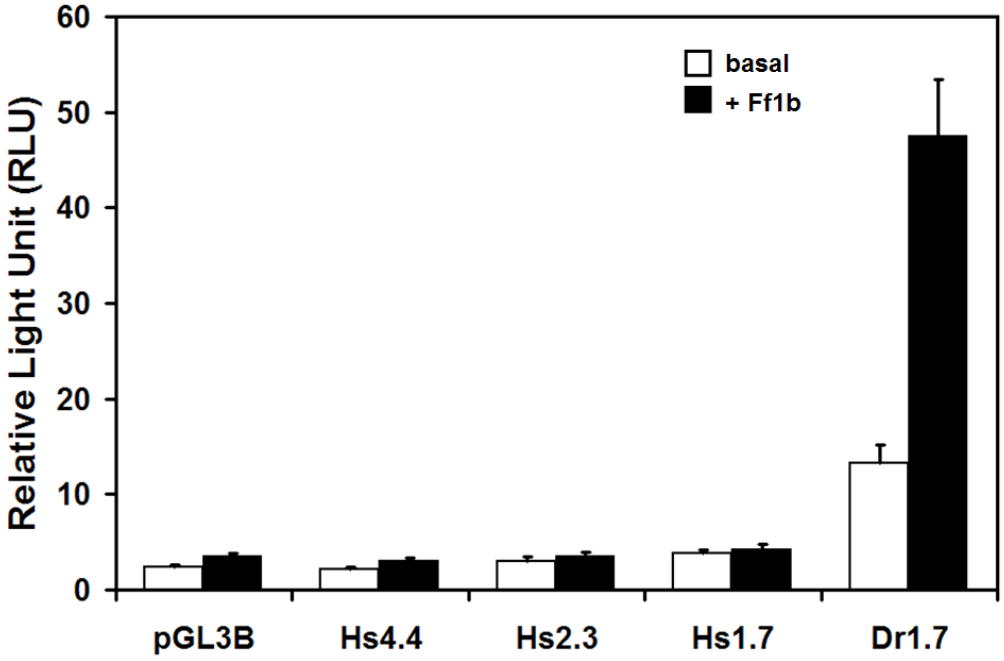

Figure 3.5 Overexpression of *ff1b* potentiates the transcriptional activity of zebrafish *cyp11a1* promoter. Embryos at one- to two-cell stage were injected with the promoterless pGL3Basic (pGL3B) or plasmids containing human *CYP11A1* promoter spanning 4.4-, 2.3-, and 1.7 kb (Hs4.4, Hs2.3, and Hs1.7) or the 1.7 kb zebrafish *cyp11a1* promoter (Dr1.7) with (closed bar) or without (open bar) the overexpression of *ff1b* from pCDNAff1b plasmid. pRL-CMV was included as a normalization control for firefly luciferase activity. Embryos (n = 25) were harvested at 14 hpf, and dual-luciferase assays were performed. Data are expressed as normalized luciferase activity measured from one representative microinjection experiment ± SEM (n = 4).

In accordance with the observation from EGFP construct injection, the three fragments of human *CYP11A1* promoter (4.4-, 2.3-, and 1.7 kb) were unable to activate luciferase reporter gene in zebrafish embryos even with the concomitant overexpression of *ff1b* (Fig. 3.5). On the other hand, the 1.7 kb promoter of zebrafish *cyp11a1* was activated to a level that was 5.6-fold (13.24 RLU) as compared to that of empty pGL3Basic vector (2.36 RLU). When the *ff1b* overexpression plasmid pcDNA3.1ff1b was co-injected, the promoter activity was enhanced to ~20-fold above the basal level or 3.6-fold of the luciferase activity measured from *cyp11a1*-luc alone. These data provided the first *in vivo* evidence of Ff1b potentiating the transcriptional activation of the zebrafish *cyp11a1* promoter. The above findings collectively indicate

that the 1.7 kb *cyp11a1* promoter of zebrafish and human display distinct functional discrepancy despite the mapping of highly conserved *cis*-elements within the two promoter.

3.4.2 Promoter activity of the human and zebrafish 1.7 kb *cyp11a1* promoter in steroidogenic and non-steroidogenic mammalian cell lines

To assess the role of this 1.7 kb putative promoter of zebrafish *cyp11a1* in cell lineage selectivity, we evaluated the expression of luciferase reporter gene directed by this promoter in comparison to its human equivalent in different lineages of cell lines *in vitro*. These include steroidogenic cell lines, Y1 (adrenocortical cells), MA-10 (testis Leydig cells), and CHO-K1 (Chinese hamster ovary), as well as non-steroidogenic cell lines, 293T (embryonic kidney cells), LβT2 (pituitary gonadotrope cells), and HepG2 (liver carcinoma cells). The 1.7 kb human promoter was expected to be active in some of these cell lines, especially those of human or rodent origin and steroidogenic including Y1, MA-10, and CHO-K1, which express *SF-1* endogenously.

As shown earlier, the 1.7 kb promoter of zebrafish *cyp11a1* was able to activate the luciferase reporter gene by 12-fold in Y1 cells (Fig. 3.3). The human 1.7 kb promoter was activated to a higher level, ~21-fold of basal level, in Y1 cells (Fig. 3.6). In CHO-K1 and MA-10 cells, the luciferase activity was increased by 4.5-fold and 6.7-fold for zebrafish promoter (Dr 1.7 kb) while the human 1.7 kb promoter (Hs 1.7 kb) again to a higher level (18.5-fold and 7.8-fold). Similarly in LβT2 cells, the zebrafish and human 1.7 kb promoter activated the luciferase reporter to 3.5-fold and 11.3-fold of basal level, respectively. Both promoters were, however, not active in HepG2 liver carcinoma cells. Intriguingly, the luciferase activity was activated to 18-fold by zebrafish promoter and to 11.6-fold by human promoter in the non-steroidogenic 293T embryonic kidney cells.

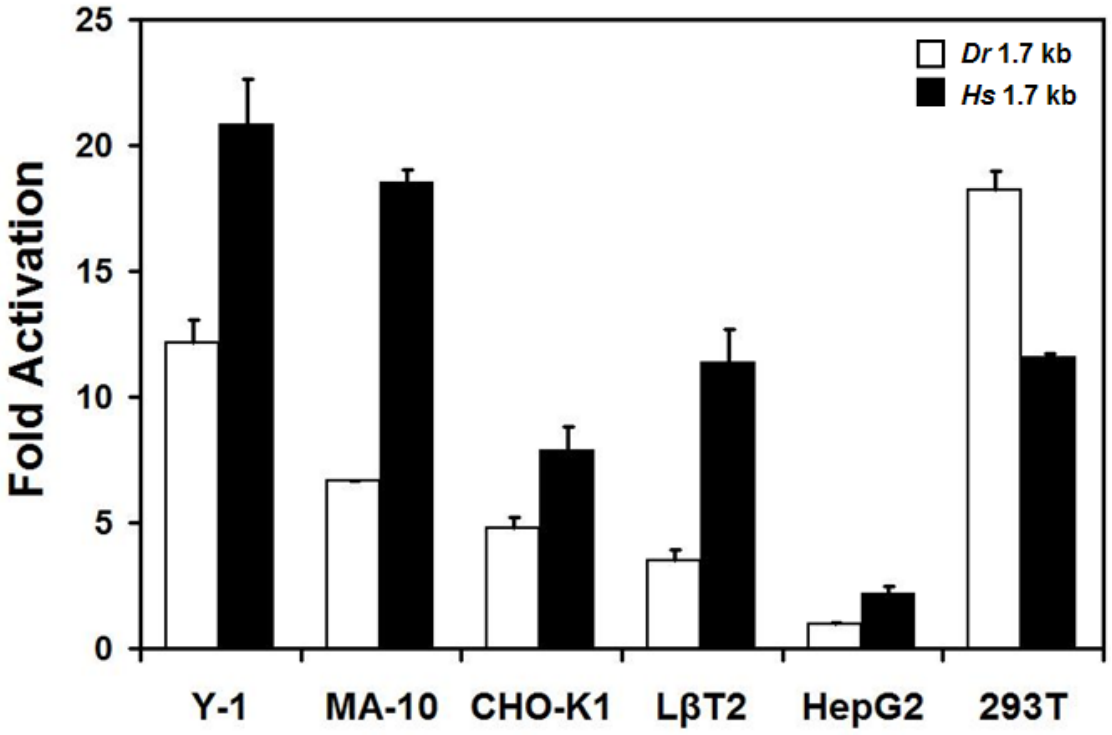

Figure 3.6 Promoter activity of the 1.7 kb *cyp11a1* promoter of zebrafish and human in different lineages of cell lines. The 1.7 kb *cyp11a1* promoter of zebrafish (Dr 1.7 kb) or human (Hs 1.7 kb) was cloned upstream to luciferase in pGL3-Basic vector and transfected into Y1 adrenocortical cells, MA-10 Leydig cells, CHO-K1 ovary cells, LβT2 gonadotrope cells, HepG2 hepatoma cells, and 293T embryonic kidney cells. Renilla luciferase expression vector, pRL-SV40, was co-transfected for normalization of transfection efficiency. Data are expressed as fold activation above the normalized luciferase activity measured from cells transfected with promoterless pGL3Basic vector (adjusted to 1-fold) from one representative experiment, and represent the mean of luciferase activity ± SEM (n = 4).

In summary, the above findings indicate that the 1.7 kb promoter of both the human and zebrafish *cyp11a1* contains regulatory elements controlling the activation of *cyp11a1* gene in different lineages of mammalian cells. Despite the demonstration of its transcriptional activity in transgenic mouse previously, the human *CYP11A1* promoter was inactive in zebrafish embryos, highlighting the possible functional difference between the zebrafish and human promoter.

3.5 Truncation analysis of the 1.7 kb zebrafish *cyp11a1* promoter

The subsequent transient transfection studies on the zebrafish promoter were performed in Y1 adrenocortical cells, as adrenal cortex represents one of the major tissues where *cyp11a1* is endogenously expressed and, thus, should provide the best cellular niche for the investigation of *cyp11a1* promoter activity. To determine the minimal length of the zebrafish *cyp11a1* promoter required for its basal activity and to look at the effect of deleting the distal FRE in this promoter, the promoter characterization began with a series of truncations on the original 1.7 kb promoter of zebrafish *cyp11a1*. Various 5' truncated fragments of the 1.7 kb promoter were generated by PCR and cloned into pGL3Basic vector for the assessment of their promoter activity. Truncation of the zebrafish *cyp11a1* promoter to 1 kb did not affect the reporter gene activity significantly (Fig. 3.7). Even when the distal binding site of Ff1b was deleted in both the 1.5 kb and 1 kb promoter fragment, the luciferase activity derived from them was comparable to that of the original 1.7 kb fragment. The luciferase activity was reduced to ~45% of 1.7 kb fragment when the promoter was truncated down to 500 bp. Nevertheless, residual luciferase activity indicates that the 500 bp promoter was still functional, probably due to the presence of an intact binding site of Ff1b proximally to the start codon. Taken together, these results indicate that 1 kb of the *cyp11a1* promoter is sufficient to drive the basal promoter activity and that the distal FRE is dispensable for basal promoter activity.

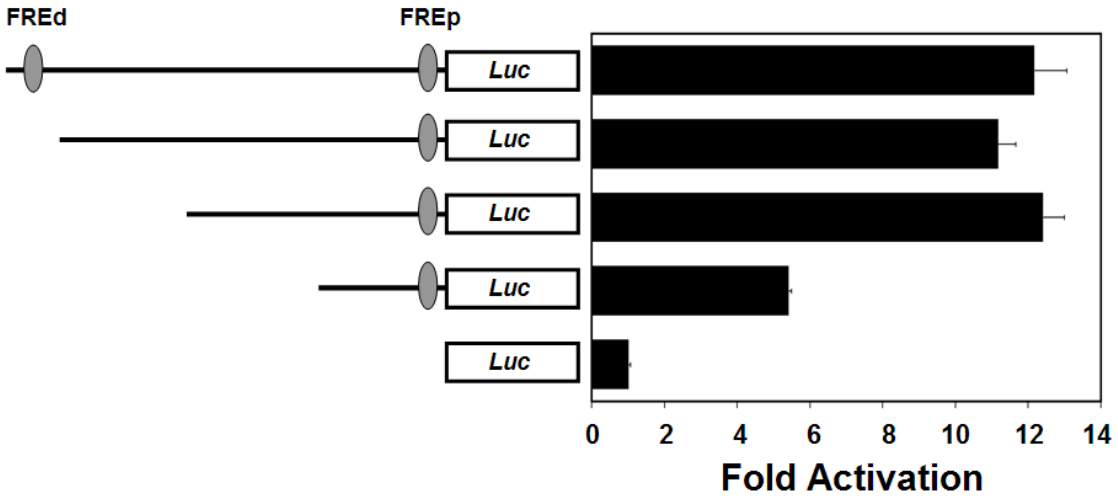

Figure 3.7 The distal FRE is dispensable for the basal promoter activity of zebrafish 1.7 kb *cyp11a1* promoter. The 1.7 kb promoter of *cyp11a1* and various truncated versions were cloned into pGL3Basic and transfected into Y1 cells for quantification of promoter activity. The relative positions and nucleotide sequences of distal FRE (FREd) and proximal FRE (FREp) are indicated. *Renilla* luciferase expression vector, pRL-SV40, was co-transfected for normalization of transfection efficiency. Data are expressed as normalized luciferase activity in relative light unit from one representative experiment, and represent the mean of luciferase activity ± SEM (n = 4).

3.6 Mutagenesis of the two FREs in the 1.7 kb zebrafish *cyp11a1* promoter

To further explore the function of the two FREs in the 1.7 kb *cyp11a1* promoter, the FREd and FREp were mutagenized either individually or both together by site-directed mutagenesis. The mutagenesis was introduced in reminiscent of that reported for FREs in human *CYP11A1* promoter where it has been demonstrated to markedly reduce SF-1 binding and *CYP11A1* promoter activity (Hsu *et al*., 2004; Hu *et al*., 2001b). For the zebrafish *cyp11a1* promoter, the third nucleotide (T) within the core recognition sequences was mutagenized into C and two nucleotides downstream to the core recognition sequences (GA) were mutagenized into TG (Fig. 3.8). As for FREp, two nucleotides upstream to the core recognition sequences (GT) were mutagenized into CA and the second nucleotide (T) within the core recognition sequences was mutagenized into a G (Fig. 3.8).

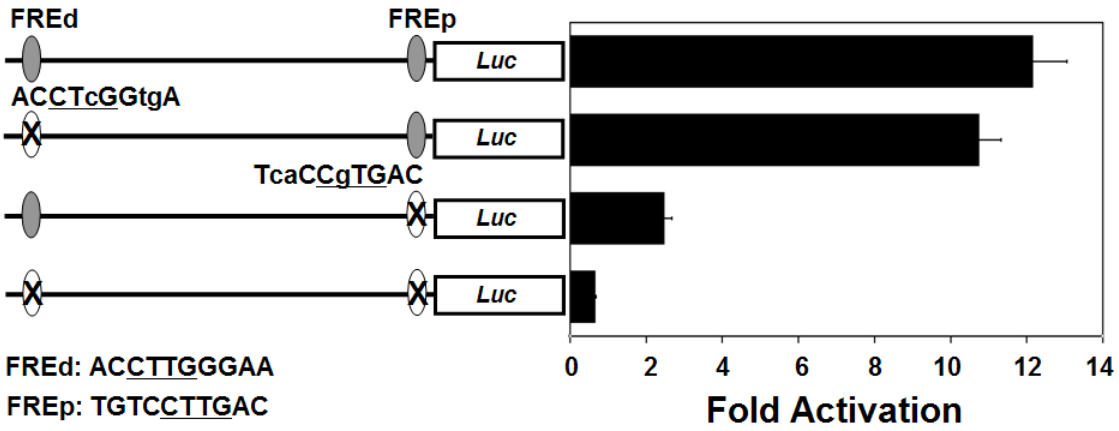

Figure 3.8 The proximal FRE is crucial for the activation of the 1.7 kb *cyp11a1* promoter. The two FREs are mutagenized individually or simultaneously in pGL3Basic plasmid and the resulting plasmids were transfected into Y1 cells for assessment of promoter activity. The relative positions and nucleotide sequences of distal FRE (FREd) and proximal FRE (FREp) are indicated with core motif underlined. Mutated residues are indicated in lower case. *Renilla* luciferase expression vector, pRL-SV40, was co-transfected for normalization of transfection efficiency. Data are expressed as normalized luciferase activity in relative light unit from one representative experiment, and represent the mean of luciferase activity ± SEM ($n = 4$).

Transient transfections into Y1 cells showed that mutagenesis in the FREp alone reduced the luciferase activity from 12-fold to 3-fold of basal level while the mutagenesis in FREd alone marginally reduced the luciferase activity from 12-fold to 10.5-fold (Fig. 3.8). The double mutation in both FREp and FREd rendered the *cyp11a1* promoter completely inactive. The intact FREd or other TFBSs present in the FREp mutant may partially compensate the function of FREp. These results demonstrate that the proximal and distal FREs do not have the same function in the transcriptional activation of the zebrafish *cyp11a1* promoter. In agreement with the findings from human *cyp11a1* promoter, the proximal FRE, which is situated in the basal promoter region, is found to be the major regulator for the core promoter activity *in vitro* whereas the function of the distal FRE in basal gene expression is less obvious (Hsu *et al*., 2004; Hu *et al*., 2001b).

3.7 Ff1b binds to both FREs *in vitro*

To determine whether Ff1b binds to the two FREs selectively, oligonucleotides containing the distal FRE (5'-GTTGACCTTGGGAAAAGTAAATG-3') and the proximal FRE (5'-GTAGTTCATTGTCCTTGACCTGTG-3') were synthesized, biotin-labeled, and tested in electrophoretic mobility shift assay (EMSA) for their interaction with Ff1b proteins. Ff1b proteins were transcribed and translated in rabbit reticulocyte *in vitro* from the pcDNA3.1ff1b plasmid using the TNT® T7 quick coupled transcription/translation system (Promega). The identity of Ff1b, which corresponded to a ~50 kDa band in a SDS-PAGE, was verified by biotin-labeling and immuno-blotting (Fig. 3.9). As expected, the ~50 kDa band did not appear in the negative control reaction where the pCDNA3.1 vector was used as template for the transcription/translation reaction *in vitro*. The rabbit reticulocyte containing Ff1b proteins was subsequently used for EMSA.

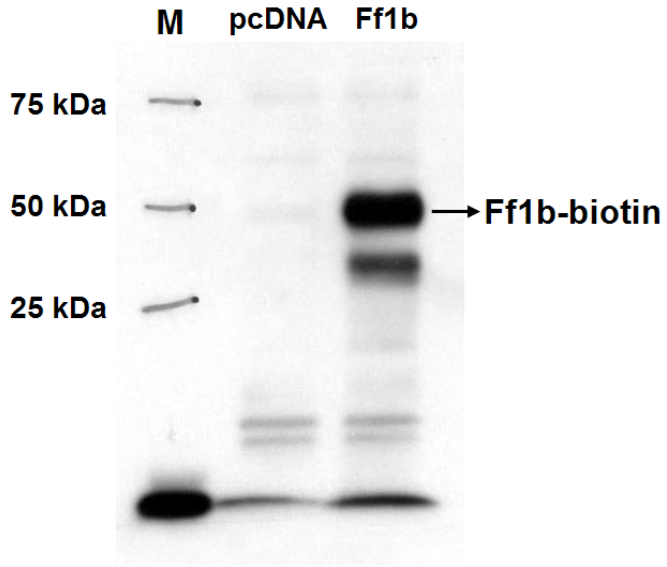

Figure 3.9 Detection of Ff1b protein synthesized from *in vitro* transcription/translation. The plasmid pcDNA3.1 or pcDNA3.1Ff1b was used as template for *in vitro* transcription/translation reaction in rabbit reticulocyte using the TNT® T7 quick coupled transcription/translation system (Promega). Newly synthesized proteins were biotin-labeled with biotinylated lysine added to the reaction as a precharged, ε-labeled biotinylated lysine-tRNA complex (Transcend™ tRNA; Promega). An aliquot (2 µl) of each reaction mixture was separated on SDS-PAGE, transferred to PVDF membrane, and the biotinylated proteins were visualized by binding Streptavidin-HRP followed by chemiluminescent detection.

As expected, no band shift was observed when the biotin-labeled oligonucleotides were incubated with reaction mixtures using the empty pcDNA3.1 vector as transcription/translation template (Fig. 3.10, lane 1 and 6). Mobility complexes were only observed when the reaction mixtures containing Ff1b proteins were used (lane 2 and 7). Ff1b proteins, however, did not bind the mutated version of both the biotin-labeled distal and proximal FRE (lane 3 and 8). The Ff1b-FRE complexes were effectively competed by 200-fold molar excess of the corresponding unlabeled FRE (lane 4 and 9). The same complexes were, however, unaffected by 200-fold molar excess of the unlabeled mutated FREs (lane 5 and 10). These observations demonstrated the specificity of Ff1b binding to both the distal and proximal FREs.

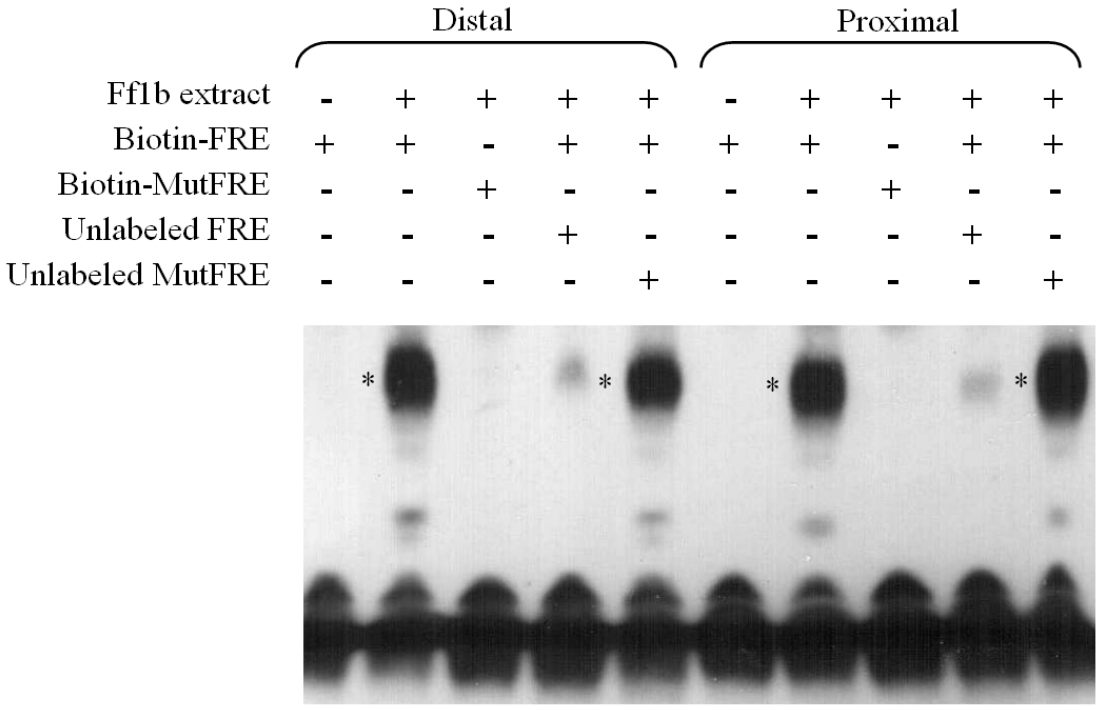

Figure 3.10 Ff1b binds to both the distal and proximal FREs in the 1.7 kb zebrafish *cyp11a1* promoter in electrophoretic mobility shift assay (EMSA). Biotin-labeled wild-type or mutated oligos (30bp) containing the distal (FREd) or proximal (FREp) were incubated with rabbit reticulocyte in which empty pcDNA vector (Lane 1 and 6) or *ff1b* overexpression plasmid pcDNA3.1ff1b (Lane 2-5 and 7-10) was used as template for *in vitro* transcription and translation. In competition assay, ~200-fold molar excess of the respective unlabeled FRE (lane 4 and 9) or mutated FRE (lane 5 and 10) was used. The FRE-Ff1b complexes are denoted by asterisks (*).

Following the discovery that Ff1b binds to both the distal and proximal FREs, the strength of Ff1b binding to the two FREs were studied by competitive binding assays. Ff1b binding to biotin-labeled FREd (Fig. 3.11A) and to biotin-labeled FREp (Fig. 3.11B) was progressively reduced by increasing concentrations of unlabeled distal and proximal FRE at 10-, 50-, 100-, and 200-fold molar excesses. Overall, the binding of Ff1b to the FREd seemed to be slightly stronger as the Ff1b-FREd complexes were competed more effectively by unlabeled FREd as compared to unlabeled FREp (Fig. 3.11A). Similarly, the Ff1b-FREp complexes were competed more effectively by unlabeled FREd as compared to unlabeled FREp (Fig. 3.11B). The strength of competition seemed to vary slightly with different range of molar ratio. At 10-50 molar excess, unlabeled FREp competed more potently than unlabeled FREd. At 100-200 molar excess, unlabeled FREd was a more potent competitor.The difference in strength of binding, was however, only marginal.

In summary, Ff1b binds to both FREs mapped in the 1.7 kb promoter of zebrafish *cyp11a1* as demonstrated by the EMSA data. The binding of Ff1b to the distal FRE seems to be slightly stronger as shown in the competitive binding assay of EMSA. These findings, however, have to be verified by more *in vivo* studies assessing the binding selectivity of Ff1b to the two FREs in different cellular context.

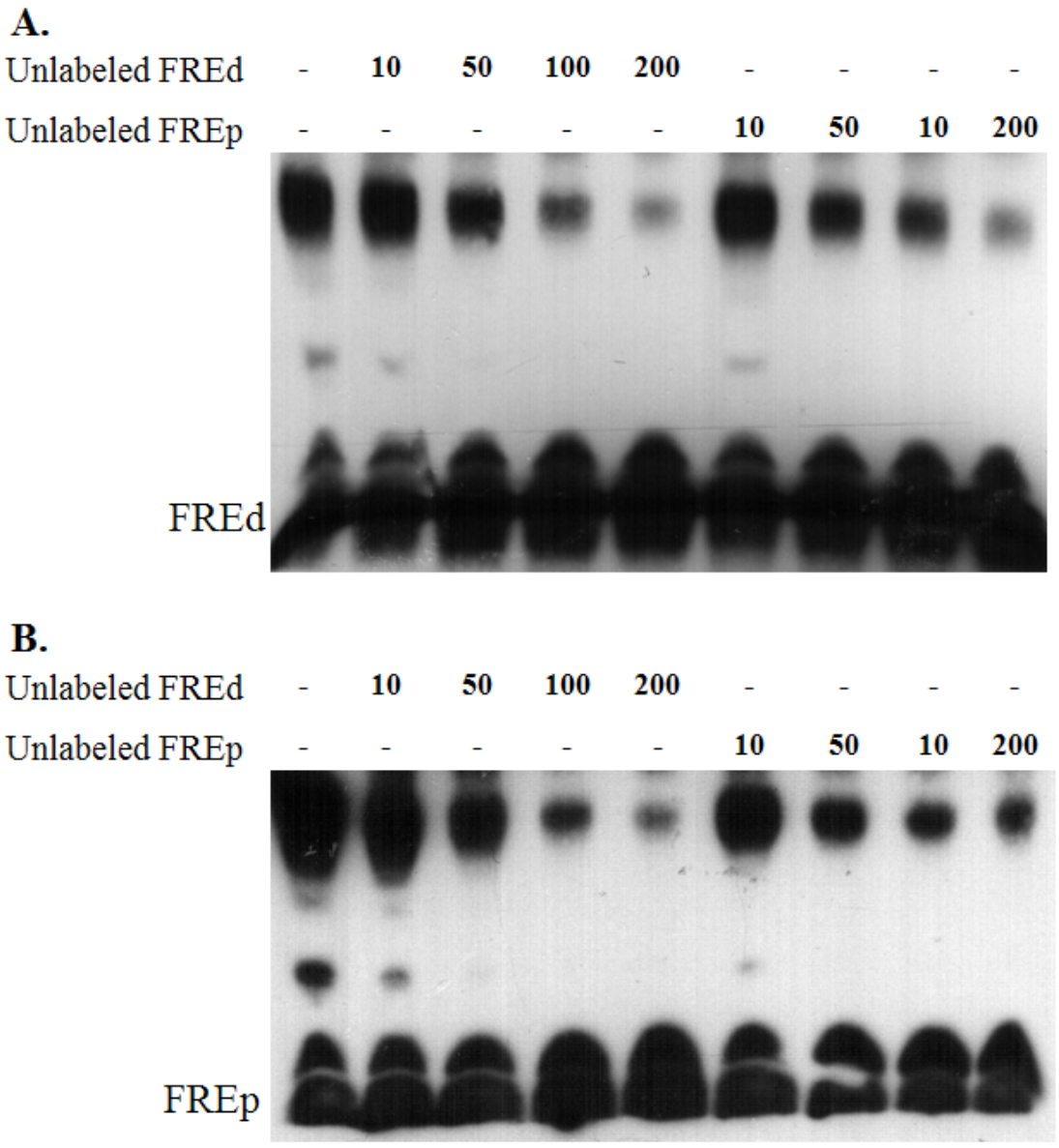

Figure 3.11 Competitive binding of the distal (FREd) and proximal (FREp) FREs in electrophoretic mobility shift assay (EMSA). Biotin-labeled FREd (A) or FREp (B) oligos (30bp) were incubated with rabbit reticulocyte in which *ff1b* overexpression construct pCDNAff1b was used as template for *in vitro* transcription and translation. In competition assay, ~10-, 50-, 100-, and 200-fold molar excess of the respective unlabeled FRE was used.

3.8 Ff1b binds to both FREs *in vivo*

To see whether Ff1b binds to the two FREs *in vivo*, the association of Ff1b with *cyp11a1* promoter was assessed by ChIP assay. A polyclonal antibody for Ff1b was raised against amino acid residues 234-248 (CAYLHQEQSGRGKLE) of Ff1b, which corresponds to the N-terminus of ligand binding domain. This custom anti-peptide production was carried out in rabbits by Biogenes (Germany) and two animals (#1659 and #1660) were immunized for each epitope chosen. The activity of the antibody produced was assessed by Western blot where a band corresponding to the size of Ff1b (~50 kDa) was detected in ovary protein extract from an adult zebrafish female. As the Ff1b antiserum from rabbit #1660 gave rise to a stronger signal in Western blot, the #1660 antiserum was subsequently used for chromatin immunoprecipitation (ChIP) assay as followed.

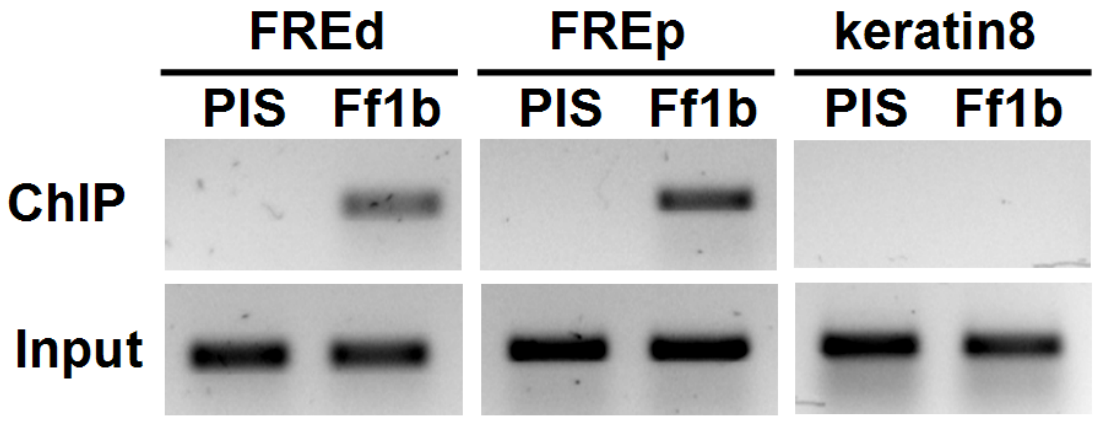

Figure 3.12 Ff1b binds to both the distal and proximal FRE *in vivo* as shown by ChIP. Chromatin was prepared from freshly dissected zebrafish ovary and immunoprecipitated with Ff1b antiserum or pre-immume serum (PIS) from the same rabbit. DNA extracted from ChIP was analyzed by PCR using primers covering the nucleotide positions -1643 and -1475 for FREd, -223 and +26 for FREp, and -471 to -255 for *keratin8* promoter, which does not contain any consensus FRE.

Chromatin was immunoprecipitated by Ff1b antiserum from ovary tissues where Ff1b is abundantly expressed (von Hofsten *et al*., 2005). In agreement with the observations in EMSA, Ff1b binds to both FREd and FREp of *cyp11a1* promoter *in vivo* as shown by the enrichment of the two promoter regions in PCR analyses following ChIP assay (Fig. 3.12). This enrichment did not take place in samples where the pre-immune serum (PIS) was used instead of Ff1b antiserum. Likewise, the enrichment was not seen on *keratin8* promoter where no consensus FRE was identified and thus, should not bind Ff1b. This data presented the first experimental evidence of Ff1b association to its target gene promoter, *cyp11a1*, *in vivo*.

3.9 Summary

A 1.7 kb 5' upstream promoter of zebrafish *cyp11a1* that was responsive to Ff1b transcriptional activity was isolated and studied extensively. This promoter fragment drived tissue-specific expression of EGFP in the zebrafish embryos and also the activation of luciferase gene in Y1 adrenocortical cells. This was in contrast to the other three gene promoters of *cyp17*, *star*, and *3β-hsd* isolated concurrently despite the fact that *cyp17* and *star* promoter contained at least one FRE. Truncation analysis done on the 1.7 kb *cyp11a1* promoter demonstrated that the truncation of this promoter down to 1 kb did not affect the basal promoter activity significantly, indicating that losing the distal FRE had no effect in the basal promoter activity. In accordance with this observation, mutagenesis studies on the two FREs suggested that the proximal FRE played central role in mediating the basal promoter activity of *cyp11a1*. Finally, this study provided the first experimental evidence of Ff1b association with its endogenous target gene promoter *cyp11a1* and also Ff1b potentiating the transcriptional activity of *cyp11a1* promoter *in vivo*. The interaction of Ff1b with both the distal and proximal FREs in the *cyp11a1* promoter was demonstrated *in vitro* by EMSA and *in vivo* by ChIP assay. All of the above findings have ascertained the conserved function of Ff1b as the transcriptional regulator of *cyp11a1*, and most likely also the other steroidogenic genes in zebrafish.

CHAPTER 4

Development of a transgenic green fluorescent lineage tracer for *ff1b*

4.1 Introduction

Our previous findings have established Ff1b as the ortholog of mammalian SF-1 in zebrafish. The first hint of Ff1b acting at multiple levels in endocrine development and function emerged from developmental analyses of its expression in zebrafish embryos. The expression of *ff1b* from the earliest stages of organogenesis in the interrenal and gonadal primordium (Chai and Chan, 2000) suggests a fundamental role in the initial differentiation of the primary steroidogenic tissues. The interrenal primordia expressing *ff1b* appear as bilateral clusters of cells located ventral to the the third somite at 20-22 hpf in close association to the pronephric primordium (Hsu *et al*., 2003). By 28 hpf, the bilateral clusters coalesce into a discrete structure at the midline and the interrenal cells are capable of producing steroids, as characterized by the presence of key steroidogenic enzymes including *cyp11a1* and *3β-hsd* (Chai and Chan, 2000; Hsu *et al*., 2003). In adult zebrafish, the steroidogenic interrenal cells are embedded in the both lobes of head kidney. Besides, *ff1b* is also expressed in the ventromedial hypothalamus (VMH), which acts as the control centre of the endocrine system, from about 24 hpf onwards (Chai and Chan, 2000), indicating a regulatory role in endocrine function. In contrast to mammalian *SF-1*, *ff1b* expression was not detected in the developing pituitary in zebrafish.

Similar to SF-1, direct insights into the roles of Ff1b in zebrafish came from morpholino (MO) knockdown studies of *ff1b*. Injection of ff1bMO into embryos led

to the development of late-appearing morphological defects that are indicative of impaired osmoregulatory functions (Chai *et al*., 2003; Hsu *et al*., 2003). In addition, the expression of two interrenal steroidogenic genes, *cyp11a1* and *3β-hsd*, were shown to be downregulated and the development of interrenal tissue was adversely affected, as judged by the complete absence of 3β-Hsd enzymatic activity. In direct contrast to observations from *Sf-1* knockout mice, the effects of morpholino knockdown of *ff1b* in other *ff1b*-expressing tissues including ventral hypothalamus and gonads were less obvious.

Despite the tremendous progress made in studying the expression pattern, knockout/knockdown, structural and chemical properties of SF-1 and Ff1b, the molecular mechanisms underlying their regulation and transcriptional activity remain largely unknown. As the interrenal of *ff1b* morphant disappeared at relatively early stages of development, it has been difficult to trace the fate of *ff1b*-expressing cells or to define the molecular basis for the loss of these cells in the downregulation of *ff1b*. For instance, it has been shown that the adrenal primordium formed but progressively regressed by apoptosis in SF-1 knockout mice (Luo *et al*., 1994). We are still not sure whether the same phenomenon took place when *ff1b* gene was knocked down by MO. Therefore, it will be extremely useful if a lineage tracer could be developed for cell lineages that express *ff1b*. In mouse, an SF-1/EGFP transgenic line has been generated using ~45 kb of SF-1 5' flanking sequence (up to Exon2) from a BAC plasmid that was placed upstream to EGFP coding sequence (Stallings *et al*., 2002). The resulting transgenic mouse displayed EGFP fluorescence in *SF-1*-expressing tissues, including the ovaries, testes, adrenal cortex, and the VMH but not in corpora lutea or the anterior pituitary gland.

In this study, we have adopted a BAC transgenesis strategy to trace the lineage of *ff1b*-expressing cells in zebrafish embryos. BAC transgenesis has emerged as a powerful approach to achieve copy number-dependent and position-independent transgenic expression (Heintz, 2000; Giraldo and Montoliu, 2001; Yang *et al*., 2006; Lakowski *et al*., 2007). We have taken advantage of recent improvements in the DNA engineering of BAC plasmid by Red/ET homologous recombination approach. This strategy allows any kind of modifications, including insertion, point mutation, sub-cloning, and deletion, at any desired site within a BAC plasmid (Muyrers *et al*., 1999; Muyrers *et al*., 2000a; Muyrers *et al*., 2000b; Zhang *et al*., 2000). In addition to the characterization of the transgenic zebrafish generated by the BAC transgenesis approach, this chapter discusses the initial evaluation of this transgenic line as a useful tool for studying the embryonic development of interrenal gland *in vivo*. The resultant transgenic line had enabled us to study the early morphogenesis of VMH and interrenal gland in a way that would not be possible in the mammalian system.

4.2 The generation of pBACff1bEx2EGFPKan by Red/ET homologous recombination

The most straightforward way to mark *ff1b*-expressing cells will be the fusion of upstream flanking sequences of *ff1b* to EGFP reporter gene. Unfortunately, initial experiments using a plasmid construct containing up to 20 kb of *ff1b* upstream sequences and 30 bp of 5' UTR fused upstream of EGFP did not recapitulate *ff1b* expression in zebrafish embryos. In addition, in-frame insertion of EGFP into Exon 2 flanked by ~3.8 kb of genomic sequences on either side did not successfully recapitulate *ff1b* expression. This indicates that elements contributing to tissue-specific regulation of *ff1b* expression are located distally from the transcription start site. Therefore, a Red/ET homologous recombination strategy was utilized to insert

the EGFP coding region into Exon2 of *ff1b* gene locus contained in a BAC construct, BACff1b2, so that EGFP expression would come under the full control of *ff1b* gene regulatory elements.

The EGFP-Kan^r cassette was designed to be inserted in-frame immediately downstream to codon 25 of *ff1b*, which is located in the first coding-exon, Exon2 (Fig. 4.1). This insertion would prevent the generation of a dominant negative mutant, as the resultant fusion Ff1b-EGFP protein does not contain an intact DNA binding domain. Red/ET homologous recombination was carried out in a DH10B bacterial host whereby the donor DNA fragment encompassing the EGFP-Kan^r cassette flanked by 75 bp and 243 bp of left and right homology arms, was used to target the genomic sequences flanking the insertion site. As the insertion site is located prior to the nuclear localization signal of Ff1b (in Exon 4), the EGFP protein will remain cytoplasmic. The recombined BAC construct is named pBACff1bEx2EGFPKan.

4.3 Assessment of transgene activity from pBACff1bEx2EGFPKan in zebrafish embryos by transient transgenesis

Microinjection of the supercoiled pBACff1bEx2EGFPKan into zebrafish embryos at 1 to 2-cell stage demonstrated that the recombined DNA containing the EGFP marker recapitulated endogenous *ff1b* expression in the VMH and their neuronal projections, as well as that in the interrenal gland. Despite the mosaic and transient nature of transgenesis, an intense expression of EGFP was detected in a variable number of cells, estimated to be comparable to the number of native *ff1b*-expressing cells. The intrinsic fluorescence of EGFP allowed a sensitive assay to determine spatial expression of the transgene.

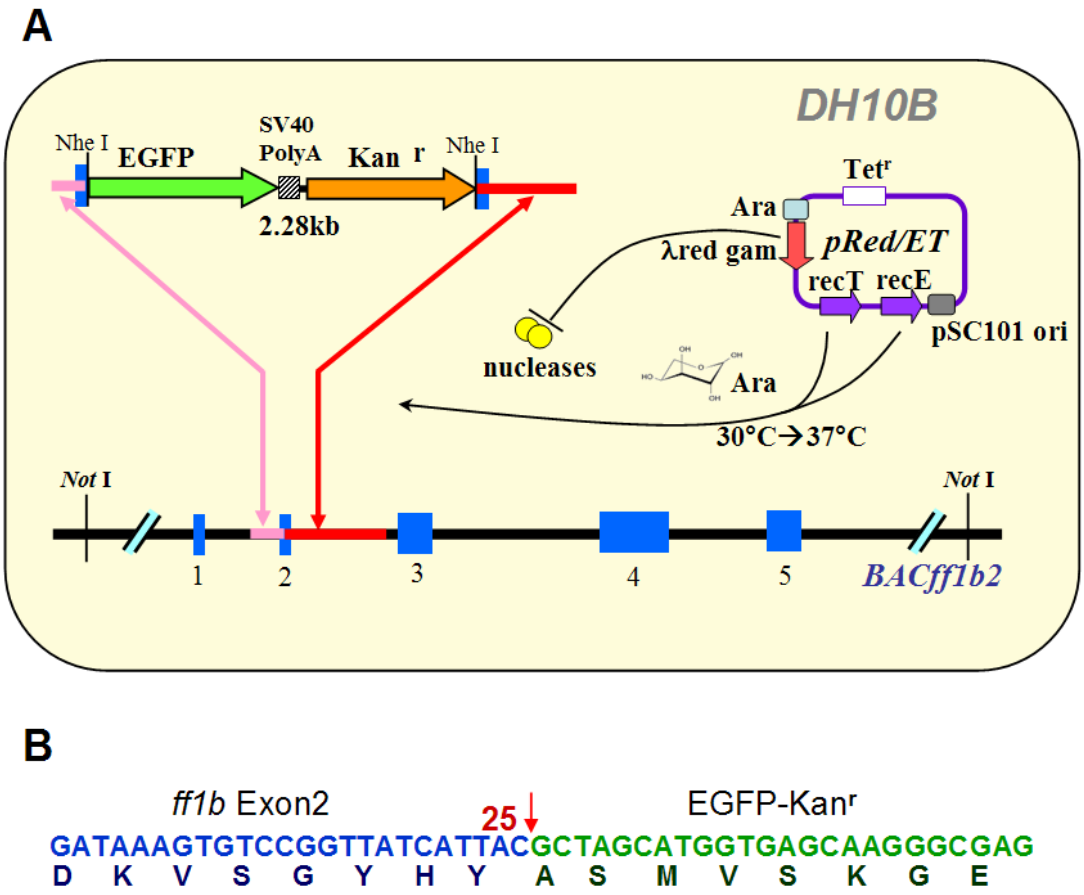

Figure 4.1 Construction of the pBACff1bEx2EGFPKan construct by Red/ET homologous recombination. (A) Schematic representation of the insertion of the EGFP-Kan^r cassette into the BACff1b2. The BACff1b2, which contains the *ff1b* locus, and pRed/ET plasmid, which encodes phage-derived proteins catalyzing homologous recombination, were transformed into *E. coli* DH10B strain. The donor DNA fragment, EGFP-Kan^r (2.28 kb) harbouring 75 bp and 243 bp of left (pink) and right (red) homology sequences targeting the insertion site in Exon 2, was subsequently transformed into the same bacteria cell. By shifting the temperature from 30 to 37°C, and L-arabinose induction, homologous recombination occurs between the homology sequences of donor and BACff1b2. The resultant recombined BAC plasmid, pBACff1bEx2EGFPKan, has the EGFP under the control of endogenous *ff1b* locus. (B) The insertion site is immediately downstream of codon 25 of *ff1b*, and is located in Exon 2. Exon 2 sequences are in blue and the successfully inserted EGFP-Kan^r sequences are in green.

Under an UV fluorescence microscope, weak EGFP expression could first be observed in the microinjected zebrafish embryos from about 28-30 hpf onwards. Images of embryos were taken only from ~34-36 hpf onwards when the EGFP signal accumulated to a level easily captured by confocal microscopy. At 36 hpf, strong EGFP expression could be detected in the VMH, otic vesicle, interrenal, and fibre-like structures in the muscle (Fig. 4.2A).

EGFP-expressing cells in the VMH appeared as one small cluster of cells lateral to the anterior tip of the neural tube beginning at about 28 hpf. As development proceeded, the number of EGFP-expressing cells increased and so did the intensity of fluorescence (Fig. 4.2B and C). Occasionally, the neuronal projections and neuronal cell body-like structures (marked by white arrow) extended from VMH were observed from the forebrain up to hindbrain but their appearances were highly mosaic. The neuronal projections from the VMH ascended dorsally to the level of tegmentum, where they made a sharp 90 degrees turn and continued to project caudally to the otic vesicle (Fig. 4.2A).

EGFP expression was detected in the interrenal gland in 30% of the embryos that showed EGFP expression following microinjection. By the time interrenal cells expressed detectable levels of EGFP at around 32-34 hpf, they had aggregated into a discrete structure ventral to the third somite (Fig. 4.2D). From 48 hpf onwards, EGFP fluorescence proliferated within the interrenal cells and began to show signs of spreading (Fig. 4.2E). Daily monitoring of injected embryos up to two weeks post-fertilization did not produce any evidence of EGFP expression in the genital ridge region. The regulation of *ff1b* expression in the genital ridge may require control elements that are located at great distances from the proximal promoter and are not present within the insert of BACff1b2. The lack of expression can also be due to the

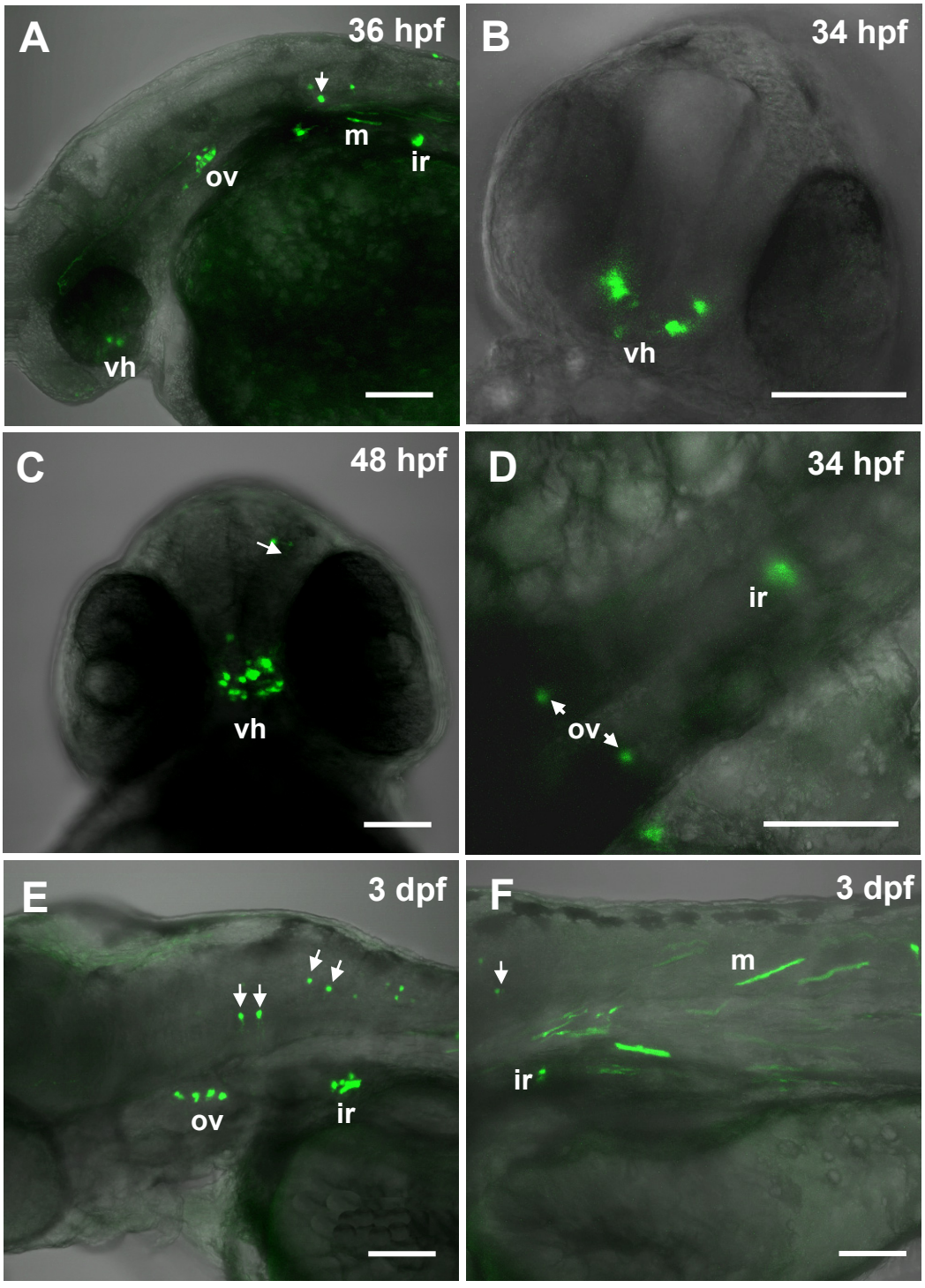

Figure 4.2 The recombined pBACFf1bEx2EGFPKan generated by Red/ET recombination targets EGFP to specific tissues in zebrafish embryos. EGFP is under the control of *ff1b* genomic regulatory elements in the recombined BAC plasmid. When the supercoiled pBACFf1bEx2EGFPKan construct was microinjected into zebrafish embryos at 1-2 cell stage, EGFP expression can be clearly seen at the ventromedial hypothalamus (A-C), and their neuronal projectios (A, C, E-F); interrenal (A, D, E-F); otic vesicle (A, D, E); and muscle (A, F). Neuronal cell body-like structures that appear alongside with the neuronal projections from VMH are highlighted by white arrows. Images were taken with confocal microscope with whole-mount live embryos at the corresponding developmental stages. Scale bars, 100 μm. Abbreviations: ir, interrenal; m, muscle; ov, otic vesicle; vh, ventral hypothalamus.

presence of repressor or the insertion site of the EGFP-Kan^r cassette, causing the expression in the genital ridge to be prohibited.

Besides the VMH and interrenal, EGFP fluorescence was also detected in the otic vesicle and fibre-like structure in the muscle (Fig. 4.2A, D, E-F). As the transient expression of the transgene was highly mosaic, it was difficult to judge which part of the muscle and the otic vesicle actually expressed EGFP. It was also difficult to postulate whether these were due to ectopic expression coming from genomic sequences contained in the BAC plasmid or they were simply non-specific expression.

Nevertheless, the transient transgenesis demonstrated that the ff1bEx2EGFP transgene was capable of marking tissues where *ff1b* gene is endogenously expressed. The mosaic nature of transient expression, however, hindered further molecular analyses. Thus, this transgene released from pBACff1bEx2EGFPKan was used to generate a stable germ-line transgenic zebrafish that will express EGFP in *ff1b*-expressing cells.

4.4 Recapitulation of *ff1b* endogenous expression in zebrafish embryos by stable transgenesis

To generate a linearized transgene for stable transgenesis, pBACff1bEx2EGFPKan was digested with restriction enzyme *Not* I to release the ~100 kb genomic DNA sequence containing the EGFP-Kan^r cassette from the pBeloBAC11 vector backbone. The linearized and purified transgene was microinjected into zebrafish embryos strictly at 1-cell stage. Embryos were checked for EGFP fluorescence at 36-48 hpf and only those showing strong EGFP expression were selected and raised up to adulthood. Out of the 135 fishes that survived to adulthood, only one positive founder was identified (transgenesis efficiency = 0.7%) and the resulting transgenic line was named ff1bEx2EGFP. Indeed, another founder

was found to produce EGFP fluorescent progenies. However, the embryos produced by this founder showed only non-specific EGFP expression in the CNS, probably due to the insertion of a truncated transgene. The low efficiency of transgenesis is probably due to the large size of transgene. Judging from the number of F_1 progeny that showed EGFP fluorescence, the germ-line transmission rate was ~40 – 50%. As expected, because of its large size, the linearized and purified transgene must be freshly prepared for microinjection to achieve a high percentage of fluorescent embryos, and subsequent stable germ-line transgenesis.

As reported for many other transgenic lines, the homozygous transgenic embryos of ff1bEx2EGFP line are not viable and only heterozygous transgenic embryos can be used for imaging and molecular analyses. The homozygous transgenic embryos are easily distinguishable from the non-fluorescent (non-transgenic) and heterozygous transgenic by their stronger EGFP fluorescence prior to 48 hpf and the development of pericardial edema from ~48 hpf onwards. Subsequently, abnormal curvatures of body axes were observed in these homozygous transgenic embryos and they generally do not survive beyond 6-7 dpf.

Notably, the EGFP transgene expression faithfully recapitulated the endogenous expression of *ff1b* in the VMH and interrenal. Weak EGFP signal was visible in the VMH and much stronger in the otic vesicle and muscle from about 20 hpf (21-somite stage) onwards. By 22 hpf, EGFP cells in the VMH accumulated to a level that could be better visualized and captured by confocal microscope (Fig. 4.3A). On the other hand, the interrenal appeared only as a small dot just above the yolk sac and ventral to the third somite in this stage. From 28 hpf onwards, the interrenal formed a more discrete structure in the same region (Fig. 4.3B). Concurrently, the

Figure 4.3 EGFP transgene expression in ff1bEx2EGFP transgenic zebrafish embryos. The expression of EGFP transgene at different developmental stages of transgenic embryos was captured by confocal (A-D; G-H) or epifluorescence (E-F) microscope. From 22 hpf onwards, EGFP could be detected in the ventromedial hypothalamus, otic vesicle, interrenal, and muscle (A). From 28 hpf, neuronal projections that extended dorsally and caudally from the ventromedial hypothalamus was apparent (B). At 48 hpf, EGFP expression from common cardiac vein appeared and the intensity of EGFP expression in ventromedial hypothalamus and associated neuronal projections, otic vesicle, interrenal, and muscle continued to increase (C, lateral view; D, dorsal view). By 3 dpf, the EGFP expression at the common cardiac vein was almost diminished and a new EGFP expression domain at the neuromasts emerged and are marked by red arrows (E). As development proceeded, EGFP expression at the ventromedial hypothalamus and interrenal continued to proliferate and increase in intensity while those in the otic vesicle and muscle became weaker (F-H). All images were captured from lateral view except for A and H, which were captured from dorsal view. Scale bars, 100 μm. Abbreviation: vh, ventromedial hypothalamus; ov, otic vesicle; ir, interrenal; m, muscle; ccv, common cardiac vein.

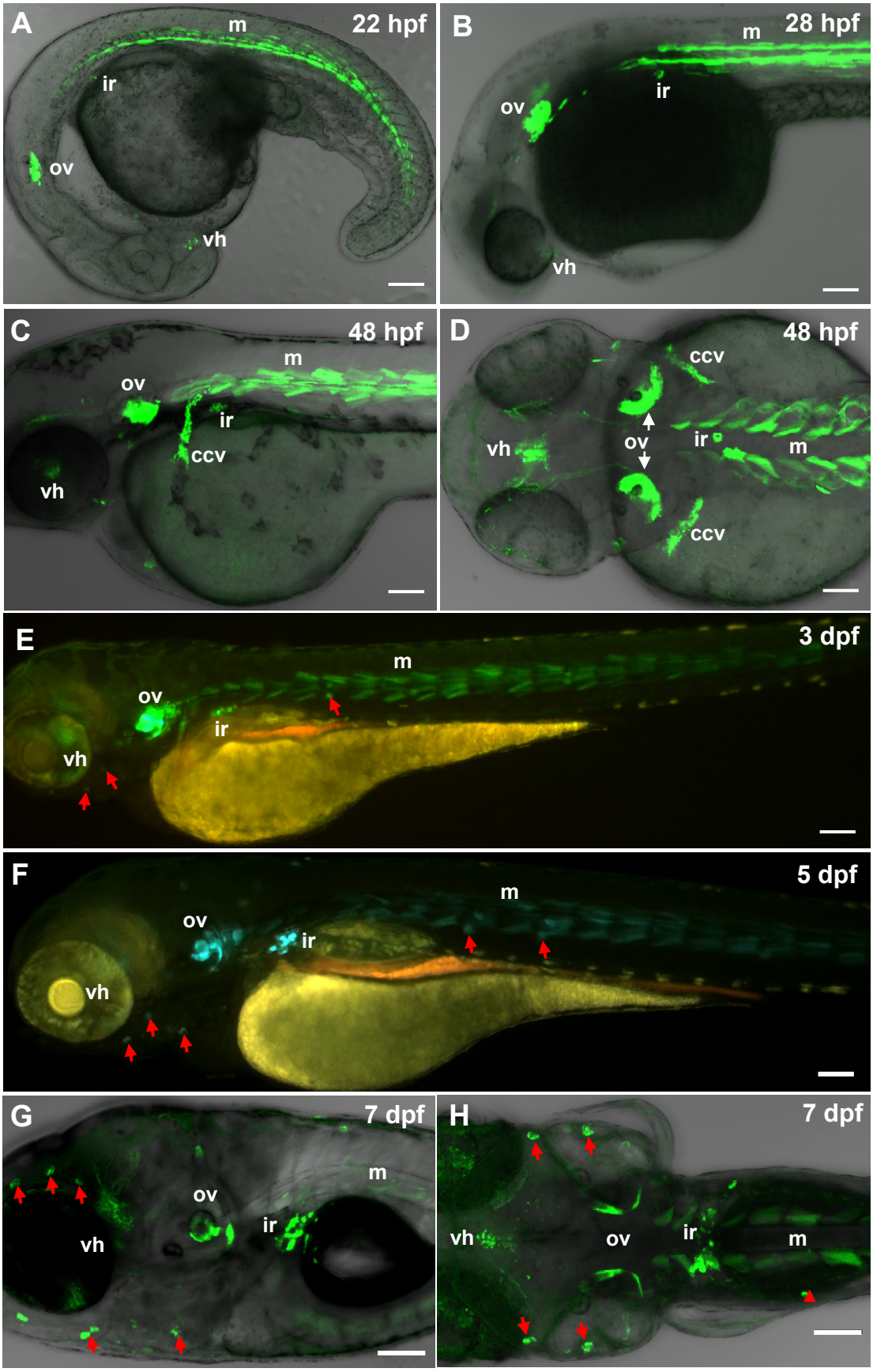
A
22 hpf
m
ir
ov
vh
B
28 hpf
m
ir
ov
vh
C
48 hpf
m
ov
ir
ccv
vh
D
48 hpf
ccv
vh
ov
ir
m
ccv
E
3 dpf
m
ov
ir
vh
F
5 dpf
m
ov
ir
vh
G
7 dpf
m
ov
ir
vh
H
7 dpf
vh
ov
ir
m

neuronal projections extended dorsally and caudally from VMH to the midbrain, otic vesicle, and muscle could be clearly visualized at this stage.

Similar to the observations in transient transgenesis (Fig. 4.2), EGFP-positive cells in the VMH and interrenal continued to proliferate as embryonic development proceeded (Fig 4.3C-H). At 48 hpf, a previously unidentified domain of transgene expression appeared at the position that corresponded to the common cardiac vein (Fig. 4.3C and D). This vein-like structure appeared bilaterally at both sides of the trunk and they extended from the second somite to the direction of heart but stopped half way through on the yolk. The expression, however, was nearly disminished by 3 dpf (Fig. 4.3E). Interestingly, transgene expression began to show up in the neuromasts (marked by red arrows) of the lateral line system from about 3 dpf onwards (Fig. 4.3 E-H). This expression was also not noticed in transient transgenesis, as these random dots could have been treated as non-specific EGFP expression or mosaic EGFP expression coming from other tissues. By 5 dpf, the spatial domain of VMH and interrenal were more or less defined and did not change much thereafter (Fig. 4.3 F-H). Conversely, the EGFP signal in the otic vesicle and the muscle became weaker as development proceeded.

In ISH, a third domain of *ff1b* expression appeared at 4 dpf as stripes of cells located along the dorsolateral peritoneal walls parallel to the eigth and ninth somite on either side of the trunk, and they have been proposed to correspond to the genital ridge which would eventually develop into gonads (Chai, 2002). However, similar to observations in transient transgenesis, monitoring of EGFP expression in the ff1bEx2EGFP larvae up to 2 weeks did not reveal any expression domain that corresponds to the genital ridge. This observation indicates that the gonad-specific

enhancer lies outside of the transgene used in this study or that a gonad-specific repressor is present in the transgene.

In contrast to the transient transgenesis, EGFP fluorescence observed in stable transgenesis was now at its full complement where the domain of expression and the fluorescence intensity increased considerably. The EGFP expression in the otic vesicle and muscle was unlikely to be ectopic expression that resulted from integration site effect, as the EGFP signal was already detected even in transient transgenesis studies. They may still represent genuine endogenous *ff1b* expression that could not be detected by ISH analyses previously.

4.4.1 EGFP transgene expression in the ventromedial hypothalamus

In the VMH of a developing zebrafish embryo, *ff1b* expression is initiated at ~24 hpf as revealed by ISH analyses (Chai and Chan, 2000). The expression pattern of the EGFP transgene in the VMH of ff1bEx2EGFP transgenic embryos was largely similar to those revealed by ISH and transient transgenesis studies of pBACff1bEx2EGFPKan. At about 20 hpf, 2 to 3 EGFP-positive cells appeared bilaterally to the anterior tip of the neural tube in the developing brain (Fig. 4.4A). The number of EGFP-positive cells increased steadily with development and by 24 hpf, the number of cells almost doubled at both sides and neuronal projections from these cells began to be visible (Fig. 4.4B). As the anterior neural axis folds, these cells were translocated caudally and dorsally to form two narrow strips of cells extending bilaterally from the midline of the rostral diencephalon by 28 hpf (Fig. 4.4C). From lateral view, it was noticed that the axonal-like projections from VMH ascended dorsally at an angle to the midbrain, where they made a sharp 90 degrees turn and continued to project caudally to the otic vesicle (Fig. 4.4D-E). Additional sectioning

Figure 4.4 EGFP transgene expression in the ventromedial hypothalamus. Confocal images of live transgenic embryos were taken from ventral (A-C), lateral (D), and dorsal (E-H) view to examine the embryonic development of ventromedial hypothalamus from 20 hpf through 7 dpf. At 20 hpf, a few EGFP-positive cells appeared bilaterally at the ventral hypothalamus (A). By 24 hpf, the number of EGFP-positive cells almost doubled and the neuronal projections from these cells could be clearly visualized (B). By 28 hpf, these cells formed two narrow strips of cells extending bilaterally from the midline of rostral diencephalon (C, ventral view). From lateral view, axonal-like projections from the ventromedial hypothalamus ascended dorsally and caudally at a sharp 90 degree trun to the midbrain (D). Proliferation and growth of these neurons continued and they eventually occupied a distinct region within the ventral hypothalamus (E-H). In some images, otic vesicle was included for a complete coverage of neuronal projections. Scale bar, 100 μm. Abbreviations: vh, ventromedial hypothalamus; ov, otic vesicle.

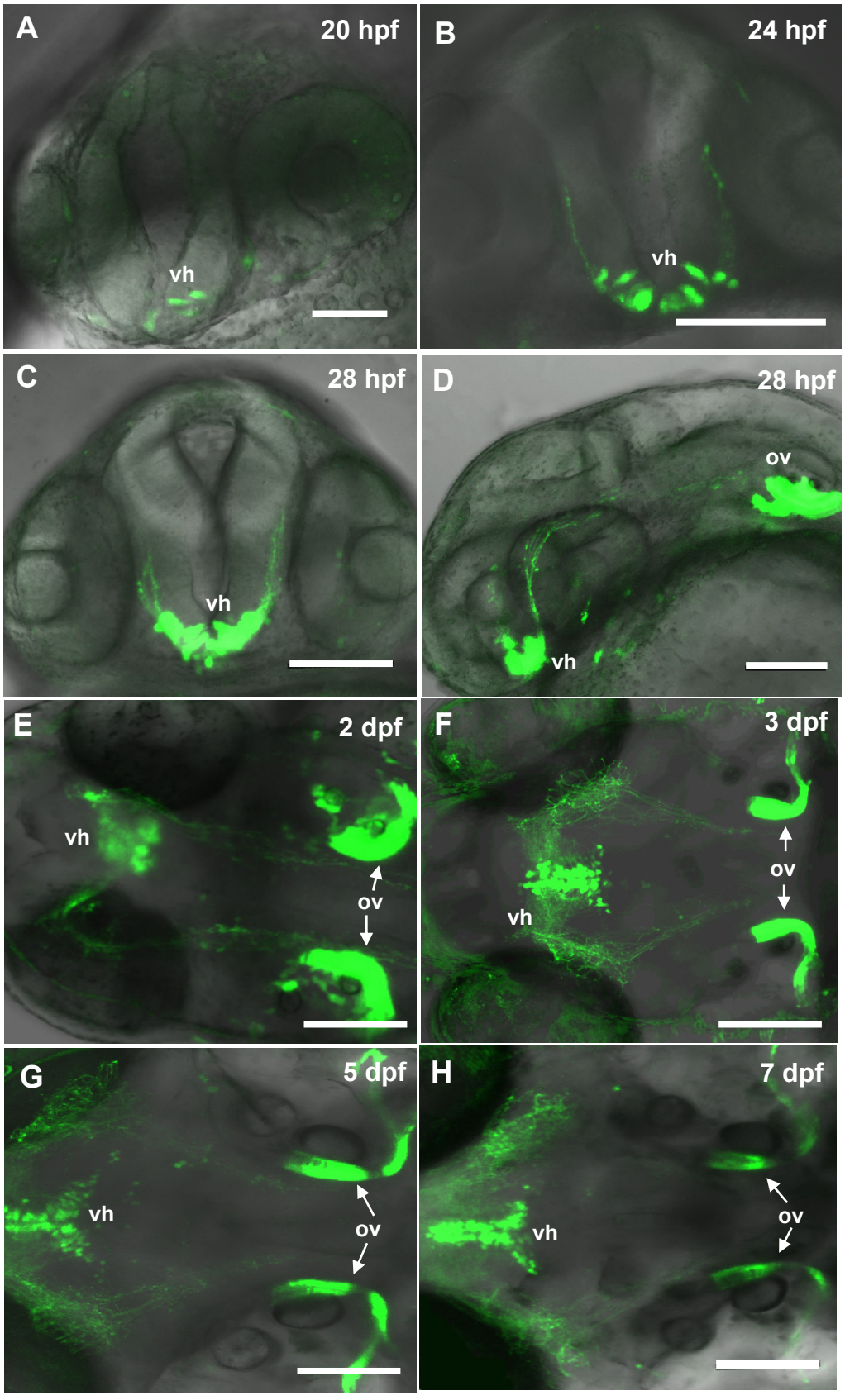
A
20 hpf
vh
B
24 hpf
vh
C
28 hpf
vh
D
28 hpf
ov
vh
E
2 dpf
vh
ov
F
3 dpf
ov
vh
G
5 dpf
vh
ov
H
7 dpf
vh
ov

of the transgenic embryos would be required to determine whether these projections directly innervated the otic vesicle in the developing zebrafish embryos.

Proliferation and growth of the VMH neurons continued and eventually they occupied a distinct region within the ventral hypothalamus (Fig. 4.4E-H). From 3 to 5 dpf, projections from the VMH neurons became more complex. In addition to the posterior projection described earlier, more localized and arborized projections resembling dendritic projections were observed, most notably laterally within the hypothalamus and midbrain.

Collectively, these data indicate that the EGFP expression not only recapitulated the endogenous *ff1b* expression but also unraveled the neuronal projections that were previously not detected by ISH analyses. The discrepancy could be largely attributed to the difference in sub-cellular domains that are revealed by ISH and fluorescence detection. While ISH detects mostly *ff1b* transcripts in the nucleus and perinuclear cytoplasm, fluorescence revealed the presence of EGFP proteins in the cytoplasm. The ability to mark the *ff1b*-expressing neurons and their projections will certainly be a valuable asset in studying the development and function of the VMH as the regulatory centre for the endocrine system.

4.4.2 EGFP transgene expression in the interrenal gland

The morphogenetic movement of interrenal primordial cells is well defined by *in situ* hybridization analyses in zebrafish embryos. At 20-22 hpf, *ff1b*-expressing interrenal cells appear in the intermediate mesoderm bilateral to the notochord and ventral to the third somite. By ~30 hpf, the two clusters of *ff1b*-expressing cells coalesced into a single cluster located slightly to the right of midline from dorsal view

(Chai and Chan, 2000; Chai *et al*., 2003; Hsu *et al*., 2003; Liu and Guo, 2006; Liu, 2007).

In the ff1bEx2EGFP transgenic embryos, EGFP was weakly expressed from the interrenal cells at ~22 hpf (Fig 4.5A-B) but it was not discernable if observed from the dorsal view. There is a possibility that the EGFP expression in the interrenal primodia prior to this stage was masked by the stronger EGFP fluorescence from the otic vesicle and the muscle. At 28 hpf, the interrenal primordium was clearly visible from top of the embryo as the cells had aggregated into a discrete structure at the midline (Fig. 4.5C).

The number of EGFP-positive cells increased significantly as the embryo continued to develop (Fig. 4.5D-F). Beginning from 3 dpf, dispersal of the main cell cluster became evident, giving rise to a few smaller clusters across the midline (Fig. 4.5D). The shape and size of these cell clusters, however, showed slight variations among different individuals as development proceeded. At 5-7 dpf, the swim bladder began to inflate and the interrenal cells could be seen to be closely associated with the dorsal and anterior end of the swim bladder.

Just like the majority of organ rudiments, the interrenal had more or less completed morphogenesis by 3-4 dpf and its development slowed down considerably. Thus, the interrenal cells continued to proliferate but at a much lower rate thereafter. In agreement with the observations in transient transgenesis, no direct neuronal connection could be observed between the EGFP-visualized neuronal tracts and the interrenal in any of the transgenic embryos, suggesting that the interrenal organ is not directly innervated by the VMH neurons. In conclusion, the ff1bEx2EGFP transgene expression faithfully recapitulates the endogenous *ff1b* in the interrenal gland. Thus,

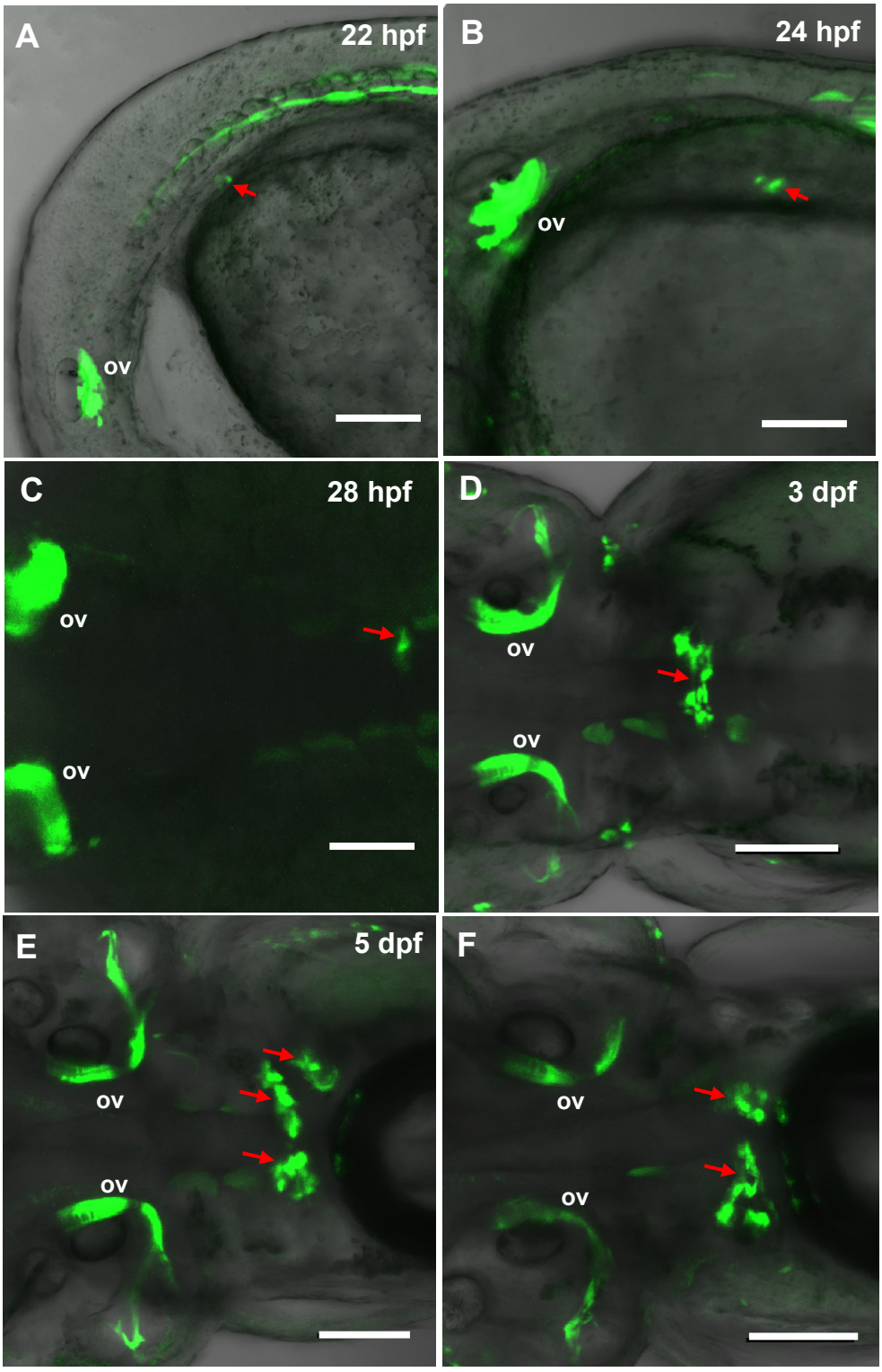

Figure 4.5 EGFP transgene expression in the interrenal gland. Confocal images of live transgenic embryos were taken from lateral (A-B), and dorsal (C-F) view to examine the embryonic development of interrenal from 22 hpf through 7 dpf. The EGFP expression at the interrenal gland was first detected at a position ventral to the third somite at 22 hpf (A). These cells of interrenal primordium continued to proliferate and occupied a region that was anterior and dorsal to the swim bladder by 7 dpf (B-F). Otic vesicle (ov) was included to indicate the orientation of embryos or larvae. Interrenal cells were highlighted with red arrows. Scale bar, 100 µm.

this transgenic line will be extremely useful in studying molecular events governing early morphogenesis of interrenal gland.

4.4.3 EGFP transgene expression in the otic vesicle

In addition to the VMH and interrenal, the otic vesicle showed unexpectedly high level of ff1bEx2EGFP transgene expression. The EGFP-positive cells were first identified in the otocyst as early as 18 hpf (17-somite). However, it was only until about 20 hpf (21-somite) that the fluorescence could be effectively captured by confocal microscopy. At this stage, the EGFP signal appeared as a semi-circle structure at the ventral epithelium of the otic placode, which was just formed by the thickening of ectoderm, from lateral view (Fig. 4.6A). By 28 hpf, the otolith seeding was complete and EGFP expression continued to occupy this ventrocaudal patch of the sensory epithelium.

As the otic vesicle continued to develop and invaginate, the EGFP expression domain became restricted and shifted gradually to the posterior region of the otocyst lumen. At 48 hpf, it occupied a region that corresponded morphologically to the maculae, which is the sensory epithelium associated with the succular and utricular otoliths (Fig. 4.6B and F). From 3 through 7 dpf, EGFP expression was greatly reduced and became restricted to the posterior crista, which is connected to the posterior macula and associated with the saccular otolith (Fig. 4.6C-E, G-I). The EGFP-expressing cells eventually appeared as two symmetrical semi-circles lining the posterior wall of otic vesicle. The thinning of this EGFP-expressing posterior layer was probably due to the thinning of epithelium as the otic vesicle organ developed.

Figure 4.6 EGFP transgene expression in the otic vesicle. Confocal images of live transgenic embryos were taken from lateral (A-E), and dorsal (F-I) view to examine the embryonic development of otic vesicle from 20 hpf through 7 dpf. From 20 hpf onwards, EGFP expression appeared at the ventral epithelium of the otic vesicle (A, B). At 48 hpf, EGFP-positive cells occupied the maculae associated with the succular and uricular otoliths (B, F). From 3 dpf through 7 dpf, the EGFP expression reduced in intensity and expression domain, after which they were restricted to the posterior crista (C-E, G-I). The orientation of embryos or larvae was kept constant with anterior to the left and dorsal to the top. The main sites of EGFP expression were highlighted with different colors in B and labeled accordingly. Scale bar, 100 μm. Abbreviations: am, anterior macula; pc, posterior cista; pm, posterior macula; s, saccular otolith; u, utricular otolith.

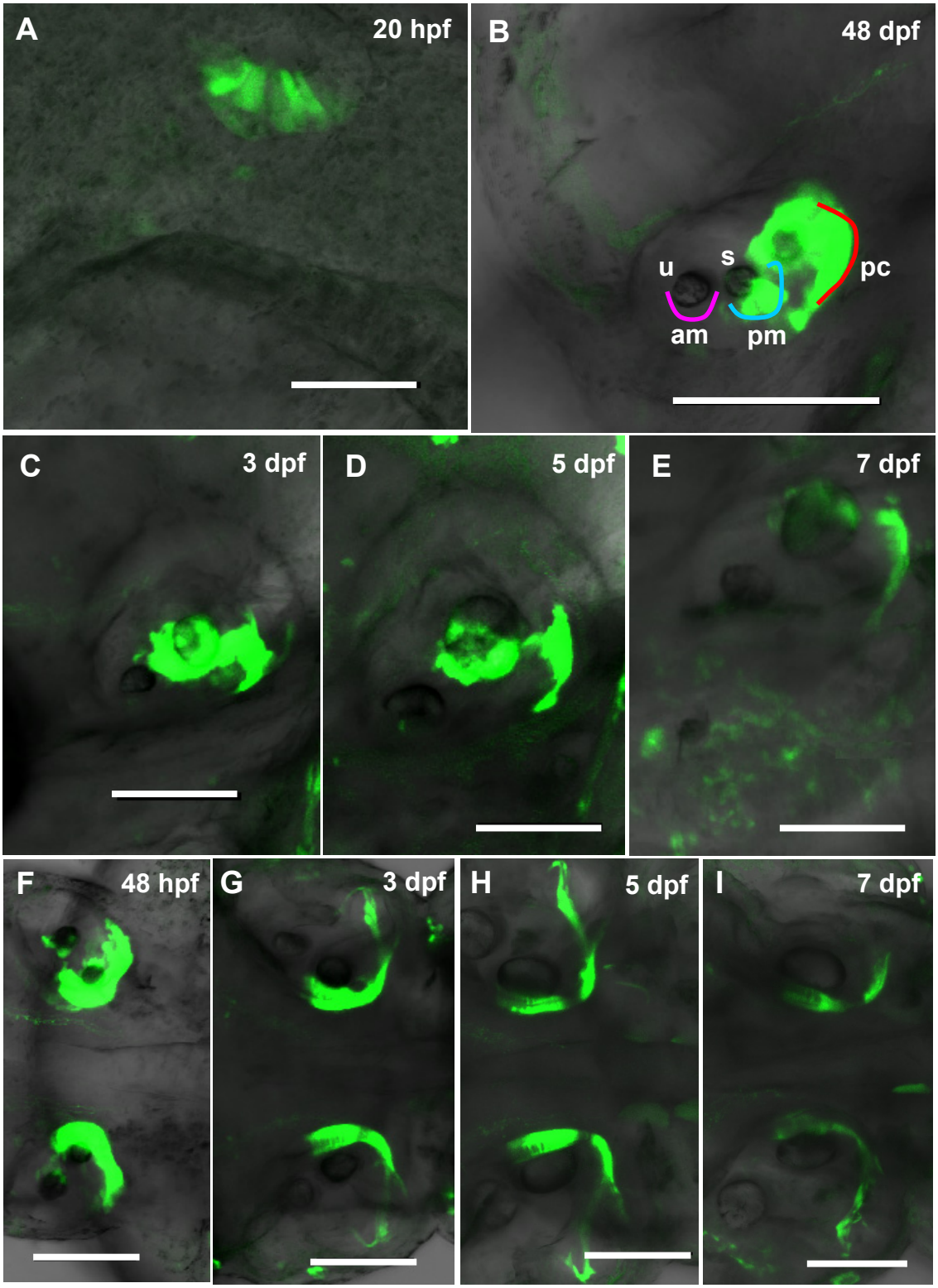
A
20 hpf
B
48 dpf
u
s
pc
am
pm
C
3 dpf
D
5 dpf
E
7 dpf
F
48 hpf
G
3 dpf
H
5 dpf
I
7 dpf

4.4.4 EGFP transgene expression in the muscle

While it was difficult to determine the exact site of EGFP expression in the skeletal muscles by transient transgenesis, the EGFP expression in stable transgenesis enabled us to do so. Weak transgene expression appeared in the skeletal muscle as early as 18 hpf (17-somite) almost coinciding with that in the otic placode. Only images from 22 hpf through 7 dpf are shown (Fig. 4.7). Strikingly, the EGFP expression in the skeletal muscles did not occupy the entire somite. Instead, they appeared as thick fibers in the centre of the each somite and seemed to be located directly lateral to the notochord (Fig. 4.7A). From the dorsal view, they appeared as two strips of rope-like structure flanking the midline at 28 hpf (Fig 4.7B).

As development continued, the expression domain decreased gradually. By 3 dpf, the thick fibers now became thin fibers organized orderly along the trunk (Fig. 4.7C). Viewing from top of the larvae, each pair of fibers was organized symmetrically and laterally to the midline (Fig. 4.7D). Each muscle fiber seemed to originate from the notochord and extended laterally and caudally in each somite. The domain and intensity of EGFP expression continued to decrease and by 7 dpf, only weak EGFP expression could be seen (Fig. 4.7 E-F).

To better localize the site of EGFP expression in the muscle, transverse cryo-sections (20 μm thickness) were prepared from 36 hpf embryos. The EGFP expression was clearly mapped to the muscle pioneer cells that will eventually form the future horizontal myoseptum (indicated by red arrows in Fig. 4.7G). They remained in contact with the notochord and become flattened cells that extend from the notochord to the lateral surface of the myotome (Du *et al*., 1997). A saggital cryo-section of the embryo at 48 hpf pointed to the same location in the muscle (Fig 4.7H).

Figure 4.7 EGFP transgene expression in the skeletal muscles. Confocal and epifluorescent (C-D, G-H) images of transgenic embryos were taken from lateral (A, C, E), and dorsal (B, D, F) view to examine the EGFP transgene expression in the muscle from 22 hpf through 7 dpf. At 22 hpf, the EGFP expression in the muscle appeared as thick fibers that were located directly lateral to the notochord (A). from dorsal view at 28 hpf, they appeared as two strips of rope-like structure flanking the midline (B). From 3 dpf through 7 dpf, the EGFP expression decreased both in intensity and expression domain as development continued (C-F). A transverse cryo-section of 36 hpf embryo at 20 μm thickness (G) and a saggital cryo-section of 48 hpf embryo at 20 μm thickness (H) indicated that the EGFP expression domain in the muscle corresponded to the muscle pioneer cells that will form the future horizontal myoseptum. The orientation of embryos or larvae was kept constant with anterior to the left and dorsal to the top. The location of EGFP expression in muscle pioneer cells bilateral to the notochord is indicated by red arrowheads. Scale bar, 100 μm. Abbreviations: ir, interrenal; n, notochord.

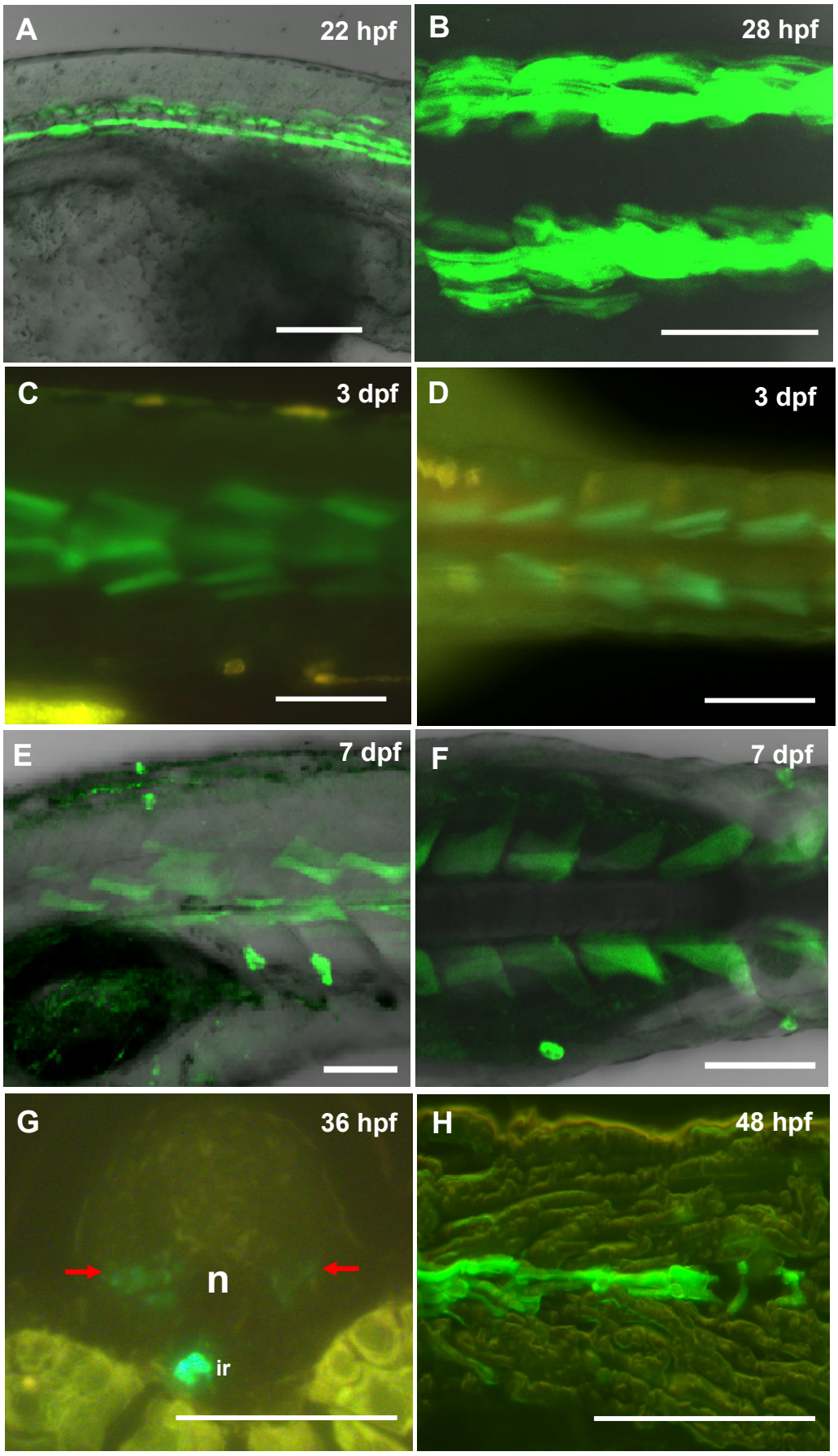
A
22 hpf
B
28 hpf
C
3 dpf
D
3 dpf
E
7 dpf
F
7 dpf
G
36 hpf
n
ir
H
48 hpf

4.5 Morpholino knockdown of *ff1b* in ff1bEx2EGFP transgenic embryos

To confirm that the ff1bEx2EGFP transgenic line fully recapitulates EGFP expression only in *ff1b*-expressing cells, the knock-down of *ff1b* gene function in this transgenic background was carried out. We were particularly interested in tracking the fate of *ff1b*-expressing cells in interrenal organogenesis in this context. Unfortunately, the EGFP transgene is expressed as a fusion protein, retaining the first 25 amino acids from Ff1b. The antisense *ff1b* morpholino, ff1bMO1, which has been used successfully for perturbing the functions of *ff1b* during embryogenesis, was designed complementary to the AUG start codon and 22 adjacent downstream ribonucleotide residues (Chai *et al*., 2003). As a result, this antisense morpholino would be able to knock down the EGFP transgene expression as well and hence defeating the purpose of lineage tracing. Therefore, new antisense morpholinos targeting different sites of *ff1b* mRNA were necessary.

4.5.1 Design of new morpholino to knock-down *ff1b* gene function

Besides blocking translation initiation in the cytosol by targeting mRNA sequences spanning the AUG codon, antisense morpholinos can also modify pre-mRNA splicing in the nucleus by targeting exon/intron splice junctions (Draper *et al*., 2001; Morcos, 2007; Moulton and Yan, 2008). After screening through the splice junctions spanning the *ff1b* pre-mRNA sequence, two antisense morpholino oligonucleotides, ff1bMO2 and ff1bMO3, which target Exon 2/Intron II and Exon 3/Intron III splice junctions, respectively, were selected and synthesized with Gene Tools Inc. (USA). Both morpholinos were 25 bases in length. Their positions across the corresponding splice junctions and oligonucleotide sequences are depicted in Figure 4.8. Both morpholinos targeted the splice donor site, and could potentially lead

to outcomes such as exon skipping, retainment of the downstream intron leading to a partial transcript, as well as, cryptic intronic or exonic splicing (http://www.gene-tools.com/node/18). The most possible outcome would be skipping of Exon 2 or Exon 3, respectively (Fig. 4.8C). With the Exon 2 skipping, translation might not be initiated properly due to a lack of AUG start codon. On the other hand, Exon 3 skipping would result in a defective Ff1b lacking Zn finger II in its DNA binding domain.

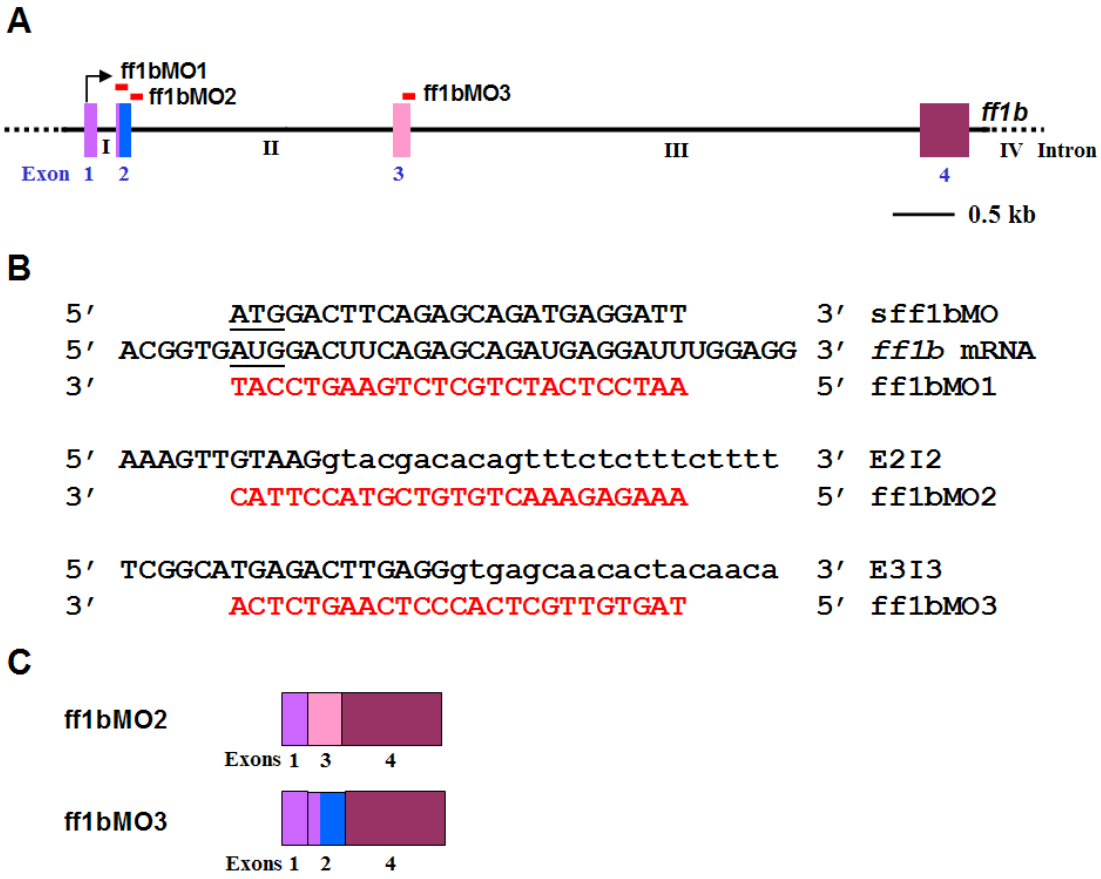

Figure 4.8 Positions and sequences of morpholino oligonucleotides used in study of *in vivo* functions of *ff1b*. (A) The relative positions of the three antisense morpholinos are indicated against the *ff1b* genomic locus. Exon regions shown in purple denote untranslated region (UTR) and those in blue denote coding region. sff1bMO, sense *ff1b* morpholino; ff1bMO1, antisense *ff1b* morpholino spanning start codon; ff1bMO2, antisense *ff1b* morpholino spanning Exon2/IntronII (E2I2) splice donor junction; ff1bMO3, antisense *ff1b* morpholino spanning Exon3/IntronIII (E3I3) splice donor junction. (B) Sequences of the morpholinos used and the corresponding sense sequences targeted by the morpholinos. The start codon is underlined. Exon and intron sequences are shown in upper and lower cases respectively. (C) The most possible outcome of ff1bMO2 and ff1bMO3 knockdown on *ff1b* transcript.

4.5.2 Determination of optimal dosage for ff1bMO2 and ff1bMO3

To determine the optimal dosage for the two newly designed morpholinos, a preliminary experiment was carried out to microinject 6.75, 11.25 and 22.5 μM final concentration of each morpholino into 1-2 cell wild type zebrafish embryos. Scoring of microinjected embryos for non-specific defects at 30 hpf suggests that the optimal working concentration for both morpholinos was 11.25 μM (Table 4.1), which is at the same range as ff1bMO1. Injected embryos were then screened at 30 hpf to determine if morpholinos caused non-specific deformation. The morphological defects that are indicative of non-specific toxicity effects include reduction of the head and eyes, an amorphous appearance of cells in the body, downward curving body axis and edema of the pericardial and yolk sac. At the dosage of 11.25 μM per embryo, less than 20% of the microinjected embryos displayed phenotypes suggestive of non-specific toxicity and this is within the the acceptable limit. In all subsequent experiments, this dosage of morpholino was used, and only embryos showing wild-type phenotype at 30 hpf were retained for further analyses.

4.5.3 Monitoring the effect of *ff1b* knockdown on interrenal development by EGFP transgene expression

The ff1bMO2 and ff1bMO3 morpholinos were microinjected into ff1bEx2EGFP transgenic embryos at 1- to 2- cell stage to a final concentration of 11.25 μM per embryo. The sense morpholino, sff1bMO (5'-ATGGACTTCAGAGCAG ATGAGGATT-3') was included as negative control. Prior to scoring for morphant phenotype class A to D at 7 dpf, the ff1bEx2EGFP embryos microinjected with 11.25 μM of ff1bMO2 and ff1bMO3 were first monitored closely for their EGFP expression in the interrenal primordia. As the

morphant phenotype of impaired osmoregulation could be largely attributed to the loss of interrenal cortisol production, close examination of interrenal morphogenesis is of central importance. Monitoring of transgene expression commenced at ~24 hpf, when weak EGFP expression could be readily detected in the interrenal, and was continued until 10 dpf. Between 36 to 48 hpf, homozygous embryos and non-fluorescent embryos were removed, and only hemizygous embryos were retained for subsequent data collection and microscopic observations.

Table 4.1 Toxicity effects of morpholinos on zebrafish embryonic development.

Morpholino	**μM**	**Wild-type (%)**	**Non-specific Morphological Defects (%)**	***n***
sff1bMO	6.75	95.5	4.0	222
	11.25	83.1	16.9	231
	22.5	40.5	59.5	257
ff1bMO1	6.75	93.7	6.3	205
	11.25	80.3	19.7	223
	22.5	30.4	69.6	214
ff1bMO2	6.75	94.3	5.7	209
	11.25	81.4	18.6	236
	22.5	33.1	66.9	254
ff1bMO3	6.75	90.5	9.5	243
	11.25	80.1	19.9	221
	22.5	30.0	70.0	217

At ~48 hpf, when the EGFP expression could be easily visualized at the developing interrenal, the morpholino-injected embryos were observed for their EGFP fluorescence at the developing interrenal gland, and eventually sorted into three groups. Those in Group I had their interrenal gland fluorescent at a level that is comparable to uninjected ff1bEx2EGFP embryos, while those in Group II had

reduced EGFP fluorescence, and Group III embryos had a complete loss of EGFP fluorescence in their interrenal gland. The proportion of morpholino-injected embryos that fell into each of the three groups is summarized in Table 4.2. Based on the percentage of embryos that showed EGFP fluorescence at their interrenal gland at this stage, the ff1bMO3 seemed to work much more efficiently than ff1bMO2.

Table 4.2 Proportions of morpholino-microinjected ff1bEx2EGFP embryos that show different degree of fluorescence in their interrenal glands at 48 hpf.

	Percentage of embryos showing EGFP in interrenal (Mean ± S.D.)			
EGFP Fluorescence	**I (Strong)**	**II (Weak)**	**III (Absent)**	***n***
sff1bMO	87.8 ± 0.87	5.9 ± 0.22	6.3 ± 0.65	354
ff1bMO2	76.6 ± 0.21	9.9 ± 1.36	13.5 ± 1.14	359
ff1bMO3	47.8 ± 3.85	21.0 ± 1.00	31.2 ± 2.85	366

Subsequent monitoring of EGFP expression in the interrenal of ff1bMO3 morphants showed encouraging correlation between this categorization and that of morphant phenotype Class A to D (Table 4.3). For instance, almost all microinjected embryos that fell into Group I at 48 hpf developed into Class A morphants (wild-type). Similarly, the majority of Group II embryos developed into Class B morphants and those in Group III generally developed into Class C and D morphants. Intriguingly, a few of the Group II embryos eventually developed into Class C morphants, while several embryos in Group III eventually started showing weak EGFP expression at their interrenal and developed into Class B morphants instead. This is most likely due to the individual variation in transgene expression level and/or tolerance of *ff1*b knockdown. Furthermore, the amount of morpholinos that were successfully delivered into each embryo was likely to vary slightly among different individuals. Nonetheless, the strong correlation between the loss of EGFP expression and the morphant

phenotype confirms that the proper development of interrenal gland is the key factor in determining the severity of morphological defects observed in *ff1b* morphants, as suggested previously by Chai *et al*. (2003).

As the ff1bMO3 worked much more effectively than ff1bMO2, only embryos microinjected with ff1bMO3 were examined in detailed for their EGFP expression in interrenal gland using confocal microscopy. In comparison to embryos injected with sff1bMO, which showed EGFP fluorescence at their interrenal gland at a level comparable to the uninjected ff1bEx2EGFP embryos (Fig. 4.9A, C, E, G), ff1bMO3 morphants that were categorized into Group III and eventually developed into Class D morphant consistently lacked fluorescent interrenal gland (Fig. 4.9B, D, F, H). This observation indicates that the formation of interrenal primordia was adversely perturbed when *ff1b* is knocked down.

4.5.4 Efficacy of ff1bMO2 and ff1bMO3 in inducing *ff1b* morphant phenotype at 7 dpf

As the phenotype of *ff1b* morphant derived from ff1bMO1 is well established (Chai *et al*., 2003; Hsu *et al*., 2003), the activity and efficacy of the two newly designed morpholinos were also assessed in comparison with it to determine if they are capable of giving rise to the same morphant phenotype in zebrafish larvae. The ff1bMO1 was microinjected into wild type zebrafish embryos and scored for morphant phenotype concurrently for comparison. The ff1bEx2EGFP embryos microinjected with sff1bMO, ff1bMO2, and ff1bMO3 morpholinos as well as wild-type embryos microinjected with ff1bMO1 were scored for morphant phenotype at 7 dpf. As reported previously, the phenotypes of the larvae could be classified into four different groups based on the severity of observed morphological defects (Table 4.3). Phenotypic changes began to appear around 5 dpf, and were fully manifested by 7 dpf.

Figure 4.9 Monitoring of EGFP transgene expression in the interrenal gland of ff1bEx2EGFP transgenic embryos following morpholino microinjections. Transgenic embryos of ff1bEx2EGFP line were microinjected with 11.25 μM of sense *ff1b* morpholino (sff1bMO) and antisense *ff1b* morpholino targeting Exon3/IntronIII splice junction (ff1bMO3) at 1 to 2 cell stage. Images of live embryos at different developmental stages (28 hpf to 5 dpf) were presented. In embryos microinjected with sff1bMO, the EGFP expression persisted at the interrenal gland in a manner that was comparable to the uninjected control from 28 hpf through 5 dpf (A, C, E, G). The EGFP expression at the interrenal was diminished in embryos microinjected with ff1bMO3 from 28 hpf through 5 dpf (B, D, F, H). EGFP expression at the interrenal gland is highlighted by red arrows. Scale bar, 100 μm.

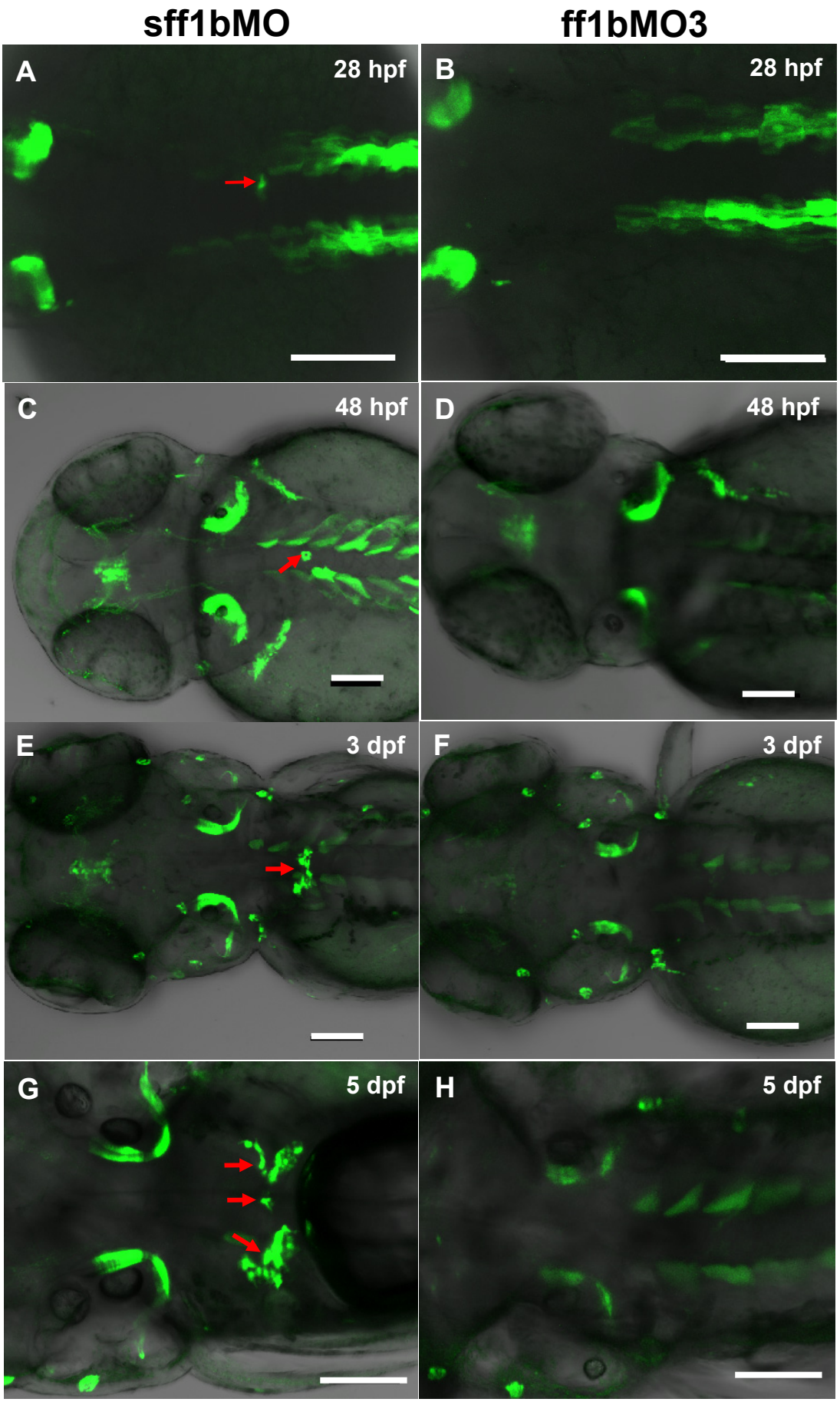
sff1bMO
ff1bMO3
A
28 hpf
B
28 hpf
C
48 hpf
D
48 hpf
E
3 dpf
F
3 dpf
G
5 dpf
H
5 dpf

Larvae were scored for morphant phenotype at 7 dpf, and repeated again at 10 dpf. In general, the phenotypes observed at 10 dpf were essentially the same as those described at 7 dpf, with the exception that fluid accumulation had become more pronounced in some embryos and the yolk sac was completely absorbed.

Table 4.3 Classification of *ff1b* morphant phenotype at 7 dpf (from Chai *et al*., 2003).

Phenotype	**Class A (Wild-type)**	**Class B**	**Class C**	**Class D**
Mouth	protruding	protruding	shortened snout	shortened snout
Swim bladder inflation	full	none	none	none
Heart beat	strong	slow	slow	slow
Pericardial sac	normal	edema	edema	edema
Blood flow	rapid	slow	none	none
Yolk sac	normal	normal	edema	severe edema
Optic sac	normal	normal	slight edema	severe edema
Yolk absorption	complete	delayed	delayed	delayed
Body axis	straight	straight	curved upward	curved upward
Blood islands	none	none	ventral tail	ventral tail

The proportion of larvae displaying the various classes of phenotypes at 7 dpf is presented in Table 4.4. Notably, ff1bMO3 knockdown of *ff1b* produced morphant phenotype at a percentage that was comparable to ff1bMO1. On the other hand, the efficacy of ff1bMO2 in perturbing *ff1b* gene function was much lower with only ~20% of microinjected embryos displayed morphant phenotype Class B to Class D. The reason underlying this discrepancy is not clear at the moment but it is a well known fact that morpholinos targeting the same mRNA function at different efficacies.

Table 4.4 Percentages of morphants exhibiting different classes of phenotypes at 7 dpf.

	Percentage of embryos (mean ± S.D.)				
Phenotype Class	**A**	**B**	**C**	**D**	***n***
sff1bMO	88.7 ± 0.38	4.8 ± 0.70	3.2 ± 0.73	3.3 ± 0.35	354
ff1bMO1	47.3 ± 1.64	20.8 ± 1.45	17.1 ± 1.56	14.8 ± 1.75	398
ff1bMO2	79.5 ± 1.67	6.7 ± 2.27	9.0 ± 0.96	4.8 ± 0.37	344
ff1bMO3	46.5 ± 3.45	22.4 ± 1.37	17.5 ± 0.14	13.6 ± 2.21	366

Besides scoring for morphant phenotype, the different classes of ff1bMO3 morphants were also subjected to microscopic analyses for EGFP expression in their interrenal gland at 7 dpf. Notably, morphants that fell into Class C and D completely lacked interrenal gland at 7 dpf (Fig. 4.10E and F). Class B morphants, on the other hand, showed residual traces of EGFP expression at their interrenal (Fig. 4.10C and D) but the fluorescent intensity and domain were both much lower than that in the Class A morphants (Fig. 4.10A and B), which were essentially the same as uninjected or sff1bMO-injected embryos.

Collectively, these findings demonstrate that the organogenesis of interrenal gland is adversely affected by *ff1b* knock-down and the severity of phenotype is directly correlated with both the presence and number of interrenal cells. This conclusion supports our hypothesis that the *ff1b* morphant phenotypes observed can be largely attributed to corticosteroid insufficiency that resulted from a reduced size or a complete lack of interrenal organ. Importantly, the morpholino knock-down experiment beautifully demonstrated the convenience offered by the ff1bEx2EGFP transgenic line to perform live imaging of interrenal morphogenesis without additional experimental manipulation of zebrafish embryos such as ISH.

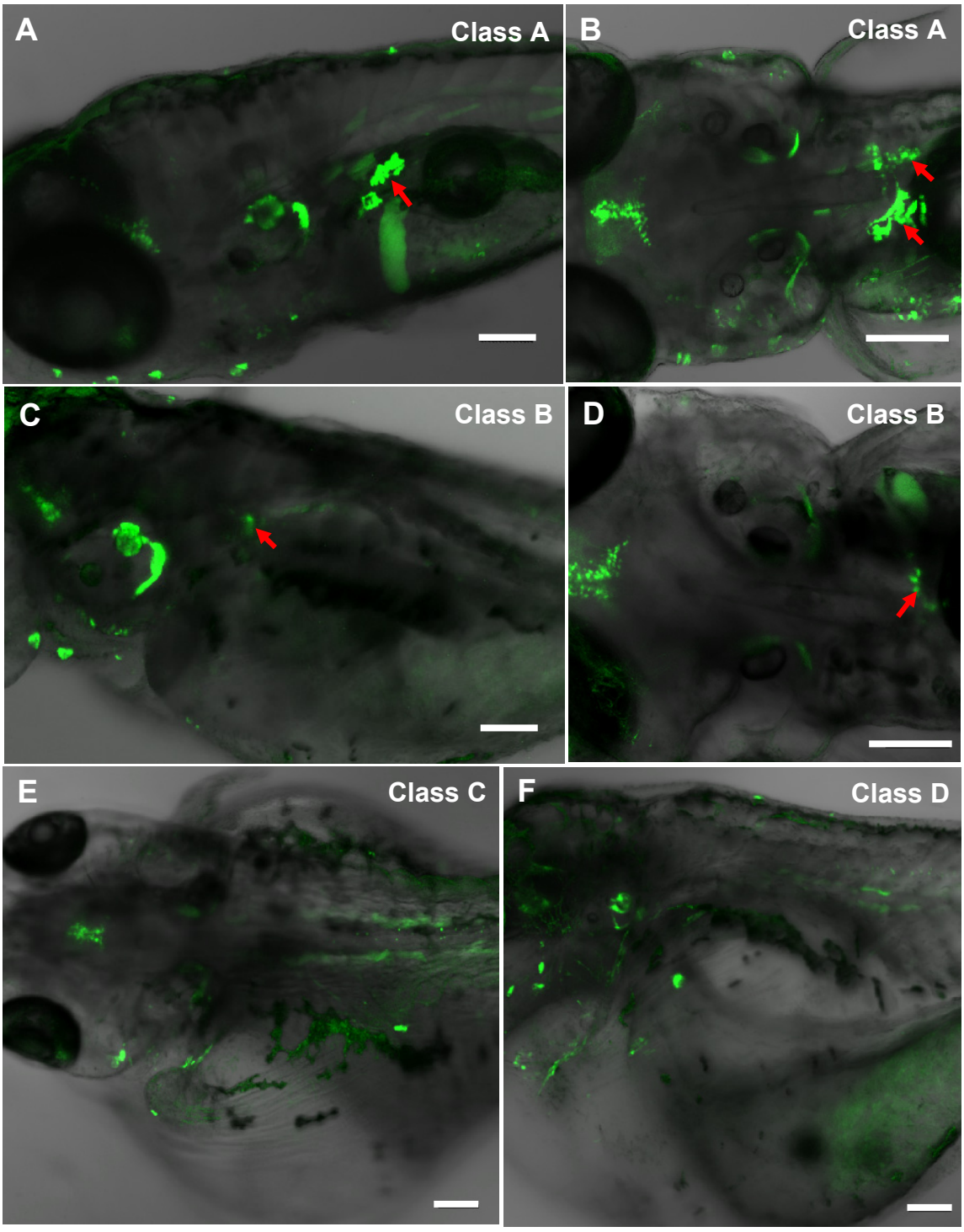

Figure 4.10 EGFP transgene expression in the interrenal gland of *ff1b* morphants at 7dpf. Ff1bEx2EGFP transgenic embryos were microinjected with *ff1b* antisense morpholino ff1bMO3 and monitored for EGFP expression in the interrenal gland. Images of morphants Class A to D at 7 dpf were captured with confocal microscopy. While Class A morphants (A-B) showed EGFP expression that was comparable to the uninjected controls at their interrenal glands, Class B morphants (C-D) showed reduced EGFP expression and Class C and D morphants (E-F) completely lacked EGFP expression at their interrenal glands. Interrenal cells are indicated by red arrows. Scale bar, 100 μm.

4.6 Treatment of ff1bEx2EGFP transgenic embryos with aminoglutethimide, a steroid inhibitor

Excessive fluid accumulation in *ff1b* morphants suggests a dysregulation of osmoregulatory functions. Since the interrenal gland is known to be essential for osmoregulation in teleosts through its secretion of corticosteroids (Norris, 2006), it is reasonable to postulate that the osmoregulatory phenotypes observed in *ff1b* morphants could have resulted from the loss of interrenal steroidogenic functions.

To test this possibility, an inhibitor-based method has been adopted previously to interfere with the steroidogenic activities of the interrenal gland in our laboratory. It was reported that the treatment of wild-type zebrafish embryos with the steroid inhibitor, aminoglutethimide (AG), resulted in late larval phenotypes that were highly reminiscent of *ff1b* morphants (Chai *et al*., 2003). However, the AG-treated larvae that displayed *ff1b* morphant-like phenotype were not examined histologically for the presence of *ff1b* transcripts or 3β-Hsd enzymatic activity in the interrenal gland. AG is a potent non-competitive inhibitor of the P450SCC enzyme (Uzgiris *et al*., 1977; Whipple *et al.*, 1978) and it is also known to inhibit aromatase activity (Graves and Salhanick, 1979; Purba *et al*., 1994). Thus, treatment of embryos with AG would be expected to inhibit *de novo* synthesis of steroids from cholesterol in the interrenal gland, thereby effecting pharmacological interrenalectomy. It will be useful and interesting to repeat this inhibition experiment in the ff1bEx2EGFP transgenic line to better understand the connection between the observed phenotypes and interrenal morphogenesis in zebrafish.

The transgenic embryos were treated with 1 mM of AG, starting from 8 hpf. Similarly, homozygous embryos and non-fluorescent embryos were removed between 36 to 48 hpf, and only hemizygous embryos were retained for subsequent data

collection and microscopic observations. The AG inhibition resulted in late larval phenotypes that were remarkably similar to those shown by *ff1b* morphants Class B to D. Subcutaneous edema became evident in ~70% of the larvae from around 7 dpf. At 10 dpf, phenotype which included edema of the cranial, curvature of the body axis, optic, pericardial and yolk sacs, a shortened snout and protrusion of the lower maxilla was clearly manifested.

Despite the similarity in the final outcome of the two lines of experiments, subtle differences were discernible. For instance, the penetrance of AG treatment was much higher than that of morpholino knockdown. Nearly 73% of treated larvae displayed the phenotype of impaired osmoregulatory functions, which were indicated by serious yolk sac edema (Table 4.5). This is probably due to the high diffusibility of AG. However, a large proportion of the AG-treated embryos (50%) displayed class B phenotype. Besides, yolk sac edema in the most severely affected AG-treated larvae was generally less extensive compared to Class C and D *ff1b* morphants. This probably reflects a better tolerance of zebrafish embryos to AG inhibition compared to *ff1b* knockdown. In contrast to *ff1b* morphants, no blood island formation was noted in AG-treated larvae. These differences indicate that the molecular mechanisms underlying *ff1b* knockdown and steroid inhibition could be different to certain extent although embryos under the two experimental strategies gave rise to similar outcome.

Table 4.5 Percentages of AG-treated embryos exhibiting different classes of *ff1b* morphant phenotypes at 7 dpf.

	Percentage of embryos (Mean ± S.D.)				
Phenotype Class	**A**	**B**	**C**	**D**	***n***
Buffer control	93.5 ± 0.70	3.0 ± 0.66	2.6 ± 0.14	1.76 ± 0.09	341
AG-treated	26.5 ± 0.81	47.5 ± 0.81	15.9 ± 0.30	10.1 ± 0.36	407

So could the morphogenesis of interrenal gland be affected in AG-treated embryos? The impaired osmoregulation observed in AG-treated larvae was probably due to the lack of glucocorticoids, as a result of AG inhibition but it should not affect the development of interrenal gland. However, there is still a possibility that a perturbation in the feedback regulation mediated by gluococorticoids may lead to a downregulation of *ff1b* and hence interrenal morphogenesis. The previous attempt of AG inhibition had not addressed these issues, partially due to the difficulty of performing ISH and immunohistochemical assays on the larvae with edema. The ff1bEx2EGFP embryos have certainly provided an ideal system to study the effect of AG inhibition on interrenal development.

Monitoring of EGFP expression in the interrenal gland of AG-treated ff1bEx2EGFP embryos revealed that the interrenal development was largely unaffected throughout embryogenesis (Fig. 4.11). Even when they started to show phenotypes of *ff1b* morphants at 7 dpf, the interrenal gland could be detected and located easily (Fig. 4.11E-H). Class A larvae showed transgene expression that was essentially the same as buffer control. While the interrenal gland was almost comparable to the buffer control in terms of size and shape, larvae of Class B to Class D generally had their interrenal gland slightly expanded and the displaced as a result of the serious edema and distortion of the whole body axis (Fig. 4.11F-H).

Taken together, these observations indicate that the morphogenesis of interrenal gland is not affected by steroid deficiency induced by AG. The observations confirm that the end product of steroidogenesis does not play a role in regulating the development of interrenal gland. Therefore, the similar morphological defects observed in *ff1b* morphants and AG-treated larvae could be largely attributed to the identical end result of the two experiments, which is gluococorticoid insufficiency.

Figure 4.11 Treatment of ff1bEx2EGFP transgenic embryos with steroid inhibitor, aminoglutethimide (AG). Transgenic ff1bEx2EGFP embryos were treated with 1 mM of AG in egg water containing 1.5 mM of HEPES buffer (pH 7.4) from 8 hpf onwards. Embryos were examined for EGFP transgene expression particularly those in the interrenal gland, at different developmental stages using epifluorescence (A, D) or confocal microscopy (B, C, E-H). From 36 hpf through 5 dpf, the EGFP expression persisted in the interrenal gland at a level that is comparable to the untreated embryos (A-D). Even when the AG-treated larvae started to show morphological defects in reminiscent of *ff1b* morphant Class A to D at 7 dpf, the EGFP expression at their interrenal glands remained largely intact (E-H). Positions of interrenal cells are indicated by red arrows. Scale bar, 100 μm.

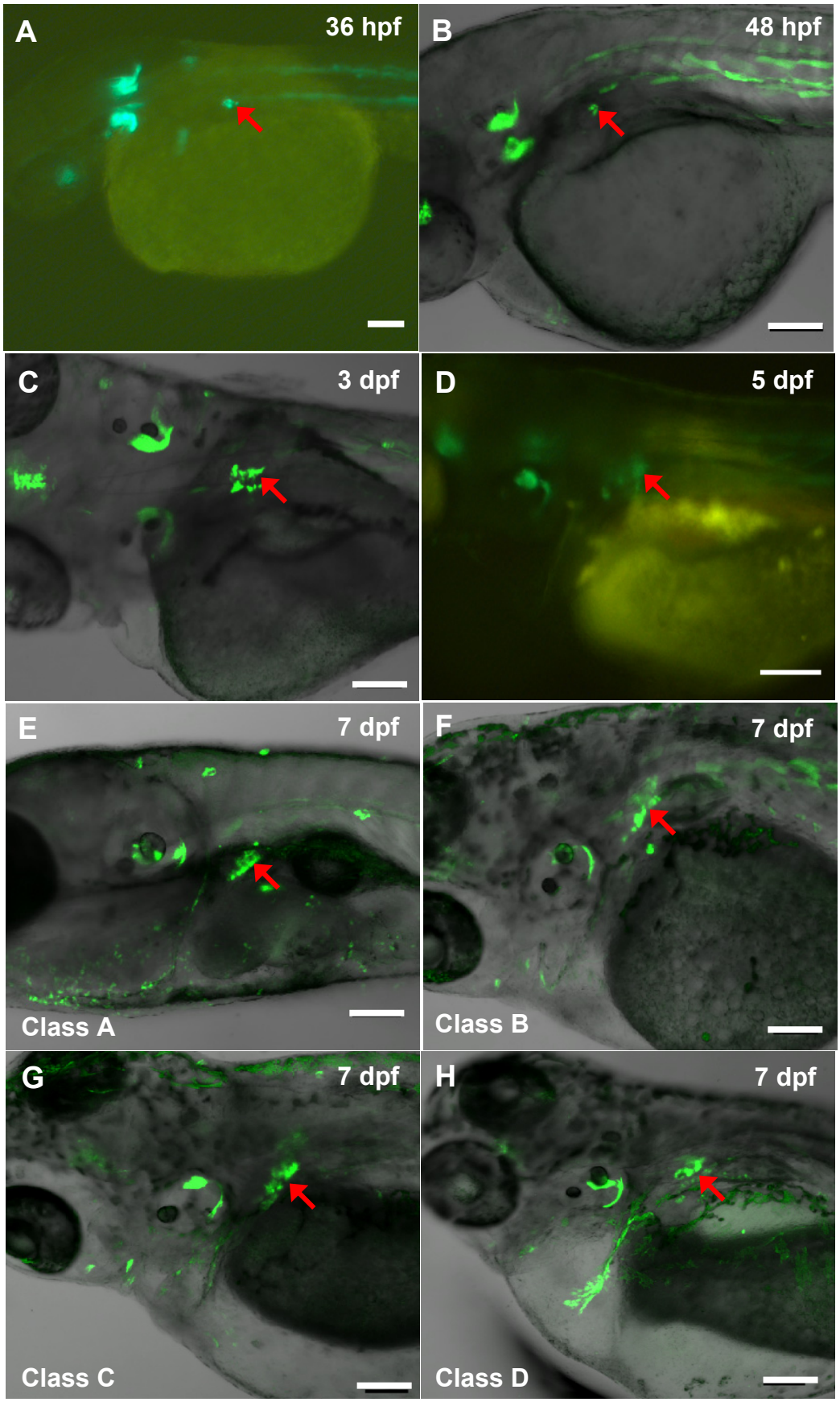
A
36 hpf
B
48 hpf
C
3 dpf
D
5 dpf
E
7 dpf
Class A
F
7 dpf
Class B
G
7 dpf
Class C
H
7 dpf
Class D

4.7 Summary

Using a BAC transgenesis strategy, we describe the first successful targeting of EGFP reporter to the VMH and interrenal gland using endogenous regulatory sequences from the zebrafish *ff1b*. In conjunction, EGFP expression was also observed in VMH-associated neuronal projections, otic vesicle, muscle pioneer cells, common cardiac vein, and neuromasts. Some of these expression domains might represent genuine *ff1b* expression *in vivo* that were not captured by ISH analyses previously. The novelty and versatility of the ff1bEx2EGFP transgenic platform to study the roles of Ff1b in endocrine development and function, particularly with regards to the interrenal gland in zebrafish, was well demonstrated by the injection of newly designed ff1bMO3 and chemical treatment with AG. Using this stable transgenic line, we were able to trace the the fate of *ff1b*-expressing cells following *ff1b* knockdown from much earlier developmental stage without the need to perform labourious ISH assays. Interestingly, lineage tracing of EGFP-expressing interrenal cells in AG-treated embryos demonstrated that the interrenal development was largely unaffected despite the fact that they showed similar phenotype of impaired osmoregulation as *ff1b* morphants. The ff1bEx2EGFP transgenic line will certainly aid in unraveling the molecular factors and mechanisms underlying the development and function of *ff1b*-expressing organs in zebrafish with much greater efficiency and propriety.

CHAPTER 5

Characterization of *ff1b* locus to identify interrenal-specific enhancers

5.1 Introduction

Ff1b is established as a master regulator of interrenal gland development in zebrafish (Chai and Chan, 2000; Chai *et al*., 2003; Hsu *et al*., 2003), in reminescent of its mammalian ortholog, *SF-1*. In mouse, *Sf-1* is required for the differentiation and maintenance of the primordia for adrenals and gonads but it is dispensable for their early formation (Luo *et al*., 1994). Apparently, additional yet unknown factors are acting upstream of SF-1 to specify the cell fate of adrenals and gonads at initial stages and to induce the onset of SF-1 expression in early embryonic development. In zebrafish, transcriptional activation of Ff1b in various endocrine organs has not been carefully analyzed but there is sufficient evidence in mammals to suggest that specific enhancers exist for individual organ expression.

It is noteworthy that the four zebrafish *ff1* isoforms isolated have expression domains that overlap, from embryonic till adult stages (Kuo *et al*., 2005). In a developing zebrafish embryo, the transcripts of *ff1a*, *ff1b*, and *ff1d* can be detected in distinct VMH subdomains that partially overlap with one another (Chai and Chan, 2000; von Hofsten *et al*., 2005; Kurrasch *et al*., 2007). Moreover, *ff1d* is transiently co-expressed with *ff1b* in the interrenal gland at about 30 hpf and they are both highly expressed in mature gonads (von Hofsten *et al*., 2005). The overlapping expression domains of *ff1* genes imply that they may regulate each other's expression. In addition, functional redundancy might exist among the Ff1 isoforms when they are co-expressed in the same cell, as they bind to the same FRE. In rodents, the expression of

SF-1 and *LRH-1* are partially overlapped in the ovary with differential expression levels in different cell types (Falender *et al*., 2003; Hinshelwood *et al*., 2003). Although the molecular mechanisms underlying the transcriptional regulation of the two genes in the ovary have not been characterized, molecular switching between the two NRs at α-inhibin promoter has been demonstrated (Weck and Mayo, 2006).

In contrast to detailed characterization of their expression patterns and functions in the endocrine tissues, the transcriptional mechanisms that direct *FF1* genes to their designated tissues remain largely undefined. Despite the identification of a few promoter elements, including an E box, a CCAAT box and three Sp1 binding sites (Daggett *et al*., 2000; Nomura *et al*., 1995; Scherrer *et al*., 2002; Woodson *et al*., 1997) that control the basal transcription of *SF-1*, subsequent investigations suggested that these regions were unable to account for the specific temporal and spatial expression of the gene. Initial effort to drive expression of reporter transgenes using short promoter fragments from mouse *Sf-1* locus failed to fully recapitulate the endogenous expression pattern of *Sf-1* (Stallings *et al*., 2002; Wilhelm and Englert, 2002; Jeays-Ward *et al*., 2003). As for zebrafish *ff1b*, the 5' upstream promoter of *ff1b* up to 20 kb did not target GFP reporter gene to *ff1b*-expressing tissues in zebrafish. These findings collectively indicate that regulatory elements governing *ff1b* and *Sf-1* expression *in vivo* are most likely located distally from the basal promoter regions.

An alternative strategy to determine potential upstream regulators of SF-1 is through the studies of gene mutations that affect *SF-1* expression. By this approach, transcription factors such as WT1 and PBX1 have been proposed to act upstream of SF-1 because *Sf-1* expression was markedly reduced in $WT1^{-/-}$ and $PBX1^{-/-}$ mice (Wilhelm and Englert, 2002; Schnabel *et al*., 2003). Direct evidence of the involvements of PBX1 in the regulation of *Sf-1* transcription came from subsequent

characterization of a fetal adrenal enhancer identified in the intron IV of mouse *Sf1* gene (Zubair *et al*., 2006).

As the tissue-specific enhancers of *SF-1* are expected to lie distally to the proximal promoter region, the effort in studying the transcriptional regulation of *SF-1* has recently switched to transgenic mouse assays that utilize BAC or even yeast artificial chromosome (YAC) plasmid, which can accommodate the entire gene locus of *Sf-1* (Karpova *et al*., 2005; Shima *et al*., 2005; Zubair *et al*., 2006). In conjunction, the *ff1b* locus from the BACff1b2 plasmid has been demonstrated to target EGFP reporter transgene specifically to *ff1b*-expressing tissues (Chapter 4). By dissecting the transgene activity of genomic fragments spanning distinct but overlapping regions of *Sf-1* locus in transgenic mouse, a highly conserved VMH enhancer (~600 bp) has been identified in intron VI of mouse and human *SF-1* loci. This enhancer is able to recapitulate the endogenous *Sf-1* expression in fetal ventromedial diencephalons till adult VMH in transgenic mice studies (Shima *et al*., 2005). Following this study, a pituitary-specific enhancer of *Sf-1* has also been recently identified in Intron VI (Shima *et al*., 2008). Subsequently, a BAC- and YAC- transgenic mouse approach has revealed a fetal adrenal enhancer (FAdE) in intron IV of mouse and human *SF-1* loci (Zubair *et al*., 2006).

The major objective of this chapter was to characterize the genomic structure of *ff1b* gene in zebrafish and to uncover the regulatory elements that are necessary to specify the temporal and spatial expression of *ff1b*. This was done by sequencing and analyzing *ff1b* gene locus contained in the BACff1b2 plasmid. We believe that specific enhancer/repressor elements are located in specific regions within or flanking the *ff1b* gene locus, distally to the basal promoter region. Each of these modules of regulatory element will control the expression of *ff1b* in a specific tissue at a specific

time. By combining Red/ET recombination-based deletions of specific genomic fragments and transient transgenesis studies in zebrafish, we managed to locate the *cis*-elements that potentially regulate the interrenal-specific expression of *ff1b* to Intron IV, which is uniquely present among all the vertebrate *FF1* genes characterized so far. Further characterization of these regulatory regions will certainly help to identify the upstream *cis*- and *trans*- factors that regulate the tissue-specific expression of *ff1b*.

5.2 Genomic structure of *ff1b*

In an effort to recover genomic sequences for the entire zebrafish *ff1b* locus, a zebrafish BAC library was screened using the PCR screening approach (Genome Systems Inc, MO, USA). This gave rise to BACff1b2, which contains at least 20 kb of 5' flanking sequences and the entire *ff1b* gene locus (~25 kb). A 16.9 kb *Eco*RI fragment encompassing the 5' flanking region of *ff1b* was isolated and completely sequenced using transposon-mediated tagging. Genomic sequences spanning the *ff1b* gene (Exon 1 through Exon 8) in the BACff1b2 were characterized by restriction enzyme subcloning and exon-containing fragments were identified by Southern blot hybridization of restricted BACff1b2 using a probe targeting Exon 4 (Chai and Chan, 2000). Large overlapping fragments were then cloned into pBluescript II SK (Stratagene) or pGEM11zf (Promega) vectors for sequencing. To access internal regions of these fragments, deletion subclones were generated by restriction enzyme digestion. DNA sequences were assembled using computer program Sequencher (version 4.8; Gene Code Corp., MI, USA). Any gaps in the contig assembly were completed by sequencing with primers targeting known sequences flanking the gap in the BACff1b2 plasmid. Notably, the entire genomic DNA insert carried by the BACff1b2 plasmid was not sequenced fully. Only the *ff1b* locus (Exon 1 to Exon 8)

with ~1 kb of 3' downstream sequences and nearly 21 kb of 5' upstream sequences has been completed and the genomic sequence is provided in Appendix I.

5.2.1 Exon/Intron organization of *ff1b* gene

Analysis of the *ff1b* locus revealed that the 2522 bp long *ff1b* transcript is encoded by 8 exons distributed over a region of approximately 25 kb (Fig. 5.1). The 5' untranslated region (UTR) is transcribed almost entirely from Exon 1 as the start codon AUG starts at the seventh nucleotide of Exon 2. Exon 8 represents the largest exon in size (1305 bp) but the final 1065 nucleotide sequences are transcribed into 3' UTR. Upstream to Exon 1, nearly 21 kb of 5' flanking sequences were completed with an AT-rich gap at position -8473 bp that could not be sequenced using BigDye (Sanger) but was estimated to be ~0.8 kb in size by PCR analysis using flanking primers (data not shown).

The genomic organization of zebrafish *ff1b* is highly conserved with that of the mouse (Ikeda *et al*., 1993; Ninomiya *et al*., 1995) and human *SF-1* (Wong *et al*., 1996), except for the presence of the additional Intron IV (Fig. 5.1). While Exon 4 in the other three zebrafish *ff1* genes and other vertebrate *FFf1* genes represents the largest coding exon and encodes the entire hinge domain region, the equivalent coding region of the zebrafish *ff1b* hinge domain is split into Exon 4 and Exon 5, thereby giving rise to the additional Intron IV. This genomic arrangement is also observed in invertebrate *FF1* genes including, *Drosophila Ftz-F1* (Fig. 5.1) and hence this intron may represent an ancestral characteristic of *FF1* genes.

The sizes and nucleotide sequences spanning all exon/intron junction sequences are presented in Table 5.1. All introns have been fully sequenced except for Intron V, which contains an AT-rich region that was recalcitrant to Sanger sequencing and is estimated to be ~1 kb in size using PCR analysis with flanking primers (data not

shown). All exon/intron junctions of *ff1b* follow the 5' GT—AG 3' rule and they are highlighted in blue (Table 5.1). Sequences of exons and introns are shown in upper and lower cases respectively and amino acids encoded at each exon/intron junction are indicated in red.

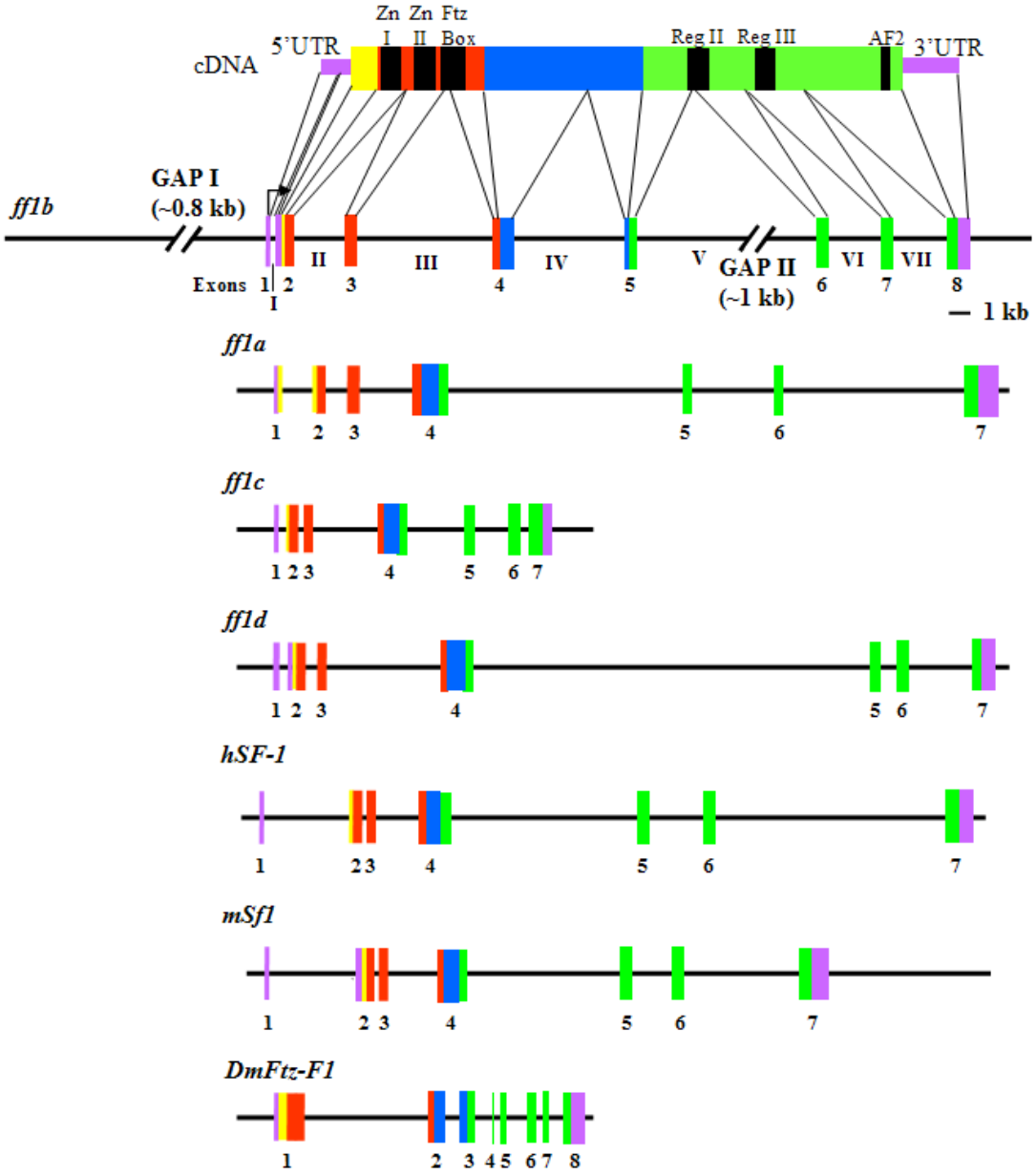

Figure 5.1 Genomic organization of the zebrafish *ff1b* gene. The exon/intron organization of *ff1b* and the corresponding protein domains encoded by the exons are indicated in different colors. The exon/intron organization of the other three zebrafish *ff1* genes, namely *ff1a*, *ff1c*, and *ff1d* as well as human *SF-1*, mouse *Sf1*, and *Ftz-F1* from *Drosophila melanogaster* (*DmFtz-F1*) are shown in parallel for comparison.

Table 5.1 Sequences spanning the exon/intron junctions of zebrafish *ff1b* gene.

Exon	bp	Donor	Intron	bp	Acceptor
1	105	TTTAATATTGAGgtattactgt	I	151	tctgtgtcagACGGTGATGGAC M D
2	108	GAAAGTTGTAAGgtacgacaca E S C K	II	2129	accatgccagGGTTTTTTCAAG G F F K
3	142	AGAGACTTGAGGgtgagcaaca R L E G	III	5576	gtcttctcagCTGTGCGTGCAG V R A D
4	440	GATGAGGAGCAGgtatgaagca D E E Q	IV	3754	gcgtgcgcagGTGAGAGGAAAG V R G K
5	157	AAGGAACTAAAGgtacggctcc K E L K	V	~10560	tgtgattcagGTGGGCGATCAG V G D Q
6	120	ACAGGACAGGAGgtgagcgtct T G Q E	VI	1792	tgtgctgcagGTGGAGCTGTCG V E L S
7	145	TCTTCAACCCCAgtgagtctca F N P S	VII	2202	tcttcctcagACGTGAAGCTCC V K L L
8	1305	CCGTTCATACCA			

5.2.2 The 5' putative promoter region of zebrafish *ff1b*

By transient transfection analyses, several *cis*-elements that regulate the basal transcription of mammalian (human, rat, and mouse) *SF-1* have been identified at its 5' proximal promoter region (Fig. 5.2). They include an E box that binds basic helix-loop-helix (bHLH) family of transcription factors (Nomura *et al*., 1995; Harris and Mellon, 1998), a CCAAT box and Sp1 binding sites (Woodson *et al*., 1997). In addition, tissue-specific transcription factors, such as GATA4 (Tremblay and Viger, 2001) and Sox9 (Shen and Ingraham, 2002), have also been implicated in the activation of *SF-1* transcription. Notably, two FREs were mapped at positions -454/-442 and +176/183 of human *SF-1* and SF-1 itself has been shown to bind the FRE present in its first intron in rat and human genes, indicating a possibility of autoregulation mechanism (Nomura *et al*., 1996).

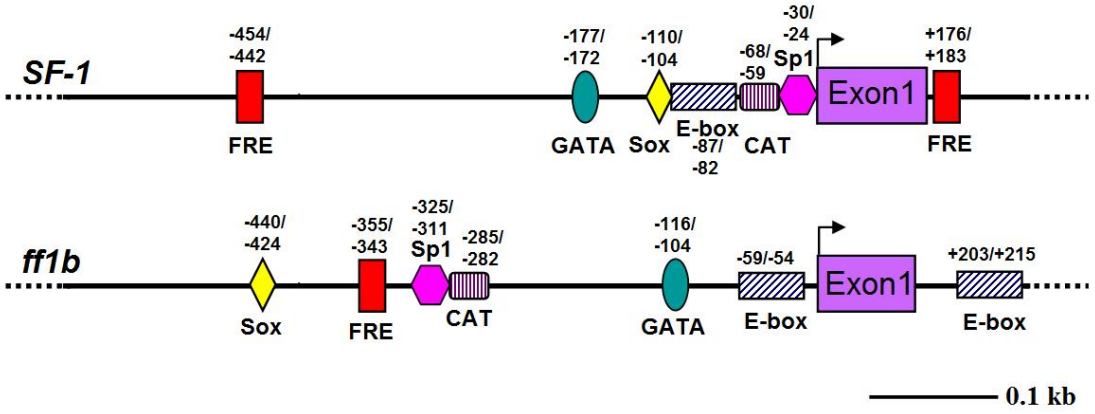

Figure 5.2 Schematic representation of *cis*-elements present in the 5' proximal promoter of mammalian *SF-1* and zebrafish *ff1b* genes. A summary of experimental findings for basal promoter of *SF-1* in human, rat and mouse is illustrated. Equivalent region of 5' promoter sequences (up to -500 bp) of zebrafish *ff1b* was analyzed computationally with MatInspector and the putative *cis*-elements are shown. Regulatory *cis*-elements are presented in different shapes and colors and their positions relative to the transcription start site (indicated by black arrowhead) are shown. Abreviations: FRE, Ftz-f1 response element; GATA, GATA protein response element; Sox, Sox protein binding sites; CAT, CAAT box; Sp1, Sp1 response element.

To identify potential transcription factor binding sites (TFBSs) that might play a role in the transcriptional activation of *ff1b*, the equivalent region of 5' proximal promoter of *ff1b* was subjected to bioinformatics analyses using the online analysis program MatInspector (www.genomatix.de). Encouragingly, similar binding elements were revealed in the basal promoter region of *ff1b* to those that were found in the human regulatory region. In close proximity to the transcription start site, motifs resembling the E-box element (-59/-54 and +203/+215) and CCAAT box (-285/-283) were found (Fig. 5.2). In addition, binding sites for *trans*-factors including GATA, Sp1 and Sox were mapped at positions -116/-104, -325/-311, and -440/-424 respectively. Although the positions of the promoter elements varied slightly between mammalian *SF-1* and zebrafish *ff1b*, the above mapping of *cis*-elements indicate that the mechanism of activating the basal promoter for *Ftz-f1* genes is largely conserved across the various vertebrate species.

5.2.3 The zebrafish *ff1b* is located on linkage group 8

Chromosomal location of the zebrafish *ff1b* has been mapped to position LG8_139.1 cM of linkage group (LG) 8 using the Heat-Shock (HS) meiotic mapping panel (Woods *et al*., 2000; Kuo *et al*., 2005). The zebrafish *ff1b* gene is localized in ctg12124 together with four other genes, namely *cyr61*, *lmo4*, nr*6a1*, and *c11orf8* (Fig. 5.3). The tight linkage of *ff1b* and *ff1d* to *nr6a1a* and *nr6a1b*, respectively, thus supports the orthology of both genes to *NR5A1* as well as confirming their relationship as gene duplicates. The *ff1d* locus on LG21 retains contiguous synteny of neighboring genes when compared to human and mouse *SF-1* locus, while the *ff1b* locus on LG8 is completely different. Thus, it appears that *ff1b* locus has undergone genomic rearrangement such as inversion and deletion, to evolve to its present genomic context (Kuo *et al*., 2005).

The zebrfish genome database at Ensembl (http://www.ensembl.org/Danio_rerio/Info/Index), however, does not give a similar syntenic arrangement of neighboring genes for the *ff1b* locus (Fig. 5.4A), and the only gene retained by both genomic maps is *cyr61*. As the current version of the zebrafish genome is still incomplete, particularly for this segment of the LG8, as well as the expected tight linkage of *nr6a1a* to *ff1b*, the *ff1b* chromosomal context derived from the HS mapping panel is likely to be the more correct version. In contrast, the genomic context predicted for *ff1d* at Ensembl genome assembly is similar to the genetic mapping analysis. However, the syntheny of downstream neighboring genes of *ff1d* is only maintained until *nek* and the next expected downstream ORF, *lhx2*, could not be identified in any close proximity to *ff1d* locus on LG21 at Ensembl database (Fig. 5.4A).

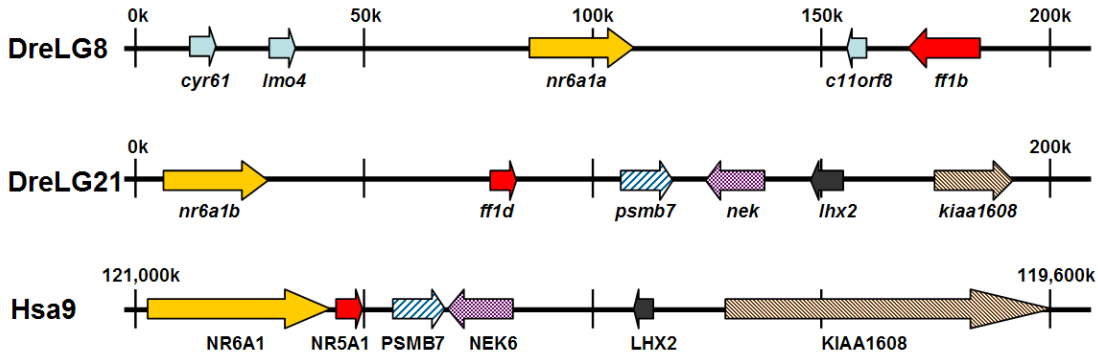

Figure 5.3. Genomic context of *ff1b* on linkage group (LG) 8 in comparison to *ff1d* and human *NR5A1* by genetic mapping. Comparison of *ff1b* and *ff1b* locus on zebrafish chromosome DreLG8 and DreLG21 to *NR5A1* locus on human chromosome Hsa9 (modified from Figure 2 of Kuo *et al*., 2005). The *ff1b* and *ff1d* genes were mapped on the LN54 radiation hybrid panel, and intercalated into the map from the Heat-Shock meiotic mapping panel on the basis of nearby markers mapped on both panels.

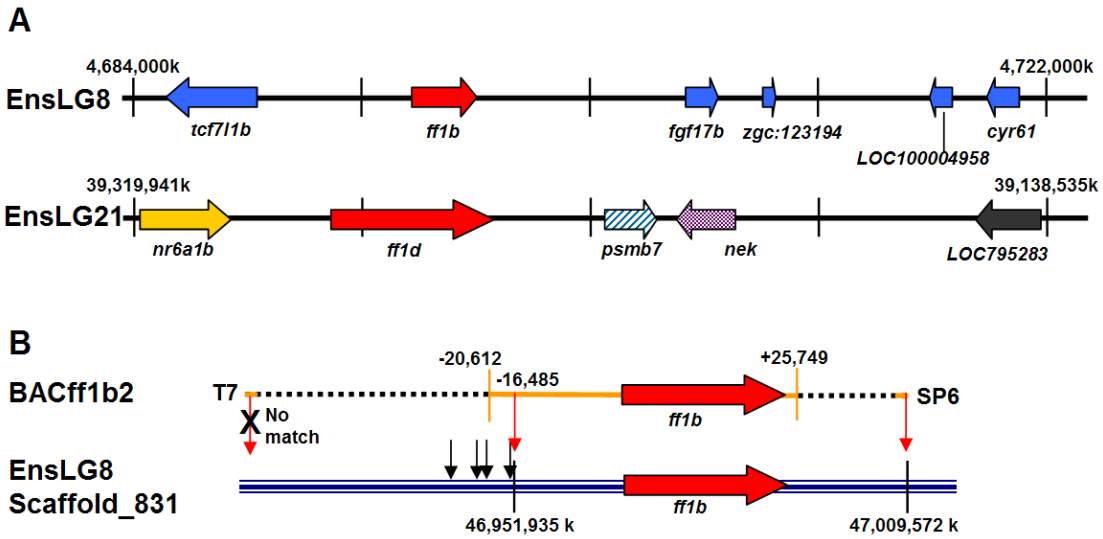

Figure 5.4 Genomic context of *ff1b* and *ff1d* on LG8 and LG21 displayed at Ensembl and mapping to the *ff1b* genomic sequences determined from BACff1b2. (A)Schematic representation of genome assembly predicted for *ff1b* and *ff1d* at Ensembl genome browser of zebrafish (Zv7). (B) Comparison of genomic sequences determined from BACff1b2 to that in scaffold_831 on LG8 at Ensembl genome browser. The genomic DNA insert in the BACff1b2 plasmid is flanked by T7 and SP6 vector priming sites at 5' and 3' end, respectively. The portions of genomic sequence that has been determined in this study are highlighted in orange. The portions of genomic DNA insert that has not been sequenced are indicated in dashed line. The corresponding genomic regions from scaffold_831 of Ensembl database that have been matched to BACff1b2 sequences are displayed underneath. The extreme 5' and 3' end of matching sequences between the two contigs are indicated by red arrows. Gaps in the genomic sequences of scaffold_831 located at the 5' upstream region of *ff1b* locus are indicated by black arrows.

The ~46 kb of genomic sequences that have been determined from the BACff1b2 was compared to zebrafish genome database (Ensembl; Fig. 5.4B). The *ff1b* locus spanning Exon 1 to Exon 8 was first mapped to position 46,968,420 to 46,993,052, which was annotated as *nr5a1a* on the contig termed scaffold_831 on LG8. The genomic sequences obtained from BACff1b2 matched the database sequence from -16,485 to +25749 bp, which corresponded to 91% of our genomic sequences spanning 46,361 bp (-20,612 to +25749 bp). Also, our genomic sequences have resolved all the remaining gaps that were present in scaffold_831 for *ff1b*, which consisted of two gaps in Intron III and one gap each in Intron IV and Intron VII.

Although the entire genomic DNA insert contained in the BACff1b2 plasmid has not been sequenced in full, the extreme 5' and 3' end sequences of the DNA insert were obtained by DNA sequencing with T7 and SP6 primers flanking the insert on pBeloBAC-11 vector. Notably, sequences at the 3' end of the genomic insert generated from SP6 priming in BACff1b2 can be mapped in scaffold_831 but not the 5' end sequences generated from T7 priming. This matching eventually gave rise to an additional 16,520 bp of genomic sequences 3' to where we have stopped sequencing in the BACff1b2 plasmid (Fig. 5.4B). Due to the presence of several unsequenced gaps in the 5' upstream region of *ff1b* locus in scaffold_831, no additional 5' upstream sequences could be matched with confidence after -16,485 bp of *ff1b*, the position where the database and the genomic DNA insert of BACff1b2 sequences last matched. As the genomic DNA insert in BACff1b2 was estimated to be ~100 kb, the 5' genomic region of *ff1b* that was not sequenced is estimated to be ~38 kb. When the sequences from -20,612 to -16,485 bp of our genomic sequences were used to perform BLAT search against the zebrafish genome, no significant matching

could be obtained, indicating that the genomic sequences spanning this region have not been completed for the on-going zebrafish genome sequencing project.

5.3 Deletions of targeted genomic regions from the recombined pBACff1bEx2EGFPAmp by Red/ET homologous recombination

The transgenesis studies using pBACff1bEx2EGFPKan described in Chapter 4 indicate that the regulatory elements that are required for *ff1b* temporal- and spatial-specific expression are contained within the *ff1b* locus in the BAC construct. Furthermore, based on the findings of mouse *Sf-1* (Shima *et al*., 2005; Zubair *et al*., 2006; Shima *et al*., 2008), the regulatory *cis*-elements governing tissue-specific expression of *ff1b* were anticipated to be localized in intronic sequences. Therefore, we have adopted a two-step counter selection, homologous recombination-based strategy to remove specific introns and genomic sequences of *ff1b* from the recombined BAC plasmid. The effect of losing those genomic fragments on the EGFP transgene expression was subsequently assessed by microinjecting the various deleted BAC contructs into zebrafish embryos.

Using the two-step counter-selection method (Section 2.8.2), specific sequences within the pBACff1bEx2EGFPAmp plasmid could be deleted by Red/ET homologous recombination. The first step of counter selection involved the insertion of the *rpsL-neo* cassette through homology arms targeting the genomic sequences to be deleted and the successfully recombined BAC construct was retrieved by kanamycin selection (Fig. 2.2). In the second step of counter-selection, the *rpsL-neo* cassette was removed and replaced by the homologous arms, thereby leading to the deletion of a particular genomic region and without leaving a selectable marker behind.

With homologous arms targeting the sequenced portion of the pBACff1bEx2EGFPAmp plasmid, we managed to specifically delete two genomic fragments spanning 10 kb and 20 kb respectively from the 5' upstream region (Fig. 5.5A). The first 5' deletion (5'10kbDel1) spans -21,342 to -11,397 bp while the second 5' deletion (5'20kbDel2) spans longer region from -21,342 to -1,012 bp. Approximately 1 kb of sequences 5' upstream to exon 1 was retained so that the basal promoter activity would not be affected by the deletion. Since the data from several transgenic mouse studies point to the presence of tissue-specific enhancer in intronic sequences, the remaining deletions were planned to target the intronic region. Thus, Intron I to Intron VII was deleted individually from the pBACff1bEx2EGFPAmp plasmid (Fig. 5.5B). It was anticipated that most of the regulatory elements governing tissue-selective expression of *ff1b* should reside within the 46 kb genomic region that has been fully sequenced in the BAC construct. Therefore, the above deletion scheme represents a good starting point to identify genomic regions that potentially contain regulatory enhancer or repressor elements of *ff1b*.

5.4 Assessment of 5' genomic deletions of *ff1b* from pBACff1bEx2EGFPAmp by transient transgenesis in zebrafish embryos

Although transgenesis studies performed previously in our laboratory demonstrated that the 5' flanking region of *ff1b* up to 20 kb lacked tissue-specific enhancer activity, there was still a possibility for the presence of repressor elements within this 5' upstream sequences. Therefore, two genomic regions spanning 10 kb and 20 kb each were deleted from the BAC construct. To study the effect of removing these 5' upstream regions, the deleted pBACff1bEx2EGFPAmp plasmids were microinjected into zebrafish embryos at 1 to 2 cell stage. At about 48 hpf, microinjected embryos were scored for EGFP expression at the expected tissues of

expression, including the VMH, neuronal projections, otic vesicle, interrenal and muscle (Table 5.2).

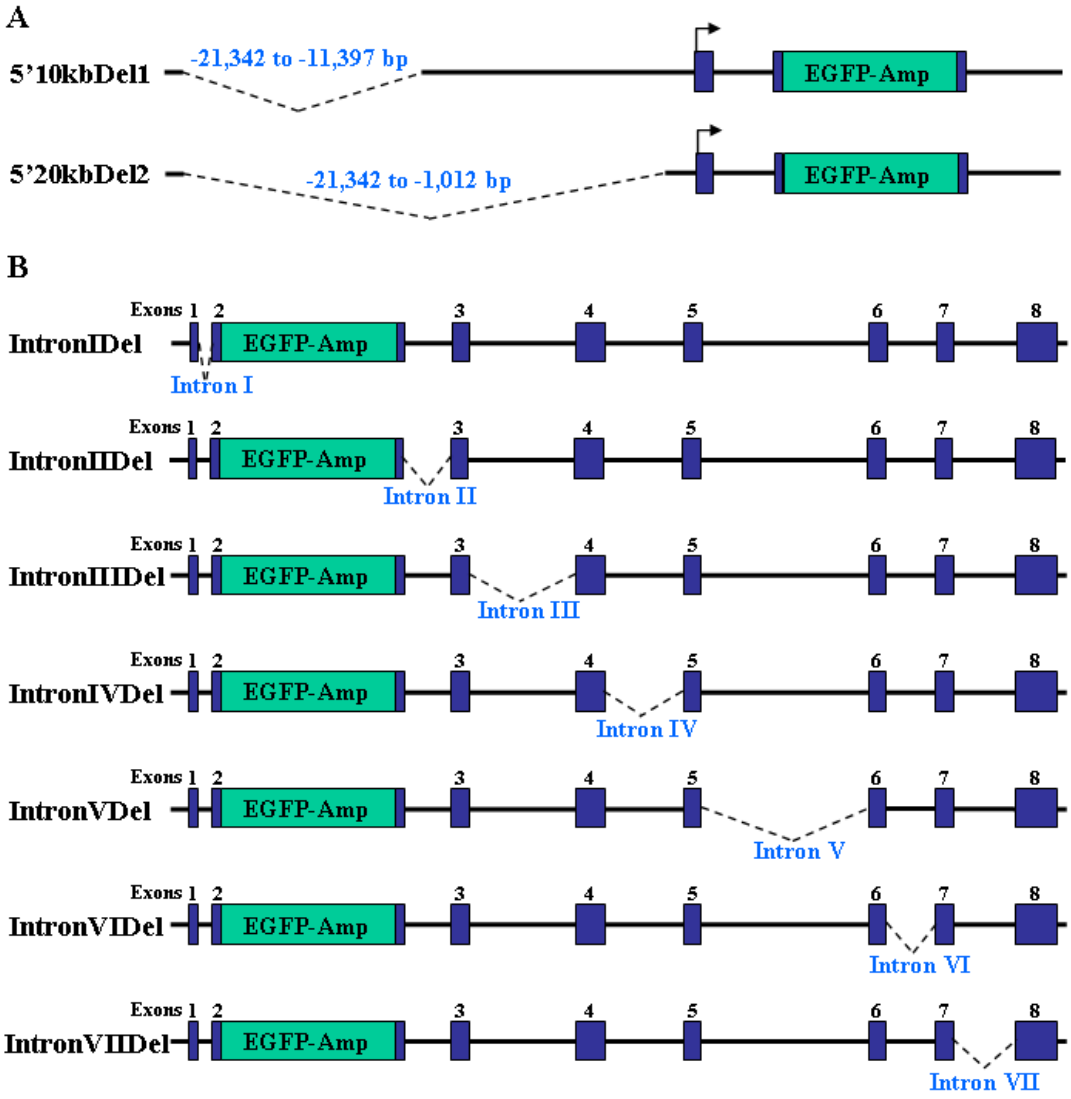

Figure 5.5 Schematic representation of Red/ET recombination-based deletions of *ff1b* genomic regions in pBACFf1bEx2EGFPAmp. (A) Specific genomic regions at the 5' flanking region and (B) introns were deleted from the pBACff1bEx2EGFPAmp construct by a two-step counter selection recombination strategy. Each genomic fragment deleted is indicated by V-shape in dash line.

As the expression pattern of EGFP transgene in transient transgenesis could be highly mosaic, our analyses took mainly qualitative differences into consideration. Thus, the effect of losing a particular genomic fragment was considered significant only when the EGFP expression at a particular tissue was completely lost in all the

embryos examined. As expected, the EGFP expression pattern at the various expected sites of expression was largely unaffected when the 5' flanking sequences of *ff1b* were removed (Table 5.2).

Table 5.2 Percentage (number) of zebrafish embryos expressing EGFP at the respective tissues at 48 hpf following microinjections of the corresponding deleted pBACff1bEx2EGFPAmp constructs. Abbreviations: VMH, ventromedial hypothalamus; NP, neuronal projections; IR, interrenal; OV, otic vesicles ; M, muscle.

	Percentage (No.) of embryos expressing EGFP at:					***n***
BAC plasmids microinjected	**VMH**	**NP**	**IR**	**OV**	**M**	
pBACff1bEx2 EGFPAmp	14.3 (75)	12.2 (64)	14.0 (73)	13.4 (70)	13.0 (68)	523
5'10kbDel1	24.8 (115)	15.8 (73)	2.1 (10)	30.0 (139)	43.2 (200)	463
5'20kbDel2	23.4 (94)	19.2 (77)	12.2 (49)	20.4 (82)	26.9 (108)	401
IntronIDel	7.5 (35)	7.0 (33)	10.5 (49)	10.6 (50)	10.8 (51)	468
IntronIIDel	17.0 (86)	14.4 (73)	8.7 (44)	16.8 (85)	10.5 (53)	506
IntronIIIDel	6.4 (33)	8.2 (42)	10.7 (55)	17.1 (88)	13.6 (70)	515
IntronIVDel	11.8 (70)	10.1 (60)	0	0	13.6 (81)	595
IntronVDel	2.7 (14)	2.3 (12)	9.7 (50)	11.7 (60)	9.7 (50)	515
IntronVIDel	8.9 (46)	9.4 (48)	9.6 (49)	13.7 (70)	8.7 (34)	510
IntronVIIDel	5.0 (25)	5.2 (26)	9.5 (47)	9.9 (49)	8.2 (41)	497

Intriguingly, the number of embryos displaying EGFP transgene expression at interrenal was dramatically reduced with the truncation of -21,342 bp to -11,397 bp (5'10kbDel1) but was unaffected with truncation spanning longer region from -21,342

bp to -1,012 bp (5'20kbDel2). These observations indicate the possibility of having positive regulatory elements for interrenal-specific expression of *ff1b* within the first 10 kb of the 5' upstream sequences. At the same time, the results could also indicate the presence of potential repressor elements that suppress interrenal-specific expression of *ff1b* within the second 10 kb of 5' upstream sequences. This postulation remains to be tested, as the truncation did not lead to a complete loss of expression at the interrenal. A more extensive deletional study of the 20 kb 5' upstream sequences would aid to map any potential regulatory elements that are relevant to interrenal-specific expression of *ff1b*.

5.5 Assessment of intronic deletions of *ff1b* from pBACff1bEx2EGFPAmp by transient transgenesis in zebrafish embryos

The tissue-specific enhancers regulating the expression of mouse *Sf-1* in the VMH, pituitary, and fetal adrenal have been identified in Intron VI and Intron IV respectively (Shima *et al*., 2005; Zubair *et al*., 2006; Shima *et al*., 2008). These enhancer sequences have been shown to be highly conserved in human *SF-1* but we could not identify the equivalent regulatory region in zebrafish by computational analyses. However, it is still reasonable to hypothesize that the regulatory elements that are responsible for the tissue-specific expression of *ff1b* could reside in one of the introns in reminiscent to the mammalian *SF-1* genes. Therefore, Intron I to Intron VII of zebrafish *ff1b* gene was deleted individually using the counter selection strategy. The effect of losing a particular intron was subsequently assessed by microinjecting the deleted pBACff1bEx2EGFPAmp plasmid into zebrafish embryos followed by monitoring of EGFP transgene expression.

Surprisingly, the deletions of most introns produced no effect on the EGFP transgene expression in tissues that are known to express the transgene (Table 5.2)

with the exception of Intron IV. Deletion of Intron IV led to a complete loss of EGFP transgene expression in the interrenal and otic vesicle, indicating that important *cis*-elements controlling the expression of *ff1b* in these tissues are located in this intron. The close association of *ff1b* expression in the otic vesicle and interrenal gland was also unexpected, as a previous ISH study (Chai and Chan, 2000) has failed to localize *ff1b* expression to the otic vesicle. Interestingly, Intron IV represents the additional, and most probably a more ancestral intron, that is not found in the human and mouse *SF-1* genes. Thus, the location of interrenal-specific regulatory elements present in this unique intron of *ff1b* could be distinctive from the FAdE that has been mapped in mouse *Sf-1*.

Intriguingly, the EGFP expression in the muscle pioneer cells remained not affected with deletions of individual introns or 5' upstream sequences. This indicates that the *cis*-elements that are responsible for the muscle-specific expression of transgene are located outside of those portions of the *ff1b* locus that were studied. At the same time, it could also point to the absence of repressor elements or gene boundary elements that are required to suppress the muscle-specific expression of *ff1b* in the endogenous genomic context.

Although EGFP expression in the VMH and associated neuronal projections was mostly not affected, the proportions of embryos showing the presence of EGFP in these locations were markedly reduced when Intron V or Intron VII was deleted. This observation highlighted the possibility that the two introns might act synergistically to regulate the VMH-specific expression of *ff1b* gene. This finding implies that the organization of regulatory elements for *ff1b* could be more complicated than what has been described for mammalian *SF-1*. Nevertheless, further characterization of the TFBSs within these introns is necessary to identify potential *cis*-elements controlling

VMH-specific expression of *ff1b*. For example, both Intron V and VII can be deleted simultaneously to see whether they are functionally related to one another.

Taken together, our recombination-based deletion scheme of removing individual introns and specific genomic sequences from the 5' flanking region, in combination with transient transgenesis using the zebrafish embryos, has successfully identified Intron IV as the candidate genomic region containing the enhancer that confers interrenal-specific expression to zebrafish *ff1b*. In addition, several other genomic regions that could potentially regulate tissue-specific expression of *ff1b* have also been identified (Fig. 5.6). By dissecting Intron IV computationally and experimentally, core *cis*-elements as well as the associated *trans*-acting factors that regulate interrenal-specific expression can now be identified. While candidate *cis*-elements that are required for VMH-specific expression of *ff1b* have not been determined with any certainty, Intron V and Intron VII might potentially be involved and they are likely to contain *cis*-elements that are important for the transcriptional regulation of *ff1b* in the VMH.

5.6 Computational analysis of Intron IV for *cis*-elements that potentially regulate interrenal-specific expression of *ff1b*

To determine the presence of *cis*-elements that contribute to the interrenal-specific expression of *ff1b*, the 3754 bp of intronic sequence was analyzed using the MatInspector program online (www.genomatix.de). Only TFBSs that were predicted with core similarity of >0.90 were considered significant. Not only *cis*-elements that bind factors which have been previously implicated in *SF-1* expression in the adrenal cortex are taken into consideration, *cis*-elements that bind novel factors that could potentially modulate interrenal-specific expression of *ff1b* have also been highlighted. The positions of these putative *cis*-elements are summarized in Table 5.3 and a closer

examination of the arrangement of these elements revealed that most of them were localized between 1900 and 3200 of Intron IV. Therefore, this genomic region of intron IV displays the highest potential in harboring a core enhancer element for interrenal expression (Fig. 5.7).

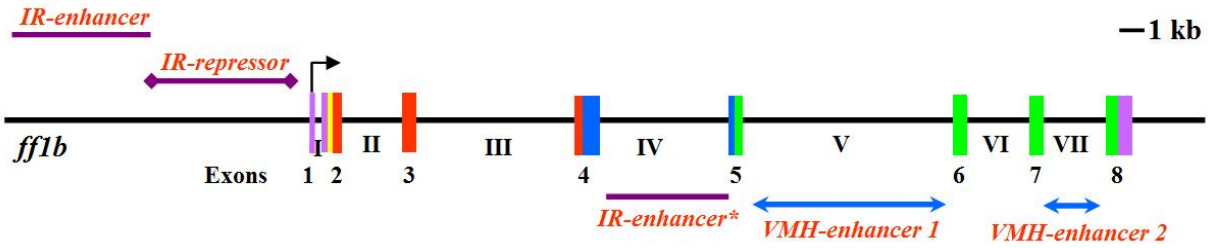

Figure 5.6 Genomic regions that harbor potential enhancer or repressor elements of *ff1b* gene. Genomic fragments that contain potential enhancer or repressor elements for interrenal- (IR) and ventromedial hypothalamus- (VMH) specific expression of *ff1b* are identified by genomic deletion and transient transgenesis studies in zebrafish embryos. Asterisk (*) indicates an absolute requirement of the genomic fragment for IR-specific expression.

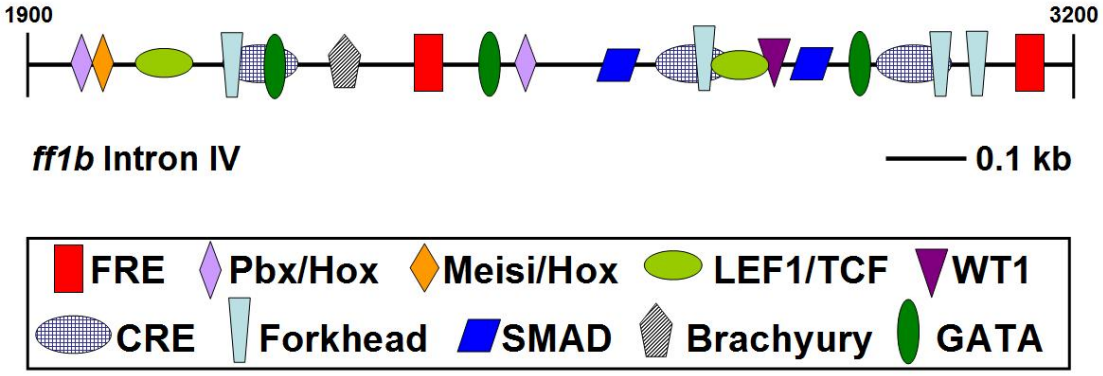

Figure 5.6 Potential *cis*-elements present between position 1900 and 3200 bp of *ff1b* Intron IV. The genomic sequences of *ff1b* Intron IV spanning 1900 to 3200 bp was analyzed bioinformatically with online prediction program MatInspector. Putative *cis*-regulatory elements that could potentially regulate the interrenal-specific expression of *ff1b* are illustrated in different shapes and colors.

Table 5.3. Positions of *cis*-elements that may potentially contribute to the interrenal-specific expression of *ff1b* in Intron IV, as predicted by MatInspector.

No	*cis*-element	Abbreviation	Position in Intron IV of *ff1b*
1	Pbx/Hox binding site	Pbx/Hox	135/151; 290/306; 761/777; 1392/1408; 1985/2001; 2502/2518
2	Meis/Hox binding site	Meis/Hox	220/234; 503/517; 805/819; 1097/1111; 1993/2007
3	FF1 response element	FRE	2383/2395; 3113/3125
4	Wilms tumor binding site	WT1	2717/2733
5	GATA binding site	GATA	144/151; 433/445; 806/818; 1401/1413; 2190/2202; 2456/2468; 2792/2804
6	cAMP response element	CRE	31/51; 526/546; 2148/2168; 2681/2701; 2841/2861
7	LEF1/TCF binding site	LEF1/TCF	2058/2074; 2689/2705;
	Brachyury binding site	Brachyury	2281/2301
8	Forkhead/Winged helix binding site	Forkhead	401/417; 838/854; 1144/1160; 2143/2153; 2686/2696; 2959/2969; 3066/3082
9	SMAD protein binding site	SMAD	1626/1634; 2615/2623; 2762/2770;

Notably, several binding sites for Pbx/Hox and Meis/Hox complexes have been mapped within Intron IV of *ff1b*. The Pbx-Hox-Meisi1 complex has been recently demonstrated to bind *cis*-elements present in Intron IV of mouse *Sf-1* and directly regulate *Sf-1* expression in the fetal adrenal of mouse (Zubair *et al*., 2006). Two FREs have been also mapped at position 2383/2395 and 3113/3125 of Intron IV, implying the presence of an autoregulatory loop in reminescent to the FAdE identified in mouse *Sf-1* locus (Zubair *et al*., 2006). Also, a binding site for WT1 has also been mapped at position 2717/2733. The expression of *wt1* at the earliest stage of adrenogonadal precursors of both mouse and zebrafish suggested that it could act as a direct upstream activator of *Sf-1* or *ff1b* and this has indeed been demonstrated in mouse (Wilhelm and Englert, 2002; Hsu *et al*., 2003). Furthermore, the ablation of this gene led to developmental defects in the adrenal cortex of mouse (Wilhelm and

Englert, 2002) and interrenal gland of zebrafish (Hsu *et al*., 2003). Another class of transcription factors that has been implicated in the transcriptional regulation of SF-1 (Tremblay and Viger, 2001) and adrenocortical development (Kiiveri *et al*., 2002) is GATA factors and several GATA binding sites have also been mapped within Intron IV.

In addition to the above TFBSs that have been directly implicated in SF-1 expression or adrenocortical development, a few other novel *cis*-elements that may potentially be involved in controlling *ff1b* expression in the interrenal have also been located. Several cAMP response elements (CRE) have been predicted with high confidence throughout Intron IV of *ff1b*. Considering the important role of cAMP in inducing the transcriptional activation of steroidogenic enzymes in adrenocortical cells, it has been proposed to regulate the expression of SF-1 (Val *et al*., 2003). Two binding sites for LEF1/TCF and one binding site for Brachyury, which are both molecular components of Wnt signaling pathway, have also been located in Intron IV. These *cis*-elements may be functional as Wnt signaling pathway is important for adrenocortical development and factors involved in this pathway could, therefore, potentially regulate the early specification of interrenal as well as the interrenal-specific expression of *ff1b* (Else and Hammer, 2005; Kim *et al*., 2008). Besides, several binding sites for transcription factors belonging to the fork head/winged helix family are present in Intron IV. This family of transcription factors are important regulators of mesoderm development (El Hodiri *et al*., 2001; Wilm *et al*., 2004). Since the interrenal gland is derived from intermediate mesoderm, transcription factors regulating mesoderm development might potentially regulate early specification of interrenal and thus *ff1b* expression as well. Lastly, three binding sites for transcription factors of the SMAD family have also been mapped. As molecular components of

transforming growth factor beta (TGFβ) signaling pathway, SMAD proteins have been shown to transcriptionally regulate *StAR* promoter in adrenocortical cells (Brand *et al*., 1998) as well as the proliferation of adrenocortical cells (Chambaz *et al*., 1996; Mesiano and Jaffe, 1997; Langlois *et al*., 2002).

Taken together, the computational prediction revealed TFBSs that are likely to play a role in directing interrrenal-specific expression of *ff1b*. Based on this prediction, Intron IV appears as a promising candidate regulating the interrenal-specific expression of *ff1b*. As the intronic sequences spanning 3754 bp is too long, a more extensive deletional/subcloning study concentrating on this fragment would be necessary. By placing distinct but overlapping genomic fragments fromIintron IV downstream to a reporter gene construct with a functional basal promoter, the transgene activity of potential enhancer can be investigated by transient transgenesis in zebrafish embryos. The functionalities of the predicted *cis*-elements can then be studied following the identification of a core enhancer of interrenal, which is anticipated to span only a few hundred basepairs.

5.7 Summary

In this chapter, the genomic organization of the zebrafish *ff1b* gene and the characterization of the gene locus to identify tissue-specific regulatory elements were described. The genomic sequences from the BACff1b2 plasmid spanning ~20 kb of 5' upstream region and ~25 kb of *ff1b* locus were almost fully sequenced, except for two AT-rich gaps in the 5' region and in Intron V, respectively. The structure of *ff1b* gene is generally conserved among vertebrate *SF-1* genes in terms of exon/intron organization, with the exception of the presence of the unique Intron IV in zebrafish. Furthermore, *cis*-elements that potentially regulate the basal transcription of *ff1b* have been mapped and they appear to be highly conserved to those reported for mammalian *SF-1*. However, the genome context of *ff1b* on LG8 does not show conserved synteny with human *SF-1*. Instead, conserved synteny to genomic arrangement of human *SF-1* is observed for *ff1d* locus on LG21. Using a recombination-based deletion strategy, specific genomic regions and introns were successfully removed from the recombined pBACff1bEx2EGFPAmp and the effect of each deletion was studied by transient transgenesis in zebrafish embryos. The preliminary findings have identified several potential enhancer/repressor-containing regions. Interestingly, Intron IV has been shown to be essential for the interrenal-specific expression of EGFP transgene, and it represents an intron that is normally preserved only in invertebrate *FF1* genes. Therefore, we have identified an ancestral intronic core enhancer that regulates the interrenal expression of *ff1b*. Computational analysis of Intron IV sequences revealed TFBSs that have been directly implicated in the expression of mouse *Sf-1* gene or adrenocortical development. In addition, a few novel *cis*-elements that may potentially mediate interrenal-specific expression of *ff1b* have been identified.

CHAPTER 6

Discussion

6.1. The zebrafish Ff1b, similarly to SF-1, plays a conserved role in the regulation of steroidogenesis

In the interrenal primordium of zebrafish, *ff1b* expression precedes that of *cyp11a1* and *3β-hsd* by about 2 hr (Chai and Chan, 2000; Hsu *et al*., 2003). Furthermore, *ff1b* knockdown by MO led to interrenal agenesis and impaired osmoregulation along with downregulation of the two steroidogenic enzymes (Chai *et al*., 2003). These observations imply a conserved role of *ff1b* in the transcriptional regulation of steroidogenic enzymes and hence steroidogenesis. To define the ability of zebrafish Ff1b to transactivate the expression of steroidogenic enzymes, the 5' putative promoter of *cyp11a1* was isolated and demonstrated to be active by transient transfection and microinjection studies. Through a series of detailed characterization of the 1.7 kb promoter of zebrafish *cyp11a1*, we provided evidence that Ff1b binds directly to the distal and proximal FRE and transactivates the *cyp11a1* promoter.

6.1.1. Ff1 potentially regulates the transcription of genes encoding steroidogenic enzymes in zebrafish

Strict temporal and spatial regulation of gene expression of steroidogenic enzymes appear to be tightly regulated by members of the NR5A subfamily of NRs. For instance, SF-1 is well established as a transcriptional regulator of all steroidogenic enzymes except for CYP11B2 (Val *et al*., 2002; Payne and Hales, 2004). LRH-1 has been reported to regulate the expression of the following steroidogenic enzymes, CYP11A1 (Kim *et al*., 2005; Hsieh *et al*., 2008), CYP17 (Zhou *et al*., 2007), CYP19 (Mendelson and Kamat, 2007; Ohmuro-Matsuyama *et al*., 2007), CYP11B1 (Wang *et*

al., 2001), and 3β-HSD (Mueller *et al*., 2006; Saxena *et al*., 2007). In Medaka, SF-1 and LRH-1 homologs have been shown to bind and transactivate the promoter region of ovarian aromatase *cyp19a1* (Watanabe *et al*., 1999) and brain *cyp19a2* (Ohmuro-Matsuyama *et al*., 2007) gene, respectively. The association of the FREs present in the promoter region of rainbow trout *cyp19a* promoter with an FF1 factor similar to SF-1 has also been demonstrated by transient transfection and EMSA assays (Kanda *et al*., 2006). Several other studies have presented the evidence of co-expression of Ff1s and steroidogenic enzymes in teleosts, without demonstrating a direct involvement of Ff1s in their transcriptional regulation (von Hofsten *et al*., 2002; Liu *et al*., 2004; von Hofsten and Olsson, 2005; Zhang *et al*., 2007).

Except for *3β-hsd*, computational analysis has revealed at least one FRE in the promoter regions of *cyp11a1*, *cyp17*, and *star*, which have been isolated by genome walking in this study. To determine the commonality of the presence of FREs in the promoter regions of steroidogenic genes, 2 kb of 5' upstream region for all the currently known zebrafish genes encoding steroidogenic enzymes were isolated *in silico* from Ensembl zebrafish genome browser. The putative regions were then analyzed computationally using MatInspector for the prediction of FREs. Notably, at least one FRE can be mapped at the 5' promoter of *cyp19a1a* (-129/-117), *17β--hsd1* (-1921/-1903, -864/-852, -129/-117), *11β-hsd2* (-1647/-1635), and *11β-hsd3* (-709/-697). The consistent presence of FREs in these promoter regions indicates that Ff1 isoforms could potentially regulate the transcription of steroidogenic enzymes. Considering the restricted expression of *ff1b* in steroidogenic tissues, these predictions imply a direct involvement of Ff1b in the regulation of these genes. At the same time, other Ff1 isoforms could also be involved if they are co-expressed in the same cells.

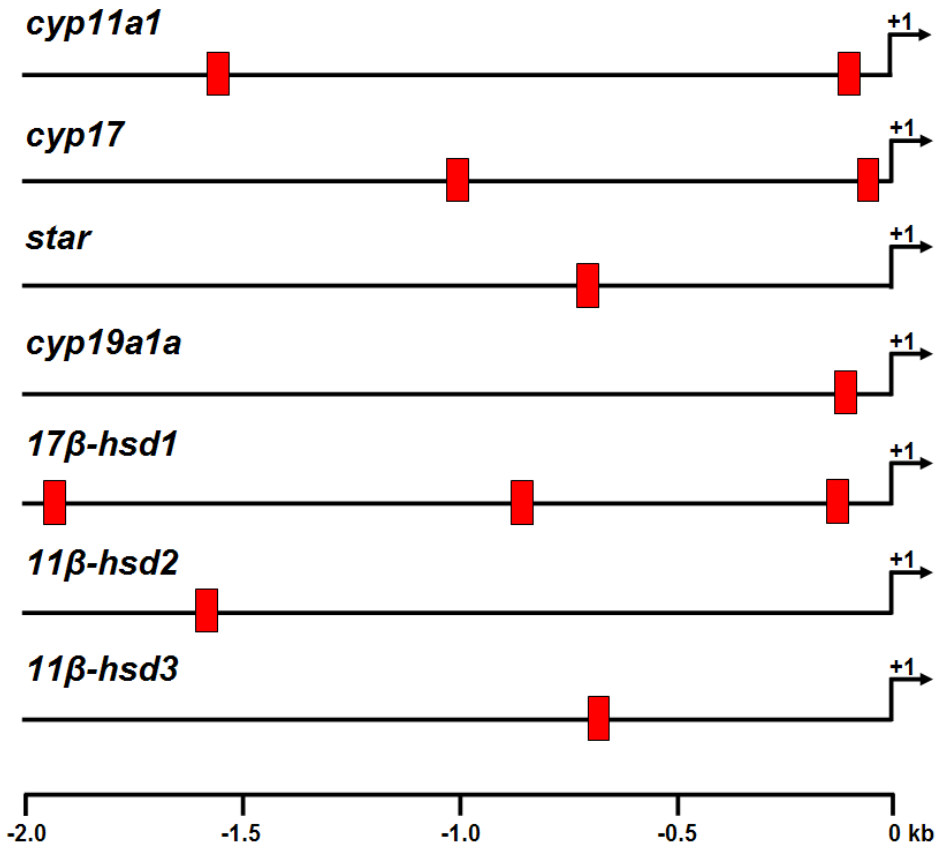

Figure 6.1 Relative positions of Ff1 response elements (FREs) identified in the 5' flanking promoter of zebrafish genes encoding steroidogenic enzymes. Two kb of 5' promoter sequences of all the currently annotated steroidogenic genes at Ensembl were isolated *in silico* and FREs, as incicated by the red boxes, were identified by online prediction program.

Although *cyp11a1* catalyzes the rate-limiting step in the steroidogenesis pathway, no previous study of this gene in zebrafish has been reported. In this study, the 1.7 kb zebrafish *cyp11a1* promoter was shown to be active using transient transfections in cell lines and transient transgenesis in zebrafish embryos. The report of the ability of Ff1b to transactivate the 1.7 kb zebrafish *cyp11a1* promoter has provided a good validation for the direct involvement of Ff1b in the transciptional regulation of *cyp11a1*, and probably also other steroidogenic enzymes in zebrafish.

6.1.2. Regulatory *cis*-elements are conserved in the zebrafish *cyp11a1* promoter

The human *CYP11A1* promoter has been very well studied and the functional roles of the following transcription factors, SF-1, Sp1, AP-1, TReP-132, AP-2, NF-1, and Ets in its transcriptional activation have been well established (Guo *et al*., 2007). Within the first 150 bp of 5' promoter, an AP-2 binding motif, a TreP-132 binding site, an FRE, and the TATA box constitutes the basal promoter. An upstream cAMP-responsive module between -1553 and -1633 consists of an FRE, and two flanking AP-1/CREB-binding sites. In addition, two adrenal-selective enhancers (AdE) together with two Sp1-binding motifs, a NF-1 binding site, and a consensus Ets binding site form a regulatory module at -1845 to -1898. These *cis*-elements are defined through many transient transfection and transgenic mouse studies.

In the zebrafish *cyp11a1* promoter, two FREs, one CRE, two Sp1 and four AP-1 binding sites have been mapped (Fig. 3.4). It is noteworthy that the presence of the two FREs in a highly conserved manner is consistent with the role of SF-1 acting as a central regulator of the transcriptional activation of steroid hydroxylases. Unlike the Tetraodon, human, and mouse *CYP11A1* promoter, the distal FRE of zebrafish *cyp11a1* promoter is not tightly associated with CRE. Nevertheless, the conservation of the two FREs, Sp1, and AP-1 transcription factor binding sites that have been implicated in the transcriptional activation of mammalian *CYP11A1* promoter indicates a conserved mode of regulation across different species. *Cis*-elements that bind known coregulators of SF-1 including Sox proteins (De Santa *et al*., 1998) , GATA factors (Tremblay and Viger, 1999), and WT-1 (Shen *et al*., 1994) have also been defined, implying a possible functions of these transcription factors in regulating the transcription of *cyp11a1* in concert with Ff1b.

6.1.3. Functional discrepancy exists between the 1.7 kb *cyp11a1* promoter of zebrafish and human despite the high degree of *cis*-element conservation

Despite the conservation of their *cis*-acting elements, the 1.7 kb zebrafish and human *cyp11a1* promoters does not appear to be functionally equivalent. In transient transfection studies, the 1.7 kb human promoter consistently activates the luciferase reporter to a higher level in all the cell lines tested including Y1, MA-10, CHO-K1, LβT2, HepG2, with exception for 293T (Section 3.4). Intriguingly, the 1.7 kb *cyp11a1* promoter of both human and zebrafish are capable of activating the luciferase reporter gene not only in cell lines of steroidogenic origins like Y1, MA-10, and CHO-K1, but also in cell lines of non-steroidogenic origins like 293T and LbT2. As LbT2 cells originate from pituitary gonadotrope, the activation of the human and zebrafish *cyp11a1* promoter is most likely attributed to the presence of endogenous SF-1. The high level of promoter activity for both human and zebrafish *cyp11a1* in 293T cells might not be surprising, as the human *CYP11A1* promoter has ben shown to be active in this cell line (Ben Zimra *et al*., 2002). This is probably due to the presence of *trans*-acting factors that are capable of assuming the role of FF1s. In placental tissue that does not express SF-1, another transcription factor named AP-2 has been shown to assume the role of SF-1 to activate the transcription of human *CYP11A1* (Ben Zimra *et al*., 2002). Intriguingly, the presence of LRH-1, which belongs to the same family of SF-1 and binds the same FRE (Fayard *et al*., 2004), did not activate both promoter in HepG2 of liver origin (where LRH-1 is endogenously expressed). This observation has highlighted the potential roles of other transcription factors that interact with Ff1b and SF-1 in regulating the tissue-specific activity of the *cyp11a1* promoter.

While the zebrafish *cyp11a1* could activate the luciferase reporter by 5.6-fold above the basal level, the human *CYP11A1* equivalent was completely inactive when they were tested in zebrafish embryos. Furthermore, the promoter activity of zebrafish

cyp11a1 can be further potentiated by co-injection of *ff1b* overexpression construct in zebrafish embryos, but not the human *CYP11A1* promoter. In addition, the 1.7 kb human promoter was unable to direct EGFP expression specifically to the interrenal and genital ridge when it was microinjected into zebrafish embryos. These observations are in disagreement with a previous study, which demonstrated that Ff1b was able to induce the promoter activity of the 2.3 kb human *CYP11A1* promoter in H1299 cells (Hsu *et al*., 2003). The disparities between transient transfection studies in cell lines and *in vivo* transgenesis studies in zebrafish embryos have underscored the *in vitro* nature of promoter analysis in cell lines. Although studying promoter activity in cell lines is useful for characterization of general properties, the findings might not be conclusive and they may not reflect the true context of transcription events *in vivo*. In this aspect, the zebrafish has provided a useful *in vivo* model for promoter analyses, as the activity of the reporter can be easily assessed by quantitative (luciferase) and qualitative (EGFP) methods.

The discrepancies between the two promoters are intriguing, considering the high degree of conservation in *cis*-elements and that the 1.7 kb human *CYP11A1* promoter of equivalent length has been able to direct *lac*Z expression specifically to the adrenals and gonads in transgenic mouse (Hu *et al*., 1999; Hu *et al*., 2001). This observation highlighted the complication of promoter analysis, as promoter regions that are sequentially conserved might not be functionally equivalent *in vivo* and vice versa. Ff1b might not bind the FREs in human promoter at an affinity that is equivalent to its binding in the zebrafish *cyp11a1* promoter. Nevertheless, both the transient transfection in cell lines and transient microinjection in zebrafish embryos confirm that the 1.7 kb zebrafish *cyp11a1* promoter is active. Most importantly, the

transactivation assays with *ff1b* co-expression has established Ff1b as a *bona fide* transcriptiona factor that is able to transactivate the *cyp11a1* promoter.

6.1.4. Functional distinction of the distal and proximal FRE in the zebrafish *cyp11a1* promoter

With the identification of two highly conserved FREs in the zebrafish *cyp11a1* promoter, similar to that reported for human and mouse, it is important to understand why this arrangement persisted. Previous studies on the human *CYP11A1* promoter have revealed that while the proximal FRE is responsible for the basal activity, the distal FRE is needed for hormonal regulation and tissue selectivity (Guo *et al*., 2007). This difference in the functionality of the two FREs is presumably due to the different *cis*-acting elements associated with each FRE. The same feature can be seen in the case of zebrafish *cyp11a1* promoter, where the distal FRE is surrounded by a CRE and binding sites for AP-1 and GATA factors while the proximal FRE is surrounded by TATA boxes and binding sites for transcription factors such as Sp1, Sox and WT-1.

Transfection of the zebrafish *cyp11a1* promoter carrying specific mutations in the two FREs, individually or simultaneously, has ascertained the pivotal role of the proximal FRE in the basal activity of *cyp11a1* promoter (Section 3.6). Thus, Ff1b bound to the proximal FRE could regulate the basal promoter activity by interacting with transcription factors in the Pol II initiation complex such as TFIIB, CBP/p300 and AP-1 (Li *et al*., 1999; Monte *et al*., 1998). Although the distal FRE seems to be dispensable in the basal promoter activity, the 1.7 kb zebrafish *cyp11a1* promoter only loses its activity completely when both the FREs are mutated, indicating that it might still play a role in regulating the basal activation of *cyp11a1* promoter, though to a

lesser extent. The importance of the distal FRE for the regulation of tissue specificity and cAMP responsiveness is not addressed by the current study.

Our EMSA and ChIP assays showed that Ff1b binds to both the distal and proximal FREs in *vitro* and *in vivo*. This is in reminescent to the findings from the human and rat *CYP11A1* promoter (Clemens *et al*., 1994; Hu *et al*., 2001). The association of SF-1 with the two FREs of human *CYP11A1* promoter has been confirmed by EMSA (Hu *et al*., 2001). In the rat *Cyp11a1* promoter, the distal (-79/-71) and proximal (-51/-43) FREs are only ~30 bp apart and SF-1 binding to the proximal FRE was shown to be stronger than to the distal FRE in EMSA (Clemens *et al*., 1994). In the current study, the competition binding assay for the two FREs of zebrafish *cyp11a1* promoter suggests differential binding of Ff1b to the two FREs at different concentration range. The binding affinity of Ff1b to the distal FRE seems to be slightly stronger than to the proximal FRE. The possible discrepancy in the binding affinity of SF-1 to the two FREs has remained largely unexplored and the significance of the differential binding affinity remains unresolved until more kinetics and biochemistry data on the SF-1-FRE interactions became available.

6.2. Generation of the ff1bEx2EGFP transgenic zebrafish: a major step for the lineage tracing of *ff1b*-expressing cells

Considering the importance of Ff1b in the development and maintenance of endocrine organs of zebrafish, a faithful lineage tracer of *ff1b*-expressing cells offers a lot of potential advantages. A fluorescent lineage tracer will enable us to fully utilize the advantage of zebrafish model to study the functional roles of Ff1b and other related factors, such as its coregulators, *in vivo*. However, this is not as straightforward as in case of many other genes where the usage of short 5' proximal promoter region is normally sufficient to drive tissue-specific expression of a

transgene. Similar to the observation for mouse *Sf-1*, the 5' proximal promoter fragment containing up to 20 kb of the zebrafish *ff1b* genomic sequences is unable to target EGFP reporter to tissues that endogenously express *ff1b*. A recombination-based strategy which involved the insertion of the EGFP reporter into Exon 2 of the zebrafish *ff1b* locus successfully recapitulated the endogenous expression of *ff1b* in zebrafish embryos. Despite the low efficiency of BAC transgenesis in zebrafish, a stable transgenic line, ff1bEx2EGFP, has been generated successfully.

6.2.1. The EGFP expression parallels the endogenous expression pattern of *ff1b* in the VMH

Using ISH, zebrafish *ff1b* transcripts can be reliably detected at ~24 hpf as two tight clusters lateral to the anterior tip of the neural tube in the VMH of developing brain (Chai and Chan, 2000). In the ff1bEx2EGFP transgenic embryos, as early as 20 hpf, weak EGFP expression can be detected in the first few *ff1b*-positive neurons in the VMH. The subsequent EGFP expression largely recapitulates the endogenous expression pattern of *ff1b* obtained by ISH. The earlier detection of these VMH neurons is expected and has allowed the confirmation that Ff1b is only established in a small group of precursor cells at the same time as the specification of VMH. In both mammals and teleosts, the molecular mechanism underlying the embryonic development of VMH in relation to SF-1 remain poorly characterized. Previous findings from our laboratory have demonstrated that *ff1b* expression in the VMH is completely absent in midline patterning mutants *one-eyed pinheaed* (*oep*) and *cyclos* (*cyc*) (Chai and Chan, 2000). Both mutants have been reported to be defective in their prechordal and floor plate formation as well as the positioning of anterior-posterior (AP) axis (Hatta *et al*., 1991; Schier *et al*., 1997; Sampath *et al*., 1998). A recent study has reported the downregulation of *ff1b* expression in the VMH in *smu* (*smo*) and *dtr*

(*gli1*) mutants and, also following *sonic hedgehog* (*shh*) overexpression (Bergeron *et al*., 2008). These observations suggest that the proper differentiation of *ff1b*-expressing cells in the VMH relies on the optimal level of Hedgehog signaling. The faithful expression of EGFP in the *ff1b*-expressing VMH neurons would aid to define the molecular mechanisms underlying the above observations.

Interestingly, the other two *ff1* isoforms, *ff1a* and *ff1d*, have both been reported to be expressed in the VMH at a level comparable to *ff1b* (Chai and Chan, 2000; von Hofsten *et al*., 2005; Kurrasch *et al*., 2007). The co-expression of *ff1* genes in the overlapping subdomains of VMH implies a molecular interaction and interplay between these genes. Nevertheless, they seem to occupy distinct but slightly overlapping subdomains of VMH. Notably, both *ff1a* and *ff1d* have been reported to be expressed in the pituitary as well (Liu *et al*., 1997; von Hofsten *et al*., 2001; von Hofsten *et al*., 2005). *ff1a* transcripts was reported to be present in the pituitary from 24 hpf up to 40 hpf (Liu *et al*., 1997; von Hofsten *et al*., 2001) but the location of this expression domain has not been confirmed by co-staining with pituitary markers. Besides,the expression of *ff1d* has also been reported in the anterior pituitary and the neurons connecting the VMH and anterior pituitary cells (von Hofsten *et al*., 2005). The significance of this observation is not clear at the moment, due to the late appearance of *ff1d* expression (only at 30 dpf) and the lack of double ISH data to confirm the localization to the pituitary. In the ff1bEx2EGFP transgenic embryos, EGFP expression is also not detected in the pituitary, in reminescent to the ISH expression pattern of *ff1b* reported till date (Chai and Chan, 2000; Kuo *et al*., 2005; Kurrasch *et al*., 2007; von Hofsten *et al*., 2005). The expression profile of *ff1b*, as revealed by EGFP and ISH detection, along with the observation from MO knockdown of *ff1b*, suggest a minimal role of *ff1b* in the development and function of

pituitary in zebrafish. As for *ff1a* and *ff1d*, the significance of their expression in the VMH and pituitary has to be further clarified with double ISH assays as well as functional studies such as MO knockdown of the two genes. The ff1bEx2EGFP transgenic embryos would provide an excellent experimental platform to further clarify the functional complexity among *ff1* genes when their expression domains overlap with one another.

6.2.2. The EGFP transgene expression parallels the endogenous expression pattern of *ff1b* in the interrenal gland

In the interrenal gland, ISH reveals that the interrenal primordium appears as two small and bilateral clusters of non-steroidogenic cells within the pronephric primordia at a location ventral to the third somite at 22 hpf (Hsu *et al*., 2003; Liu, 2007). The interrenal primordia proliferate in tight association with the endothelium as development proceeds (Liu and Guo, 2006; Liu, 2007). Before the initiation of steroidogenesis (by 28-30 hpf), the bilateral clusters coalesced into a single structure at the midline, and migrates out of the pronephric field (Chai and Chan, 2000; Hsu *et al*., 2003). In the ff1bEx2EGFP embryos, EGFP expression can be readily detected at the interrenal primordium by 20 hpf. By 28 hpf, the EGFP expression strongly reminesce of the endogenous *ff1b* expression.

The morphogenetic movement of interrenal cells has been shown to be influenced by the endothelium. In the *cloche* mutant that lacks endocardium and endothelial cells in the major trunk (Liao *et al*., 1997), the convergence of the bilateral interrenal primordia at the midline is disrupted (Liu and Guo, 2006). As the interrenal gland is in close proximity to the notochord, its ontogenic development has also been proposed to be associated with midline signaling. In *oep* mutant, the interrenal primordia fail to fuse together and they are displaced to ectopic bilateral locations

(Chai and Chan, 2000; Hsu *et al*., 2003). In another midline signaling *flh* mutant which lacks notochord, the interrenal primordia remain at their original locations without fusing together by 36 hpf (Hsu *et al*., 2003).

The sonic hedgehog (SHH) signaling also represents one of the major signaling coming from the midline structure. In sharp contrast to an earlier report which demonstrated that the interrenal primordium, as revealed by *cyp11a1* detection, remains largely intact in SHH mutants *smu* and *syu* (Hsu *et al*., 2003), a microarray study has recently established a direct involvement of SHH signaling in interrenal and pronephric organogenesis in zebrafish (Bergeron *et al*., 2008). As reported by Bergeron *et al*. (2008), the interrenal expression of *ff1b* was absent in SHH signaling mutant *smu* and significantly reduced in another mutant *dtr*, but expanded following *shh* overexpression by mRNA microinjection. The discrepancy between the two reports is intriguing, as it seems to suggest that *ff1b* is indispensable for *cyp11a1* expression in the interrenal primordium in the *smu* mutant. Nevertheless, it is important to consider that the ISH detection of the two genes was performed at different time frame (24 hpf for *ff1b* versus 36 hpf for *cyp11a1*). It is unlikely that the expression of *cyp11a1* is independent of *ff1b*, as the MO knockdown of *ff1b* gene function has reproducibly resulted in a downregulation of *cyp11a1* expression (Chai *et al*., 2003; Hsu *et al*., 2003). Moreover, the current study has also definitively established a direct involvement of Ff1b in the transcriptional regulation of *cyp11a1* in zebrafish.

In the mammals, signaling pathways mediated by extracellular growth factors such as the Wnt signaling and TGFβ signaling have been implicated in the differentiation, proliferation and maintenance of adrenocortical tissues. The Wnt signaling pathway has been shown to regulate the embryonic development of a

number of organs, including adrenal cortex (Grigoryan *et al*., 2008). The Wnt-4 KO mice display abnormalities in the differentiation of definitive zone in their adrenal gland and defects in cell migration of adrenocortical precursors (Vainio *et al*., 1999; Heikkila *et al*., 2002). The targeted disruption of β-catenin, as an effector of canonical Wnt signaling pathway, has been shown to impair the differentiation and proliferation of adrenocortical precursors (Kim *et al*., 2008). Besides, the proliferation of adrenocortical cells has been linked to the TGFβ signaling pathway (Mesiano and Jaffe, 1997; Langlois *et al*., 2002) though detailed molecular or genetic data have not been reported. While the involvement of the aforementioned signaling pathways in adrenocortical differentiation and maintenance is not totally unexpected, the molecular mechanisms underlying them remain largely uncharacterized at the moment.

6.2.3. The EGFP fluorescence unravels the axonal projections of *ff1b*-expressing neurons in the VMH to the otic vesicles and telencephalon

In addition to the faithful recapitulation of *ff1b* expression in the VMH, the EGFP expression in ff1bEx2EGFP transgenic embryos revealed neuronal projections from VMH that was previously not detectable by ISH. Apparently, immunolocalization of Ff1b would not reveal the cellular processes of these neurons as Ff1b is a nuclear targeted protein. Similarly, ISH assays only reveal *ff1b* transcripts in the nucleus and perinuclear cytoplasm. In contrast, the EGFP expression driven by the ff1bEx2EGFP transgene in this study resides entirely in the cytoplasm, and this might have contributed to the visualization of those neuronal projections. Also, the accumulation of the fusion Ff1b-EGFP protein could have augmented the fluorescence signal as compared to the chromogenic detection method employed in ISH. The EGFP fluorescence in the neuronal projections and additional neurons could also have resulted from transneuronal transfer of EGFP molecules across synaptic

contacts. For example, EGFP has been previously shown to be able to transport across synaptic junctions when it is put under the control of appropriate signal such as that from the BDNF (Kohara *et al*., 2001), a known target gene of SF-1. As the same expression pattern was observed in transient transgenesis, we can rule out the possibility of postional effect that could have resulted from the transgene integration site in the genome.

Interestingly, some of these neuronal projections seem to directly contact the otic vesicle, another EGFP-expressing domain. The neuronal connections between the two organs required detailed histological assays. The direct innervation of inner ear by VMH neurons has not been previously documented for any species, including mouse. In mammals, direct neuronal connection between VMH and muscle through the lordosis reflex circuit has been described (Flanagan-Cato *et al*., 2001). The existence of similar connection between the *ff1b*-expressing VMH neurons and other peripheral tissues in zebrafish remains to be explored. The innervations from VMH to the muscle would need detailed histological examination of the ff1bEx2EGFP transgenic embryos.

The VMH is known to regulate a broad array of behavioral and homeostatic functions, including digestive, affective, and sexual behaviors as well as obesity and energy balance (Canteras *et al*., 1994). The expression of mammalian SF-1 specifically in the dorsomedial and central sub-domains of VMH is well defined and SF-1 is known to control the cyto-architecture of neuronal subtypes in the VMH, presumaly by regulating cell migration (Davis *et al*., 2004; McClellan *et al*., 2006). Furthermore, CNS-specific KO of SF-1 highlights its role in modulating anxiety behavior. However, the exact functions of SF-1-positive neurons in the mammalian VMH have remained undefined.

In the mammals, the neuronal projections of *SF-1* expressing neurons in the VMH remain largely uncharacterized, mainly due to the lack of a traceble marker in these neuronal projections. Moreover, in mammalian model, *in vivo* lineage tracing of VMH neurons is extremely difficult, especially during embryonic development, and the study of these neurons as well as their projections often involves laborious sectioning and immunohistochemistry assays that might eventually alter the original strutural organizations. The ability to discern axonal and dendritic projections from VMH neurons would be an important step in understanding their functions. By tracing their projections, useful insights may be gained about the targets that they innervate as well as major neuronal networks that they may interact with in the CNS. Such information will be instructive for the understanding of the physiological processes that they might be involved in. Thus, the ability to visualize the neuronal projections from *ff1b*-expressing cells in the ff1bEx2EGFP transgenic embryos should find wide applications in the study of VMH development and function.

6.2.4. The unexpected sites of EGFP expression in ff1bEx2EGFP transgenic embryos at the otic vesicle, muscle pioneer cells, common cardiac vein, and neuromasts

Several unexpected EGFP-expressing domains are observed in the ff1bEx2EGFP transgenic embryos. They include the otic vesicles, slow muscle pioneer cells, common cardiac vein, and neuromasts. These expression domains have not been detected by *ff1b* ISH nor have they been reported in other species. As the EGFP expression in the otic vesicles and muscle is observed even in transient transgenesis when microinjected with supercoiled pBACff1bEx2EGFPKan, the transgene expression is not likely to be due to integration site. Indeed, the effect of integration site on transgene expression is known to be a major factor for shorter transgenes (a few kb), but often a minor factor for transgenes derived from large DNA

constructs like BAC. In transient transgenesis studies, the EGFP expression in the common cardiac vein and the scattered distribution of EGFP-expressing neuromasts could have been overlooked, as they were usually highly mosaic. The study of a single transgenic line of ff1bEx2EGFP in this study does not allow us to conclude whether the EGFP signal from the common cardiac vein and neuromasts could have resulted from ectopic expression caused by integration site.

Although the EGFP expression in the muscle pioneer cells was unexpected, the expression domain in the muscle has indeed been described for Drosophila *FF1* genes and all the zebrafish *ff1* isoforms. In *Drosophila*, the betaFF1 receptor has been demonstrated to regulate muscle contraction events that drive the morphogenetic movements at the prepupal-pupal transition stage (Fortier *et al*., 2003). In zebrafish, *ff1a* has been shown to be expressed specifically in the adaxial and slow muscle precursors. A series of gene knockdown and overexpression studies have demonstrated a role of Ff1a in the morphogenesis of both the fast and slow myofibril assembly in response to Hedgehog signaling and in cooperation with Prox1 (Sheela *et al*., 2005). Strong expression of *ff1c* and weak expression of *ff1d* in the adult muscle tissue have been previously described (Kuo *et al*., 2005). Interestingly, weak expression of *ff1b* in the muscle of adult zebrafish has also been demonstrated in our laboratory by RT-PCR (Chai, 2002), implying a possibility of *ff1b* expression in the muscle. If the expression of *ff1b* in the muscle pioneer cells is genuine, it is then inexplicable that the strong expression in the muscle at early developmental stage, as revealed by the EGFP fluorescence, is undetectable by ISH.

Analogous to the EGFP expression in the neuronal projections of VMH, a few of the aforementioned explanations could hold true for the unexpected expression in the otic vesicle and muscle pioneer cells. They could still potentially represent

endogenous expression domains of *ff1b* and the discrepancy between fluorescence visualization and ISH detection is most likely due to the difference in the detection limit and sensitivity of the two methods. Otherwise, the additional expression domains could be attributed to non-specific enhancer present in the genomic insert of BACff1b2 plasmid. Unfortunately, we are unable to map any ORF with high confidence within the sequenced portion of genomic DNA insert in the BAC plasmid, thereby unable to extrapolate the possible influence of genes surrounding *ff1b* locus. It is noteworthy that with the exception of the interrenal gland, other EGFP expression domains in the ff1bEx2EGFP embryos remain largely unaffected following *ff1b* MO knockdown. This observation indicates that the continued expression of EGFP in these tissues is not dependent on *ff1b*.

Although we have not managed to map any known ORF in the sequenced portion of BACff1b2 plasmid, the presence of the extreme 5' or 3' genomic sequences from the neighboring genes might still be influential on the EGFP expression pattern. By genetic mapping, the nearest neighbor gene of *ff1b* is predicted as *c11orf8* (Kuo *et al*., 2005). However, the only expression data available for this gene is from a genetic screen that aims to identify factors responsible for breast tumor suppression (Seitz *et al*., 2006) and it could not account for the EGFP expression in the otic vesicle and muscle pioneer cells. The next nearest known neighbor of *ff1b* is predicted to be *nr6a1a*, which is commonly known as germ cell nuclear factor (*gcnf*). Its expression is predominantly found in the germ cell of gonads (Chung and Cooney, 2001). Intriguingly, *Gcnf* KO mice display severe defects in somitogenesis from early stage of development although its functional role in this aspect has not been explored (Chung *et al*., 2001). This raises the possibility of GCNF involvement and expression in the muscle. In zebrafish, *gcnf* has been cloned and characterized in terms of its

expression in the ovary and testis (Braat *et al*., 1999). With more detailed expression profiling of *gcnf* as well as more complete genomic sequences between *gcnf* and *ff1b*, we will be able to see whether any muscle-specific distal enhancer of this gene could be present in the BAC transgene and thereby interefere with the EGFP expression.

All in all, the successful recapitulation of *ff1b* expression in the VMH and interrenal gland together with the unexpected transgene expression highlights the complexity of gene regualtion, as in many other transgenic studies. In many cases, the length of transgene does not necessarily correlate with the extent of recapitulating the endogenous expression of a gene. Recently, there are even reports suggesting interchromosomal regulation of gene expression. In the most complex case of gene regulation, the transcription modulation may involve not only the *cis*-elements (promoter, enhancer, and repressor) and corresponding *trans*-factors (specific transcription factors, nuclear proteins, and chromatin remodeling factors), but also a whole concert of long range and dynamic intra- or inter- chromosomal interactions at specific sub-nuclear compartments (Bartkuhn and Renkawitz, 2008; Kumaran *et al*., 2008; Osborne and Eskiw, 2008). The transcriptional regulation of many genes and the interactions among individual genes in the context of whole genome is far more complex than previously thought (Gerstein *et al*., 2007; Keller and Harel, 2007). Nevertheless, the unexpected sites of EGFP expression in ff1bEx2EGFP embryos have not interfere with the usability of this transgenic line to perform lineage tracing studies, at least for the VMH and interrenal gland, which currently represent two major sites of endogenous *ff1b* expression.

6.3. The ff1bEx2EGFP stable line provides a versatile transgenic platform to study early morphogenesis of interrenal gland

The ff1bEx2EGFP transgenic embryos have undoubtedly provided a useful *in vivo* system to trace the fate of *ff1b*-expressing cells, particularly those in the VMH and interrenal gland. More importantly, the zebrafish embryos are highly amenable to a broad range of experimental manipulations such as gene knockdown by MO, overexpression and rescue, chemical treatment with small molecules, just to mention a few. Although the homozygous transgenic embryos are not viable, as reported for many other transgenic lines, the hemi-zygous embryos are reliable enough for data collection. The direct visualization of EGFP fluorescence in these embryos offerred a level of convenience that was previously unavailable, allowing for instance the fate tracing of *ff1b*-expressing cells in live embryos.

6.3.1. The EGFP transgene allows the tracing of *ff1b*-expressing interrenal cells from early developmental stage

The MO knockdown of *ff1b* resulted in late larval phenotypes that are indicative of impaired osmoregulation. The morphants can be classified according to the severity of the subcutaneous edema (Chai *et al*., 2003). The knockdown of *ff1b* gene function by MO has been re-examined using the ff1bEx2EGFP transgenic line in the current study. The EGFP expression in the *ff1b* morphants of ff1bEx2EGFP embryos has allowed for the live monitoring of the size of interrenal primordia from early stages of development, before the morphant phenotypes are manifested at 5-6 dpf. It is noteworthy that the EGFP expression of the interrenal correlated strongly with the severity of subcutaneous edema in *ff1b* morphants. All embryos that showed no EGFP at the interrenal gland at 48 hpf developed into Class C and D morphants, whereas embryos that showed weak or reduced, and normal EGFP expression at the interrenal at 48 hpf consistently developed into Class B and Class A morphants,

respectively. It was previously reported that a portion of ff1bMO1-injected larvae retained positive staining for 3β-Hsd enzymatic activity, and they eventually developed into Class A morphants (Chai *et al*., 2003). This is in contrast to the finding in this study, where a good 47.8% of ff1bMO3-injected embryos retain interrenal EGFP expression that is comparable to the uninjected controls, and almost all of them (46.5%) developed into Class A morphant at 7 dpf. The discrepancy is probably due to the higher sensitivity of EGFP detection as compared to the chromogenic enzymatic assays of 3β-Hsd. However, the ability of the EGFP-positive interrenal cells to carry out steroidogenesis has not been examined in the current study. Considering the normal morphology of Class A morphants at 7 dpf, it is likely that the EGFP-positive interrenal cells are capable of producing steroids, at least to a level that is sufficient to maintain the normal osmoregulatory functions in zebrafish.

The existence of intermediate phenotypes between the wild-type and the most severe knockdown of *ff1b* has highlighted the influence of technical variations in microinjection as well as a potential correlation to the dosage-sensitivity of Ff1b. Concomitantly, compensatory functions from other *ff1* isoforms, particularly *ff1d* that has been shown to be transiently expressed in the interrenal primordium (von Hofsten *et al*., 2005), may also play a role. As of any other microinjection experiments, the amount of ff1bMO3 delivered into the ff1bEx2EGFP embryos may vary slightly from one individual to another, thereby giving rise to a range of different MO dosage, and hence different classes of severity. We envisage that the milder morphant phenotypes, i.e. Class B, probably correspond to a genetic condition of haploinsufficiency while the most severe morphant phenotypes, i.e. Class C and D, probably correspond to a nearly KO genetic background. The potential correlation to the dosage-sensitive effect

of Ff1b can be further ascertained with a targeted mutagenesis of *ff1b* gene, which is now technically possible in zebrafish (Meng *et al*., 2008; Woods and Schier, 2008).

It is now known that most genes do not give rise to obvious phenotype when their dosage is reduced by 50%, in hemizygotes, or increased by 50%, in duplication-bearing animals (Hodgkin, 2005). Such changes in gene dosage usually do have a small impact on viability but the reduction in viability is not easily discernible at the level of a single gene. The dosage-sensitive effect of Ff1 receptors has been previously described. In mammals, the drastic phenotypes of heterozygous mutation of SF-1 imply that this receptor acts in a dosage-sensitive manner. In human, heterozygous G35E mutation which is located in the first zinc finger of the DBD causes complete sex reversal in 46XY affected individual, and major adrenal failure (Achermann *et al*., 1999). In another heterozygous R255L mutation of human SF-1 which is located in the hinge region, bilateral adrenal agenesis was observed without a defect in sexual differentiation (Biason-Lauber and Schoenle, 2000). Although not as obvious as in humans, haploinsufficiency of SF-1 in mice induces adrenal hypoplasia in both male and female at E15.5 (Bland *et al*., 2000). Just recently, the increased dosage of SF-1 has been shown to trigger cell proliferation in adrenocortical cells through concerted modulations of cell cycle and apoptosis (Doghman *et al*., 2007). These findings collectively suggest that SF-1 works as a dosage-sensitive NR to ensure the proper differentiation and function of adrenal cortex in human and mouse. Considering the functional homology of Ff1b to SF-1 and the existence of several severity classes of *ff1b* morphants, Ff1b could potentially act in a dosage-sensitive manner in zebrafish.

6.3.2. The interrenal primordium is completely absent in the most severe knockdown of *ff1b* gene function

In SF-1 KO studies, the developmental abnormalities observed at birth are not apparent during precocious development. Thus, the bipotential gonad appears to be normal and is colonized by primordial germ cells prior to sex determination at E10.5. Furthermore, the adrenal and gonadal primordia subsequently separate and migrate to the correct positions. However, when sex determination commences at E12-E12.5, gonads and adrenal primordia in these mice progressively regress by apoptosis (Luo *et al*., 1994; Luo *et al*., 1995). These observations indicate that SF-1 is dispensable for the early specification of the adrenogonadal primordia but is crucial for their subsequent differentiation, proliferation, and maintenance. Considering the highly conserved function of Ff1b to mammalian SF-1, it is reasonable to ask whether Ff1b modulate the morphogenesis of interrenal in zebrafish in a similar manner.

Our MO knockdown of *ff1b* gene function using ff1bMO3 in ff1bEx2EGFP transgenic embryos demonstrated that in severe case of knockdown, the interrenal promordia did not form at all (Section 4.5). The complete absence of the interrenal primordia in these Class C and Class D morphants suggests that Ff1b is important for both the early specification and subsequent maintenance of interrenal functions. This is in contrast to the phenomenon observed for SF-1 in mouse. While the lack of interrenal primordium could reflect a true mechanism by which Ff1b acts to regulate the morphogenesis of interrenal, it could also partially due to the technical inability to detect the weak fluorescence from the early interrenal primordium, which is deeply embedded underneath the third somites in whole-mount ff1bEx2EGFP embryos. The adoption of imaging systems of higher sensitivity and penetration, e.g. two-photon confocal microscopy, as well as histological sections of the morphants at early stage of interrenal specification (18- 20 hpf) would help to further clarify this issue.

6.3.3. The formation of interrenal primordium is independent of glucocorticoids

The osmoregulatory defects observed in *ff1b* morphants are largely attributed to the loss of *ff1b* gene function and the loss of production of corticosteroids from the interrenal gland. In conjunction, chemical treatment of zebrafish embryos with steroid inhibitor aminoglutethimide (AG) has been shown to produce similar larval phenotypes that are indicative of impaired osmoregulation (Chai *et al*., 2003). While *ff1b* MO perturbs *ff1b* gene function and results in the downregulation of *cyp11a1* expression, the AG inhibitor disrupts the enzymatic function of Cyp11a1 and Cyp19 directly. Although the perturbation is directed at different level of regulation, both experiments ultimately resulted in the dysregulation of steroid biosynthesis and, thus, gluococorticoid insufficiency and impaired osmoregulatory function. However, the presence of interrenal primordia in the AG-treated larvae has not been examined. Ff1bEx2EGFP transgenic embryos treated with AG showed normal development of the interrenal gland throughout the study period (Section 4.6). At 7 dpf, the position and EGFP-expressing domain of the interrenal gland appeares to be slightly displaced and it is most likely attributed to the distortion of the whole body axis and associated organs in the larvae as a result of the edema phenotype.

Indeed, AG inhibits only the activity of steroidogenic enzymes Cyp11a1 and Cyp19, resulting in glucocorticoid insufficiency, which would presumably upset the balance of steroidogenesis pathways as well as the feedback regulation by the end product of steroidogenesis (primarily costisol). The perturbation could potentially alter the steroidogenic activity of interrenal primordia via gluococorticoid-mediated regulatiory pathways. However, it does not necessarily affect the expression of *ff1b* and *ff1b*-regulated morphogenesis of interrenal gland. Interestingly, a glucocorticoid response element can be mapped at position -637/-619 bp of *ff1b* promoter, indicating

a possibility of glucocorticoid regulation on *ff1b* expression. Nevertheless, the AG AG-treated embryos that retain their interrenal glands indicate otherwise. ISH detection of *cyp11a1* transcripts together with ISH and enzymatic assays of *3β-hsd* have established that the zebrafish interrenal cells are capable of producing steroids as early as 24 hpf although the interrenal organogenesis is not yet completed (Chai *et al*., 2003; Hsu *et al*., 2003). The assessment of steroidogenic activity of interrenal primoridia that persisted in the AG-treated ff1bEx2EGFP embryos would aid to pinpoint whether the steroidogenic functions of the EGFP-positive interrenal cells are still retained.

It is noteworthy that blood island formation was not observed in the ventral tail of AG-treated larvae and the yolk sac edema in the most severely affected AG-treated larvae was less extensive compare to Class D *ff1b* morphants. These disparities indicate that the chemical inhibition of steroidogenic enzymes is not as severe as the disruption of *ff1b* gene function, which presumably downregulates the expression of all steroidogenic enzymes. Nevertheless, the penetrance of AG inhibition is significantly higher (73%) in comparison to MO knockdown by ff1bMO3 (54%) though most of the AG-treated larvae displayed Class B morphant phenotypes. The higher penetrance of chemical treatment in comparison to microinjection is no unusual as the immersion of zebrafish embryos/larvae in AG-containing egg water is anticipated to produce less variation in delivery amount in comparison to the mechanical delivery of MO by microinjection. The AG inhibition experiment has undoubtedly demonstrated the versatility and realiability of the ff1bEx2EGFP transgenic line for studying the effect of small molecules on interrenal development.

Consistent with our findings, a search through the literature revealed that glucocorticoids have not been reported to influence the embryonic development of

adrenal cortex. Generally, the fetal adrenal produces only low amount of cortisol until late gestation stage (Muglia *et al*., 1995; Miller, 1998). Evidence from KO studies of gluococorticoid receptor (GR) indicate that glucocorticoids play crucial roles in modulating the development of lung, thymus, liver, and adrenal medulla (Cole *et al*., 1995). Nevertheless, the moderately elevated level of corticosterone and sharp increase in ACTH level following the loss of glucocorticoids or gluococorticoid receptor function indicate a dysregulation of HPA axis, which is most likely attributed to defective feedback modulation (Schmid *et al*., 1995).

6.4. The conserved genomic organization of *ff1b*

To elucidate the genomic organization of zebrafish *ff1b*, ~46 kb of genomic sequences encompassing the *ff1b* locus has been sequenced. The genomic sequence obtained matched almost completely to the *nr5a1a (ff1b)* locus annotated in scaffold_831 of LG8. With the exception of an additional Intron IV, genomic structure of *ff1b* is conserved to that of human and mouse SF-1. Intriguingly, the intron is uniquely found in *ff1b* gene but not the other three zebrafish *ff1* genes. The *ff1b* genomic sequences determined in this study have set a stage for the manipulations of genomic sequences to delineate *cis*-regulatory elements that modulate the tissue-restricted expression of *ff1b* in zebrafish.

6.4.1. The presence of a unique Intron IV in zebrafish *ff1b* gene

In contrast to all other vertebrate *FF1* genes characterized so far, the zebrafish *ff1b* is organized into eight exons spanning a total genomic region of 25 kb. Generally, Exon 4 of vertebrate FF1 genes represents the largest exon and it encodes the entire hinge domain. In zebrafish *ff1b*, the presence of the unique Intron IV splits this exon into Exon 4 and Exon 5. The remaining *ff1a* (Lin *et al*., 2000), *ff1c* (Xia, 2001), and

ff1d (annotated as *nr5a1b* in LG21 of Ensembl genome database Zv7) also lack this intron. An *in silico* examination of currently annotated *nr5a1* genes in other teleosts including stickleback (*Gasterosteus aculeatus*), medaka (*Oryzias latipes*), fugu (*Takifugu rubripes*), and tetraodon (*Tetraodon nigroviridis*) at the Ensemble genome database (www.ensembl.org) revealed that the presence of this intron is unique to *ff1b* in the teleost lineage. In invertebrate *FF1* genes of *D. melanogaster* (*Ftz-F1*) and *C. elegans* (*cnhr*) genes, the presence of an intron in the corresponding position is noted, albeit at a much smaller size.

Although independent and repetitive gain of introns has been reported in several fish lineages, (Venkatesh *et al*., 1999; Zhaxybayeva and Gogarten, 2003) subsequent evolutionary analyses of more completed genomes suggest that intron loss is far more predominant than intron gain during the process of evolution (Zhaxybayeva and Gogarten, 2003; Carmel *et al*., 2007; Loh *et al*., 2008; Sharpton *et al*., 2008). Considering the presence of a similar intron in invertebrate *FF1* genes and the absence of it in all other vertebrate *FF1* genes characterized so far, the presence of the extra intron in zebrafish *ff1b* is likely to represent an ancestral feature of *FF1* genes, which was subsequently lost in most other teleost and tetrapod lineages during evolution.

6.4.2. Conserved *cis*-regulatory elements in the *ff1b* promoter

Computational analysis of the proximal promoter of *ff1b* reveals conserved *cis*-regulatory elements that are involved in basal transcription (Section 5.2.2). Two putative E-box elements have been identified, with a full consensus motif located in Intron I (+203/+215) and a second less conserved motif (CAAGTG) located at –59/-54. With the exception of human *NR5A2*, all other vertebrate *FF1* gene promoters characterized lack a TATA box, (Zhang *et al*., 2001). The E-box elements are utilized

instead for transcription initiation of mouse *SF-1* (Ninomiya *et al*., 1995), rat *SF-1* (Nomura *et al*., 1995; Harris and Mellon, 1998), human *SF-1* (Woodson *et al*., 1997; Oba *et al*., 2000), bovine *SF-1* (Oba *et al*., 2000) and mouse *LRH-1* (Pare *et al*., 2001). The E-box motifs that are located in close proximity to the TSS are known to be essential for maximal promoter activation while E-box elements located in introns are able to induce gene transcription. For instance, an E-box element located at the Exon 1/Intron I junction of the human norepinephrine transporter gene regulates not only the transcription initiation but also the splicing of the gene (Kim *et al*., 2001). Similarly, an intronic E-box located at position +767 bp of the acetylcholinesterase (AChE) gene has been shown to be functional for myogenin-induced expression during myogenesis (Angus *et al*., 2001).

A putative FRE at position -355 to -343 of *ff1b* promoter indicates the possibility of autoregulation of *ff1b* transcription by Ff1b itself. For the rat SF-1 gene, an FRE in Intron I has been demonstrated to bind SF-1 itself and modulate the transcriptional activation of SF-1 gene (Nomura *et al*., 1996). However, studies on human and mouse promoter of SF-1 revealed that such autoregulatory mechanism does not take place (Oba *et al*., 2000; Woodson *et al*., 1997) despite the presence of an FRE at a corresponding region in the promoters of these genes. Recently, an FRE in the Intron IV of mouse *Sf-1* gene has also been implicated in an autoregulatory loop that maintains the fetal adrenal-specific expression of SF-1 (Zubair *et al*., 2006). There might be inter-species difference in the autoregulation of SF-1 genes and more *in vivo* data would be needed to confirm the previous findings which were mostly derived from transient transfection studies *in vitro*.

The characterization of mammalian SF-1 promoter has also revealed a Sp1 binding site that is important for their activity in steroidogenic cell lines (Scherrer *et*

al., 2002; Woodson *et al*., 1997). Furthermore, the expression of many adrenocortical-specific genes such as *CYP11A1* (Guo *et al*., 2003), *StAR* (Sugawara *et al*., 2000), *CYP21B* (Kagawa and Waterman, 1991), *CYP17* (Borroni *et al*., 1997) and *AKR1B7* (Aigueperse *et al*., 2001) have been shown to require Sp1 binding. Hence, the presence of a putative Sp1 site at location -325/-311 bp of *ff1b* proximal promoter is likely to be involved in the modulation of *ff1b* expression in the interrenal gland. Two other tissue-specific transcription factors have been implicated in the transcriptional regulation of mammalian SF-1, namely SOX9 and GATA4 (Tremblay and Viger, 2001). The regulation by the two transcription factors, however, seems to be confined to gonadal cell lineages. The presence of binding sites for the two factors in *ff1b* 5' promoter indicates that possible functionality of these elements in modulating gonad-specific expression of *ff1b*.

6.4.3. Zebrafish *ff1b* locus does not show conserved synteny with human SF-1

The genome context of zebrafish *ff1* genes in terms of their conserved syntennies with human NR5A paralogues have been reported by Kuo et al. (2005). The four zerbafish *ff1* genes, namely *ff1a*, *ff1b*, *ff1c*, and *ff1d*, have been mapped to chromosomal location LG22_40.9 cM, LG8_139.1 cM, LG3_80.3 cM and LG21_36.7 cM, respectively, using the HS meiotic panel (Woods *et al*., 2000). Although the expression and functional analyses have undoubtedly placed *ff1b* as an ortholog of human *NR5A1*, the phylogenetic and genetic mapping analyses suggests *ff1d* as the true ortholog of *NR5A1*. The examination of genomic context surrounding *ff1b* and *ff1d* indicates that *ff1d*, but not *ff1b*, shows conserved long-range syntenies with human *NR5A1*. It is likely that regulatory sequences of *ff1d,* as the duplicate of *ff1b*, may have been allowed more freedom to change during evolution due to the maintenance of its duplicate gene *ff1b*. The presence of an ancestral intron in

zebrafish *ff1b* and the conserved synteny between *ff1d* and human *NR5A1* suggests *ff1b* as the ancestral copy of the two duplicated genes (*ff1b* and *ff1d*). The ancestral *ff1b* gene was subsequently lost in the tetrapod lineages and its function has been retained by its duplicated gene.

Although the genetic maps are generated with high confidence, they would eventually need to be verified by data from genomic sequence assembly. This proves to be rather difficult at the moment as the sequencing of zebrafish genome is still incomplete and the sequence assembly is still in a draft version. It is noteworthy that the genomic context displayed at the Ensembl genome assembly is quite different from that shown by genetic mapping and even the *nr6a1a* gene that is closely associated with *ff1b* cannot be located in close proximity to *ff1b* on LG8. Since no ORF could be localized in the known genomic sequences of BACff1b plasmid, the *c11orf8* that supposedly lies 3' downstream of *ff1b* is likely to reside in genomic region beyond the genomic DNA insert studied.

6.5. A potential repressor element is present at the 5' upstream flanking region of *ff1b*

The inability of the 20 kb long fragment of *ff1b* 5' flanking sequences to drive tissue-specific expression of EGFP in zebrafish embryos indicates not only the absence of tissu-specific enhancer elements within this region, but also the existence of potential repressor elements. This mode of regulation, however, has largely been overlooked for most transcription regulation studies, mainly because it is technically far more difficult to identify a true repressor than a true enhancer. Nevertheless, many complex modes of gene regulation involve modules of enhancer and repressor *cis*-elements, acting in concert with their associated *trans*-factors, to bring upon a particular pattern of gene expression (Hawkins and Ren, 2006; Wallace and

Felsenfeld, 2007; Bartkuhn and Renkawitz, 2008). Till date, the only study that has investigated the effect of repressor-like element is the assessment of a histone acetylation boundary present between the mouse *Sf-1* and *Gcnf* genes (Ishihara and Morohashi, 2005). This study has identified an insulator element residing between the two genes that contains bind sites for the insulator protein CTCF and a nuclear matrix attachment region (MAR). Experimental evidences from ChIP and DNase I suggested that the chromatin architecture induced by this insulator is responsible for the the regulation of distinct expression patterns of *Gcnf* and *Sf-1*. Ths study, however, did not identify the associated *trans*-factors or *cis*-elements that specifically repress the expression of *Sf-1* in *Gcnf*-expressing cells, and *vice versa*.

When the 5' flanking sequences spanning -21,342 to -11,397 bp of *ff1b* locus was deleted from the pBACff1bEx2EGFPAmp plasmid, a sharp decrease in the number of embryos showing EGFP at interrenal gland is noted (Section 5.4). This decrease was, however, relieved with longer deletion spanning -21,342 to -1,012 bp. These results point to the presence of a potential enhancer element in the genomic region spanning -21,342 and -11,397 bp, and at the same time the presence of a potential repressor element in the genomic region spanning -11,397 and -1,012 bp. Taken the previous finding on the transcriptional activity of *ff1b* 5' sequences into account, the possibility of the presence of a repressor element seems to be higher. Nonetheless, it is currently difficult to map the true repressor and associated *trans*-factors from the long genomic region spanning 10 kb.

6.6. An intron deletion strategy using Red/ET method localizes an interrenal-specific enhancer to Intron IV of zebrafish *ff1b*

The realization of the enhancer for VMH, adrenal, and pituitary specific expression is located in the intron of mouse *Sf-1* and that these enhancers are highly

conserved and could be located in the human SF-1. However, this conservation does not seem to extend to the zebrafish *ff1b*. Using the Red/ET recombination strategy, individual intron is deleted and the ability of the remaining introns to drive the EGFP expression was assessed in microinjected zebrafish embryos (Section 5.5). This has allowed for the localization of an interrenal-specific enhancer to Intron IV of *ff1b*.

6.6.1. Intron IV of *ff1b* contains regulatory elements that are essential for interrenal-specific expression

A recent study has reported the identification of a fetal adrenal enhancer (FAdE), spanning 0.6 kb, in the Intron IV of mouse SF-1 gene (Zubair *et al*., 2006). The *lac*Z reporter gene expression driven by the FAdE enhancer is only restricted to the fetal stage of adrenal cortex, indicating the presence of temporal-specific enhancer elsewhere to modulate the adrenal-specific expression of SF-1 in the postnatal and adult stages. Although the enhancer was shown to be highly conserved between human and mouse, bioinformatics analysis suggest that the conservation does not seem to extend to zebrafish *ff1b* nor *ff1d*. It is likely that the high degree of sequence divergence between zebrafish and mouse, especially in the non-coding genomic regions, has hindered the idenfitication of the equivalent of FAdE enhancer by sequence homology. Nevertheless, similar *cis*-elements and corresponding *trans*-factors may still be involved for the specification of interrenal-specific expression of *ff1b* considering the conserved roles of *ff1b* in interrenal development, as well as, the conserved ontogeny between mammalian adrenal and zebrafish interrenal.

In this study, we report the identification of a putative interrenal-specific enhancer in Intron IV of *ff1b* gene following a combination of deletional analyses spanning *ff1b* locus and trasient transgenesis in zebrafish embryos. The deletion of the entire Intron IV (3754 bp) from the pBACff1bEx2EGFPAmp plasmid led to complete

disappearance of EGFP expression in the interrenal and otic vesicle. Although the close association of otic vesicle-specific transgene expression to that of interrenal gland cannot be explained, the resulting transgene expression pattern indicates that Intron IV contains regulatory elements that are indispensable in mediating the interrenal-specific expression of *ff1b*. Intriguingly, the interrenal-specific enhancer resides in Intron IV of *ff1b*, which is uniquely present among all other vertebrate *FF1* genes characterized so far. Thus, Intron IV of mouse *Sf-1* where the FAdE resides does not correspond to the Intron IV of zebrafish *ff1b* where the interrenal enhancer resides. Since the Intron IV of zebrafish *ff1b* represents an ancestral feature of *FF1* genes, the interrenal enhancer that has been identified in this study is likely to represent an ancestral enhancer in regulating the interrenal-specific expression of *ff1b*. Most probably, this intron was subsequently lost in the tetrapod lineages after which the enhancer was relocated to Intron IV of mouse *Sf-1*, which corresponds to Intron V of zebrafish *ff1b*, via a currently undefinable evolutionary mechanism.

In the mouse FAdE, the Pbx/Prep and Pbx/Hox sites were shown to mediate the initiation of SF-1 transcription in the fetal adrenal while the FREs and associated SF-1 have been implicated in the autoregulation and maintenance of SF-1 transcription (Zubair *et al*., 2006). Within position 1900 to 3200 of *ff1b* Intron IV, which harbors a high concentration of putative *cis*-elements, two FREs and several binding sites for Pbx/Hox and Pbx/Meis1 have been mapped. Prep1 and Meis1 are closely related factors that both belong to the TALE class of homeodomain transcription factors and they bind the same DNA motif (Berthelsen *et al*., 1998). While PBX1 has been repeatedly implicated in the modulation of SF-1 expression in the adrenal cortex in mammals (Schnabel *et al*., 2003; Else and Hammer, 2005; Hammer *et al*., 2005; Zubair *et al*., 2006; Lichtenauer *et al*., 2007), a collaborative

study in our laboratory demonstrated that the zebrafish *pbx1* is not expressed in the interrenal gland at embryonic stages up to 3 dpf (Dr Teoh Pick Har and Dr Alexander Chong Shu Chien, personal communication). However, detection of *pbx1* transcripts in the head kidney of adult zebrafish by RT-PCR indicates that it may still play a role in maintaining the expression of *ff1b* in the interrenal gland. During embryonic stage, *pbx1* function might be assumed by other *pbx* isoforms or its expression level is below the detection limit of ISH.

Several other novel *cis*-elements that may be potentially involved in controlling *ff1b* expression in the interrenal have also been mapped. Several cAMP response elements have been predicted with high confidence. Although *SF-1* has been demonstrated to regulate a number of target genes in a cAMP-dependent manner, it is still not established whether cAMP signaling pathway directly modulate the expression of *SF-1*. The connection of *ff1b* transcription to cAMP cannot be ruled out currently considering the important role of cAMP in inducing the expression of most steroidogenic enzymes in the interrenal.

The Wnt signaling pathway has been shown to be important for adrenocortical development and factors involved in this pathway could potentially regulate the early specification of adrenal cortex as well as the adrenocortical expression of SF-1 (Else and Hammer, 2005; Kim *et al*., 2008). In Intron IV of *ff1b*, two binding sites for LEF1/TCF and one binding site for Brachyury, which are both molecular components of Wnt signaling pathway important for embryogenesis (Technau, 2001; Galceran *et al*., 2004), have been predicted. Also, a number of binding sites for fork head/winged helix family of transcription factors have been mapped within Intron IV. This family of transcription factors have been implicated in the modulation of mesoderm development (El Hodiri *et al*., 2001; Wilm *et al*., 2004) and hence may potentially

regulate early events of interrenal morphogenesis and *ff1b* expression. Lastly, three binding sites for SMAD family of transcription factors have been predicted. SMAD proteins are components of transforming growth factor beta (TGFβ) signaling pathway, which has been implicated in the transcriptional regulation of *StAR* gene in adrenocortical cells (Brand *et al*., 1998) as well as the proliferation of adrenocortical cells (Chambaz *et al*., 1996; Mesiano and Jaffe, 1997; Langlois *et al*., 2002). Thus, they could also potentially regulate the expression of *ff1b* in maintaining the proper expansion of interrenal cell domain.

6.6.2. Intron V and Intron VI may potentially regulate the VMH-specific expression of *ff1b*

A 503-bp core VMH-specific enhancer has been localized to Intron VI of *Sf-1* using transgenic mouse assays (Shima *et al*., 2005). Mutagenesis and EMSA analyses revealed that the transcriptional activity of this enhancer is mediated through tight cooperation between an activating and a suppressive element, and the activating element is likely to bind homeobox protein Nkx2.1. In reminescent to the FAdE, the VMH enhancer has been shown to be highly conserved in Intron VI of human *SF-1*. Bioinformatic analysis has not managed to identify an equivalent region in zebrafish *ff1b* or *ff1d* by sequence homology. In our intron deletion studies, the number of embryos expressing transgene in the VMH and neuronal projections decreased markedly with the deletion of Intron V or Intron VII, indicating that they may potentially regulate the VMH-specific expression of *ff1b*. However, residual transgene expression in VMH following the deletion of Intron V or Intron VII alone indicates that they are not absolutely required for VMH-specific expression. Although their roles in regulating the expression of *ff1b* in the VMH cannot be properly defined at the moment, further studies on the two introns as well as simultaneous deletion of

them would most likely lend more insights into the molecular mechanisms underlying the VMH-specific expression of *ff1b*.

6.7. Conclusions

This study has presented multiple approaches to study the zebrafish *ff1b* gene, particularly with regard to its functional roles in the ontogenic development of interrenal gland. Detailed analysis of the two FREs identified within the 1.7 kb zebraifsh *cyp11a1* promoter and the demonstration of Ff1b transactivation activity and association with this promoter have established Ff1b as a *bona fide* transcription factor that is directly involved in the transactivation of *cyp11a1*. The presence of FREs in the putative promoter regions of other annotated steroidogenic genes of zebrafish suggest that this transcriptional regulation is likely to extend to most steroidogenic enzymes. These findings have further ascertained the roles of Ff1b as the central regulator of steroidogenesis, similar to that already described for mammalian SF-1, indicating a conserved mode of regulation for steroidogenesis over 450 million years of evolution. The co-expression of the other three zebrafish *ff1* isoforms within *ff1b*-expressing cells remains to be established and the resolution of this would then fully define the extent of transcriptional influence of Ff1b.

The sequenced portion of zebrafish *ff1b* locus determined in this study matches scaffold_831 of zebrafish LG8 (Ensembl) and when sequences from these two sources of BAC genomic sequences were combined, about 60 kb of genomic sequences encompassing zebrafish *ff1b* could be clearly defined and established. The ~100 kb genomic sequences contained within the BAC construct are sufficient to direct expression of EGFP to all the relevant tissues that are known to express *ff1b* as previously determined by ISH. However, additional EGFP expression were seen in the otic vesicle, muscle pioneer cells, common cardiac vein, and neuromasts, and it is

reasonable to conclude that either the upstream 5' DNA sequences were responsible or the actual *ff1b* genomic locus contains previously undetermined *cis*-elements. With the exception of the otic vesicle, as *ff1b* expression also disappeared when Intron IV is deleted, we have specifically determined that the same enhancer located within Intron IV is also functional in otic vesicle. Despite the presence of broader EGFP expression domain in the ff1bEx2EGFP embryos, the transgene has allowed us to study the fate of *ff1b*-expressing cells in the developing VMH and interrenal gland in a manner not previously possible. The availability of the ff1bEx2EGFP transgenic zebrafish line will thus allow the upstream regulators and coregulators of *ff1b* to be worked out rapidly, which is currently difficult to perform with the mouse SF-1 lineage-tracing model.

Using Red/ET recombination strategy, we have devised a novel and rapid strategy to specifically delete intronic enhancers, which is particularly suited for genes with such arrangement of core enhancers. This strategy can also be widely applicable to the removal of large tract of DNA, as well as, to make small deletions. Thus, when combined with transient microinjection assay into zebrafish embryos, we have been able to rapidly narrow down the required core enhancer that is responsible for directing *ff1b* expression in the interrenal and otic vesicle.

After comparison of the various *FF1* genes, we conclude that *ff1b* is the ancestral ortholog of *SF-1* lineage, and that in the other vertebrate classes, this ancestral ortholog is lost and that only the *ff1d* (*SF-1*) lineage persisted. Indeed, LRH-1 is derived subsequently from the SF-1 ortholog. The interrenal enhancer identified in *ff1b* should in fact be the ancestral enhancer and that the interrenal enhancer found in *ff1d*/*SF-1* lineage is likely to be acquired after the initial duplication, followed by

the loss of the ancestral intron. While this remains speculative, a through characterization of the *ff1d* isoform should be able to confirm this interpretation.

6.8. Future perspectives

The promoter analysis of *cyp11a1* has established firmly the direct involvement of Ff1b in the transcriptional regulation of steroidogenic enzymes. With the isolation and extensive characterization of the *cyp11a1*, an endogenous target gene promoter that is strictly regulated by Ff1b is now available. It is, therefore, amenable to a whole series of investigations with regards to the transactivation activity of zebrafish Ff1b. For instance, the involvement of the two FREs in cAMP responsiveness of the *cyp11a1* promoter can be further defined by transient transfections with hormonal treatments (e.g. with forskolin). Most importantly, the *cyp11a1* promoter can be used as a platform to delineate the transcriptional activity of Ff1b with regards to the influence of coregulators using transient transfections in cell lines or transactivation assay by microinjections into zebrafish embryos.

An important reagent presented in this study is the successful generation of an Ff1b antibody that works efficiently in ChIP assay. It is now possible to study the *in vivo* occupancy of Ff1b with potential target gene promoters. More importantly, it will enable us to perform genome-wide profiling of Ff1b binding sites using strategies such as ChIP-on-chip (Hudson and Snyder, 2006; Tavera-Mendoza *et al*., 2006), SABE (Chen, 2006), and PET-ChIP (Hudson and Snyder, 2006). By combining the data from the genome-wide analysis with computational analysis to identify Ff1 target genes (Bowler *et al*., 2006), we will be able to identify novel target genes of Ff1b that are involved in the morphogenesis and ontogenic development of interrenal gland and VMH. With the ff1bEx2EGFP line, this effort would even be more meaningful as EGFP-positive interrenal or VMH cells can be readily isolated from early stages of

embryonic development by fluorescence activated cell sorting (FACS). The fluorescent *ff1b*-expressing cells isolated by this method can also be used for other molecular analyses such as real-time RT-PCR, transcriptome profiling by microarray and SAGE, etc. This line of experiment is currently on-going in our laboratory and they are anticipated to greatly aid in identifying novel upstream and downstream factors of Ff1b that cooperatively play a role in the development of VMH and interrenal gland.

Although we have not determined whether the disparities in EGFP transgene and endogenous expression revealed by ISH are due to the absence of regulatory elements or the presence of interfering regulatory elements in the transgenic construct, or even the integration site of the transgene, further studies could be carried out to determine which of these hypotheses are correct. Several experimental approaches could be undertaken to investigate the genomic sequences that are required for *ff1b* expression in these endocrine tissues. For instance, multiple transgenic constructs encompassing truncated or additional genomic sequences could be used to explore whether the genomic sequences 5' or 3' to *ff1b* locus are needed to activate or suppress the expression of the EGFP reporter. In addition, genomic sequences that have been shown to potentially contain regulatory *cis*-elements should be sub-cloned into a reporter vector and assessed for their ability to drive tissue-specific expression.

By tracing the EGFP expression in ff1bEx2EGFP transgenic embryos, we can now perform real-time observation of morphogenetic movement of *ff1b*-expressing cells in the developing embryos without the need for subsequent ISH and immunohistochemistry assays, which will often alter the integrity of the embryos. This has opened up a whole new avenue of live imaging experiments utilizing the developing zebrafish embryos. For instance, one interesting experiment would be the

study of migration of *ff1b*-expressing neurons in the developing VMH and to dissect the target sites of their neuronal projections. Moreover, the easy manipulations of zebrafish embryos has made the transgenic line an excellent *in vivo* system to screen for molecules or genetic mutations that affect the development of VMH, interrenal gland, or any other EGFP-expressing tissues.

Functional studies can also be performed by crossing the ff1bEx2EGFP transgenic line with other mutant or transgenic lines. For example, the interrenal gland morphogenesis has been demonstrated to be dependent on midline signaling (Chai and Chan, 2000; Hsu *et al*., 2003). A simple cross between the ff1bEx2EGFP line and mutant zebrafish lines such as *oep* and *flh* (or any other signaling mutant line that could potentially affect interrenal development) would provide a convenient platform to study the molecular mechanisms underlying their connections. Besides mutant lines, crossing with other transgenic lines that express different fluorescent markers driven by genes related to *ff1b* would also provide useful functional data. For instance, we are currently generating a red fluorescent transgenic line for the tracing of *prox1*, which has been proposed as a transcriptional repressor of *ff1b* (Liu *et al*., 2003). A double fluorescent transgenic line of *ff1b* and *prox1* would provide useful insights in to the mechanism by which the two transcription factors interact with each other to modulate important developmental events such as interrenal morphogenesis.

Last but not least, the putative interrenal-specific core enhancer that has been localized to Intron IV of *ff1b* needs to be further delineated. As Intron IV spans 3754 bp and core enhancer elements usually encompass only a few hundred bp of nucleotide sequences, additional fine deletion and truncation analyses need to be carried out. Not only should we aimed to identify the core enhancer element responsible for interrenal-specific expression, we should be able to simultaneously

establish the upstream *trans*-acting factors that interact with the *cis*-elements located in the enhancer. More importantly, this core enhancer would eventually enable us to generate another stable transgenic line that expresses fluorescent marker specifically in the interrenal gland only. Besides Intron IV, other genomic regions that potentially contain regulatory elements responsible for directing *ff1b* expression to other specific tissues should also be further analyzed by deletions spanning shorter regions and sub-cloning of smaller and overlapping fragments into a reporter vector. These include the 10 kb 5' upstream sequences that potentially contain an interrenal repressor as well as Intron V and Intron VI as they potentially contain VMH-specific enhancer.

With the findings delivered from this study and the above experimental plan in place, we will be able to gain useful insights into the mechanisms by which Ff1b regulates the development of interrenal gland and VMH, particularly in terms of its upstream regulators and its downstream gene targets. Importantly, the zebrafish transgenic model serves as an excellent developmental platform to deliver new and reliable findings that could be hardly achieved in the mouse model. Furthermore, the ontogeny of the endocrine development and functions have been shown to be highly conserved between zebrafish and mammals, indicating that key aspects of endocrine function could be readily and reliably addressed using a more amenable vertebrate model species like the zebrafish. Together, with the active research of SF-1 and LRH-1 in the mammalian system, and the experimental findings that have been generated for zebrafish Ff1s, we now have a good chance to unravel the complex molecular networks that use this sub-family of NR as an important transcriptional modulators of diverse biological processes, particularly in the maintenance of endocrine development and function of the HPA and HPG axes.

Bibliography

Achermann,J.C., Ito,M., Ito,M., Hindmarsh,P.C., and Jameson,J.L. (1999). A mutation in the gene encoding steroidogenic factor-1 causes XY sex reversal and adrenal failure in humans. Nat. Genet. *22*, 125-126.

Ahlgren,R., Suske,G., Waterman,M.R., and Lund,J. (1999). Role of Sp1 in cAMP-dependent transcriptional regulation of the bovine CYP11A gene. J. Biol. Chem. *274*, 19422-19428.

Aigueperse,C., Val,P., Pacot,C., Darne,C., Lalli,E., Sassone-Corsi,P., Veyssiere,G., Jean,C., and Martinez,A. (2001). SF-1 (steroidogenic factor-1), C/EBPbeta (CCAAT/enhancer binding protein), and ubiquitous transcription factors NF1 (nuclear factor 1) and Sp1 (selective promoter factor 1) are required for regulation of the mouse aldose reductase-like gene (AKR1B7) expression in adrenocortical cells. Mol. Endocrinol. *15*, 93-111.

Amores,A., Force,A., Yan,Y.L., Joly,L., Amemiya,C., Fritz,A., Ho,R.K., Langeland,J., Prince,V., Wang,Y.L., Westerfield,M., Ekker,M., and Postlethwait,J.H. (1998). Zebrafish hox clusters and vertebrate genome evolution. Science *282*, 1711-1714.

Angus,L.M., Chan,R.Y., and Jasmin,B.J. (2001). Role of intronic E- and N-box motifs in the transcriptional induction of the acetylcholinesterase gene during myogenic differentiation. J. Biol. Chem. *276*, 17603-17609.

Annicotte,J.S., Fayard,E., Swift,G.H., Selander,L., Edlund,H., Tanaka,T., Kodama,T., Schoonjans,K., and Auwerx,J. (2003). Pancreatic-duodenal homeobox 1 regulates expression of liver receptor homolog 1 during pancreas development. Mol. Cell Biol. *23*, 6713-6724.

Bartkuhn,M. and Renkawitz,R. (2008). Long range chromatin interactions involved in gene regulation. Biochim. Biophys. Acta *1783*, 2161-2166.

Bassett,M.H., Zhang,Y., Clyne,C., White,P.C., and Rainey,W.E. (2002). Differential regulation of aldosterone synthase and 11beta-hydroxylase transcription by steroidogenic factor-1. J. Mol. Endocrinol. *28*, 125-135.

Ben Zimra,M., Koler,M., and Orly,J. (2002). Transcription of cholesterol side-chain cleavage cytochrome P450 in the placenta: activating protein-2 assumes the role of steroidogenic factor-1 by binding to an overlapping promoter element. Mol. Endocrinol. *16*, 1864-1880.

Bentley,P.J. (1998). Comparative vertebrate endocrinology. Cambridge University Press).

Bergeron,S.A., Milla,L.A., Villegas,R., Shen,M.C., Burgess,S.M., Allende,M.L., Karlstrom,R.O., and Palma,V. (2008). Expression profiling identifies novel Hh/Gli-regulated genes in developing zebrafish embryos. Genomics *91*, 165-177.

Bernichtein,S., Alevizaki,M., and Huhtaniemi,I. (2008). Is the adrenal cortex a target for gonadotropins? Trends Endocrinol. Metab *19*, 231-238.

Berthelsen,J., Zappavigna,V., Mavilio,F., and Blasi,F. (1998). Prep1, a novel functional partner of Pbx proteins. EMBO J. *17*, 1423-1433.

Biason-Lauber,A. and Schoenle,E.J. (2000). Apparently normal ovarian differentiation in a prepubertal girl with transcriptionally inactive steroidogenic factor 1 (NR5A1/SF-1) and adrenocortical insufficiency. Am. J. Hum. Genet. *67*, 1563-1568.

Birk,O.S., Casiano,D.E., Wassif,C.A., Cogliati,T., Zhao,L., Zhao,Y., Grinberg,A., Huang,S., Kreidberg,J.A., Parker,K.L., Porter,F.D., and Westphal,H. (2000). The LIM homeobox gene Lhx9 is essential for mouse gonad formation. Nature *403*, 909-913.

Bland,M.L., Desclozeaux,M., and Ingraham,H.A. (2003). Tissue growth and remodeling of the embryonic and adult adrenal gland. Ann. N. Y. Acad. Sci. *995*, 59-72.

Bland,M.L., Jamieson,C.A., Akana,S.F., Bornstein,S.R., Eisenhofer,G., Dallman,M.F., and Ingraham,H.A. (2000). Haploinsufficiency of steroidogenic factor-1 in mice disrupts adrenal development leading to an impaired stress response. Proc. Natl. Acad. Sci. U. S. A *97*, 14488-14493.

Boerboom,D., Pilon,N., Behdjani,R., Silversides,D.W., and Sirois,J. (2000). Expression and regulation of transcripts encoding two members of the NR5A nuclear receptor subfamily of orphan nuclear receptors, steroidogenic factor-1 and NR5A2, in equine ovarian cells during the ovulatory process. Endocrinology *141*, 4647-4656.

Bornstein,S.R. and Vaudry,H. (1998). Paracrine and neuroendocrine regulation of the adrenal gland--basic and clinical aspects. Horm. Metab Res. *30*, 292-296.

Borroni,R., Liu,Z., Simpson,E.R., and Hinshelwood,M.M. (1997). A putative binding site for Sp1 is involved in transcriptional regulation of CYP17 gene expression in bovine ovary. Endocrinology *138*, 2011-2020.

Borud,B., Hoang,T., Bakke,M., Jacob,A.L., Lund,J., and Mellgren,G. (2002). The nuclear receptor coactivators p300/CBP/cointegrator-associated protein (p/CIP) and transcription intermediary factor 2 (TIF2) differentially regulate PKA-stimulated transcriptional activity of steroidogenic factor 1. Mol. Endocrinol. *16*, 757-773.

Borud,B., Mellgren,G., Lund,J., and Bakke,M. (2003). Cloning and characterization of a novel zinc finger protein that modulates the transcriptional activity of nuclear receptors. Mol. Endocrinol. *17*, 2303-2319.

Botrugno,O.A., Fayard,E., Annicotte,J.S., Haby,C., Brennan,T., Wendling,O., Tanaka,T., Kodama,T., Thomas,W., Auwerx,J., and Schoonjans,K. (2004). Synergy between LRH-1 and beta-catenin induces G1 cyclin-mediated cell proliferation. Mol. Cell *15*, 499-509.

Bowler,T., Kosman,D., Licht,J.D., and Pick,L. (2006). Computational identification of Ftz/Ftz-F1 downstream target genes. Dev. Biol. *299*, 78-90.

Braat,A.K., Zandbergen,M.A., De Vries,E., Van Der,B.B., Bogerd,J., and Goos,H.J. (1999). Cloning and expression of the zebrafish germ cell nuclear factor. Mol. Reprod. Dev. *53*, 369-375.

Brand,C., Souchelnytskiy,S., Chambaz,E.M., Feige,J.J., and Bailly,S. (1998). Smad3 is involved in the intracellular signaling pathways that mediate the inhibitory effects of transforming growth factor-beta on StAR expression. Biochem. Biophys. Res. Commun. *253*, 780-785.

Burris,T.P., Guo,W., Le,T., and McCabe,E.R. (1995). Identification of a putative steroidogenic factor-1 response element in the DAX-1 promoter. Biochem. Biophys. Res. Commun. *214*, 576-581.

Bury,N.R. and Sturm,A. (2007). Evolution of the corticosteroid receptor signalling pathway in fish. Gen. Comp Endocrinol. *153*, 47-56.

Busygina,T.V., Vasiliev,G.V., Klimova,N.V., Ignatieva,E.V., and Osadchuk,A.V. (2005). Binding sites for transcription factor SF-1 in promoter regions of genes encoding mouse steroidogenesis enzymes 3betaHSDI and P450c17. Biochemistry (Mosc.) *70*, 1152-1156.

Campbell,L.A., Faivre,E.J., Show,M.D., Ingraham,J.G., Flinders,J., Gross,J.D., and Ingraham,H.A. (2008). Modification of SF- 1 (NR5A1) Results in Decreased Recognition of SUMO-Sensitive Target Genes. Mol. Cell Biol.

Canteras,N.S., Simerly,R.B., and Swanson,L.W. (1994). Organization of projections from the ventromedial nucleus of the hypothalamus: a Phaseolus vulgaris-leucoagglutinin study in the rat. J. Comp Neurol. *348*, 41-79.

Cao,G., Garcia,C.K., Wyne,K.L., Schultz,R.A., Parker,K.L., and Hobbs,H.H. (1997). Structure and localization of the human gene encoding SR-BI/CLA-1. Evidence for transcriptional control by steroidogenic factor 1. J. Biol. Chem. *272*, 33068-33076.

Carlone,D.L. and Richards,J.S. (1997). Functional interactions, phosphorylation, and levels of 3',5'-cyclic adenosine monophosphate-regulatory element binding protein and steroidogenic factor-1 mediate hormone-regulated and constitutive expression of aromatase in gonadal cells. Mol. Endocrinol. *11*, 292-304.

Carmel,L., Wolf,Y.I., Rogozin,I.B., and Koonin,E.V. (2007). Three distinct modes of intron dynamics in the evolution of eukaryotes. Genome Res. *17*, 1034-1044.

Carson-Jurica,M.A., Schrader,W.T., and O'Malley,B.W. (1990). Steroid receptor family: structure and functions. Endocr. Rev. *11*, 201-220.

Cartharius,K., Frech,K., Grote,K., Klocke,B., Haltmeier,M., Klingenhoff,A., Frisch,M., Bayerlein,M., and Werner,T. (2005). MatInspector and beyond: promoter analysis based on transcription factor binding sites. Bioinformatics. *21*, 2933-2942.

Castillo-Olivares,A., Campos,J.A., Pandak,W.M., and Gil,G. (2004). The role of alpha1-fetoprotein transcription factor/LRH-1 in bile acid biosynthesis: a known nuclear receptor activator that can act as a suppressor of bile acid biosynthesis. J. Biol. Chem. *279*, 16813-16821.

Castillo-Olivares,A. and Gil,G. (2000). Alpha 1-fetoprotein transcription factor is required for the expression of sterol 12alpha -hydroxylase, the specific enzyme for cholic acid synthesis. Potential role in the bile acid-mediated regulation of gene transcription. J. Biol. Chem. *275*, 17793-17799.

Chai,C. (2002). Ph.D Thesis: Characterization and developmental analysis of a zebrafish Ftz-F1 gene, ff1b (nr5a4). Department of Biological Sciences, National University of Singapore).

Chai,C. and Chan,W.K. (2000). Developmental expression of a novel Ftz-F1 homologue, ff1b (NR5A4), in the zebrafish Danio rerio. Mech. Dev. *91*, 421-426.

Chai,C., Liu,Y.W., and Chan,W.K. (2003). Ff1b is required for the development of steroidogenic component of the zebrafish interrenal organ. Dev. Biol. *260*, 226-244.

Chambaz,E.M., Souchelnitskiy,S., Pellerin,S., Defaye,G., Cochet,C., and Feige,J.J. (1996). Transforming growth factors-beta s: a multifunctional cytokine family. Implication in the regulation of adrenocortical cell endocrine functions. Horm. Res. *45*, 222-226.

Chan,W.K. and Tan,C.H. (1988). Aminoglutethimide augments follicle-stimulating hormone-induced aromatase activity in cultured porcine granulosa cells. Endocrinology *122*, 2290-2298.

Chen,C. and Guo,I.C. (2000). Effect of cAMP on protein binding activities of three elements in upstream promoter of human CYP11A1 gene. Life Sci. *67*, 2045-2049.

Chen,F., Ma,L., Dawson,P.A., Sinal,C.J., Sehayek,E., Gonzalez,F.J., Breslow,J., Ananthanarayanan,M., and Shneider,B.L. (2003). Liver receptor homologue-1 mediates species- and cell line-specific bile acid-dependent negative feedback regulation of the apical sodium-dependent bile acid transporter. J. Biol. Chem. *278*, 19909-19916.

Chen,J. (2006). Serial analysis of binding elements for human transcription factors. Nat. Protoc. *1*, 1481-1493.

Chinn,A.M., Ciais,D., Bailly,S., Chambaz,E., LaMarre,J., and Feige,J.J. (2002). Identification of two novel ACTH-responsive genes encoding manganese-dependent superoxide dismutase (SOD2) and the zinc finger protein TIS11b [tetradecanoyl phorbol acetate (TPA)-inducible sequence 11b]. Mol. Endocrinol. *16*, 1417-1427.

Chou,S.J., Lai,K.N., and Chung,B. (1996). Characterization of the upstream sequence of the human CYP11A1 gene for cell type-specific expression. J. Biol. Chem. *271*, 22125-22129.

Chung,A.C. and Cooney,A.J. (2001). Germ cell nuclear factor. Int. J. Biochem. Cell Biol. *33*, 1141-1146.

Chung,A.C., Katz,D., Pereira,F.A., Jackson,K.J., DeMayo,F.J., Cooney,A.J., and O'Malley,B.W. (2001). Loss of orphan receptor germ cell nuclear factor function results in ectopic development of the tail bud and a novel posterior truncation. Mol. Cell Biol. *21*, 663-677.

Clemens,J.W., Lala,D.S., Parker,K.L., and Richards,J.S. (1994). Steroidogenic factor-1 binding and transcriptional activity of the cholesterol side-chain cleavage promoter in rat granulosa cells. Endocrinology *134*, 1499-1508.

Cole,T.J., Blendy,J.A., Monaghan,A.P., Krieglstein,K., Schmid,W., Aguzzi,A., Fantuzzi,G., Hummler,E., Unsicker,K., and Schutz,G. (1995). Targeted disruption of the glucocorticoid receptor gene blocks adrenergic chromaffin cell development and severely retards lung maturation. Genes Dev. *9*, 1608-1621.

Coulter,C.L. (2005). Fetal adrenal development: insight gained from adrenal tumors. Trends Endocrinol. Metab *16*, 235-242.

Couzinet,B., Meduri,G., Lecce,M.G., Young,J., Brailly,S., Loosfelt,H., Milgrom,E., and Schaison,G. (2001). The postmenopausal ovary is not a major androgen-producing gland. J. Clin. Endocrinol. Metab *86*, 5060-5066.

Crawford,P.A., Dorn,C., Sadovsky,Y., and Milbrandt,J. (1998). Nuclear receptor DAX-1 recruits nuclear receptor corepressor N-CoR to steroidogenic factor 1. Mol. Cell Biol. *18*, 2949-2956.

Crawford,P.A., Polish,J.A., Ganpule,G., and Sadovsky,Y. (1997a). The activation function-2 hexamer of steroidogenic factor-1 is required, but not sufficient for potentiation by SRC-1. Mol. Endocrinol. *11*, 1626-1635.

Crawford,P.A., Sadovsky,Y., and Milbrandt,J. (1997b). Nuclear receptor steroidogenic factor 1 directs embryonic stem cells toward the steroidogenic lineage. Mol. Cell Biol. *17*, 3997-4006.

Curtin,D., Ferris,H.A., Hakli,M., Gibson,M., Janne,O.A., Palvimo,J.J., and Shupnik,M.A. (2004). Small nuclear RING finger protein stimulates the rat luteinizing hormone-beta promoter by interacting with Sp1 and steroidogenic factor-1 and protects from androgen suppression. Mol. Endocrinol. *18*, 1263-1276.

Daggett,M.A., Rice,D.A., and Heckert,L.L. (2000). Expression of steroidogenic factor 1 in the testis requires an E box and CCAAT box in its promoter proximal region. Biol. Reprod. *62*, 670-679.

Dallman,M.F., Akana,S.F., Jacobson,L., Levin,N., Cascio,C.S., and Shinsako,J. (1987). Characterization of corticosterone feedback regulation of ACTH secretion. Ann. N. Y. Acad. Sci. *512*, 402-414.

Davis,A.M., Seney,M.L., Stallings,N.R., Zhao,L., Parker,K.L., and Tobet,S.A. (2004). Loss of steroidogenic factor 1 alters cellular topography in the mouse ventromedial nucleus of the hypothalamus. J. Neurobiol. *60*, 424-436.

De Santa,B.P., Bonneaud,N., Boizet,B., Desclozeaux,M., Moniot,B., Sudbeck,P., Scherer,G., Poulat,F., and Berta,P. (1998a). Direct interaction of SRY-related protein SOX9 and steroidogenic factor 1 regulates transcription of the human anti-Mullerian hormone gene. Mol. Cell Biol. *18*, 6653-6665.

De Santa,B.P., Mejean,C., Moniot,B., Malcles,M.H., Berta,P., and Boizet-Bonhoure,B. (2001). Steroidogenic factor-1 contributes to the cyclic-adenosine monophosphate down-regulation of human SRY gene expression. Biol. Reprod. *64*, 775-783.

De Santa,B.P., Moniot,B., Poulat,F., and Berta,P. (2000). Expression and subcellular localization of SF-1, SOX9, WT1, and AMH proteins during early human testicular development. Dev. Dyn. *217*, 293-298.

De Santa,B.P., Moniot,B., Poulat,F., Boizet,B., and Berta,P. (1998b). Steroidogenic factor-1 regulates transcription of the human anti-mullerian hormone receptor. J. Biol. Chem. *273*, 29654-29660.

Dellovade,T.L., Young,M., Ross,E.P., Henderson,R., Caron,K., Parker,K., and Tobet,S.A. (2000). Disruption of the gene encoding SF-1 alters the distribution of hypothalamic neuronal phenotypes. J. Comp Neurol. *423*, 579-589.

Desclozeaux,M., Krylova,I.N., Horn,F., Fletterick,R.J., and Ingraham,H.A. (2002). Phosphorylation and intramolecular stabilization of the ligand binding domain in the nuclear receptor steroidogenic factor 1. Mol. Cell Biol. *22*, 7193-7203.

Doghman,M., Karpova,T., Rodrigues,G.A., Arhatte,M., De Moura,J., Cavalli,L.R., Virolle,V., Barbry,P., Zambetti,G.P., Figueiredo,B.C., Heckert,L.L., and Lalli,E. (2007). Increased steroidogenic factor-1 dosage triggers adrenocortical cell proliferation and cancer. Mol. Endocrinol. *21*, 2968-2987.

Draper,B.W., Morcos,P.A., and Kimmel,C.B. (2001). Inhibition of zebrafish fgf8 pre-mRNA splicing with morpholino oligos: a quantifiable method for gene knockdown. Genesis. *30*, 154-156.

Drean,Y.L., Liu,D., Wong,A.O., Xiong,F., and Hew,C.L. (1996). Steroidogenic factor 1 and estradiol receptor act in synergism to regulate the expression of the salmon gonadotropin II beta subunit gene. Mol. Endocrinol. *10*, 217-229.

Du,S.J., Devoto,S.H., Westerfield,M., and Moon,R.T. (1997). Positive and negative regulation of muscle cell identity by members of the hedgehog and TGF-beta gene families. J. Cell Biol. *139*, 145-156.

Duarte,J., Perriere,G., Laudet,V., and Robinson-Rechavi,M. (2002). NUREBASE: database of nuclear hormone receptors. Nucleic Acids Res. *30*, 364-368.

Duval,D.L., Nelson,S.E., and Clay,C.M. (1997). A binding site for steroidogenic factor-1 is part of a complex enhancer that mediates expression of the murine gonadotropin-releasing hormone receptor gene. Biol. Reprod. *56*, 160-168.

Ehrhart-Bornstein,M. and Hilbers,U. (1998). Neuroendocrine properties of adrenocortical cells. Horm. Metab Res. *30*, 436-439.

Ehrhart-Bornstein,M., Hinson,J.P., Bornstein,S.R., Scherbaum,W.A., and Vinson,G.P. (1998). Intraadrenal interactions in the regulation of adrenocortical steroidogenesis. Endocr. Rev. *19*, 101-143.

El Hodiri,H., Bhatia-Dey,N., Kenyon,K., Ault,K., Dirksen,M., and Jamrich,M. (2001). Fox (forkhead) genes are involved in the dorso-ventral patterning of the Xenopus mesoderm. Int. J. Dev. Biol. *45*, 265-271.

Else,T. and Hammer,G.D. (2005). Genetic analysis of adrenal absence: agenesis and aplasia. Trends Endocrinol. Metab *16*, 458-468.

Escriva,H., Bertrand,S., and Laudet,V. (2004). The evolution of the nuclear receptor superfamily. Essays Biochem. *40*, 11-26.

Falender,A.E., Lanz,R., Malenfant,D., Belanger,L., and Richards,J.S. (2003). Differential expression of steroidogenic factor-1 and FTF/LRH-1 in the rodent ovary. Endocrinology *144*, 3598-3610.

Fayard,E., Auwerx,J., and Schoonjans,K. (2004). LRH-1: an orphan nuclear receptor involved in development, metabolism and steroidogenesis. Trends Cell Biol. *14*, 250-260.

Fayard,E., Schoonjans,K., Annicotte,J.S., and Auwerx,J. (2003). Liver receptor homolog 1 controls the expression of carboxyl ester lipase. J. Biol. Chem. *278*, 35725-35731.

Fitzpatrick,S.L. and Richards,J.S. (1993). cis-acting elements of the rat aromatase promoter required for cyclic adenosine 3',5'-monophosphate induction in ovarian granulosa cells and constitutive expression in R2C Leydig cells. Mol. Endocrinol. *7*, 341-354.

Flanagan-Cato,L.M., Calizo,L.H., and Daniels,D. (2001). The synaptic organization of VMH neurons that mediate the effects of estrogen on sexual behavior. Horm. Behav. *40*, 178-182.

Fortier,T.M., Vasa,P.P., and Woodard,C.T. (2003). Orphan nuclear receptor betaFTZ-F1 is required for muscle-driven morphogenetic events at the prepupal-pupal transition in Drosophila melanogaster. Dev. Biol. *257*, 153-165.

Fowkes,R.C., Desclozeaux,M., Patel,M.V., Aylwin,S.J., King,P., Ingraham,H.A., and Burrin,J.M. (2003). Steroidogenic factor-1 and the gonadotrope-specific element enhance

basal and pituitary adenylate cyclase-activating polypeptide-stimulated transcription of the human glycoprotein hormone alpha-subunit gene in gonadotropes. Mol. Endocrinol. *17*, 2177-2188.

Galarneau,L., Pare,J.F., Allard,D., Hamel,D., Levesque,L., Tugwood,J.D., Green,S., and Belanger,L. (1996). The alpha1-fetoprotein locus is activated by a nuclear receptor of the Drosophila FTZ-F1 family. Mol. Cell Biol. *16*, 3853-3865.

Galceran,J., Sustmann,C., Hsu,S.C., Folberth,S., and Grosschedl,R. (2004). LEF1-mediated regulation of Delta-like1 links Wnt and Notch signaling in somitogenesis. Genes Dev. *18*, 2718-2723.

Gao,D.M., Wang,L.F., Liu,J., Kong,Y.Y., Wang,Y., and Xie,Y.H. (2006). Expression of mouse liver receptor homologue 1 in embryonic stem cells is directed by a novel promoter. FEBS Lett. *580*, 1702-1708.

Germain,P., Staels,B., Dacquet,C., Spedding,M., and Laudet,V. (2006). Overview of nomenclature of nuclear receptors. Pharmacol. Rev. *58*, 685-704.

Gerstein,M.B., Bruce,C., Rozowsky,J.S., Zheng,D., Du,J., Korbel,J.O., Emanuelsson,O., Zhang,Z.D., Weissman,S., and Snyder,M. (2007). What is a gene, post-ENCODE? History and updated definition. Genome Res. *17*, 669-681.

Giguere,V. (1999). Orphan nuclear receptors: from gene to function. Endocr. Rev. *20*, 689-725.

Giraldo,P. and Montoliu,L. (2001). Size matters: use of YACs, BACs and PACs in transgenic animals. Transgenic Res. *10*, 83-103.

Gizard,F., Lavallee,B., DeWitte,F., Teissier,E., Staels,B., and Hum,D.W. (2002). The transcriptional regulating protein of 132 kDa (TReP-132) enhances P450scc gene transcription through interaction with steroidogenic factor-1 in human adrenal cells. J. Biol. Chem. *277*, 39144-39155.

Gizard,F., Robillard,R., Barbier,O., Quatannens,B., Faucompre,A., Revillion,F., Peyrat,J.P., Staels,B., and Hum,D.W. (2005). TReP-132 controls cell proliferation by regulating the expression of the cyclin-dependent kinase inhibitors p21WAF1/Cip1 and p27Kip1. Mol. Cell Biol. *25*, 4335-4348.

Goodwin,B., Jones,S.A., Price,R.R., Watson,M.A., McKee,D.D., Moore,L.B., Galardi,C., Wilson,J.G., Lewis,M.C., Roth,M.E., Maloney,P.R., Willson,T.M., and Kliewer,S.A. (2000). A regulatory cascade of the nuclear receptors FXR, SHP-1, and LRH-1 represses bile acid biosynthesis. Mol. Cell *6*, 517-526.

Grassi,M.E., Basari,F., and Chimenti,C. (1997). Adrenocortical and adrenomedullary homologs in eight species of adult and developing teleosts: morphology, histology, and immunohistochemistry. Gen. Comp Endocrinol. *108*, 483-496.

Graves,P.E. and Salhanick,H.A. (1979). Stereoselective inhibition of aromatase by enantiomers of aminoglutethimide. Endocrinology *105*, 52-57.

Grigoryan,T., Wend,P., Klaus,A., and Birchmeier,W. (2008). Deciphering the function of canonical Wnt signals in development and disease: conditional loss- and gain-of-function mutations of beta-catenin in mice. Genes Dev. *22*, 2308-2341.

Gronemeyer,H., Gustafsson,J.A., and Laudet,V. (2004). Principles for modulation of the nuclear receptor superfamily. Nat. Rev. Drug Discov. *3*, 950-964.

Gu,P., Goodwin,B., Chung,A.C., Xu,X., Wheeler,D.A., Price,R.R., Galardi,C., Peng,L., Latour,A.M., Koller,B.H., Gossen,J., Kliewer,S.A., and Cooney,A.J. (2005). Orphan nuclear receptor LRH-1 is required to maintain Oct4 expression at the epiblast stage of embryonic development. Mol. Cell Biol. *25*, 3492-3505.

Gummow,B.M., Winnay,J.N., and Hammer,G.D. (2003). Convergence of Wnt signaling and steroidogenic factor-1 (SF-1) on transcription of the rat inhibin alpha gene. J. Biol. Chem. *278*, 26572-26579.

Guo,I.C., Hu,M.C., and Chung,B.C. (2003). Transcriptional regulation of CYP11A1. J. Biomed. Sci. *10*, 593-598.

Guo,I.C., Huang,C.Y., Wang,C.K., and Chung,B.C. (2007a). Activating protein-1 cooperates with steroidogenic factor-1 to regulate 3',5'-cyclic adenosine 5'-monophosphate-dependent human CYP11A1 transcription in vitro and in vivo. Endocrinology *148*, 1804-1812.

Guo,I.C., Shih,M.C., Lan,H.C., Hsu,N.C., Hu,M.C., and Chung,B.C. (2007b). Transcriptional regulation of human CYP11A1 in gonads and adrenals. J. Biomed. Sci. *14*, 509-515.

Guo,I.C., Tsai,H.M., and Chung,B.C. (1994). Actions of two different cAMP-responsive sequences and an enhancer of the human CYP11A1 (P450scc) gene in adrenal Y1 and placental JEG-3 cells. J. Biol. Chem. *269*, 6362-6369.

Gurates,B., Amsterdam,A., Tamura,M., Yang,S., Zhou,J., Fang,Z., Amin,S., Sebastian,S., and Bulun,S.E. (2003). WT1 and DAX-1 regulate SF-1-mediated human P450arom gene expression in gonadal cells. Mol. Cell Endocrinol. *208*, 61-75.

Gurates,B., Sebastian,S., Yang,S., Zhou,J., Tamura,M., Fang,Z., Suzuki,T., Sasano,H., and Bulun,S.E. (2002). WT1 and DAX-1 inhibit aromatase P450 expression in human endometrial and endometriotic stromal cells. J. Clin. Endocrinol. Metab *87*, 4369-4377.

Haisenleder,D.J., Yasin,M., Dalkin,A.C., Gilrain,J., and Marshall,J.C. (1996). GnRH regulates steroidogenic factor-1 (SF-1) gene expression in the rat pituitary. Endocrinology *137*, 5719-5722.

Halvorson,L.M., Ito,M., Jameson,J.L., and Chin,W.W. (1998). Steroidogenic factor-1 and early growth response protein 1 act through two composite DNA binding sites to regulate luteinizing hormone beta-subunit gene expression. J. Biol. Chem. *273*, 14712-14720.

Halvorson,L.M., Kaiser,U.B., and Chin,W.W. (1996). Stimulation of luteinizing hormone beta gene promoter activity by the orphan nuclear receptor, steroidogenic factor-1. J. Biol. Chem. *271*, 6645-6650.

Hammer,G.D. and Ingraham,H.A. (1999). Steroidogenic factor-1: its role in endocrine organ development and differentiation. Front Neuroendocrinol. *20*, 199-223.

Hammer,G.D., Krylova,I., Zhang,Y., Darimont,B.D., Simpson,K., Weigel,N.L., and Ingraham,H.A. (1999). Phosphorylation of the nuclear receptor SF-1 modulates cofactor recruitment: integration of hormone signaling in reproduction and stress. Mol. Cell *3*, 521-526.

Hammer,G.D., Parker,K.L., and Schimmer,B.P. (2005). Minireview: transcriptional regulation of adrenocortical development. Endocrinology *146*, 1018-1024.

Hanley,N.A., Rainey,W.E., Wilson,D.I., Ball,S.G., and Parker,K.L. (2001). Expression profiles of SF-1, DAX1, and CYP17 in the human fetal adrenal gland: potential interactions in gene regulation. Mol. Endocrinol. *15*, 57-68.

Harris,A.N. and Mellon,P.L. (1998). The basic helix-loop-helix, leucine zipper transcription factor, USF (upstream stimulatory factor), is a key regulator of SF-1 (steroidogenic factor-1) gene expression in pituitary gonadotrope and steroidogenic cells. Mol. Endocrinol. *12*, 714-726.

Hatano,O., Takakusu,A., Nomura,M., and Morohashi,K. (1996). Identical origin of adrenal cortex and gonad revealed by expression profiles of Ad4BP/SF-1. Genes Cells *1*, 663-671.

Hatta,K., Kimmel,C.B., Ho,R.K., and Walker,C. (1991). The cyclops mutation blocks specification of the floor plate of the zebrafish central nervous system. Nature *350*, 339-341.

Hawkins,R.D. and Ren,B. (2006). Genome-wide location analysis: insights on transcriptional regulation. Hum. Mol. Genet. *15 Spec No 1*, R1-R7.

Heckert,L.L. (2001). Activation of the rat follicle-stimulating hormone receptor promoter by steroidogenic factor 1 is blocked by protein kinase a and requires upstream stimulatory factor binding to a proximal E box element. Mol. Endocrinol. *15*, 704-715.

Heikkila,M., Peltoketo,H., Leppaluoto,J., Ilves,M., Vuolteenaho,O., and Vainio,S. (2002). Wnt-4 deficiency alters mouse adrenal cortex function, reducing aldosterone production. Endocrinology *143*, 4358-4365.

Heintz,N. (2000). Analysis of mammalian central nervous system gene expression and function using bacterial artificial chromosome-mediated transgenesis. Hum. Mol. Genet. *9*, 937-943.

Hillier,S.G. (2001). Gonadotropic control of ovarian follicular growth and development. Mol. Cell Endocrinol. *179*, 39-46.

Hinshelwood,M.M., Repa,J.J., Shelton,J.M., Richardson,J.A., Mangelsdorf,D.J., and Mendelson,C.R. (2003). Expression of LRH-1 and SF-1 in the mouse ovary: localization in different cell types correlates with differing function. Mol. Cell Endocrinol. *207*, 39-45.

Hinson,J.P., Purbrick,A., Cameron,L.A., and Kapas,S. (1994). The role of neuropeptides in the regulation of adrenal zona fasciculata/reticularis function. Effects of vasoactive intestinal polypeptide, substance P, neuropeptide Y, Met- and Leu-enkephalin and neurotensin on corticosterone secretion in the intact perfused rat adrenal gland in situ. Neuropeptides *26*, 391-397.

Hodgkin,J. (2005). Karyotype, ploidy, and gene dosage. WormBook. 1-9.

Honda,S., Morohashi,K., Nomura,M., Takeya,H., Kitajima,M., and Omura,T. (1993). Ad4BP regulating steroidogenic P-450 gene is a member of steroid hormone receptor superfamily. J. Biol. Chem. *268*, 7494-7502.

Hsieh,H.T., Wang,C.H., Wu,M.L., Yang,F.M., Tai,Y.C., and Hu,M.C. (2008). PIASy inhibits LRH-1-dependent CYP11A1 expression by competing for SRC-1 binding. Biochem. J.

Hsu,H.J., Hsu,N.C., Hu,M.C., and Chung,B.C. (2006). Steroidogenesis in zebrafish and mouse models. Mol. Cell Endocrinol. *248*, 160-163.

Hsu,H.J., Lin,G., and Chung,B.C. (2003). Parallel early development of zebrafish interrenal glands and pronephros: differential control by wt1 and ff1b. Development *130*, 2107-2116.

Hsu,H.J., Lin,G., and Chung,B.C. (2004a). Parallel early development of zebrafish interrenal glands and pronephros: differential control by wt1 and ff1b. Endocr. Res. *30*, 803.

Hsu,N.C., Shih,M.C., and Chung,B.C. (2004b). Study of the function of proximal SF-1 binding sites on Cyp11A1 promoter. Endocr. Res. *30*, 813-814.

Hu,M.C., Chiang,E.F., Tong,S.K., Lai,W., Hsu,N.C., Wang,L.C., and Chung,B.C. (2001a). Regulation of steroidogenesis in transgenic mice and zebrafish. Mol. Cell Endocrinol. *171*, 9-14.

Hu,M.C., Chou,S.J., Huang,Y.Y., Hsu,N.C., Li,H., and Chung,B.C. (1999). Tissue-specific, hormonal, and developmental regulation of SCC-LacZ expression in transgenic mice leads to adrenocortical zone characterization. Endocrinology *140*, 5609-5618.

Hu,M.C., Hsu,N.C., Pai,C.I., Wang,C.K., and Chung,B. (2001b). Functions of the upstream and proximal steroidogenic factor 1 (SF-1)-binding sites in the CYP11A1 promoter in basal transcription and hormonal response. Mol. Endocrinol. *15*, 812-818.

Hu,Z., Zhuang,L., Guan,X., Meng,J., and Dufau,M.L. (1997). Steroidogenic factor-1 is an essential transcriptional activator for gonad-specific expression of promoter I of the rat prolactin receptor gene. J. Biol. Chem. *272*, 14263-14271.

Hudson,M.E. and Snyder,M. (2006). High-throughput methods of regulatory element discovery. Biotechniques *41*, 673, 675, 677.

Ikeda,Y., Lala,D.S., Luo,X., Kim,E., Moisan,M.P., and Parker,K.L. (1993). Characterization of the mouse FTZ-F1 gene, which encodes a key regulator of steroid hydroxylase gene expression. Mol. Endocrinol. *7*, 852-860.

Ikeda,Y., Luo,X., Abbud,R., Nilson,J.H., and Parker,K.L. (1995). The nuclear receptor steroidogenic factor 1 is essential for the formation of the ventromedial hypothalamic nucleus. Mol. Endocrinol. *9*, 478-486.

Ikeda,Y., Shen,W.H., Ingraham,H.A., and Parker,K.L. (1994). Developmental expression of mouse steroidogenic factor-1, an essential regulator of the steroid hydroxylases. Mol. Endocrinol. *8*, 654-662.

Ingraham,H.A., Lala,D.S., Ikeda,Y., Luo,X., Shen,W.H., Nachtigal,M.W., Abbud,R., Nilson,J.H., and Parker,K.L. (1994). The nuclear receptor steroidogenic factor 1 acts at multiple levels of the reproductive axis. Genes Dev. *8*, 2302-2312.

Inokuchi,A., Hinoshita,E., Iwamoto,Y., Kohno,K., Kuwano,M., and Uchiumi,T. (2001). Enhanced expression of the human multidrug resistance protein 3 by bile salt in human enterocytes. A transcriptional control of a plausible bile acid transporter. J. Biol. Chem. *276*, 46822-46829.

Ishihara,S.L. and Morohashi,K. (2005). A boundary for histone acetylation allows distinct expression patterns of the Ad4BP/SF-1 and GCNF loci in adrenal cortex cells. Biochem. Biophys. Res. Commun. *329*, 554-562.

Ito,M., Park,Y., Weck,J., Mayo,K.E., and Jameson,J.L. (2000). Synergistic activation of the inhibin alpha-promoter by steroidogenic factor-1 and cyclic adenosine 3',5'-monophosphate. Mol. Endocrinol. *14*, 66-81.

Ito,M., Yu,R., and Jameson,J.L. (1997). DAX-1 inhibits SF-1-mediated transactivation via a carboxy-terminal domain that is deleted in adrenal hypoplasia congenita. Mol. Cell Biol. *17*, 1476-1483.

Ito,M., Yu,R.N., and Jameson,J.L. (1998). Steroidogenic factor-1 contains a carboxy-terminal transcriptional activation domain that interacts with steroid receptor coactivator-1. Mol. Endocrinol. *12*, 290-301.

Jacob,A.L., Lund,J., Martinez,P., and Hedin,L. (2001). Acetylation of steroidogenic factor 1 protein regulates its transcriptional activity and recruits the coactivator GCN5. J. Biol. Chem. *276*, 37659-37664.

Jacobs,S.B., Coss,D., McGillivray,S.M., and Mellon,P.L. (2003). Nuclear factor Y and steroidogenic factor 1 physically and functionally interact to contribute to cell-specific expression of the mouse Follicle-stimulating hormone-beta gene. Mol. Endocrinol. *17*, 1470-1483.

Jaillon,O., Aury,J.M., Brunet,F., Petit,J.L., Stange-Thomann,N., Mauceli,E., Bouneau,L., Fischer,C., Ozouf-Costaz,C., Bernot,A., Nicaud,S., Jaffe,D., Fisher,S., Lutfalla,G., Dossat,C., Segurens,B., Dasilva,C., Salanoubat,M., Levy,M., Boudet,N., Castellano,S., Anthouard,V., Jubin,C., Castelli,V., Katinka,M., Vacherie,B., Biemont,C., Skalli,Z., Cattolico,L., Poulain,J., De,B., V, Cruaud,C., Duprat,S., Brottier,P., Coutanceau,J.P., Gouzy,J., Parra,G., Lardier,G., Chapple,C., McKernan,K.J., McEwan,P., Bosak,S., Kellis,M., Volff,J.N., Guigo,R., Zody,M.C., Mesirov,J., Lindblad-Toh,K., Birren,B., Nusbaum,C., Kahn,D., Robinson-Rechavi,M., Laudet,V., Schachter,V., Quetier,F., Saurin,W., Scarpelli,C., Wincker,P., Lander,E.S., Weissenbach,J., and Roest,C.H. (2004). Genome duplication in the teleost fish Tetraodon nigroviridis reveals the early vertebrate proto-karyotype. Nature *431*, 946-957.

Jeays-Ward,K., Hoyle,C., Brennan,J., Dandonneau,M., Alldus,G., Capel,B., and Swain,A. (2003). Endothelial and steroidogenic cell migration are regulated by WNT4 in the developing mammalian gonad. Development *130*, 3663-3670.

Jepsen,K. and Rosenfeld,M.G. (2002). Biological roles and mechanistic actions of co-repressor complexes. J. Cell Sci. *115*, 689-698.

Jeyasuria,P., Ikeda,Y., Jamin,S.P., Zhao,L., De Rooij,D.G., Themmen,A.P., Behringer,R.R., and Parker,K.L. (2004). Cell-specific knockout of steroidogenic factor 1 reveals its essential roles in gonadal function. Mol. Endocrinol. *18*, 1610-1619.

Jiang,J.Q., Young,G., Kobayashi,T., and Nagahama,Y. (1998). Eel (Anguilla japonica) testis 11beta-hydroxylase gene is expressed in interrenal tissue and its product lacks aldosterone synthesizing activity. Mol. Cell Endocrinol. *146*, 207-211.

Jorgensen,J.S. and Nilson,J.H. (2001). AR suppresses transcription of the LHbeta subunit by interacting with steroidogenic factor-1. Mol. Endocrinol. *15*, 1505-1516.

Kabe,Y., Goto,M., Shima,D., Imai,T., Wada,T., Morohashi,K., Shirakawa,M., Hirose,S., and Handa,H. (1999). The role of human MBF1 as a transcriptional coactivator. J. Biol. Chem. *274*, 34196-34202.

Kagawa,N. and Waterman,M.R. (1991). Evidence that an adrenal-specific nuclear protein regulates the cAMP responsiveness of the human CYP21B (P450C21) gene. J. Biol. Chem. *266*, 11199-11204.

Kanayama,T., Arito,M., So,K., Hachimura,S., Inoue,J., and Sato,R. (2007). Interaction between sterol regulatory element-binding proteins and liver receptor homolog-1 reciprocally suppresses their transcriptional activities. J. Biol. Chem. *282*, 10290-10298.

Kanda,H., Okubo,T., Omori,N., Niihara,H., Matsumoto,N., Yamada,K., Yoshimoto,S., Ito,M., Yamashita,S., Shiba,T., and Takamatsu,N. (2006). Transcriptional regulation of the rainbow trout CYP19a gene by FTZ-F1 homologue. J. Steroid Biochem. Mol. Biol. *99*, 85-92.

Karlsson,J., von Hofsten,J., and Olsson,P.E. (2001). Generating transparent zebrafish: a refined method to improve detection of gene expression during embryonic development. Mar. Biotechnol. (NY) *3*, 522-527.

Karpova,T., Maran,R.R., Presley,J., Scherrer,S.P., Tejada,L., and Heckert,L.L. (2005a). Transgenic rescue of SF-1-null mice. Ann. N. Y. Acad. Sci. *1061*, 55-64.

Karpova,T., Presley,J., Manimaran,R.R., Scherrer,S.P., Tejada,L., Peterson,K.R., and Heckert,L.L. (2005b). A FTZ-F1-containing yeast artificial chromosome recapitulates expression of steroidogenic factor 1 in vivo. Mol. Endocrinol. *19*, 2549-2563.

Kawabe,K., Shikayama,T., Tsuboi,H., Oka,S., Oba,K., Yanase,T., Nawata,H., and Morohashi,K. (1999). Dax-1 as one of the target genes of Ad4BP/SF-1. Mol. Endocrinol. *13*, 1267-1284.

Keller,E.F. and Harel,D. (2007). Beyond the gene. PLoS. ONE. *2*, e1231.

Kiiveri,S., Liu,J., Westerholm-Ormio,M., Narita,N., Wilson,D.B., Voutilainen,R., and Heikinheimo,M. (2002). Differential expression of GATA-4 and GATA-6 in fetal and adult mouse and human adrenal tissue. Endocrinology *143*, 3136-3143.

Kim,A.C., Reuter,A.L., Zubair,M., Else,T., Serecky,K., Bingham,N.C., Lavery,G.G., Parker,K.L., and Hammer,G.D. (2008a). Targeted disruption of beta-catenin in Sf1-expressing cells impairs development and maintenance of the adrenal cortex. Development *135*, 2593-2602.

Kim,C.H., Ardayfio,P., and Kim,K.S. (2001). An E-box motif residing in the exon/intron 1 junction regulates both transcriptional activation and splicing of the human norepinephrine transporter gene. J. Biol. Chem. *276*, 24797-24805.

Kim,J.W., Havelock,J.C., Carr,B.R., and Attia,G.R. (2005). The orphan nuclear receptor, liver receptor homolog-1, regulates cholesterol side-chain cleavage cytochrome p450 enzyme in human granulosa cells. J. Clin. Endocrinol. Metab *90*, 1678-1685.

Kim,K.W., Zhao,L., and Parker,K.L. (2008b). Central nervous system-specific knockout of steroidogenic factor 1. Mol. Cell Endocrinol.

Kimmel,C.B., Ballard,W.W., Kimmel,S.R., Ullmann,B., and Schilling,T.F. (1995). Stages of embryonic development of the zebrafish. Dev. Dyn. *203*, 253-310.

Kishimoto,M., Fujiki,R., Takezawa,S., Sasaki,Y., Nakamura,T., Yamaoka,K., Kitagawa,H., and Kato,S. (2006). Nuclear receptor mediated gene regulation through chromatin remodeling and histone modifications. Endocr. J. *53*, 157-172.

Kohara,K., Kitamura,A., Morishima,M., and Tsumoto,T. (2001). Activity-dependent transfer of brain-derived neurotrophic factor to postsynaptic neurons. Science *291*, 2419-2423.

Komatsu,T., Mizusaki,H., Mukai,T., Ogawa,H., Baba,D., Shirakawa,M., Hatakeyama,S., Nakayama,K.I., Yamamoto,H., Kikuchi,A., and Morohashi,K. (2004). Small ubiquitin-like modifier 1 (SUMO-1) modification of the synergy control motif of Ad4 binding protein/steroidogenic factor 1 (Ad4BP/SF-1) regulates synergistic transcription between Ad4BP/SF-1 and Sox9. Mol. Endocrinol. *18*, 2451-2462.

Koskimies,P., Levallet,J., Sipila,P., Huhtaniemi,I., and Poutanen,M. (2002). Murine relaxin-like factor promoter: functional characterization and regulation by transcription factors steroidogenic factor 1 and DAX-1. Endocrinology *143*, 909-919.

Kotomura,N., Ninomiya,Y., Umesono,K., and Niwa,O. (1997). Transcriptional regulation by competition between ELP isoforms and nuclear receptors. Biochem. Biophys. Res. Commun. *230*, 407-412.

Kretz,O., Reichardt,H.M., Schutz,G., and Bock,R. (1999). Corticotropin-releasing hormone expression is the major target for glucocorticoid feedback-control at the hypothalamic level. Brain Res. *818*, 488-491.

Krylova,I.N., Sablin,E.P., Moore,J., Xu,R.X., Waitt,G.M., MacKay,J.A., Juzumiene,D., Bynum,J.M., Madauss,K., Montana,V., Lebedeva,L., Suzawa,M., Williams,J.D., Williams,S.P., Guy,R.K., Thornton,J.W., Fletterick,R.J., Willson,T.M., and Ingraham,H.A. (2005). Structural analyses reveal phosphatidyl inositols as ligands for the NR5 orphan receptors SF-1 and LRH-1. Cell *120*, 343-355.

Kumaran,R.I., Thakar,R., and Spector,D.L. (2008). Chromatin dynamics and gene positioning. Cell *132*, 929-934.

Kuo,M.W., Postlethwait,J., Lee,W.C., Lou,S.W., Chan,W.K., and Chung,B.C. (2005). Gene duplication, gene loss and evolution of expression domains in the vertebrate nuclear receptor NR5A (Ftz-F1) family. Biochem. J. *389*, 19-26.

Kurrasch,D.M., Cheung,C.C., Lee,F.Y., Tran,P.V., Hata,K., and Ingraham,H.A. (2007). The neonatal ventromedial hypothalamus transcriptome reveals novel markers with spatially distinct patterning. J. Neurosci. *27*, 13624-13634.

Labelle-Dumais,C., Jacob-Wagner,M., Pare,J.F., Belanger,L., and Dufort,D. (2006). Nuclear receptor NR5A2 is required for proper primitive streak morphogenesis. Dev. Dyn. *235*, 3359-3369.

Lakowski,J., Majumder,A., and Lauderdale,J.D. (2007). Mechanisms controlling Pax6 isoform expression in the retina have been conserved between teleosts and mammals. Dev. Biol. *307*, 498-520.

Lala,D.S., Rice,D.A., and Parker,K.L. (1992). Steroidogenic factor I, a key regulator of steroidogenic enzyme expression, is the mouse homolog of fushi tarazu-factor I. Mol. Endocrinol. *6*, 1249-1258.

Lala,D.S., Syka,P.M., Lazarchik,S.B., Mangelsdorf,D.J., Parker,K.L., and Heyman,R.A. (1997). Activation of the orphan nuclear receptor steroidogenic factor 1 by oxysterols. Proc. Natl. Acad. Sci. U. S. A *94*, 4895-4900.

Lan,H.C., Li,H.J., Lin,G., Lai,P.Y., and Chung,B.C. (2007). Cyclic AMP stimulates SF-1-dependent CYP11A1 expression through homeodomain-interacting protein kinase 3-mediated Jun N-terminal kinase and c-Jun phosphorylation. Mol. Cell Biol. *27*, 2027-2036.

Langlois,D., Li,J.Y., and Saez,J.M. (2002). Development and function of the human fetal adrenal cortex. J. Pediatr. Endocrinol. Metab *15 Suppl 5*, 1311-1322.

Lanz,R.B., Jericevic,Z., Zuercher,W.J., Watkins,C., Steffen,D.L., Margolis,R., and McKenna,N.J. (2006). Nuclear Receptor Signaling Atlas (www.nursa.org): hyperlinking the nuclear receptor signaling community. Nucleic Acids Res. *34*, D221-D226.

Laudet,V. (1997). Evolution of the nuclear receptor superfamily: early diversification from an ancestral orphan receptor. J. Mol. Endocrinol. *19*, 207-226.

Laudet,V. and Adelmant,G. (1995). Nuclear receptors. Lonesome orphans. Curr. Biol. *5*, 124-127.

Lavorgna,G., Karim,F.D., Thummel,C.S., and Wu,C. (1993). Potential role for a FTZ-F1 steroid receptor superfamily member in the control of Drosophila metamorphosis. Proc. Natl. Acad. Sci. U. S. A *90*, 3004-3008.

Lavorgna,G., Ueda,H., Clos,J., and Wu,C. (1991). FTZ-F1, a steroid hormone receptor-like protein implicated in the activation of fushi tarazu. Science *252*, 848-851.

Lee,M.B., Lebedeva,L.A., Suzawa,M., Wadekar,S.A., Desclozeaux,M., and Ingraham,H.A. (2005). The DEAD-box protein DP103 (Ddx20 or Gemin-3) represses orphan nuclear receptor activity via SUMO modification. Mol. Cell Biol. *25*, 1879-1890.

Lee,Y.K., Choi,Y.H., Chua,S., Park,Y.J., and Moore,D.D. (2006). Phosphorylation of the hinge domain of the nuclear hormone receptor LRH-1 stimulates transactivation. J. Biol. Chem. *281*, 7850-7855.

Lee,Y.K. and Moore,D.D. (2002). Dual mechanisms for repression of the monomeric orphan receptor liver receptor homologous protein-1 by the orphan small heterodimer partner. J. Biol. Chem. *277*, 2463-2467.

Lee,Y.K. and Moore,D.D. (2008). Liver receptor homolog-1, an emerging metabolic modulator. Front Biosci. *13*, 5950-5958.

Lee,Y.K., Parker,K.L., Choi,H.S., and Moore,D.D. (1999). Activation of the promoter of the orphan receptor SHP by orphan receptors that bind DNA as monomers. J. Biol. Chem. *274*, 20869-20873.

Levallet,J., Koskimies,P., Rahman,N., and Huhtaniemi,I. (2001). The promoter of murine follicle-stimulating hormone receptor: functional characterization and regulation by transcription factor steroidogenic factor 1. Mol. Endocrinol. *15*, 80-92.

Li,L.A., Chiang,E.F., Chen,J.C., Hsu,N.C., Chen,Y.J., and Chung,B.C. (1999). Function of steroidogenic factor 1 domains in nuclear localization, transactivation, and interaction with transcription factor TFIIB and c-Jun. Mol. Endocrinol. *13*, 1588-1598.

Li,Y., Choi,M., Suino,K., Kovach,A., Daugherty,J., Kliewer,S.A., and Xu,H.E. (2005). Structural and biochemical basis for selective repression of the orphan nuclear receptor liver receptor homolog 1 by small heterodimer partner. Proc. Natl. Acad. Sci. U. S. A *102*, 9505-9510.

Li,Y., Lambert,M.H., and Xu,H.E. (2003). Activation of nuclear receptors: a perspective from structural genomics. Structure. *11*, 741-746.

Liao,W., Bisgrove,B.W., Sawyer,H., Hug,B., Bell,B., Peters,K., Grunwald,D.J., and Stainier,D.Y. (1997). The zebrafish gene cloche acts upstream of a flk-1 homologue to regulate endothelial cell differentiation. Development *124*, 381-389.

Lichtenauer,U.D., Duchniewicz,M., Kolanczyk,M., Hoeflich,A., Hahner,S., Else,T., Bicknell,A.B., Zemojtel,T., Stallings,N.R., Schulte,D.M., Kamps,M.P., Hammer,G.D., Scheele,J.S., and Beuschlein,F. (2007). Pre-B-cell transcription factor 1 and steroidogenic factor 1 synergistically regulate adrenocortical growth and steroidogenesis. Endocrinology *148*, 693-704.

Lin,W., Wang,H.W., Sum,C., Liu,D., Hew,C.L., and Chung,B. (2000). Zebrafish ftz-f1 gene has two promoters, is alternatively spliced, and is expressed in digestive organs. Biochem. J. *348 Pt 2*, 439-446.

Liu,D., Chandy,M., Lee,S.K., Le Drean,Y., Ando,H., Xiong,F., Woon,L.J., and Hew,C.L. (2000). A zebrafish ftz-F1 (Fushi tarazu factor 1) homologue requires multiple subdomains in the D and E regions for its transcriptional activity. J. Biol. Chem. *275*, 16758-16766.

Liu,D., Le Drean,Y., Ekker,M., Xiong,F., and Hew,C.L. (1997). Teleost FTZ-F1 homolog and its splicing variant determine the expression of the salmon gonadotropin IIbeta subunit gene. Mol. Endocrinol. *11*, 877-890.

Liu,D.L., Liu,W.Z., Li,Q.L., Wang,H.M., Qian,D., Treuter,E., and Zhu,C. (2003a). Expression and functional analysis of liver receptor homologue 1 as a potential steroidogenic factor in rat ovary. Biol. Reprod. *69*, 508-517.

Liu,X., Liang,B., and Zhang,S. (2004). Sequence and expression of cytochrome P450 aromatase and FTZ-F1 genes in the protandrous black porgy (Acanthopagrus schlegeli). Gen. Comp Endocrinol. *138*, 247-254.

Liu,Y.W. (2007). Interrenal organogenesis in the zebrafish model. Organogenesis *3*, 44-48.

Liu,Y.W., Gao,W., Teh,H.L., Tan,J.H., and Chan,W.K. (2003b). Prox1 is a novel coregulator of Ff1b and is involved in the embryonic development of the zebra fish interrenal primordium. Mol. Cell Biol. *23*, 7243-7255.

Liu,Y.W. and Guo,L. (2006). Endothelium is required for the promotion of interrenal morphogenetic movement during early zebrafish development. Dev. Biol. *297*, 44-58.

Loh,Y.H., Brenner,S., and Venkatesh,B. (2008). Investigation of loss and gain of introns in the compact genomes of pufferfishes (Fugu and Tetraodon). Mol. Biol. Evol. *25*, 526-535.

Lu,T.T., Makishima,M., Repa,J.J., Schoonjans,K., Kerr,T.A., Auwerx,J., and Mangelsdorf,D.J. (2000). Molecular basis for feedback regulation of bile acid synthesis by nuclear receptors. Mol. Cell *6*, 507-515.

Luo,X., Ikeda,Y., and Parker,K.L. (1994). A cell-specific nuclear receptor is essential for adrenal and gonadal development and sexual differentiation. Cell *77*, 481-490.

Luo,X., Ikeda,Y., Schlosser,D.A., and Parker,K.L. (1995). Steroidogenic factor 1 is the essential transcript of the mouse Ftz-F1 gene. Mol. Endocrinol. *9*, 1233-1239.

Luo,Y., Liang,C.P., and Tall,A.R. (2001). The orphan nuclear receptor LRH-1 potentiates the sterol-mediated induction of the human CETP gene by liver X receptor. J. Biol. Chem. *276*, 24767-24773.

Mangelsdorf,D.J., Thummel,C., Beato,M., Herrlich,P., Schutz,G., Umesono,K., Blumberg,B., Kastner,P., Mark,M., Chambon,P., and Evans,R.M. (1995). The nuclear receptor superfamily: the second decade. Cell *83*, 835-839.

Marchal,R., Naville,D., Durand,P., Begeot,M., and Penhoat,A. (1998). A steroidogenic factor-1 binding element is essential for basal human ACTH receptor gene transcription. Biochem. Biophys. Res. Commun. *247*, 28-32.

Margolis,R.N., Evans,R.M., and O'Malley,B.W. (2005). The Nuclear Receptor Signaling Atlas: development of a functional atlas of nuclear receptors. Mol. Endocrinol. *19*, 2433-2436.

Martinez,A., Val,P., Jean,C., Veyssiere,G., and Lefrancois-Martinez,A.M. (2002). SF-1 controls the expression of the scavenger gene akr1b7: in vitro and in vivo approaches. Endocr. Res. *28*, 515-518.

Martinez,A., Val,P., Sahut-Barnola,I., Aigueperse,C., Veyssiere,G., and Lefrancois-Martinez,A.M. (2003). Steroidogenic factor-1 controls the aldose reductase akr1b7 gene promoter in transgenic mice through an atypical binding site. Endocrinology *144*, 2111-2120.

Mascaro,C., Nadal,A., Hegardt,F.G., Marrero,P.F., and Haro,D. (2000). Contribution of steroidogenic factor 1 to the regulation of cholesterol synthesis. Biochem. J. *350 Pt 3*, 785-790.

McClellan,K.M., Parker,K.L., and Tobet,S. (2006). Development of the ventromedial nucleus of the hypothalamus. Front Neuroendocrinol. *27*, 193-209.

McCormick,S.D., Regish,A., O'Dea,M.F., and Shrimpton,J.M. (2008). Are we missing a mineralocorticoid in teleost fish? Effects of cortisol, deoxycorticosterone and aldosterone on osmoregulation, gill Na+,K+ -ATPase activity and isoform mRNA levels in Atlantic salmon. Gen. Comp Endocrinol. *157*, 35-40.

McGonnell,I.M. and Fowkes,R.C. (2006). Fishing for gene function--endocrine modelling in the zebrafish. J. Endocrinol. *189*, 425-439.

Mellon,S.H. and Bair,S.R. (1998). 25-Hydroxycholesterol is not a ligand for the orphan nuclear receptor steroidogenic factor-1 (SF-1). Endocrinology *139*, 3026-3029.

Mendelson,C.R. and Kamat,A. (2007). Mechanisms in the regulation of aromatase in developing ovary and placenta. J. Steroid Biochem. Mol. Biol. *106*, 62-70.

Meng,X., Noyes,M.B., Zhu,L.J., Lawson,N.D., and Wolfe,S.A. (2008). Targeted gene inactivation in zebrafish using engineered zinc-finger nucleases. Nat. Biotechnol. *26*, 695-701.

Mesiano,S. and Jaffe,R.B. (1997). Role of growth factors in the developmental regulation of the human fetal adrenal cortex. Steroids *62*, 62-72.

Miller,C.A., Ingmer,H., and Cohen,S.N. (1995). Boundaries of the pSC101 minimal replicon are conditional. J. Bacteriol. *177*, 4865-4871.

Miller,W.L. (1998). Steroid hormone biosynthesis and actions in the materno-feto-placental unit. Clin. Perinatol. *25*, 799-817, v.

Mizusaki,H., Kawabe,K., Mukai,T., Ariyoshi,E., Kasahara,M., Yoshioka,H., Swain,A., and Morohashi,K. (2003). Dax-1 (dosage-sensitive sex reversal-adrenal hypoplasia congenita critical region on the X chromosome, gene 1) gene transcription is regulated by wnt4 in the female developing gonad. Mol. Endocrinol. *17*, 507-519.

Monte,D., DeWitte,F., and Hum,D.W. (1998). Regulation of the human P450scc gene by steroidogenic factor 1 is mediated by CBP/p300. J. Biol. Chem. *273*, 4585-4591.

Morcos,P.A. (2007). Achieving targeted and quantifiable alteration of mRNA splicing with Morpholino oligos. Biochem. Biophys. Res. Commun. *358*, 521-527.

Morohashi,K., Honda,S., Inomata,Y., Handa,H., and Omura,T. (1992). A common trans-acting factor, Ad4-binding protein, to the promoters of steroidogenic P-450s. J. Biol. Chem. *267*, 17913-17919.

Morohashi,K., Iida,H., Nomura,M., Hatano,O., Honda,S., Tsukiyama,T., Niwa,O., Hara,T., Takakusu,A., Shibata,Y., and . (1994). Functional difference between Ad4BP and ELP, and their distributions in steroidogenic tissues. Mol. Endocrinol. *8*, 643-653.

Morohashi,K., Tsuboi-Asai,H., Matsushita,S., Suda,M., Nakashima,M., Sasano,H., Hataba,Y., Li,C.L., Fukata,J., Irie,J., Watanabe,T., Nagura,H., and Li,E. (1999). Structural and functional abnormalities in the spleen of an mFtz-F1 gene-disrupted mouse. Blood *93*, 1586-1594.

Moulton,J.D. and Yan,Y.L. (2008). Using Morpholinos to control gene expression. Curr. Protoc. Mol. Biol. *Chapter 26*, Unit.

Mueller,M., Cima,I., Noti,M., Fuhrer,A., Jakob,S., Dubuquoy,L., Schoonjans,K., and Brunner,T. (2006). The nuclear receptor LRH-1 critically regulates extra-adrenal glucocorticoid synthesis in the intestine. J. Exp. Med. *203*, 2057-2062.

Muglia,L., Jacobson,L., Dikkes,P., and Majzoub,J.A. (1995). Corticotropin-releasing hormone deficiency reveals major fetal but not adult glucocorticoid need. Nature *373*, 427-432.

Muyrers,J.P., Zhang,Y., Benes,V., Testa,G., Ansorge,W., and Stewart,A.F. (2000a). Point mutation of bacterial artificial chromosomes by ET recombination. EMBO Rep. *1*, 239-243.

Muyrers,J.P., Zhang,Y., and Stewart,A.F. (2000b). ET-cloning: think recombination first. Genet. Eng (N. Y.) *22*, 77-98.

Muyrers,J.P., Zhang,Y., Testa,G., and Stewart,A.F. (1999). Rapid modification of bacterial artificial chromosomes by ET-recombination. Nucleic Acids Res. *27*, 1555-1557.

Nachtigal,M.W., Hirokawa,Y., Enyeart-VanHouten,D.L., Flanagan,J.N., Hammer,G.D., and Ingraham,H.A. (1998). Wilms' tumor 1 and Dax-1 modulate the orphan nuclear receptor SF-1 in sex-specific gene expression. Cell *93*, 445-454.

Nagy,L. and Schwabe,J.W. (2004). Mechanism of the nuclear receptor molecular switch. Trends Biochem. Sci. *29*, 317-324.

Nandi,J. (1962). The structure of the interrenal gland in teleost fishes. Berkeley and Los Angeles California: University of California Press).

Naruse,K., Tanaka,M., Mita,K., Shima,A., Postlethwait,J., and Mitani,H. (2004). A medaka gene map: the trace of ancestral vertebrate proto-chromosomes revealed by comparative gene mapping. Genome Res. *14*, 820-828.

Nash,D.M., Hess,S.A., White,B.A., and Peluso,J.J. (1998). Steroidogenic factor-1 regulates the rate of proliferation of normal and neoplastic rat ovarian surface epithelial cells in vitro. Endocrinology *139*, 4663-4671.

Naville,D., Penhoat,A., Durand,P., and Begeot,M. (1999). Three steroidogenic factor-1 binding elements are required for constitutive and cAMP-regulated expression of the human adrenocorticotropin receptor gene. Biochem. Biophys. Res. Commun. *255*, 28-33.

Naville,D., Penhoat,A., Marchal,R., Durand,P., and Begeot,M. (1998). SF-1 and the transcriptional regulation of the human ACTH receptor gene. Endocr. Res. *24*, 391-395.

Nelson,D.R. (2003). Comparison of P450s from human and fugu: 420 million years of vertebrate P450 evolution. Arch. Biochem. Biophys. *409*, 18-24.

Ngan,E.S., Cheng,P.K., Leung,P.C., and Chow,B.K. (1999). Steroidogenic factor-1 interacts with a gonadotrope-specific element within the first exon of the human gonadotropin-releasing hormone receptor gene to mediate gonadotrope-specific expression. Endocrinology *140*, 2452-2462.

Ninomiya,Y., Kotomura,N., and Niwa,O. (1996). Analysis of DNase I hypersensitive site of the ELP gene. Biochem. Biophys. Res. Commun. *222*, 632-638.

Ninomiya,Y., Okada,M., Kotomura,N., Suzuki,K., Tsukiyama,T., and Niwa,O. (1995). Genomic organization and isoforms of the mouse ELP gene. J. Biochem. *118*, 380-389.

Nolte,R.T., Wisely,G.B., Westin,S., Cobb,J.E., Lambert,M.H., Kurokawa,R., Rosenfeld,M.G., Willson,T.M., Glass,C.K., and Milburn,M.V. (1998). Ligand binding and co-activator assembly of the peroxisome proliferator-activated receptor-gamma. Nature *395*, 137-143.

Nomura,M., Bartsch,S., Nawata,H., Omura,T., and Morohashi,K. (1995). An E box element is required for the expression of the ad4bp gene, a mammalian homologue of ftz-f1 gene, which is essential for adrenal and gonadal development. J. Biol. Chem. *270*, 7453-7461.

Nomura,M., Nawata,H., and Morohashi,K. (1996). Autoregulatory loop in the regulation of the mammalian ftz-f1 gene. J. Biol. Chem. *271*, 8243-8249.

Norris,D.O. (2006). Vertebrate endocrinology. Elsevier Academic Press).

Nuclear Receptors Nomenclature Committee (1999). A unified nomenclature system for the nuclear receptor superfamily. Cell *97*, 161-163.

O'Malley,B.W., Qin,J., and Lanz,R.B. (2008). Cracking the coregulator codes. Curr. Opin. Cell Biol. *20*, 310-315.

Oba,K., Yanase,T., Ichino,I., Goto,K., Takayanagi,R., and Nawata,H. (2000). Transcriptional regulation of the human FTZ-F1 gene encoding Ad4BP/SF-1. J. Biochem. *128*, 517-528.

Ohmuro-Matsuyama,Y., Okubo,K., Matsuda,M., Ijiri,S., Wang,D., Guan,G., Suzuki,T., Matsuyama,M., Morohashi,K., and Nagahama,Y. (2007). Liver receptor homologue-1 (LRH-1) activates the promoter of brain aromatase (cyp19a2) in a teleost fish, the medaka, Oryzias latipes. Mol. Reprod. Dev. *74*, 1065-1071.

Orban,P.C., Chui,D., and Marth,J.D. (1992). Tissue- and site-specific DNA recombination in transgenic mice. Proc. Natl. Acad. Sci. U. S. A *89*, 6861-6865.

Osborne,C.S. and Eskiw,C.H. (2008). Where shall we meet? A role for genome organisation and nuclear sub-compartments in mediating interchromosomal interactions. J. Cell Biochem. *104*, 1553-1561.

Ou,Q., Mouillet,J.F., Yan,X., Dorn,C., Crawford,P.A., and Sadovsky,Y. (2001). The DEAD box protein DP103 is a regulator of steroidogenic factor-1. Mol. Endocrinol. *15*, 69-79.

Pabon,J.E., Li,X., Lei,Z.M., Sanfilippo,J.S., Yussman,M.A., and Rao,C.V. (1996). Novel presence of luteinizing hormone/chorionic gonadotropin receptors in human adrenal glands. J. Clin. Endocrinol. Metab *81*, 2397-2400.

Pare,J.F., Malenfant,D., Courtemanche,C., Jacob-Wagner,M., Roy,S., Allard,D., and Belanger,L. (2004). The fetoprotein transcription factor (FTF) gene is essential to embryogenesis and cholesterol homeostasis and is regulated by a DR4 element. J. Biol. Chem. *279*, 21206-21216.

Pare,J.F., Roy,S., Galarneau,L., and Belanger,L. (2001). The mouse fetoprotein transcription factor (FTF) gene promoter is regulated by three GATA elements with tandem E box and Nkx motifs, and FTF in turn activates the Hnf3beta, Hnf4alpha, and Hnf1alpha gene promoters. J. Biol. Chem. *276*, 13136-13144.

Patel,M.V., McKay,I.A., and Burrin,J.M. (2001). Transcriptional regulators of steroidogenesis, DAX-1 and SF-1, are expressed in human skin. J. Invest Dermatol. *117*, 1559-1565.

Payne,A.H. and Hales,D.B. (2004). Overview of steroidogenic enzymes in the pathway from cholesterol to active steroid hormones. Endocr. Rev. *25*, 947-970.

Payne,D.N. and Adcock,I.M. (2001). Molecular mechanisms of corticosteroid actions. Paediatr. Respir. Rev. *2*, 145-150.

Peng,N., Kim,J.W., Rainey,W.E., Carr,B.R., and Attia,G.R. (2003). The role of the orphan nuclear receptor, liver receptor homologue-1, in the regulation of human corpus luteum 3beta-hydroxysteroid dehydrogenase type II. J. Clin. Endocrinol. Metab *88*, 6020-6028.

Pestell,R.G., Hammond,V.E., and Crawford,R.J. (1993). Molecular cloning and characterization of the cyclic AMP-responsive ovine CYP11A1 (cholesterol side-chain cleavage) gene promoter: DNase 1 protection of conserved consensus elements. J. Mol. Endocrinol. *10*, 297-311.

Peter,R.E., Yu,K.-L., Marchant,T.A., and Rosenblum,P.M. (1990). Direct neural regulation of teleost adenohypophysis. J. Exp. Zool. *4*, 84-89.

Pfeifer,S.M., Furth,E.E., Ohba,T., Chang,Y.J., Rennert,H., Sakuragi,N., Billheimer,J.T., and Strauss,J.F., III (1993). Sterol carrier protein 2: a role in steroid hormone synthesis? J. Steroid Biochem. Mol. Biol. *47*, 167-172.

Pick,L., Anderson,W.R., Shultz,J., and Woodard,C.T. (2006). The Ftz-F1 family: Orphan receptors regulated by novel protein-protein interactions. Advances in Developmental Biology *16*, 255-296.

Pieri,I., Klein,M., Bayertz,C., Gerspach,J., van der,P.A., Pfizenmaier,K., and Eisel,U. (1999). Regulation of the murine NMDA-receptor-subunit NR2C promoter by Sp1 and fushi tarazu factor1 (FTZ-F1) homologues. Eur. J. Neurosci. *11*, 2083-2092.

Pincas,H., Amoyel,K., Counis,R., and Laverriere,J.N. (2001). Proximal cis-acting elements, including steroidogenic factor 1, mediate the efficiency of a distal enhancer in the promoter of the rat gonadotropin-releasing hormone receptor gene. Mol. Endocrinol. *15*, 319-337.

Postlethwait,J.H., Yan,Y.L., Gates,M.A., Horne,S., Amores,A., Brownlie,A., Donovan,A., Egan,E.S., Force,A., Gong,Z., Goutel,C., Fritz,A., Kelsh,R., Knapik,E., Liao,E., Paw,B., Ransom,D., Singer,A., Thomson,M., Abduljabbar,T.S., Yelick,P., Beier,D., Joly,J.S., Larhammar,D., Rosa,F., Westerfield,M., Zon,L.I., Johnson,S.L., and Talbot,W.S. (1998). Vertebrate genome evolution and the zebrafish gene map. Nat. Genet. *18*, 345-349.

Purba,H.S., King,E.J., Richert,P., and Bhatnagar,A.S. (1994). Effect of aromatase inhibitors on estrogen 2-hydroxylase in rat liver. J. Steroid Biochem. Mol. Biol. *48*, 215-219.

Qin,J., Gao,D.M., Jiang,Q.F., Zhou,Q., Kong,Y.Y., Wang,Y., and Xie,Y.H. (2004). Prospero-related homeobox (Prox1) is a corepressor of human liver receptor homolog-1 and suppresses the transcription of the cholesterol 7-alpha-hydroxylase gene. Mol. Endocrinol. *18*, 2424-2439.

Rainey,W.E., Saner,K., and Schimmer,B.P. (2004). Adrenocortical cell lines. Mol. Cell Endocrinol. *228*, 23-38.

Ramayya,M.S., Zhou,J., Kino,T., Segars,J.H., Bondy,C.A., and Chrousos,G.P. (1997). Steroidogenic factor 1 messenger ribonucleic acid expression in steroidogenic and nonsteroidogenic human tissues: Northern blot and in situ hybridization studies. J. Clin. Endocrinol. Metab *82*, 1799-1806.

Rausa,F.M., Galarneau,L., Belanger,L., and Costa,R.H. (1999). The nuclear receptor fetoprotein transcription factor is coexpressed with its target gene HNF-3beta in the developing murine liver, intestine and pancreas. Mech. Dev. *89*, 185-188.

Reinhart,A.J., Williams,S.C., Clark,B.J., and Stocco,D.M. (1999). SF-1 (steroidogenic factor-1) and C/EBP beta (CCAAT/enhancer binding protein-beta) cooperate to regulate the murine StAR (steroidogenic acute regulatory) promoter. Mol. Endocrinol. *13*, 729-741.

Rice,D.A., Mouw,A.R., Bogerd,A.M., and Parker,K.L. (1991). A shared promoter element regulates the expression of three steroidogenic enzymes. Mol. Endocrinol. *5*, 1552-1561.

Robinson-Rechavi,M., Carpentier,A.S., Duffraisse,M., and Laudet,V. (2001). How many nuclear hormone receptors are there in the human genome? Trends Genet. *17*, 554-556.

Rocha,R.M., Leme-Dos Santos,H.S., Vicentini,C.A., and Da Cruz,C. (2001). Structural and ultrastructural characteristics of interrenal gland and chromaffin cell of matrinxa, Brycon cephalus Gunther 1869 (Teleostei-Characidae). Anat. Histol. Embryol. *30*, 351-355.

Ruau,D., Duarte,J., Ourjdal,T., Perriere,G., Laudet,V., and Robinson-Rechavi,M. (2004). Update of NUREBASE: nuclear hormone receptor functional genomics. Nucleic Acids Res. *32*, D165-D167.

Sablin,E.P., Krylova,I.N., Fletterick,R.J., and Ingraham,H.A. (2003). Structural basis for ligand-independent activation of the orphan nuclear receptor LRH-1. Mol. Cell *11*, 1575-1585.

Sadovsky,Y., Crawford,P.A., Woodson,K.G., Polish,J.A., Clements,M.A., Tourtellotte,L.M., Simburger,K., and Milbrandt,J. (1995). Mice deficient in the orphan receptor steroidogenic factor 1 lack adrenal glands and gonads but express P450 side-chain-cleavage enzyme in the placenta and have normal embryonic serum levels of corticosteroids. Proc. Natl. Acad. Sci. U. S. A *92*, 10939-10943.

Safi,R., Kovacic,A., Gaillard,S., Murata,Y., Simpson,E.R., McDonnell,D.P., and Clyne,C.D. (2005). Coactivation of liver receptor homologue-1 by peroxisome proliferator-activated receptor gamma coactivator-1alpha on aromatase promoter II and its inhibition by activated retinoid X receptor suggest a novel target for breast-specific antiestrogen therapy. Cancer Res. *65*, 11762-11770.

Sairam,M.R. and Krishnamurthy,H. (2001). The role of follicle-stimulating hormone in spermatogenesis: lessons from knockout animal models. Arch. Med. Res. *32*, 601-608.

Sambook J. and Russel D. (2000). Molecular Cloning: A Laboratory Manual. Cold Spring Harbor Laboratory *Third edition*.

Sampath,K., Rubinstein,A.L., Cheng,A.M., Liang,J.O., Fekany,K., Solnica-Krezel,L., Korzh,V., Halpern,M.E., and Wright,C.V. (1998). Induction of the zebrafish ventral brain and floorplate requires cyclops/nodal signalling. Nature *395*, 185-189.

Sauer,B. and Henderson,N. (1988). Site-specific DNA recombination in mammalian cells by the Cre recombinase of bacteriophage P1. Proc. Natl. Acad. Sci. U. S. A *85*, 5166-5170.

Sauer,B. and Henderson,N. (1989). Cre-stimulated recombination at loxP-containing DNA sequences placed into the mammalian genome. Nucleic Acids Res. *17*, 147-161.

Savkur,R.S. and Burris,T.P. (2004). The coactivator LXXLL nuclear receptor recognition motif. J. Pept. Res. *63*, 207-212.

Saxena,D., Escamilla-Hernandez,R., Little-Ihrig,L., and Zeleznik,A.J. (2007). Liver receptor homolog-1 and steroidogenic factor-1 have similar actions on rat granulosa cell steroidogenesis. Endocrinology *148*, 726-734.

Scherrer,S.P., Rice,D.A., and Heckert,L.L. (2002). Expression of steroidogenic factor 1 in the testis requires an interactive array of elements within its proximal promoter. Biol. Reprod. *67*, 1509-1521.

Schier,A.F., Neuhauss,S.C., Helde,K.A., Talbot,W.S., and Driever,W. (1997). The one-eyed pinhead gene functions in mesoderm and endoderm formation in zebrafish and interacts with no tail. Development *124*, 327-342.

Schmid,W., Cole,T.J., Blendy,J.A., and Schutz,G. (1995). Molecular genetic analysis of glucocorticoid signalling in development. J. Steroid Biochem. Mol. Biol. *53*, 33-35.

Schnabel,C.A., Selleri,L., and Cleary,M.L. (2003). Pbx1 is essential for adrenal development and urogenital differentiation. Genesis. *37*, 123-130.

Schoneveld,O.J., Gaemers,I.C., and Lamers,W.H. (2004). Mechanisms of glucocorticoid signalling. Biochim. Biophys. Acta *1680*, 114-128.

Schoonjans,K., Annicotte,J.S., Huby,T., Botrugno,O.A., Fayard,E., Ueda,Y., Chapman,J., and Auwerx,J. (2002). Liver receptor homolog 1 controls the expression of the scavenger receptor class B type I. EMBO Rep. *3*, 1181-1187.

Seitz,S., Korsching,E., Weimer,J., Jacobsen,A., Arnold,N., Meindl,A., Arnold,W., Gustavus,D., Klebig,C., Petersen,I., and Scherneck,S. (2006). Genetic background of different cancer cell lines influences the gene set involved in chromosome 8 mediated breast tumor suppression. Genes Chromosomes. Cancer *45*, 612-627.

Sewer,M.B., Dammer,E.B., and Jagarlapudi,S. (2007). Transcriptional regulation of adrenocortical steroidogenic gene expression. Drug Metab Rev. *39*, 371-388.

Sharpton,T.J., Neafsey,D.E., Galagan,J.E., and Taylor,J.W. (2008). Mechanisms of intron gain and loss in Cryptococcus. Genome Biol. *9*, R24.

Sheela,S.G., Lee,W.C., Lin,W.W., and Chung,B.C. (2005). Zebrafish ftz-f1a (nuclear receptor 5a2) functions in skeletal muscle organization. Dev. Biol. *286*, 377-390.

Shen,J.H. and Ingraham,H.A. (2002). Regulation of the orphan nuclear receptor steroidogenic factor 1 by Sox proteins. Mol. Endocrinol. *16*, 529-540.

Shen,W.H., Moore,C.C., Ikeda,Y., Parker,K.L., and Ingraham,H.A. (1994). Nuclear receptor steroidogenic factor 1 regulates the mullerian inhibiting substance gene: a link to the sex determination cascade. Cell *77*, 651-661.

Sher,N., Yivgi-Ohana,N., and Orly,J. (2007). Transcriptional regulation of the cholesterol side chain cleavage cytochrome P450 gene (CYP11A1) revisited: binding of GATA, cyclic adenosine 3',5'-monophosphate response element-binding protein and activating protein (AP)-1 proteins to a distal novel cluster of cis-regulatory elements potentiates AP-2 and steroidogenic factor-1-dependent gene expression in the rodent placenta and ovary. Mol. Endocrinol. *21*, 948-962.

Shi,Y., Schonemann,M.D., and Mellon,S.H. (2008). Regulation of P450c17 expression in the early embryo depends on GATA factors. Endocrinology.

Shima,Y., Zubair,M., Ishihara,S., Shinohara,Y., Oka,S., Kimura,S., Okamoto,S., Minokoshi,Y., Suita,S., and Morohashi,K. (2005). Ventromedial hypothalamic nucleus-specific enhancer of Ad4BP/SF-1 gene. Mol. Endocrinol. *19*, 2812-2823.

Shima,Y., Zubair,M., Komatsu,T., Oka,S., Yokoyama,C., Tachibana,T., Hjalt,T.A., Drouin,J., and Morohashi,K. (2008). Pituitary homeobox 2 regulates adrenal4 binding protein/steroidogenic factor-1 gene transcription in the pituitary gonadotrope through interaction with the intronic enhancer. Mol. Endocrinol. *22*, 1633-1646.

Shinoda,K., Lei,H., Yoshii,H., Nomura,M., Nagano,M., Shiba,H., Sasaki,H., Osawa,Y., Ninomiya,Y., Niwa,O., and . (1995). Developmental defects of the ventromedial hypothalamic nucleus and pituitary gonadotroph in the Ftz-F1 disrupted mice. Dev. Dyn. *204*, 22-29.

Siebert,P.D., Chenchik,A., Kellogg,D.E., Lukyanov,K.A., and Lukyanov,S.A. (1995). An improved PCR method for walking in uncloned genomic DNA. Nucleic Acids Res. *23*, 1087-1088.

Sirianni,R., Seely,J.B., Attia,G., Stocco,D.M., Carr,B.R., Pezzi,V., and Rainey,W.E. (2002). Liver receptor homologue-1 is expressed in human steroidogenic tissues and activates transcription of genes encoding steroidogenic enzymes. J. Endocrinol. *174*, R13-R17.

Smirnov,A.N. (2002). Nuclear receptors: nomenclature, ligands, mechanisms of their effects on gene expression. Biochemistry (Mosc.) *67*, 957-977.

Stallings,N.R., Hanley,N.A., Majdic,G., Zhao,L., Bakke,M., and Parker,K.L. (2002). Development of a transgenic green fluorescent protein lineage marker for steroidogenic factor 1. Mol. Endocrinol. *16*, 2360-2370.

Stocco,D.M. (2000). The role of the StAR protein in steroidogenesis: challenges for the future. J. Endocrinol. *164*, 247-253.

Sugawara,T., Abe,S., Sakuragi,N., Fujimoto,Y., Nomura,E., Fujieda,K., Saito,M., and Fujimoto,S. (2001). RIP 140 modulates transcription of the steroidogenic acute regulatory protein gene through interactions with both SF-1 and DAX-1. Endocrinology *142*, 3570-3577.

Sugawara,T., Saito,M., and Fujimoto,S. (2000). Sp1 and SF-1 interact and cooperate in the regulation of human steroidogenic acute regulatory protein gene expression. Endocrinology *141*, 2895-2903.

Suzuki,T., Kasahara,M., Yoshioka,H., Morohashi,K., and Umesono,K. (2003). LXXLL-related motifs in Dax-1 have target specificity for the orphan nuclear receptors Ad4BP/SF-1 and LRH-1. Mol. Cell Biol. *23*, 238-249.

Tan,J.H., Quek,S.I., and Chan,W.K. (2005). Cloning, genomic organization, and expression analysis of zebrafish nuclear receptor coactivator, TIF2. Zebrafish. *2*, 33-46.

Tavera-Mendoza,L.E., Mader,S., and White,J.H. (2006). Genome-wide approaches for identification of nuclear receptor target genes. Nucl. Recept. Signal. *4*, e018.

Taylor,J.S., Braasch,I., Frickey,T., Meyer,A., and Van de,P.Y. (2003). Genome duplication, a trait shared by 22000 species of ray-finned fish. Genome Res. *13*, 382-390.

Technau,U. (2001). Brachyury, the blastopore and the evolution of the mesoderm. Bioessays *23*, 788-794.

Tremblay,J.J. and Drouin,J. (1999). Egr-1 is a downstream effector of GnRH and synergizes by direct interaction with Ptx1 and SF-1 to enhance luteinizing hormone beta gene transcription. Mol. Cell Biol. *19*, 2567-2576.

Tremblay,J.J., Lanctot,C., and Drouin,J. (1998). The pan-pituitary activator of transcription, Ptx1 (pituitary homeobox 1), acts in synergy with SF-1 and Pit1 and is an upstream regulator of the Lim-homeodomain gene Lim3/Lhx3. Mol. Endocrinol. *12*, 428-441.

Tremblay,J.J., Marcil,A., Gauthier,Y., and Drouin,J. (1999). Ptx1 regulates SF-1 activity by an interaction that mimics the role of the ligand-binding domain. EMBO J. *18*, 3431-3441.

Tremblay,J.J. and Viger,R.S. (1999). Transcription factor GATA-4 enhances Mullerian inhibiting substance gene transcription through a direct interaction with the nuclear receptor SF-1. Mol. Endocrinol. *13*, 1388-1401.

Tremblay,J.J. and Viger,R.S. (2001a). GATA factors differentially activate multiple gonadal promoters through conserved GATA regulatory elements. Endocrinology *142*, 977-986.

Tremblay,J.J. and Viger,R.S. (2001b). Nuclear receptor Dax-1 represses the transcriptional cooperation between GATA-4 and SF-1 in Sertoli cells. Biol. Reprod. *64*, 1191-1199.

Ueda,H., Sonoda,S., Brown,J.L., Scott,M.P., and Wu,C. (1990). A sequence-specific DNA-binding protein that activates fushi tarazu segmentation gene expression. Genes Dev. *4*, 624-635.

Unsicker,K., Huber,K., Schutz,G., and Kalcheim,C. (2005). The chromaffin cell and its development. Neurochem. Res. *30*, 921-925.

Uzgiris,V.I., Whipple,C.A., and Salhanick,H.A. (1977). Stereoselective inhibition of cholesterol side chain cleavage by enantiomers of aminoglutethimide. Endocrinology *101*, 89-92.

Vainio,S., Heikkila,M., Kispert,A., Chin,N., and McMahon,A.P. (1999). Female development in mammals is regulated by Wnt-4 signalling. Nature *397*, 405-409.

Val,P., Aigueperse,C., Lefrancois-Martinez,A.M., Jean,C., Veyssiere,G., and Martinez,A. (2002). Role of three SF-1 binding sites in the expression of the mvdp/akr1-b7 isocaproaldehyde reductase in Y1 cells. Endocr. Res. *28*, 527-533.

Val,P., Lefrancois-Martinez,A.M., Veyssiere,G., and Martinez,A. (2003). SF-1 a key player in the development and differentiation of steroidogenic tissues. Nucl. Recept. *1*, 8.

Venkatesh,B., Ning,Y., and Brenner,S. (1999). Late changes in spliceosomal introns define clades in vertebrate evolution. Proc. Natl. Acad. Sci. U. S. A *96*, 10267-10271.

von Hofsten,J., Jones,I., Karlsson,J., and Olsson,P.E. (2001). Developmental expression patterns of FTZ-F1 homologues in zebrafish (Danio rerio). Gen. Comp Endocrinol. *121*, 146-155.

von Hofsten,J., Karlsson,J., Jones,I., and Olsson,P.E. (2002). Expression and regulation of fushi tarazu factor-1 and steroidogenic genes during reproduction in Arctic char (Salvelinus alpinus). Biol. Reprod. *67*, 1297-1304.

von Hofsten,J., Larsson,A., and Olsson,P.E. (2005). Novel steroidogenic factor-1 homolog (ff1d) is coexpressed with anti-Mullerian hormone (AMH) in zebrafish. Dev. Dyn. *233*, 595-604.

von Hofsten,J. and Olsson,P.E. (2005). Zebrafish sex determination and differentiation: involvement of FTZ-F1 genes. Reprod. Biol. Endocrinol. *3*, 63.

Wallace,J.A. and Felsenfeld,G. (2007). We gather together: insulators and genome organization. Curr. Opin. Genet. Dev. *17*, 400-407.

Wang,D.S., Kobayashi,T., Zhou,L.Y., Paul-Prasanth,B., Ijiri,S., Sakai,F., Okubo,K., Morohashi,K., and Nagahama,Y. (2007). Foxl2 up-regulates aromatase gene transcription in a female-specific manner by binding to the promoter as well as interacting with ad4 binding protein/steroidogenic factor 1. Mol. Endocrinol. *21*, 712-725.

Wang,W., Zhang,C., Marimuthu,A., Krupka,H.I., Tabrizizad,M., Shelloe,R., Mehra,U., Eng,K., Nguyen,H., Settachatgul,C., Powell,B., Milburn,M.V., and West,B.L. (2005). The crystal structures of human steroidogenic factor-1 and liver receptor homologue-1. Proc. Natl. Acad. Sci. U. S. A *102*, 7505-7510.

Wang,Z.N., Bassett,M., and Rainey,W.E. (2001). Liver receptor homologue-1 is expressed in the adrenal and can regulate transcription of 11 beta-hydroxylase. J. Mol. Endocrinol. *27*, 255-258.

Watanabe,M., Tanaka,M., Kobayashi,D., Yoshiura,Y., Oba,Y., and Nagahama,Y. (1999). Medaka (Oryzias latipes) FTZ-F1 potentially regulates the transcription of P-450 aromatase in

ovarian follicles: cDNA cloning and functional characterization. Mol. Cell Endocrinol. *149*, 221-228.

Watanabe,N., Inoue,H., and Fujii-Kuriyama,Y. (1994). Regulatory mechanisms of cAMP-dependent and cell-specific expression of human steroidogenic cytochrome P450scc (CYP11A1) gene. Eur. J. Biochem. *222*, 825-834.

Weck,J. and Mayo,K.E. (2006). Switching of NR5A proteins associated with the inhibin alpha-subunit gene promoter after activation of the gene in granulosa cells. Mol. Endocrinol. *20*, 1090-1103.

Wehrenberg,U., Ivell,R., Jansen,M., von Goedecke,S., and Walther,N. (1994). Two orphan receptors binding to a common site are involved in the regulation of the oxytocin gene in the bovine ovary. Proc. Natl. Acad. Sci. U. S. A *91*, 1440-1444.

Wei,X., Sasaki,M., Huang,H., Dawson,V.L., and Dawson,T.M. (2002). The orphan nuclear receptor, steroidogenic factor 1, regulates neuronal nitric oxide synthase gene expression in pituitary gonadotropes. Mol. Endocrinol. *16*, 2828-2839.

Westerfield,M. (2000). The zebrafish book. A guide for the laboratory use of zebrafish (Danio rerio). Univ. of Oregon Press, Eugene.).

Whipple,C.A., Colton,T., Strauss,J.M., Hourihan,J., and Salhanick,H.A. (1978). Comparison of luteolytic potencies of aminoglutethimide enantiomers in the rabbit and rat. Endocrinology *103*, 1605-1610.

Wilhelm,D. and Englert,C. (2002). The Wilms tumor suppressor WT1 regulates early gonad development by activation of Sf1. Genes Dev. *16*, 1839-1851.

Wilm,B., James,R.G., Schultheiss,T.M., and Hogan,B.L. (2004). The forkhead genes, Foxc1 and Foxc2, regulate paraxial versus intermediate mesoderm cell fate. Dev. Biol. *271*, 176-189.

Wilson,T.E., Fahrner,T.J., and Milbrandt,J. (1993). The orphan receptors NGFI-B and steroidogenic factor 1 establish monomer binding as a third paradigm of nuclear receptor-DNA interaction. Mol. Cell Biol. *13*, 5794-5804.

Winnay,J.N. and Hammer,G.D. (2006). Adrenocorticotropic hormone-mediated signaling cascades coordinate a cyclic pattern of steroidogenic factor 1-dependent transcriptional activation. Mol. Endocrinol. *20*, 147-166.

Wolf,I.M., Heitzer,M.D., Grubisha,M., and DeFranco,D.B. (2008). Coactivators and nuclear receptor transactivation. J. Cell Biochem. *104*, 1580-1586.

Wong,M., Ramayya,M.S., Chrousos,G.P., Driggers,P.H., and Parker,K.L. (1996). Cloning and sequence analysis of the human gene encoding steroidogenic factor 1. J. Mol. Endocrinol. *17*, 139-147.

Woods,I.G., Kelly,P.D., Chu,F., Ngo-Hazelett,P., Yan,Y.L., Huang,H., Postlethwait,J.H., and Talbot,W.S. (2000). A comparative map of the zebrafish genome. Genome Res. *10*, 1903-1914.

Woods,I.G. and Schier,A.F. (2008). Targeted mutagenesis in zebrafish. Nat. Biotechnol. *26*, 650-651.

Woodson,K.G., Crawford,P.A., Sadovsky,Y., and Milbrandt,J. (1997). Characterization of the promoter of SF-1, an orphan nuclear receptor required for adrenal and gonadal development. Mol. Endocrinol. *11*, 117-126.

Xia,J. (2003). M.S. Thesis. Singapore: National University of Singapore. Characterization of zebrafish *ff1c* gene.

Xu,P.L., Kong,Y.Y., Xie,Y.H., and Wang,Y. (2003). Corepressor SMRT specifically represses the transcriptional activity of orphan nuclear receptor hB1F/hLRH-1. Sheng Wu Hua Xue. Yu Sheng Wu Wu Li Xue. Bao. (Shanghai) *35*, 897-903.

Xu,P.L., Liu,Y.Q., Shan,S.F., Kong,Y.Y., Zhou,Q., Li,M., Ding,J.P., Xie,Y.H., and Wang,Y. (2004). Molecular mechanism for the potentiation of the transcriptional activity of human liver receptor homolog 1 by steroid receptor coactivator-1. Mol. Endocrinol. *18*, 1887-1905.

Yang,W.H., Heaton,J.H., Brevig,H., Mukherjee,S., Iniguez-Lluhi,J.A., and Hammer,G.D. (2008). SUMOylation Inhibits SF-1 Activity by Reducing CDK7 Mediated Serine 203 Phosphorylation. Mol. Cell Biol.

Yang,Y., Zhang,M., Eggertsen,G., and Chiang,J.Y. (2002). On the mechanism of bile acid inhibition of rat sterol 12alpha-hydroxylase gene (CYP8B1) transcription: roles of alpha-fetoprotein transcription factor and hepatocyte nuclear factor 4alpha. Biochim. Biophys. Acta *1583*, 63-73.

Yang,Z., Jiang,H., Chachainasakul,T., Gong,S., Yang,X.W., Heintz,N., and Lin,S. (2006). Modified bacterial artificial chromosomes for zebrafish transgenesis. Methods *39*, 183-188.

Yudt,M.R. and Cidlowski,J.A. (2002). The glucocorticoid receptor: coding a diversity of proteins and responses through a single gene. Mol. Endocrinol. *16*, 1719-1726.

Zhang,C.K., Lin,W., Cai,Y.N., Xu,P.L., Dong,H., Li,M., Kong,Y.Y., Fu,G., Xie,Y.H., Huang,G.M., and Wang,Y. (2001). Characterization of the genomic structure and tissue-specific promoter of the human nuclear receptor NR5A2 (hB1F) gene. Gene *273*, 239-249.

Zhang,P. and Mellon,S.H. (1996). The orphan nuclear receptor steroidogenic factor-1 regulates the cyclic adenosine 3',5'-monophosphate-mediated transcriptional activation of rat cytochrome P450c17 (17 alpha-hydroxylase/c17-20 lyase). Mol. Endocrinol. *10*, 147-158.

Zhang,W., Zhang,Y., Zhang,L., Zhao,H., Li,X., Huang,H., and Lin,H. (2007). The mRNA expression of P450 aromatase, gonadotropin beta-subunits and FTZ-F1 in the orange-spotted grouper (Epinephelus Coioides) during 17alpha-methyltestosterone-induced precocious sex change. Mol. Reprod. Dev. *74*, 665-673.

Zhang,Y., Buchholz,F., Muyrers,J.P., and Stewart,A.F. (1998). A new logic for DNA engineering using recombination in Escherichia coli. Nat. Genet. *20*, 123-128.

Zhang,Y., Muyrers,J.P., Testa,G., and Stewart,A.F. (2000). DNA cloning by homologous recombination in Escherichia coli. Nat. Biotechnol. *18*, 1314-1317.

Zhao,L., Bakke,M., Krimkevich,Y., Cushman,L.J., Parlow,A.F., Camper,S.A., and Parker,K.L. (2001a). Steroidogenic factor 1 (SF1) is essential for pituitary gonadotrope function. Development *128*, 147-154.

Zhao,L., Bakke,M., and Parker,K.L. (2001b). Pituitary-specific knockout of steroidogenic factor 1. Mol. Cell Endocrinol. *185*, 27-32.

Zhao,L., Kim,K.W., Ikeda,Y., Anderson,K.K., Beck,L., Chase,S., Tobet,S.A., and Parker,K.L. (2008). Central nervous system-specific knockout of steroidogenic factor 1 results in increased anxiety-like behavior. Mol. Endocrinol. *22*, 1403-1415.

Zhao,Y., Yang,Z., Phelan,J.K., Wheeler,D.A., Lin,S., and McCabe,E.R. (2006). Zebrafish dax1 is required for development of the interrenal organ, the adrenal cortex equivalent. Mol. Endocrinol. *20*, 2630-2640.

Zhaxybayeva,O. and Gogarten,J.P. (2003). Spliceosomal introns: new insights into their evolution. Curr. Biol. *13*, R764-R766.

Zhou,L.Y., Wang,D.S., Shibata,Y., Paul-Prasanth,B., Suzuki,A., and Nagahama,Y. (2007). Characterization, expression and transcriptional regulation of P450c17-I and -II in the medaka, Oryzias latipes. Biochem. Biophys. Res. Commun. *362*, 619-625.

Zubair,M., Ishihara,S., Oka,S., Okumura,K., and Morohashi,K. (2006). Two-step regulation of Ad4BP/SF-1 gene transcription during fetal adrenal development: initiation by a Hox-Pbx1-Prep1 complex and maintenance via autoregulation by Ad4BP/SF-1. Mol. Cell Biol. *26*, 4111-4121.

Zubair,M., Oka,S., Ishihara,S., and Morohashi,K. (2002). Analysis of Ad4BP/SF-1 gene regulatory region. Endocr. Res. *28*, 535.

Zubair,M., Parker,K.L., and Morohashi,K. (2008). Developmental links between the fetal and adult zones of the adrenal cortex revealed by lineage tracing. Mol. Cell Biol. *28*, 7030-7040.